The Extraction, Characterisation and Application of Novel Collagen-Based Bio-Materials Derived from Rhizostomas pulmo For Tissue Engineering Applications

Widdowson, Jonathan P.

The Extraction, Characterisation and Application of Novel Collagen-Based Bio-Materials Derived from *Rhizostomas pulmo* For Tissue Engineering Applications

Jonathan P Widdowson

BSc (Genetics), Swansea University

A thesis submitted to Swansea University in partial fulfilment of the requirements for the degree of Doctor of Philosophy

DECLARATION

This work has not previously been accepted in substance for any degree and is not being concurrently submitted in candidature for any degree.

Signed ..... (candidate)

Date .....

STATEMENT 1

This thesis is the result of my own investigations, except where otherwise stated.

Other sources are acknowledged by footnotes giving explicit references. A bibliography is appended.

Signed ..... (candidate)

Date .....

STATEMENT 2

I hereby give consent for my thesis, if accepted, to be available for photocopying and for inter-library loans **after expiry of a bar on access approved by Swansea University.**

Signed ..... (candidate)

Date .....

Swansea University
Prifysgol Abertawe

THESIS SUMMARY

Candidate's Surname / Family Name:

Widdowson

Candidate's Forenames:

Jonathan Peter

Candidate for the Degree of:

PhD

Full title of thesis:

The Extraction, Characterisation and Application of Novel Collagen-Based Bio-Materials Derived from *Rhizostomas pulmo* For Tissue Engineering Applications

Summary:

Collagen is the most abundant protein in animals, and as such provides the optimal polymer for use in tissue engineering and regenerative medicine applications. The electrospinning of collagen presents a simple, scalable method for the production of biocompatible scaffolds, however recent findings have shown that collagen is irreversibly denatured into gelatin when electrospun using fluorinated alcohols. The work contained within this thesis describes the production of an industrially relevant, scalable process for the extraction of acid soluble collagen. The characterisation of this collagen is carried out, and the optimisation for use in bio-printing is assessed.

This thesis introduces a novel, collagen derived biomaterial, termed Single Alpha-Chain Collagen, and the methods for its production are discussed within. Both Acid Soluble and Single Alpha-Chain Collagens are characterised using common techniques, including Sodium Dodecyl Sulphate PolyAcrylamide Gel Electrophoresis and Fourier Transform InfraRed spectroscopy. The benefits of Single Alpha-Chain Collagen include a higher solubility profile than has been previously shown by other native collagens, permitting the production of novel prototype medical devices. Single Alpha-Chain Collagen extracts can be electrospun from benign solvents and physiological buffer systems, while preserving the nativity of the protein. Furthermore, it is shown within that Single Alpha-Chain Collagen extracts possess the ability to refibrillise into triple helical collagen when exposed to physiological buffers, a feature which is retained, even after electrospinning is carried out. The implications of these findings are compared to the literature as a solution to the current issues facing the electrospinning of collagen.

Contents

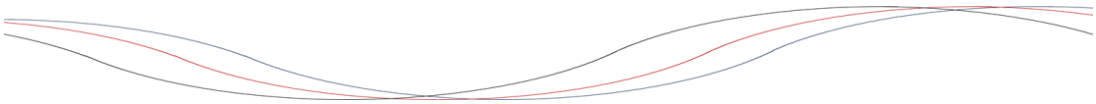

I dedicate this work to my loving mother and father. You have supported me throughout this journey and none of this would be possible without your love and care.

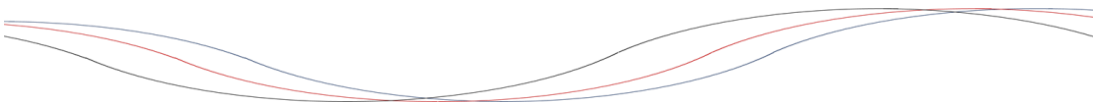

Acknowledgements

I would like to thank my supervisor Dr Chris Wright for his support, guidance and advice throughout my PhD, this work and the amazing opportunities it has afforded would not be possible without you.

I acknowledge my parents for their continuous support, not just during my higher education in Swansea, but for supporting me throughout my life. You have allowed me the opportunity to explore a career that would not be possible without you.

I thank my family and friends for their support throughout my PhD, whether it be a simple conversation, or cheering me up when things seemed dire, this would not have been possible without you.

Finally, I would like to thank Swansea University, for guiding my higher education experience, from arriving as an undergrad, through my PhD and beyond into my professional career, where I have always felt at home within these halls.

Contribution

I would like to thank Aled Lewis for his assistance and training for Scanning Electron Microscopy, and for assisting in carrying out X-Ray Diffraction experiments.

I would also like to thank Christopher Mortimer for training on the use of needle and needle-less electrospinning equipment.

Finally, I would like to thank Stephen Mandale for training in the building and control of the membrane filtration systems, and for assistance with processing the raw materials.

Mendeley Desktop was used as the reference management software for the collection and formatting of references within this thesis.

List of Tables

List of Figures

Abbreviations

ECM	Extra Cellular Matrix
BSE	Bovine Spongiform Encephalopathy
TSE	Transmissible Spongiform Encephalopathy
TFF	Tangential Flow Filtration
SACC	Single Alpha-Chain Collagen
ASC	Acid Soluble Collagen
HFP	1,1,1,3,3,3-hexafluoro-2-propanol
SDS PAGE	Sodium Dodecyl Sulphate Polyacrylamide Gel Electrophoresis
SEM	Scanning Electron Microscopy
FTIR	Fourier Transform Infrared Spectroscopy
TFE	2,2,2-trifluoroethanol
HFM	Hollow Fibre Membrane
MMP	Matrix Metalloproteinases
CD	Circular Dichroism
NaOH	Sodium Hydroxide
PBS	Phosphate Buffered Saline
AcOH	Acetic (Ethanoic) Acid
DSC	Differential Scanning Calorimetry
EDC	1-ethyl-3-(3-dimethylaminopropyl) carbodiimide hydrochloride
NHS	N-hydroxysuccinimide
TG	Transglutaminase
LO	Lysyl Oxidase
GP	Genipin
PCT	Patent Cooperation Treaty
PEO	Polyethylene Oxide
PCL	Polycaprolactone
AFM	Atomic Force Microscopy

1 Introduction

1.1 General Introduction

Collagen is a highly conserved protein which can be found right across the animal spectrum, from ancient sponges to mammals. The primary structure of collagen is defined by Glycine -X-Y repeats, where X can be any amino acid, and Y is often proline or hydroxyproline (Shoulders and Raines 2010). The individual alpha-chains form a left-handed helix, and the three chains wind around one another in a right handed superhelix. (Myllyharju and Kivirikko 2001).

Throughout this work, the main focus will be on the use of collagens which are fully fibril forming, including types I and II, due to their use in creating a biomimetic extracellular matrix (ECM) for tissue engineering (Rho et al. 2006; Zhu et al. 2009; Heydarkhan-Hagvall et al. 2008). These proteins have been utilised for a potential scaffold for use in applications ranging from 3D cell culture (Zhong et al. 2006) and wound dressings (Doillon and Silver 1986; Mathangi Ramakrishnan et al. 2013), drug delivery (Lee, Singla, and Lee 2001), as well as artificial tissue (Bell et al. 1981) and progress towards organ production.

Collagen is a primary component of many tissues found in the body; it acts as a fibre network with the function of supporting cellular growth within the ECM. This functionality makes collagen a key biomaterial that can be harnessed for the repair and control of tissues. Thus, there is a wealth of research that has studied collagen's bioactive and mechanical properties in order to optimise the delivery of its functionality for healthcare. Collagen is now widely used within regenerative medicine because of its excellent biocompatibility and versatility in fabrication methods where it can be blended to form composites with improved features such as mechanical stiffness; an important determinant of cell behaviour.

Collagen is traditionally isolated from mammalian animals using decellularization in sodium hydroxide followed by solubilisation in acetic acid with the use of centrifugation to purify the extract. Collagen has been extracted from a range of sources, but is commonly obtained from bovine, porcine and equine sources for *in vivo*

use (Silvipriya et al. 2015). However, these sources have potential problems with the risk of Bovine Spongiform Encephalopathy (BSE), other Transmittable Spongiform Encephalopathies (TSEs) and potential viral vectors that could be transmissible to humans (Asher 1999; Lupi 2002). More recently, jellyfish and other marine animals have emerged as a source of collagen that is an attractive alternative to existing sources due to a plentiful supply (J. Williams 2015) and a safer source through a lack of BSE risk and potential viral vectors (Song et al. 2006).

Membrane processing presents a diverse field which encompasses the separation of materials from one another, based on size, charge, shape or other specific qualities. Conventionally, membranes act as a barrier which allows liquids and dissolved solids to pass as a filtrate while retaining solids which are larger than the pores of the membrane. Focusing on protein extractions, tangential flow filtration (TFF) based systems for separating proteins have been described previously in regards to whey protein (Zydney 1998) among many others (Howard & Chase 2010). However, collagen has not been successfully processed in this way, due mainly to the unsuitability of starting materials such as bovine hide, with solid material capable of blocking fibres and will reduce efficacy.

Once isolated, collagen can be used in an array of fabrication methods which are useful in the production of functional biomaterial-based scaffolds suitable for regenerative medicine. Bioprinting is rapidly becoming a new method for the fabrication of complex three-dimensional structures, while traditional freeze-drying techniques facilitate the formation of open pore structures for cell migration.

Electrospinning has for many years offered the simplest solution for creating nanofibre materials from biological polymers. Many variations on electrospinning have been developed, covering scale up, fibre alignment and many other modifications to improve the efficacy of the scaffold to a given niche. However the use of collagen in electrospinning has raised questions in recent years, surrounding the use of fluorinated alcohols to dissolve the polymer in order to permit electrospinning (Zeugolis et al. 2008a).

1.2 Background

Multicellular animals require a combination of macromolecules to bind together cells, provide structural integrity within tissues and facilitate overall stability. This is achieved by the ECM, a highly organised network of glycoproteins, proteoglycans and glycosaminoglycans. The ECM provides physical stability while also promoting cell growth, migration, differentiation and adhesion by acting as a substrate for the cells to bind to. The composition of the ECM varies depending on the tissue composition, in direct governance with the surrounding cell types, and while certain cell types are responsible for the production of the ECM, the interactions with ECM components and membrane receptors causes the activation and upregulation of cellular signalling pathways associated with controlling gene expression.

The manufacture of collagen fibres and structures have seen many different techniques employed, these include fibre extrusion (Enea et al. 2011), lyophilisation (Lowe et al. 2016) and 3D printing (Nocera et al. 2018), though none of these processes are suitable to produce the nanofibre structures required to accurately mimic the ECM. Electrospinning of collagen materials has now emerged as a key method by which the functional properties of collagen can be engineered and efficiently incorporated into medical devices with applications within wound healing, tissue engineering and drug delivery.

This chapter introduces the collagen structure and its functional context within the body, examining its background as a biomaterial. This will serve to justify the growing research interest, and main theme of this thesis, focussing on the fabrication of collagen fibres through electrospinning.

1.3 Molecular Structure

Collagen is a highly conserved protein which can be found right across the animal spectrum, from ancient sponges to mammals. The primary structure of collagen has Glycine -X-Y repeats, where X can be any amino acid, and Y is often proline or hydroxyproline (Shoulders and Raines 2010), The individual chains form a left-handed helix, and the three chains wind around one another in a right handed

superhelix. (Myllyharju and Kivirikko 2001). This forms the characteristic tertiary structure of a triple helix (Figure 1.1) and makes collagen fibres insoluble with high tensile strength (Gelse, Pöschl, and Aigner 2003). Collagen is produced and secreted predominantly by fibroblast cells. The process follows the standard pathway for a secreted protein, where the precursor collagen chains are synthesised as a longer chain termed procollagen. These chains are transported to the lumen of the rough endoplasmic reticulum where the procollagen undergoes modifications such as glycosylation. Specific proline and lysine residues in the central region of the chains undergo hydroxylation before disulphide bonds are formed between N and C terminal propeptide sequences to align the three chains and begin the formation of the triple helix from C to N terminus (Lodish et al. 2000). The final assembly of collagen within the ECM is a discontinuous super twisted right-handed microfibril.

1.4 Overview

The work presented here will explore the use of TFF systems in order to aid the scalable extraction of acid soluble collagen (ASC), while also permitting the extraction of a novel collagen extract, termed single alpha-chain collagen (SACC). The work will then explore how SACC may present a solution to the problems shown with the electrospinning of collagen scaffolds, while retaining the nativity required to reform triple helical fibres under physiological conditions.

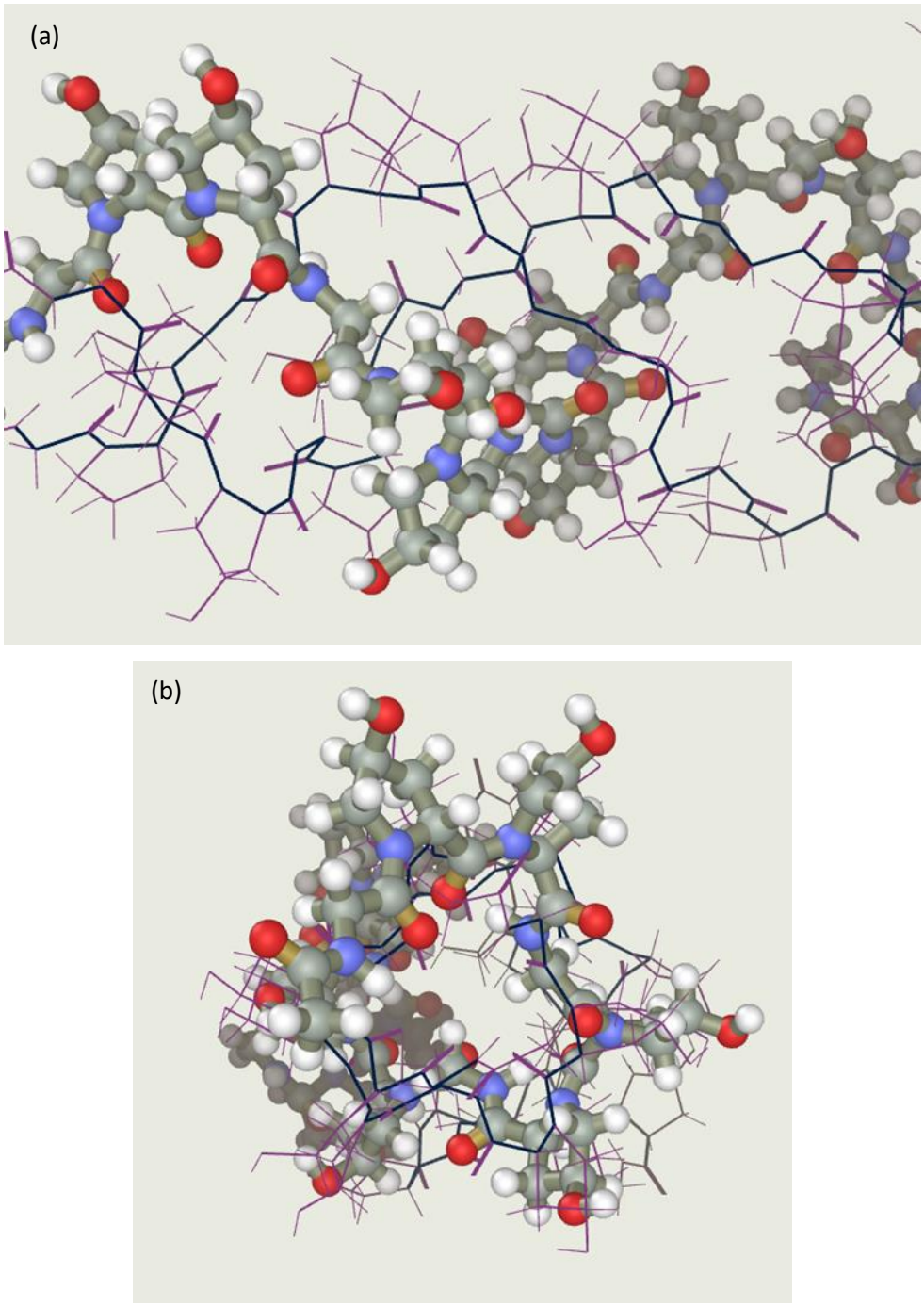

Figure 1.1 Triple helix peptide of Gly-Pro-Hyp repeats arranged with a hybrid Lui Storey and Conjugate Descent optimisation (LS-CD) using Abalone software to build amino acid structure. The repeated banding structure of the helix can be observed in a right handed superhelix. (a) shows side-on view of the triple helix chains, with a single alpha chain highlighted with ball and stick style. (b) shows view looking down the triple helix, showing the right-hand super-helix direction.

1.5 Aims and Objectives

This thesis will explore the extraction, purification and applications of collagen-based bio-materials derived from jellyfish. Initial explorations will aim to describe an improved method for the production of collagen, with particular optimisation for the processing and extraction of acid soluble collagen from jellyfish. The development of a scalable process will allow the extraction and purification of acid soluble collagen at commercial scale without damaging product quality, but greatly reducing overhead costs due to the reduced man-hours required and the improved characteristics with low batch to batch variation. This will focus on the use of hollow fibre membranes to remove the need for the use of cellulose diafiltration bags and centrifugation from the extraction process, which are currently both rate limiting stages, with a limit on commercial scalability and associated high costs.

The study will then explore the isolation of purified collagen alpha chains, a separation of the triple helical, gamma chains of collagen into single alpha helices, which retain their secondary alpha helix structure and are soluble in buffered salt solutions; these are able to undergo electrospinning without the use of harsh solvents such as 1,1,1,3,3,3-hexafluoro-2-propanol (HFP). The α-chains also retain the ability to reform into triple helical collagen molecules in physiological conditions. This material is characterised to confirm these unique characteristics and compare their attributes to acid soluble collagen.

The work then follows to examine the ASC and alpha chain extracts for their applications in regenerative medicine and tissue engineering, using techniques such as electrospinning and 3D-bioprinting to produce biomimetic scaffolds suited to replicate the conditions of the extracellular matrix.

The overall aim of this work is to improve the current landscape of the use of collagen in regenerative medicine. Major objectives for the work are the creation of a scalable system for the extraction of high-quality ASC, the creation of a new biomaterial that is able to retain the native features of triple helical collagen and for that material to be suitable for electrospinning as a solution to the issues currently faced within the field, as well as the use of other formulations for the creation of prototype regenerative medicine and tissue engineering scaffolds.

1.6 Thesis Outline

This thesis consists of 7 chapters.

Chapter 1 outlines the background of collagen, the motivation behind this work, the aims and objectives and structure of the thesis.

Chapter 2 is a literature review which presents the knowledge of collagen, with its extraction, characterisation and applications for electrospinning as reported in the literature, as well as currently known interactions of collagen with cellular systems. Discussion into the nativity of collagen when electrospun is conducted and assessed, in order to explain the current landscape for collagen electrospinning, and the issues presented within.

Chapter 3 presents the experimental techniques conducted in this work. These consist of methods used to measure the key variables in the extraction of collagen. This chapter also describes techniques used to characterise the collagen extracts, including sodium dodecyl sulphate polyacrylamide gel electrophoresis (SDS PAGE), scanning electron microscopy (SEM), and fourier transform infrared (FTIR) analysis. Finally, commonly used techniques for the production of scaffolds, including electrospinning, crosslinking, gelation methods, freeze drying and 3D bio-printing are described.

Chapter 4 Examines the currently used methods for producing collagen and describes the sequential scale-up of the developed jellyfish collagen extraction technology, based on hollow fibre filtration techniques. This chapter then characterises the acid soluble collagen produced to compare with traditional extraction methods.

Chapter 5 describes and characterises a novel collagen-based bio-material, termed single alpha chain collagen, including the adaptation to the process developed in Chapter 4, and then examines and compares the unique characteristics of this biomaterial with acid soluble collagen.

Chapter 6 demonstrates the applications for both acid soluble and single alpha-chain collagens, using techniques such as electrospinning and bio-printing, and then characterises these scaffolds.

Chapter 7 summarises the results obtained within this thesis, their relation to the literature discussed in Chapter 2 and presents the critical issues arising from this work, as well as the direction for future research based on the findings of this work.

2 Literature Review

2.1 Introduction

The simplest depiction of multicellular animals requires a combination of macromolecules to bind cells together, provide structural integrity in tissues and allow the overall stability seen in animals. This is achieved by the ECM a highly organised network of glycoproteins, proteoglycans and glycosaminoglycans. The ECM provides physical stability while promoting cell growth, including migration, differentiation and adhesion by acting as a substrate for the cells. The composition of the ECM varies depending on the tissue, in direct governance from the surrounding cell types. While cells are responsible for the production of ECM, the interactions with ECM components and membrane receptors cause the activation and upregulation of specific cellular signalling pathways associated with controlling gene expression. Within the ECM, collagens are the main group of structural proteins. They are in fact the most abundant protein found in animals, providing between 25-35% of the whole-body protein. To date, there are 28 forms of collagen as described in Table 2.1, all of which share the characteristic triple helix structure of Gly-X-Y repeats.

Variance in the amino acid composition in collagen can be observed to have distinct influence in the host organism, for example, the amino acid repeat Gly-Gly-Y which is found in abundance in the type I collagen of rainbow trout (11% of total triple helical region for the α3 (1) chain). This is shown to loosen the helix in the trout's skin sufficiently to lower denaturation temperature by 0.5% compared with muscle collagen of the same fish (Saito et al. 2001). Furthermore, a reduction in the overall abundance of proline in position II and proline hydroxylation in position III, as can be seen in marine animals shows a reduction in denaturation temperature when compared with mammals (Nagai et al. 2000; Barzideh et al. 2014a; Nalinanon et al. 2007; Engel and Bächinger 2005). It is this reduced temperature which is a hindrance in the use of marine collagens for tissue engineering in humans. The current overall consensus suggests that the thermal stability of collagen for a given species is correlated with the surrounding environmental temperature, and body temperature (Rigby 1968). The detailed analysis of the molecular folding and nucleation steps in the formation of

collagen triple helix peptides has been examined in detail by (Xu, Bhate, and Brodsky 2002).

The origins in the use of collagen are rooted to the use of gelatine in food products. Gelatine is a denatured form of collagen which was produced and used in the late medieval period by boiling animal products, while the first patent awarded for gelatine production occurred in England in 1754 ("Gelatin" 2018). Collagen has been used for many decades in different applications within healthcare and cosmetics. The repeating pattern structure, while difficult to examine at the time, was first partially examined within the tendon of kangaroo and catgut during the 1930s using x-ray diffraction (Clark et al. 1935; Wyckoff, Corey, and Biscoe 1935). This first insight into the morphology of collagen at a molecular level led to research spanning the last nine decades. Notable developments following this research focussed mainly on describing the monomers which form collagen; the quaternary packing structure of collagen was described by the work of Ramachandran, which elucidated the triple helical packing structure of fibrillar collagens with three chains entangled. This was further described as one chain in helix form, coiling in the opposing direction to the other two (Ramachandran, Doyle, and Bloot 1968). This model was modified by groups around the world to gradually understand the complex structures which underpin collagen (Venkatraman 2017).

Other work detailing the packing structure of collagen monomers led to many misconceptions regarding how the secondary structure of collagen is described. This includes whether collagen forms microfibrils or staggered sheets (Wess et al. 1998). The microfibrillar structure of collagen within major structures including cornea and tendon have been imaged using electron microscopy (Holmes et al. 2001; Holmes and Kadler 2006; Raspanti, Ottani, and Ruggeri 1990). This has led to the accepted description of collagen packing structure as a discontinuous super twisted right handed microfibril; the subunit for tropocollagen within tissues (Petruska and Hodge 1964).

Today, collagens are used across the scientific spectrum, from life science research as a basic 3D scaffold for cell culture, work in tissue engineering advances, to composite biomaterials for structural materials research. There are several medical uses for collagen already available, as well as in the cosmetic industry, where variants of collagen are advertised for their appearance enhancing and rejuvenating effects. There has been a large debate surrounding the need for collagen to become more

versatile, unfortunately at present harsh solvents are often required for usable concentrations above 10% to be achieved (Dong et al. 2009); these solvents are shown to cause denaturation of the collagen into gelatine derivatives (Zeugolis et al. 2008a).

Table 2.1 – Collagen proteins classified by their form with additional details on proteins which are poorly classified

Type	Form	Additional Details
I, II, III, V, XI	**Fibrillar**	**Full Triple Helix Fibril Formation**
IV	**Non-Fibrillar**	**Basement Membrane Protein**
VI, VII	**Non-Fibrillar**	**Cell Anchoring Proteins**
VIII, X	**Non-Fibrillar**	**Short Chain**
IX, XII, XIV, XVI, XIX, XX, XXI, XXII	**Non-Fibrillar**	**Fibril Associated Collagens with Interrupted Triple Helices (FACIT)**
XIII, XVII, XXIII	**Non-Fibrillar**	**Membrane Associated Collagens with Interrupted Triple Helices (MACIT)**
XV	**Non-Fibrillar**	**Multiple Triple Helix Domains with Interruptions (Multiplexin)**
XVIII	**Non-Fibrillar**	**Basement Membrane – Cleaved to form Endostatin Peptide for Proteolytic Cleavage**
XXIV	**Fibrillar**	**May Regulate Type I Fibrillogenesis**
XXV	**Non-Fibrillar**	**Brain-Specific membrane bound collagen. Proteolytic processing releases CLAC which interacts with senile plaques in Alzheimer's disease**
XXVI	**Non-Fibrillar**	**May play an important role in adult reproductive organs as well as their development**
XXVII	**Non-Fibrillar**	**May play a role in calcification of cartilage and the transition of cartilage to bone**
XXVIII	**Non-Fibrillar**	**Present in neuronal cells and their surrounding basement membranes**

2.2 Extraction of Collagen

Collagen is traditionally isolated from mammalian animals using solubilisation in acetic acid. The process commonly begins with the desired tissue to be used being washed, blended and soaked in sodium hydroxide, to allow cellular matter to be disrupted. Following this, centrifugation is carried out to collect the raw acellular extract, which is then solubilised in acid to facilitate the breakage of intra-molecular bonds and partial digestion of non-helical telomeres. The solution typically then undergoes a series of centrifugation and subsequent redissolution in acid, usually with the addition of salt at various stages to precipitate out the soluble collagen, accompanied with dialysis to then remove the salts (Schmidt et al. 2016). The process typically produces a relatively pure extract of acid soluble collagen with low yield (Xiong et al. 2009). The use of pepsins to digest collagen which would traditionally be insoluble, is a modern addition to increase the yield of extractions. This allowed collagen to be extracted from sources such as cartilage. The use of pepsins causes a significant increase in the removal of the non-helical telomeric regions of collagen, which should not be disruptive to the α-helical structure of collagen (Miller 1972). The use of a base, usually sodium hydroxide was added to disrupt the cells and strips them from the collagen matrix.

These extraction processes have been adapted and modified in many ways, though yield has never been shown to rise above 2% from wet weight or 20% dry weight, and some groups have modified the technique used to determine yield, based on hydroxyproline content to demonstrate small increases in yield more dramatically (Nalinanon et al. 2007).

While a range of sources have been used for collagen extraction, it is commonly obtained from bovine, porcine and equine sources for *in vivo* use (Silvipriya et al. 2015). The risks of BSEs, TSEs and potential viral vectors that could be transmissible to humans are ever-present within mammalian extracts of collagen (Asher 1999; Lupi 2002). More recently, the use of jellyfish and other marine animals as a source of collagen has become an attractive alternative to existing sources due to a plentiful supply (Williams 2015). These present a safer source through the lack of BSE risk and potential viral vectors (Song et al. 2006) and market trends expect an increase in the

use of non-mammalian collagen in the future. The low denaturation temperatures seen with marine collagens is a major drawback for their use for *in vitro* or *in vivo* testing (Addad et al. 2011; Kittiphattanabawon et al. 2010; Bae et al. 2008; Sadowska, Kołodziejska, and Niecikowska 2003).

2.2.1 Jellyfish

Jellyfish are commonly found in coastal regions and can be found in every ocean globally. All jellyfish belong to the phylum Cnidaria, and subphylum Medusozoa. The use of jellyfish belonging to the class of Scyphozoa, also termed the 'true jellyfish' are the main interest of this work. Their development, as seen in Figure 2.1 involves a surface dwelling stage, usually in the planktonic medusa form and a bottom dwelling polyp stage, which gives rise to new medusa when conditions are optimal (Hyman 1940). The reproduction of these species usually follows that of gonochorists, namely with separate male and female sexes. They have gonads located in their stomach lining, and when produced, mature gametes are expelled through the mouth opening, which often enter their planktonic phase of development. The Scyphozoa class of true jellyfish are believed to have existed since the Cambrian Fortunian Stage (Liu et al. 2017), and many species remain extant today.

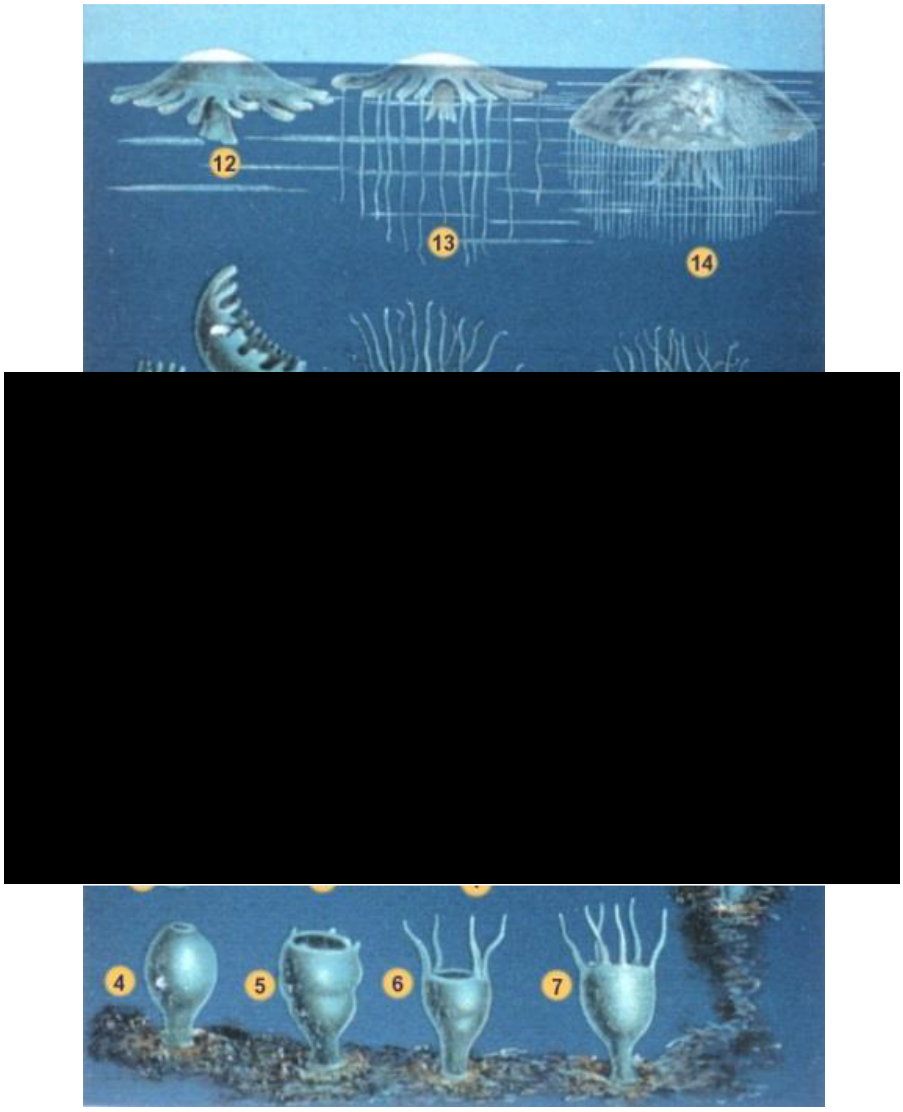

Figure 2.1 - Typical Life Cycle of the Scyphozoa class of jellyfish (Schleiden, 1869).

2.2.2 Extraction of Jellyfish Derived Collagen

The extraction of collagen from jellyfish has been carried out using traditional extraction methods, which can yield collagen which is either acid solubilised (ASC) or pepsin solubilised (PSC). These methods respectively produce ‘telo’ and ‘atelo’ collagens, named due to the amount of the telomeric domains which have been removed from the collagen chains to aid solubilisation. The use of telo and atelo collagens varies in their need, where ASC is more useful in applications which include

or require gel formation, or the reformation of collagen fibres and PSC is more useful in applications where increased solubility is desirable.

By use of Jellyfish in the extraction of collagens, it is possible to avoid overuse of animals which have other uses, for example, bovine collagen is commonly extracted from the skin of calves and adult male bulls, this skin is however also valuable in the production of leather. The avoidance of the use of mammalian species also helps to prevent the potential spread of TSEs which include BSEs in cattle, and can be present in humans, including Creutzfeldt - Jakob disease (CJD). These diseases are caused by misfolded proteins known as prions (Clarke, Jackson, and Collinge 2001), and cause neurodegeneration of the brain to give a sponge like appearance. The spread of these diseases are of concern worldwide, and in Europe the legislation surrounding TSEs is heavily regulated (Regulation (EC) 999/2001), including the testing, control and prevention of any suspected animal suspected of carrying any TSE from entering the food chain. This regulation however does not apply to any animal product which is used in cosmetic, medicinal products or medical devices, including both starting and intermediate materials and products. The reduced conditions surrounding the use of TSE animals in these fields and research, gives rise to the potential for collagen extracted from contaminated samples to be extracted, carrying with it a prion, which may be used as an injectable or in a medical device and may transmit the disease.

Once extracted, collagen can be used to form tissue scaffolds based upon various methods. Often a solution of collagen is lyophilised using freeze drying to form an open architecture-based scaffold which is ideal for cell migration. This collagen can also be integrated into a solution of HFP or 2,2,2-trifluoroethanol (TFE) on its own or as a copolymer and electrospun to form nanofibre scaffolds (Chen, Mo, and Qing 2007). In both instances the resulting scaffold must be crosslinked using various chemical (Barnes et al. 2007), enzymatic (Torres-Giner, Gimeno-Alcañiz, et al. 2009a) or photoreactive methods (Cherfan et al. 2013) due to the extraction processing of the collagen which renders the material soluble to physiological and acidic conditions. For marine collagens, there has been significant research into crosslinking these materials to improve these characteristics (Addad et al. 2011), but studies suggest that an achievable native collagen scaffold is unlikely when using marine collagens due to their inherent molecular structure (Li et al. 2013) as described above in further detail.

Regardless of source, the currently available extraction techniques do not prove suitable for industrial production, leading to the high cost of collagen to the research market at ~£1800 per gram (Sigma Aldrich, UK, 2018). The above processes also typically produce fragments of protein, which survive extraction and reduce protein purity, which is typically defined in specifications as >90% within α, β and γ regions. Further to this, the above processes do not typically deal with endotoxin content, product clarity, and their small batch sizes usually results in high batch-batch variation, which leads to an array of problems for end users, including a disparity in the gelation characteristics of the collagen.

2.2.3 Membrane Processes

Membrane processing is a diverse field which encompasses the separation of materials from one another, based on size, charge, shape or other specific qualities. Traditionally, membranes act as a barrier which allows liquid to pass as a filtrate while retaining solids. Membrane processing technologies have developed thoroughly since the first commercially viable membranes were produced in the 1950s (Loeb 1981). The field has experienced several decades of growth, and the methods of membrane filtration have expanded drastically to include several techniques and membrane modifications. Hollow fibre membrane (HFM) filtration emerged in the 1960s as a type of tangential flow filtration. HFM filters use fibres of small diameter while also increasing surface area by containing hundreds and more often thousands of individual fibres in one housing in order to facilitate the filtration of solutions that would ordinarily cake a dead-end filtration membrane.

HFM's are usually distinguished by their pore size, with microfiltration (100-5000 nm), ultrafiltration (5-50 nm), dialysis (2-5 nm) and reverse-osmosis (0.2-0.5 nm) membranes being commonly applied in applications due to their accessibility and non-fouling nature (Sakai 1994). These membranes have applications in medical, pharmaceutical, food, and water treatment industries. Medical applications include haemodialysis (2-5 nm) and extracorporeal membrane oxygenation (artificial lung, 5-8 nm) (Reed 2016), as well as supplementary applications such as protein separations

(<1,000 - >100,000 NMWCO), bacterial sterilisation (0.2-0.45 µm) and virus removal (5–50 nm) (Duek et al. 2012). Focusing on protein extractions, TFF based systems for separating proteins has been described previously in regards to whey protein (Zydney 1998) among others (Li and Chase 2010). Collagen had not been successfully applied using these techniques, due mainly to the unsuitability of starting materials such as bovine hide to being processed in this way, particularly in regards of hollow fibres, where any solid material is capable of blocking fibres and reducing efficacy. Flat sheet TFF has been used previously with specially produced membranes to purify and concentrate collagen peptides of 30-50kDa (Shen et al. 2009), demonstrating the possibility for TFF processes to be applied to full chain collagen extraction procedures. Research is slowly emerging in the use of membranes for collagen purification, with a proceedings paper on the use of spiral wound membranes for collagen fraction separation (Catalina et al. 2009), as well as collagen type I used to test membrane retention (Aspelund and Glatz 2010). Patents surrounding the use of ultrafiltration technologies in the concentration of collagen are being published, revealing the novelty of this technology for the application to collagen extraction (Chang et al. 2017).

2.3 Collagen Nanofibers and Wound Healing

Following injury of the skin, the natural processes of wound healing begin to repair the skin, beginning with the formation of blood clots. These clots become a scab at the surface, sealing the wound; fibroblasts migrate into the lower regions of the blood clot from the edges of the surrounding tissue. The fibroblasts begin breaking down the clot and replacing it with scar tissue formed of collagen fibres (Clark 1996; Clark 2012). The deposited collagen differs from healthy tissue by its alignment structure; where normal skin typically contains a ‘basket weave’ fibre structure, the scar tissue develops single directional aligned fibres of collagen as remodelling occurs by continual interaction with fibroblasts (Dallon 1998; Dallon, Sherratt, and Maini- 1999; Dallon and Sherratt 2000).

Collagen fibres are deposited and arranged in linear format during wound closure, and this causes a weakening of the tissue once restored, referred to as scarring, the

degree of scar severity is dependent on a wide array of factors, including age (Ashcroft, Horan, and Ferguson 1998), skin colour (Murray, Pollack, and Pinnell 1981), and location (Bayat, McGrouther, and Ferguson 2003). This scarring occurs due to the repair, or incomplete regeneration of the tissue (Min, Wang, and Orr 2006b), rather than the regeneration seen in non-injured skin which acts as an exact copy of morphology and functionality (Min, Wang, and Orr 2006a).

Collagen plays a role in aiding regeneration at all stages of wound healing during the repair and regeneration of the tissues (Brett 2008). Thus, the extraction and fabrication of collagen fibres through processes such as electrospinning has great potential in terms of bioactivity and control. Indeed, the ultimate wound dressing or tissue engineering device must be a highly accurate analogue of the natural tissue and the ECM. Modern techniques are striving to achieve this through improved fabrication of 3D fibrous materials in parallel with stem cell research. The efficient electrospinning of collagen, maintaining its integrity and functionality, is arguably the optimum technique and choice of polymer for achieving this; other polymers do not currently have the innate functionality and biocompatibility.

Collagen has been shown to be an essential part of wound regeneration, beginning when platelets aggregate around exposed collagen as part of the body's own process for physically blocking the wound and ceasing blood flow. During the inflammation phase, the peptide fragments of collagen have a chemotactic effect in the recruitment of cells essential to wound healing, while the collagen derived peptides stimulate fibroblast proliferation during the proliferation phase (Schultz and Mast 1999; Brett 2008). Collagen has also been shown to aid in vessel reformation with endothelial cells (Montesano, Orci, and Vassalli 1983).

When migrating cells such as keratinocytes encounter type 1 collagen in a wound, the cells secrete matrix metalloproteinases (MMPs) which denature the collagen to gelatine in order to expose the active RGD site (Arg-Gly-Asp) sequences, which are responsible for the creation of granulation tissue (Brett 2008). Previous research has also shown that when the collagen triple helix is unwound through partial denaturation, elements of the molecule are exposed that up regulate many pathways important in wound healing (Banerjee, Suguna, and Shanthi 2015; Castillo-Briceño Patricia et al. 2011).

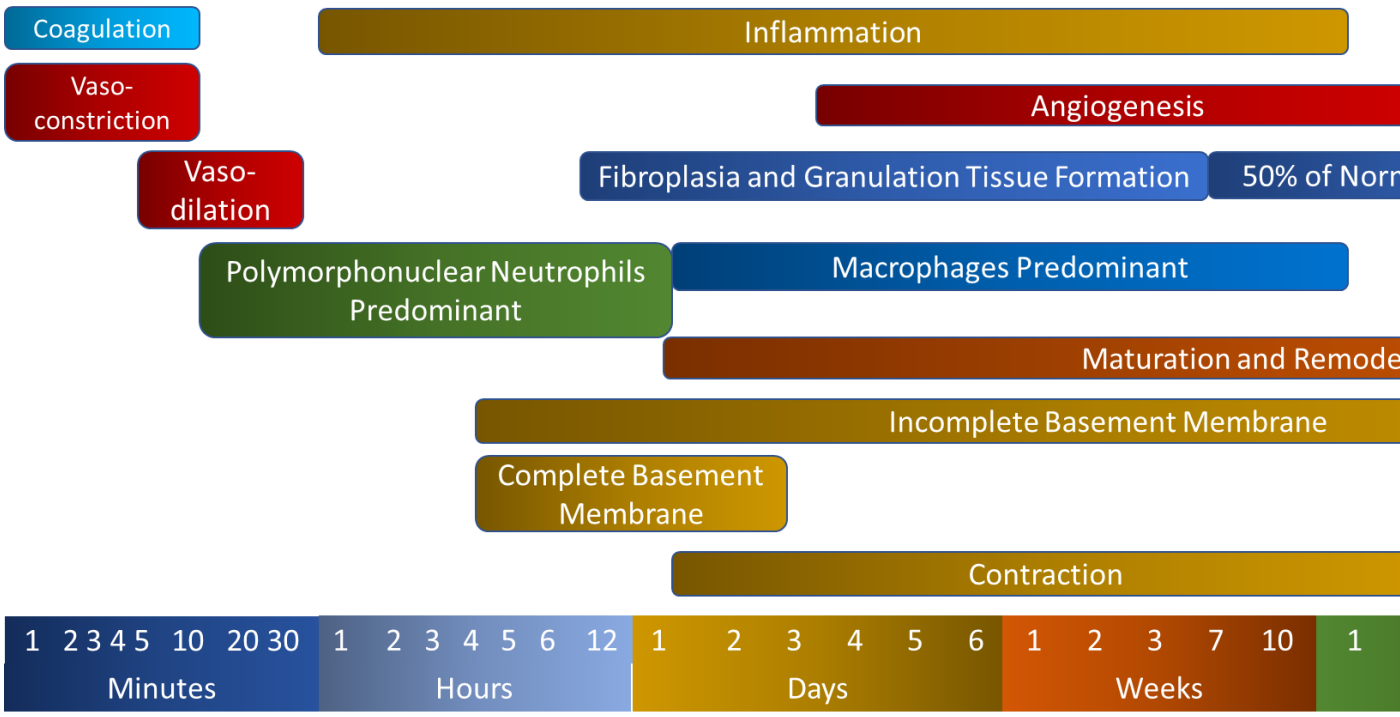

Figure 2.2 Wound regeneration timeline based on (Häggström 2014).

Despite this, collagen accumulation does not occur until the third day of wound healing, during the as termed ‘late phase’ (Clark 1998). Collagen is an essential part of the later stages of wound healing, where the collagen matrix is compacted by fibroblasts using their actin-rich microfilament structures (Ehrlich & Moyer 2013). Collagen in combination with the α1β1 integrin aids the proliferation of fibroblasts (Pozzi et al. 1998), which is a vital process to restore the structure of the extra cellular matrix in a wound.

The maturation phase of tissue repair begins when levels of collagen production and degradation equalise (Greenhalgh 1998). Throughout maturation, type III collagen, produced during proliferation, is replaced by type I collagen (Dealey 1999). The timeline for these events are seen in Figure 2.2

2.4 Fabrication methods

There is an array of fabrication methods which can be used to produce functional biomaterial-based scaffolds suitable for regenerative medicine. Bioprinting is quickly becoming a favoured method for the fabrication of complex 3-dimensional structures, while traditional freeze-drying techniques facilitate the formation of open pore structures for cell migration.

Electrospinning has for many years offered the simplest solution for creating nanofibre materials from biological polymers. Many variations on electrospinning have been developed, covering scale up, fibre alignment and many other modifications to improve the efficacy of the scaffold to a given niche.

2.4.1 Bioprinting

The act of bioprinting combines biomaterials, cells and often growth factors to produce three-dimensional structures which attempt to mimic natural biological structures (Singh and Thomas 2018). In line with polymer 3D printing technologies, layer-by-layer deposition is the currently favoured method in scaffold production, using bioinks as the printing material. The process typically deposits a layer of bioink into a bath or slurry of supporting material which allows complex structures to be

created, with the slurry being melted or dissolved away after printing is complete, and the term bio-paper is quickly becoming the favoured term (Lee et al. 2012; Manappallil 2018). Bioprinting is progressing to produce scaffolds which can be implanted and integrate within the body, whether cartilage, ligaments or more complex structures. Recent work is progressing to further expand the possibilities of the 3D bioprinting of human organs (Liu et al. 2018).

Post bioprinting process developments surround the use of bioreactors with specialised conditions to mimic the natural environment of the printed tissue, including compression for cartilage scaffolds (Chua and Yeong 2015).

The main issues arising from bioprinting are currently the high cost of machinery, unreliability of the printing process, ethical restraints and the lack of crucial elements within a complex tissue, such as vascularisation, which makes maintenance of the large numbers of cells required difficult, often leading to cell death within the central depths of the tissue. The other issue currently affecting these methods is resolution, where many standard bioprinters, or modified polymer printers are unable to recreate the level of detail needed to sufficiently replicate complex tissue structure (Malkoc 2018).

2.4.2 Freeze Drying

Freeze drying a solution of collagen is one of the simplest formulation methods for producing a three-dimensional architecture for cellular scaffolds. The collagen lyophilised using freeze drying to form an open architecture-based scaffold which is ideal for cell migration (Gaspar et al. 2011). The solution is typically frozen at a controlled rate to guide crystal ice dimensions which later dictate pore diameter, while the frozen scaffolds are then sublimated to leave behind a sheet like sponge of collagen, suitable for seeding with cells. The use of this technology lends itself to the creation of moulds in which the collagen can be dried, giving a shape which is desirable to a given application, for example cartilage within the ear and nose. The problem with such a simple technique is the ineffectiveness of the process to create multifactorial scaffolds, which are essential in the creation of complex tissues and

organs, while freeze-dried sponges are most commonly the same density with the same porosity throughout the entirety of the scaffold.

2.5 Electrospinning of Collagen Nanofiber Membranes

Electrospinning of soluble collagens provides a suitable way of producing scaffolds which closely mimic the high porosity and surface area often seen in the ECM of tissues, and thus presents great potential in the fabrication of 3D constructs for tissue engineering and wound healing.

Electrospinning was developed in the first half of the 20th century (Formhals 1934), and further investigated with added detail (Reneker and Chun 1996; Reneker et al. 2000); though the origins of the process were initially explored by (Boys 1887), and arguably by (Gilbert 1628), where electro-spraying occurred through the addition of electrically charged amber near water. Patents related to collagen electrospinning were first filed in the late 1990s (Simpson et al. 2003), with journal articles in the early 2000s describing the use of HFP to electrospin collagen (Matthews et al. 2002).

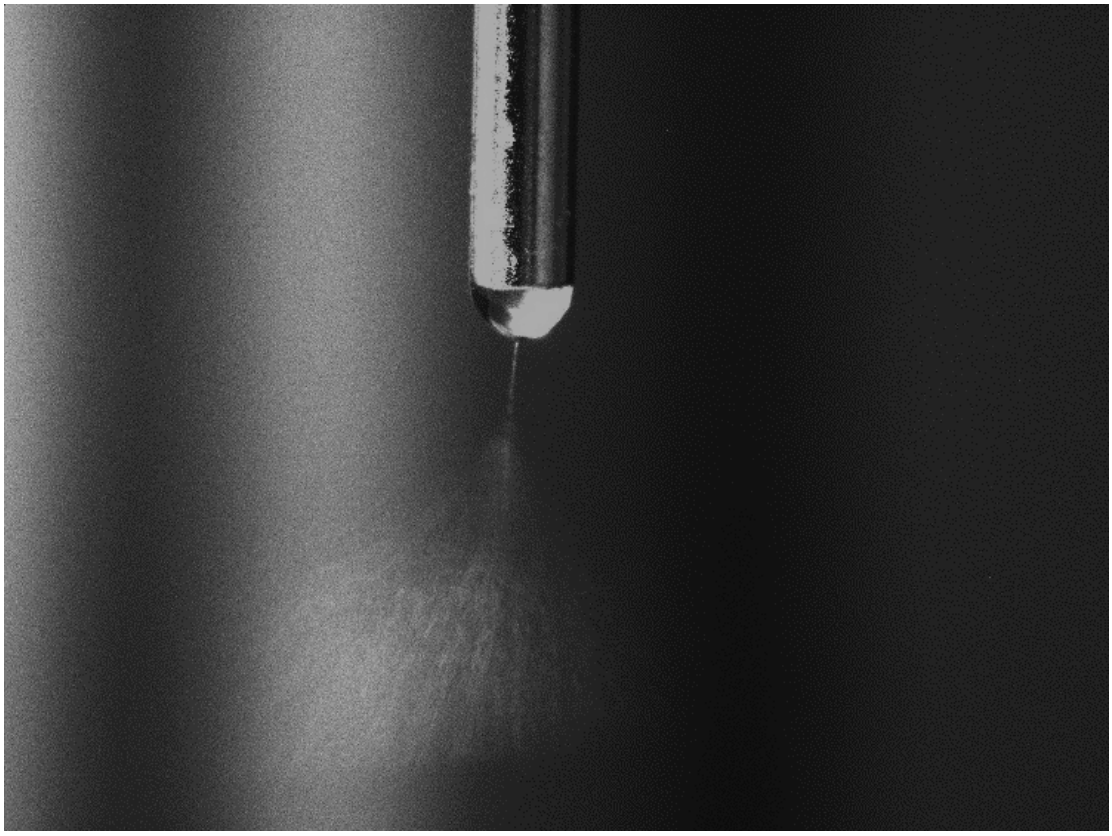

Figure 2.3 - Collagen solution being electrospun with constant droplet being replenished and a single Taylor cone producing a jet of collagen solution which lands on the grounding target as collagen nanofibres.

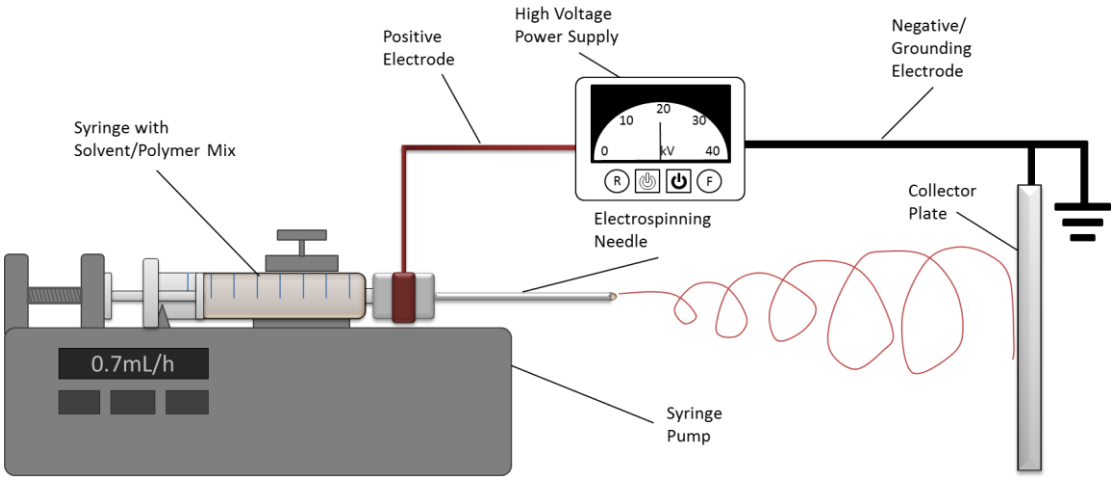

Figure 2.4 - A basic electrospinning set up using a syringe pump and high voltage power supply connected with a grounded collector plate.

The process of needle electrospinning produces a jet from a Taylor cone as seen in Figure 2.3 and involves a simple process detailed in Figure 2.4, which briefly consists of a high voltage power supply that supplies positive charge to an electrospinning needle and a grounding electrode coupled to the collector plate. The electrospinning needle is supplied by a syringe loaded with polymer and solvent which is fed at a controlled rate using a syringe pump. Electrospinning setups can be either horizontal or vertical depending on solution properties such as low viscosity liquids using gravity to prevent spraying of material onto the mat.

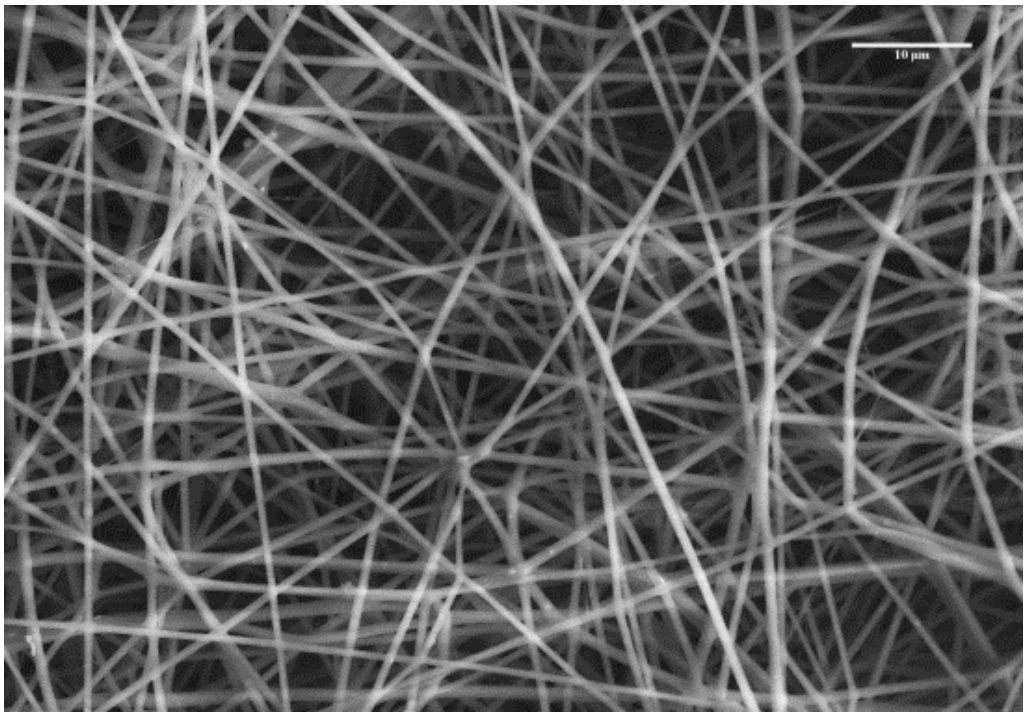

Figure 2.5 - SEM Micrograph of needle electrospun collagen fibres. Magnification of 1500X. Fibre Diameter is shown to be 646nm ± 121nm. Scale Bar = 10µm.

The optimised conditions for collagen electrospinning are dependent on the quality of collagen, as described later in this chapter as well as being down to individual electrospinning setups in different research groups. The most commonly used solvent, HFP is generally optimum for dissolving an 8% (w/v) concentration of collagen, though this has been as high as 20% (Li et al. 2015). A distance in the range of 8-20cm and voltage of 15-25kV is commonly used, while flow rate varies widely between

groups, but usually hovers around 1mL/h (Matthews et al. 2002; Rho et al. 2006; Zhou et al. 2016). Most groups have carried out electrospinning on bench scale standard setups as shown in Figure 2.4, with the replacement of the static grounding target with a rotating mandrel collector in some articles (Dong et al. 2009; Zhong et al. 2006) or other designs to collect the fibres (Buttafoco et al. 2006). Once produced, the scaffolds are examined by SEM as in Figure 2.5 in order to assess fibre diameter, porosity and beading density.

The applications of collagen electrospun mats utilise the native functionality of collagen as part of the ECM, namely adherence, migration, proliferation and differentiation of cells alongside the establishment of morphological structure that allows the supply of nutrients, the diffusion of gases and the removal of metabolites to aid cell growth and tissue maintenance. For example, when tissues are damaged, as in the case of burn victims, the cellular re-growth cannot effectively occur due to the absence of material, which can result in the formation of scar tissue or open wounds. The application of a collagen scaffold to the wound has the potential to promote re-growth of healthy tissue and prevent scar tissue formation. The addition of cells to the scaffold can provide a graft of tissue such as skin, or using chondrogenic cell types, cartilage can be produced. With the parameters of the scaffold changed to produce tightly aligned fibres, osteoblasts can help to promote calcification leading to bone growth. Collagen nanofibrous membranes are currently utilised in the areas shown in Table 2.2.

Table 2.2 – Example fields and uses for collagen electrospun nanofibre membranes

FIELD	USE	EXAMPLES
TISSUE ENGINEERING	Artificial Skin, Blood Vessels, Tendon	(Law et al. 2017; He et al. 2005; Chainani et al. 2013)
REGENERATIVE MEDICINE	Bio-resorbable Grafts	(Sell et al. 2009)
WOUND DRESSINGS	Bio-active Bandage	(Zahedi et al. 2010)
DRUG DELIVERY	Controlled Release	(Hall Barrientos et al. 2017)
3D CELL CULTURE	Model Skin	(Nisbet et al. 2009)
DRUG SCREENING / TRIALS	Model System	(Hartman et al. 2009)

The most researched of these areas are the use of collagen nanofibres for wound dressings and tissue engineering. These topics have garnered much attention, particularly over the past decade, and many reviews have been produced to examine them (Ma et al. 2005; Pham, Sharma, and Mikos 2006; Vasita and Katti 2006; Lu and Guo 2018; Mortimer, Widdowson, and Wright 2018). Despite the apparent interest in collagen as an effective biomaterial, there are large issues which currently surround its use in regenerative medicine, focused mainly on the use of current fluoroalcohols and their denaturing effects on collagen and other proteins when used for electrospinning, but also on the need to crosslink the electrospun scaffolds and the effects of the use of some of these agents, particularly glutaraldehyde.

2.5.1 The Nativity of Electrospun Collagen Nanofiber Membranes

There is an ongoing debate on the use of collagen in the field of electrospinning, particularly around the potential denaturation of the protein during this process, possibly resulting in the denatured form of collagen, known as gelatin. The effect of such a finding would result in a reduced similarity to the natural ECM, in which collagen is a major constituent. This would make electrospun collagen a less appealing prospect to those trying to create an analogous *in vitro* version of the ECM for cell-based applications.

One major paper on the topic (Zeugolis et al. 2008a), utilises an array of techniques to visualise the presence or absence of the native collagen α-helical structure, which can be identified by the presence of the 67nm banding pattern, as well as using the furrier transforming infa-red spectroscopy (FTIR) footprint of collagen when compared to a gelatin standard. The group attempt to answer the question of whether the electrospinning process denatures the protein, removing their ability to form the triple helical arrangement which results in the quarter staggered banding pattern seen in native collagen, also known as the D-banding pattern. To this end, the group uses HFP, and TFE as solvents to dissolve the collagen; These were the commonly used solvents for the electrospinning of collagen and remain the favoured choice at the time of writing. The re-dissolved fibres were analysed using a variety of techniques including transmission electron microscopy (TEM) and circular dichroism (CD) to detect the presence of the α-chain structures present in native collagen. Their findings suggest initially that the electrospun fibres are denatured, where 99.5% of collagen is converted to gelatin. It should be noted that denaturation of collagens which have been dissolved in fluorinated alcohols (HFP or TFE) without electrospinning taking place remains high (93%), suggesting that it is the reaction with these solvents which have caused denaturation to occur before electrospinning has taken place, and as such it is impossible to tell from the findings whether the electrospinning of these fibres causes any significant further denaturation. It would have been useful as a further experiment of this study to carry out their self-assembly testing on dissolved samples of electrospun collagen to give an indication if renaturation of the collagen fibres is possible following fluoroalcohol based electrospinning.

In 2008, the aforementioned solvents were the only solvents found to be viable for electrospinning collagen, due to the lack of quality assurance, with some collagens being less soluble in acetic acid than others (Zeugolis et al. 2008b). In the following year, Dong et al published research using a benign solvent mixture of phosphate buffered saline (PBS) and ethanol to dissolve and electrospin their collagen. The paper suggests the mixture allows for the electrospinning of collagen without denaturation prior to electrospinning as seen with HFP and TFE (Dong et al. 2009). This is backed up using FTIR data to compare the electrospun scaffolds to native collagen. This group however failed to investigate the presence or absence of banding present in the collagen fibres produced, and their findings of water-soluble collagen both before and

post electrospinning provide little reassurance, as collagen should remain relatively insoluble in water, but rather unable to hold form when moistened.

Other groups have since attempted different solvent systems to replace fluoroalcohols in the electrospinning of collagen, such as Liu et al, who use 40% acetic acid to electrospin a 25% collagen solution and examine the degree of degradation compared to HFP using CD (Liu et al. 2010). The group found a helical fraction of 28.89% for acetic acid and 12.51% for HFP but failed to further examine other qualities such as presence of periodic D-banding or FTIR amide 1-2 peak ratios. Barrientos et al produced co-electrospun nanofibres of PEO and collagen blends with a 1% collagen in an 8% total polymer concentration in HFP which when examined with atomic force microscopy (AFM) clearly displayed the periodic D-banding pattern of collagen within the fibres (Hall Barrientos et al. 2017). DSC measurements are not sufficiently clear due to PEO being included as a copolymer. No further examination of the fibres displayed data to suggest denaturation of the collagen had significantly occurred or been prevented, despite acknowledgement from the group that HFP is known to denature collagen.

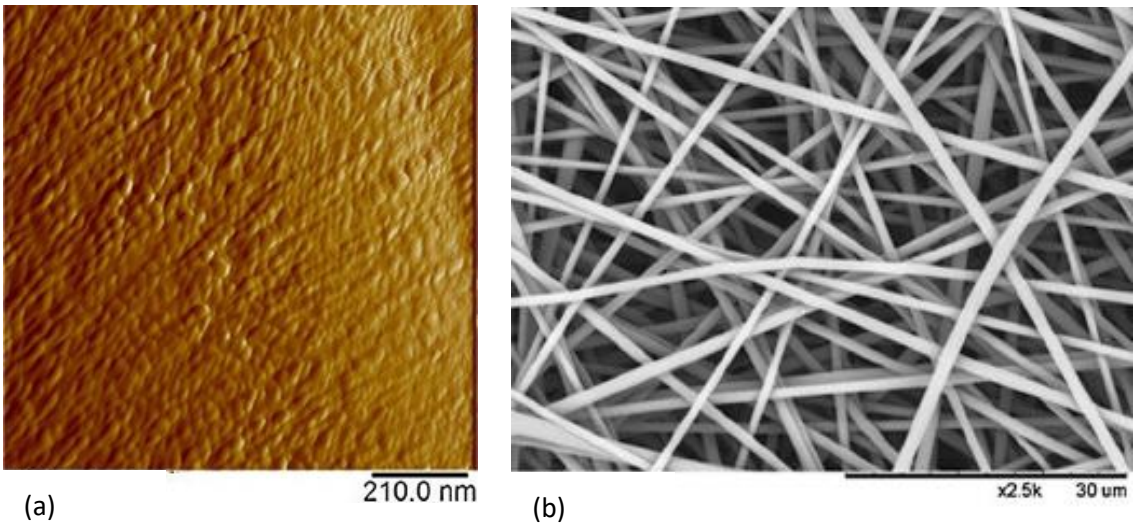

Figure 2.6 – (a) AFM image of a PLA-Collagen electrospun fibre displaying periodic D-banding pattern typical of collagen. (b) SEM image of PLA-Collagen electrospun fibres. Modified to renumber from (Hall Barrientos et al. 2017) Distributed under ("Creative Commons — Attribution 4.0 International" 2018)

In order to fully assess the true nature of collagen post electrospinning, the collagen must be extensively tested using several parameters. There is little literature into electrospinning of collagen nanofibers dissolved in a benign solvent which would not significantly alter the ability of collagen to form its native triple helical structure and this will require thorough experimentation to be carried out. The parameters to effectively determine the retention of the collagen's native structure include those tested by (Dong et al. 2009; Zeugolis et al. 2008a); namely to include TEM analysis, SEM analysis, CD, FTIR and finally differential scanning calorimetry (DSC) experimentation. Together, these techniques can show the definitive presence of collagen or gelatin in the product, by examining the α-helix formation and assess any changes in denaturation temperature.

There are, however, disparities in the argument proposed by Zeugolis *et al.*, in particular when groups have observed the characteristic 67nm banding pattern (which is typically only seen in native collagen fibres) on electrospun collagen fibres. Groups such as (Matthews et al. 2002) have shown this to be present in collagen electrospun fibres produced using HFP as the solvent system as seen in Figure 2.7.

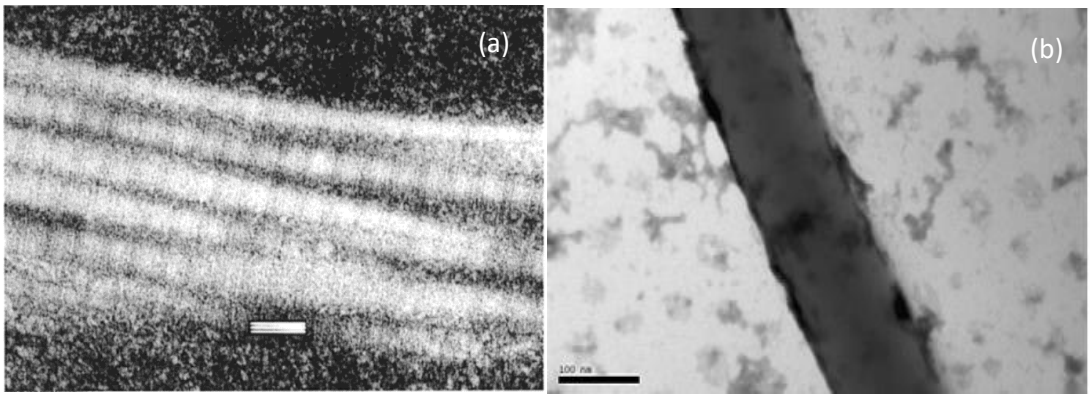

Figure 2.7 – Comparison of TEM images of electrospun collagen fibres from: (a) Electrospun calfskin collagen displaying 67nm banding pattern within fibre. (Scale bar = 100nm). Reprinted with permission from (Matthews et al. 2002). Copyright 2002 American Chemical Society. (b) Electrospun collagen produced in house which has no banding present (Scale Bar = 100nm). Reprinted with permission from (Zeugolis et al. 2008a). *Copyright 2008 Elsevier.*

The main issue is the lack of complete transparency present in research findings, particularly when techniques that examine only small areas of a sample are used such as TEM. This can lead to picking of particular features present in a sample where it represents a minority; Zeugolis did after all show a 99.5% denaturation, meaning 0.5% of triple helix could be present. Therefore, more research is required to determine the exact reasons that collagen may be denatured when being electrospun and exactly how much is caused by each influencing factor of the process.

As well as the use of solvent being of concern, the quality of the extract of collagen being used also affects how well the solution can be electrospun (Zeugolis et al. 2008a). This relates to many factors from extraction conditions with critical points which must be addressed. Figure 2.8 shows how a number of extraction conditions can influence collagen production.

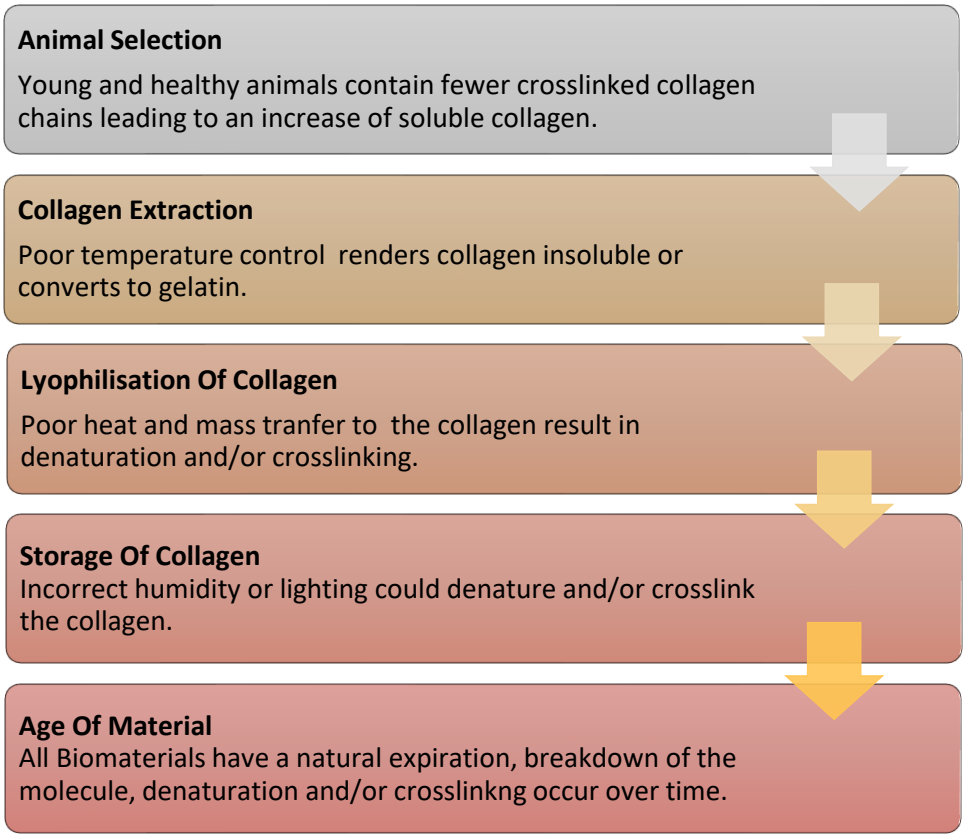

Figure 2.8 - Chart of extraction stages which contain critical points necessary to avoid solubility issues with collagen extracts Adapted with permission from (Zeugolis et al., 2008b). Copyright 2008 Taylor & Francis.

It is because of these issues that collagen has remained an undesirable polymer for electrospinning and some research has moved onto gelatin electrospinning (Sajkiewicz and Kołbuk 2014). This denatured form of collagen is a much more affordable alternative to collagen which is much more easily handled using benign solvents such as acetic acid and phosphate buffered saline.

Research on the electrospinning of native collagen has stalled in recent years, due to the condemning findings of the Zeugolis group, and papers published in the post 2008 years have either proceeded in the use of fluoroalcohols, knowing their denaturing effects (Torres-Giner, et al. 2009b; Chen et al. 2010), or attempted solvent systems which reduce the denaturing aspects of the process (Wakuda et al. 2018; Jiang et al. 2013; Dong et al. 2009). This has diverted attention away from applied scaffolds produced by electrospinning collagen and stunted progression in the fields of tissue engineering and regenerative medicine.

2.5.2 Disparities in the Extraction and Electrospinning of Collagen

The use of marine collagen has seen a significant increase in recent years, with fish scales and jellyfish extractions and applications being described by several authors. There are several statements in the production of these materials which display conflicting factors, affecting the outcomes of claims made by the various authors, with confusion and disparity arising mainly due to the originating use of collagen-based products in the history of geographically isolated cultures. Western cultures have used animal derivatives such as collagen for centuries in the production of products such as stock and glue. These processes have historically centred on the use of boiled animal parts which are not useful in other applications (meat, hide etc.). The use of these techniques meant that gelatin was commonly used in western cultures as far back as the 1400s (“Gelatin” 2018). In eastern cultures, particularly West Asia and India, where fish, rice and other staple diets, as well as a lower reliance on livestock farming for religious and geographical reasons meant that the use of cattle was less common. This led to a limited use of meat-based stocks and broths, so the distinction between gelatin and native collagen were less separated, leading to confusion in the distinguishing features between denatured and native versions of the

protein. The terms ‘hydrolysed collagen’ or ‘denatured whole chain collagen’ are commonly used in these areas, which further distort the distinguishing characteristics of collagen and gelatin.

This lack of clarity has led to the disparities seen in current literature surrounding collagen, with both extraction and electrospinning claims being incorrectly stated, either by use of hydrolysed collagen, or a denaturation of native collagen into gelatin (Le Corre-Bordes, Hofman, and Hall 2018). This has further led to a confusion within the field as to certain results around solvent systems and conditions used in the electrospinning of these biomaterials. It is hypothesised that the disparity between marine and mammalian extracts of collagen and their ability to electrospin is due to poor handling of raw materials and use, supported by matching electrospinning conditions for gelatin experiments (Erencia et al. 2014).The work carried out within this thesis, will demonstrate the effects of handling techniques that denature the collagen, permitting electrospinning under the conditions used for gelatin.

2.5.3 Crosslinking of Electrospun Collagen Nanofiber Membranes

For physiologically soluble polymers it is usually required that the scaffold is crosslinked. Glutaraldehyde has for many years been regarded as the standard method of crosslinking (Niu et al. 2013), particularly with proteins due to its efficiency and high degree of crosslinking across different polymers (Barbosa et al. 2014). This chemical has many setbacks with regard to tissue engineering scaffolds, foremost the calcification of scaffolds and surrounding tissues which are exposed to residual crosslinking agent which may lead to device failure (Golomb et al. 1987). In recent years, alternatives to glutaraldehyde have arisen with the desire to increase cytocompatibility *in vivo,* examples of these can be seen in Table 2.3.

Table 2.3 - Examples of crosslinking agents used for physiologically soluble polymers in electrospinning applications to increase cytocompatibility in comparison with glutaraldehyde and their corresponding polymers.

Crosslinking Agent	Example Polymers for Use	Type
1-ethyl-3-(3-dimethylaminopropyl) carbodiimide hydrochloride (EDC)	Any Protein	Chemical
Genipin	Any Protein	Chemical
Rose Bengal & 532nm excitation	Collagen	Photochemical
Citric Acid	Zein, Collagen	Chemical
Thermal cycling induced crystallisation	PVA	Thermal
Lysyl Oxidase	Collagen	Native Enzymatic

Niu *et al.* compared PCL/Collagen scaffolds which were crosslinked with either glutaraldehyde vapour or genipin and examined their efficacy with cell infiltration, survival and proliferation (Niu et al., 2013). They found that nanofibre based scaffolds increased cell proliferation while microfibre scaffolds showed better infiltration of cells. They also showed that genipin showed higher levels of cytocompatibility than scaffolds crosslinked with glutaraldehyde. The increased use of less cytotoxic crosslinking agents shows a shift in the field away from the use of compounds that undo the beneficial effects of electrospun scaffolds.

EDC has arisen as the favoured crosslinking agent for electrospun collagen scaffolds but is not itself without issues. First described in relation to electrospun collagen by Barnes *et al.* in 2007, the technique uses EDC alone or in combination with N-hydroxysuccinimide (NHS) (Barnes et al. 2007). The group showed that the crosslinker was successfully able to create an insoluble electrospun collagen scaffold by linking the carboxylic functional groups of aspartic and glutamic amino acids to form O-isoacylurea, which then undergoes nucleophilic attack by the amine functional

groups of lysine and hydroxylysine amino acids on adjacent collagen fibrils, creating an iso-peptide bond. The group found that when EDC crosslinking is used, the fibrous structure of collagen is lost as seen in Figure 2.9. This has been observed by other groups (Dong et al. 2009) and techniques such as those seen in Figure 2.10, which stretch or compress the scaffold have successfully prevented the loss of fibres in the scaffolds.

Work carried out in house by our research group have utilised a method which injects EDC over collagen samples which are being compressed by a frame, reducing the potential points which can shrink and lose its fibrous state, as can be observed in Figure 2.10, the inserts demonstrate crosslinked collagen fibres produced in house, crosslinked with EDC using method b.

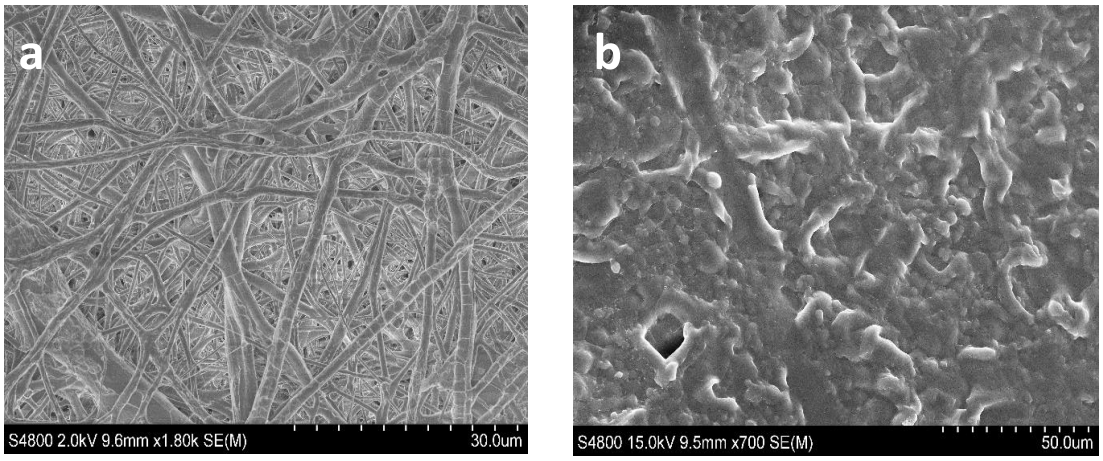

Figure 2.9 – SEM images of electrospun collagen fibres (a) before EDC crosslinking (b) after EDC crosslinking. Scale Bars = (a) 30µm (b) 50µm.

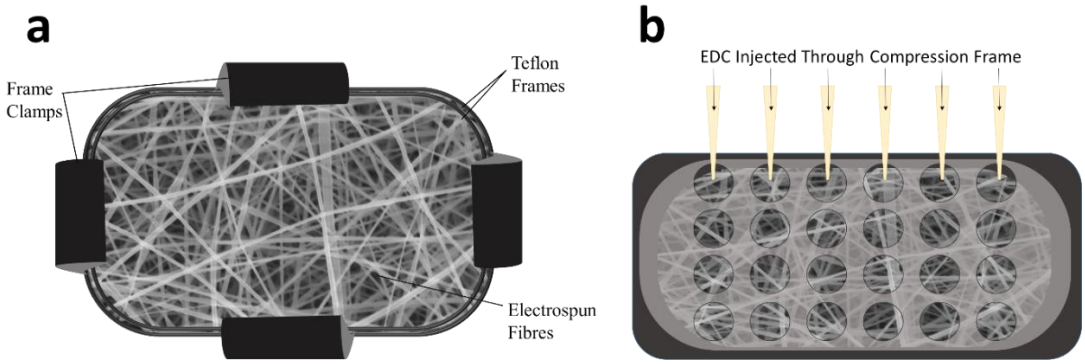

Figure 2.10 – Different compression methods for preventing the loss of fibres seen when electrospun collagen scaffolds are crosslinked with EDC. (a) Teflon frame method used by (Dong et al. 2009). (b) Compression frame with EDC injection ports used in house.

Liu *et al*, used rose bengal as a photo-initiator for 532nm excitation with an argon laser, showing scaffold integrity after 21 days, with a scaffold weight loss of 47.7% on day 7 and 68.9% on day 15 (Liu et al. 2010). The scaffolds retained their nanofibre structure, despite the weight loss, with apparent reduction in fibre diameters. The group note however, that in order for the crosslinking to occur, the rose bengal treated scaffolds need to be immersed in either water or ethanol prior to laser excitation, the former of which would immediately degrade the scaffold, the latter of which can remain and if not removed may be cytotoxic to cells (Widdowson et al. 2017).

Enzymatic crosslinking may offer a biologically acceptable method to stabilise electrospun collagen chains, and the use of transglutaminase (TG) for this purpose has been examined (Torres-Giner, Gimeno-Alcañiz, et al. 2009a). TG acts to catalyse the formation of amide crosslinks between glutamine and lysine residues (O Halloran et al. 2006). This has been shown to be non-cytotoxic and can be used on scaffolds which are seeded with cells. The technique has the downside that the increase in mechanical integrity is low, reducing its effectiveness (Halloran et al. 2008; Orban et al. 2004).

Lysyl oxidase (LO) is an alternative to TG which can be used for the enzymatic crosslinking of electrospun collagen (Hapach et al. 2015). LO facilitates the formation of intra- and inter-molecular covalent crosslinks between collagen fibres, which are essential for collagen fibril formation (Prockop et al. 1979). This is hindered by the limited access to isolated LO for use in a crosslinking solution, with many studies

using transfection (Lau, Gobin, and West 2006) or hypoxia induction (Makris et al. 2014) in cells to produce endogenous LO instead. This would not suit the application for electrospun collagen sufficiently due to the immediate dissolution of collagen in the culture medium.

Physical methods have also been examined for the crosslinking of electrospun collagen scaffolds. Drexler and Powell assessed the well documented process of dehydrothermal (DHT) crosslinking for its effectiveness when applied to electrospun collagen scaffolds (Drexler and Powell 2011). The group found potential for its effectiveness, with degradation by collagenase being significantly lower than the uncrosslinked control samples, and almost equal to EDC crosslinked samples. The DHT scaffolds were not as resistant as DHT & EDC samples and displayed a lower increase in strength than with EDC or DHT & EDC combined. Finally, the group found significantly lower fibroblast cell viability than the EDC crosslinked scaffolds when assessed by a metabolic activity (MTT) assay. The results suggest that the use of DTT may allow for the reduced use of chemical crosslinkers, for applications where accelerated cell regeneration is less important, such as dressings and intubations.

There is a positive move away from the use of glutaraldehyde for crosslinking of electrospun collagen scaffolds, and a growing selection of alternative crosslinkers is becoming apparent through the literature, which have lower cytotoxic effects than glutaraldehyde, benefitting the surrounding tissues upon implantation. The issue still remains that collagen requires crosslinking after electrospinning in order to prevent solubilisation and this issue needs to be addressed as the currently accepted hypothesis is that this is due to the denaturation of the collagen which has been electrospun (Torres-Giner, et al. 2009b).

2.6 Modification of Electrospun Collagen Nanofiber Membranes for Different Tissues

One of the largest challenges with electrospun scaffolds is not simply the degree of porosity, which is usually in the region of 91.6% (Li et al. 2002), but how accessible the pores are for cell infiltration. Wang *et al*. propose the use of the Darcy permeability coefficients to determine how cells will respond to surfaces and the architecture of

tissue engineering scaffolds through their porosity (Wang et al. 2010). They also describe 3 types of pore shown in Figure 2.11; a blind end pore leads to a section of scaffold where material cannot infiltrate further. A closed pore is isolated inside the scaffold and is therefore inaccessible to cells. The desirable architecture is an open pore network where the pores branch between each other and allow cell migration to occur. Blind end pores are often found in electrospun scaffolds which can be seen as cells becoming confluent on the outside of the scaffold without sufficient inward infiltration, as seen in Figure 2.12.

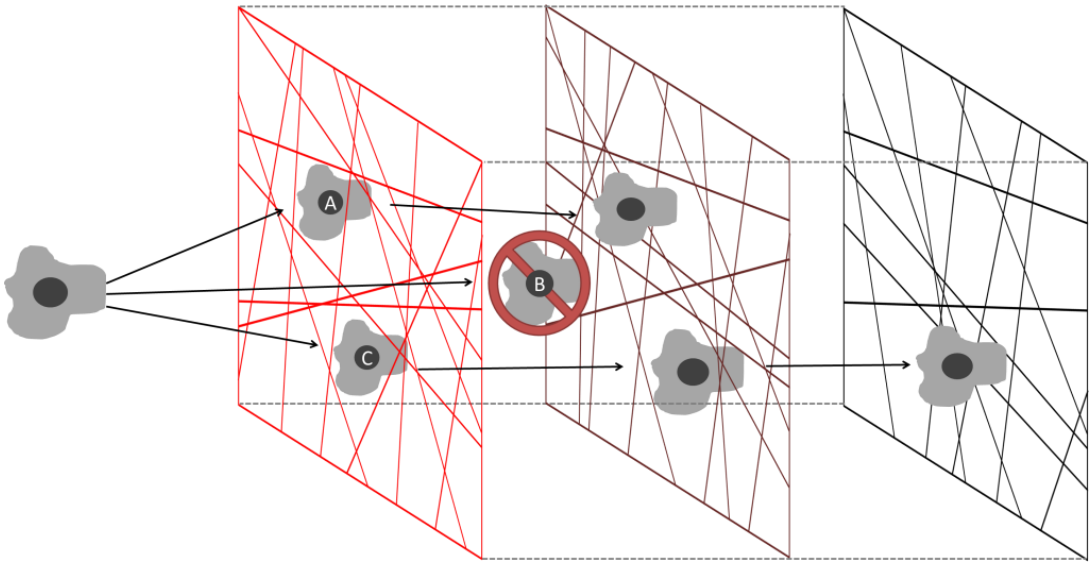

Figure 2.11 - Cell migration is influenced by 3 types of pore: A: Blind end pore where cells cannot completely infiltrate. B: A closed pore inside the scaffold cannot be accessed by cells. C: Open pore network allowing complete cellular infiltration. Reprinted from (Mortimer, Widdowson, and Wright 2018). Distributed from ("Creative Commons — Attribution 3.0 International" 2018)

Li *et al.* assessed the state of nanofibrous scaffolds for tissue engineering, with great focus on the technology of electrospinning (Li, Shanti, & Tuan, 2006). This review looked into the ideal characteristics for a tissue engineered scaffold, and the questions which should be answered for a particular niche. These begin with architecture; whether the fibres are of aligned or random orientation. The porosity of a scaffold must allow for cell migration and nutrient diffusion. If a scaffold is to recreate blood vessels, it is essential that the red blood cells are contained. This is one

of the potential limitations of an electrospun scaffold, as pore size cannot be easily controlled during production. To avoid this, various methods such as salt leaching have been employed to increase and control pore size (Lee et al. 2005).

The mechanical properties of a scaffold must also be assessed to match the niche it will be integrated into as these can have drastic effects on cell morphology, cell proliferation and differentiation (Hubbell 1995). Chang & Wang reviewed how scaffold topography and chemistry influence cell growth on a given scaffold in a given niche (Chang and Wang 2011).

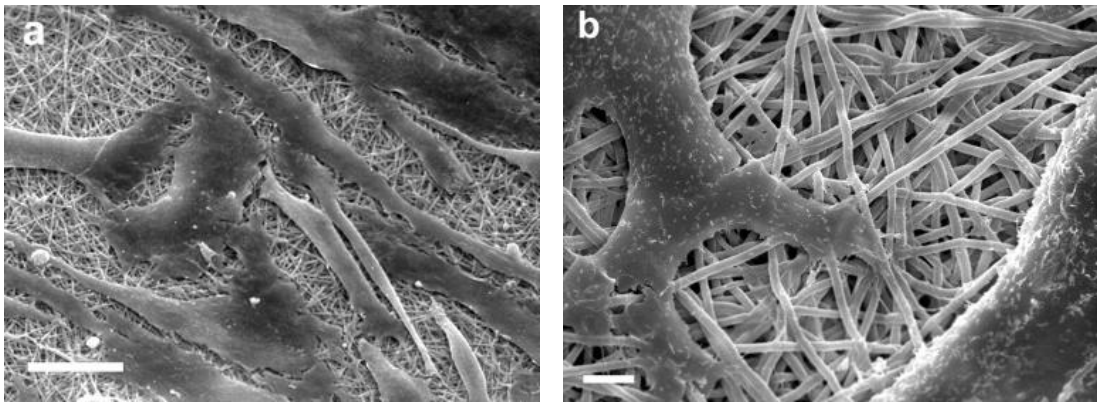

Figure 2.12 - SEM images of Vascular Wall Mesenchymal Stem Cells grown on genipin (5%) crosslinked mats for 7 days. Bars: (a) 50 µm and (b) 5 µm. Reprinted with permission from (Panzavolta et al. 2011). Copyright 2010 Elsevier Ltd.

2.6.1 Ideal Characteristics in Cell Interactions

The ideal conditions for cellular growth of a particular cell type rely on a very well controlled niche, and in order for tissue engineering scaffolds to best suit the growth of a specific cell type, it must be optimised to meet the unique requirements of each cellular environment. Many of the current market offerings were reviewed by (Zhong, Zhang, and Lim 2010) which noted a lack of electrospun collagen dressings being used currently in wound healing applications. The following will detail some of the most commonly tested cell types on electrospun scaffolds and how control has been exerted to meet the unique requirements necessary for cell expansion and infiltration.

2.6.2 Mesenchymal Stem Cells

Mesenchymal stem cells (MSCs) have been used extensively to assess the basic attributes of electrospun collagen scaffolds. Shih et al demonstrated that culturing of MSCs on an electrospun collagen scaffold had no effect on the osteogenic differentiation pathway when compared to the standard polystyrene cell culture flasks (Shih et al. 2006). Further work was carried out by (Li et al. 2005), which compared various ECM proteins. They found that cellular growth was faster on these than the standard tissue culture treated polystyrene (TCPS). This showed maintenance of typical fibroblastoid morphologies seen in Figure 2.13 that human embryonic palatal mesenchymal (HEPM) cells attach, spread and form oriented monolayers on protein fibre matrices.

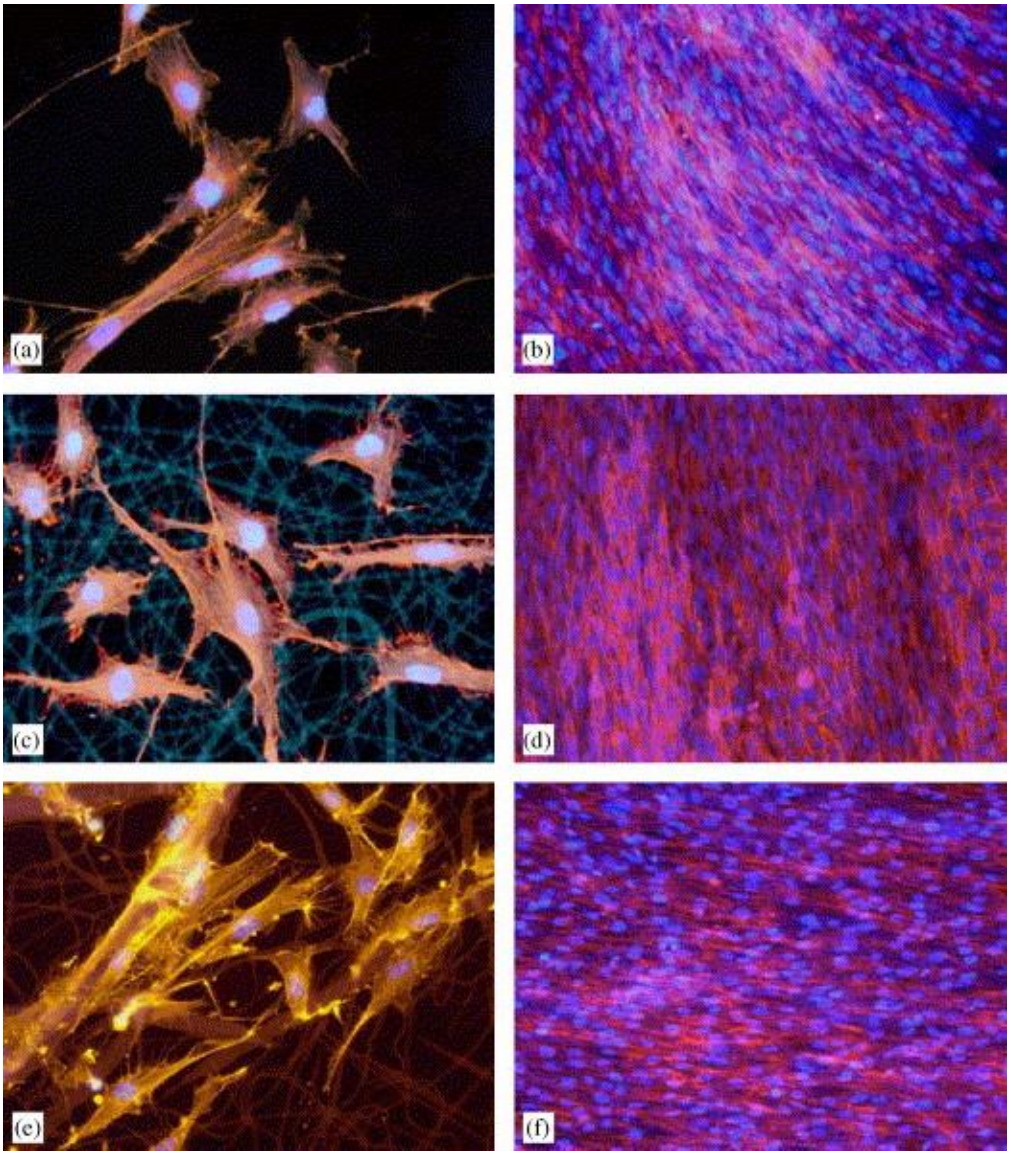

Figure 2.13 - Morphology of HEPM cells on protein fibre matrices. Staining for nuclei-bisbenzimide (blue), actin cytoskeleton-phalloidin (red), fibres-autofluorescence. (a, b) TCPS; (c, d) Gelatin; (e, f) Elastin; (a, c, e) HEPM after 48 h in culture (original magnification 400×); (b, d, f) HEPM monolayer at confluence after 72 h in culture (original magnification 200×). Reprinted with permission from (M. Li et al. 2005). Copyright 2005 Elsevier Ltd.

2.6.3 Fibroblasts

As a major cell component in the formation and renewal of the dermis, in particular the excretion of collagen, fibroblasts are of particular interest in collagen-based tissue engineering of skin grafting materials. Due to the interest in collagen as a bio-active wound dressing material, it is important that the interactions between electrospun collagen scaffolds and fibroblasts is examined in great detail. Zhong *et al*. produced aligned nanofibres of collagen to compare the growth of rabbit conjunctiva fibroblasts with randomly orientated scaffolds. They found that despite experiencing lower initial cell adhesion in the aligned samples, higher cell proliferation and confluence was seen and the shape and directional growth of the cells was seen to follow the alignment of the collagen fibres (Zhong et al. 2006). The findings of this study failed to point out that linear regeneration of tissue forming a wound closure result in a weakened, incomplete repair; described above to form scar tissue, this is an undesirable quality in a tissue engineered scaffold. This may have good applications in other tissues however, particularly those which naturally require alignment, such as muscle and bone.

The use of coaxial electrospinning by (Zhang et al. 2005) allowed the production of collagen / poly(ϵ-caprolactone) (PCL) (core / shell) coaxial nanofibres which could be compared to PCL nanofibres coated in collagen. The group compared proliferation and cell morphology for human dermal fibroblasts (HDF) between the groups of coaxial, coated, pure collagen and PCL fibres and found that the 3 groups containing collagen experienced significantly higher proliferation than virgin PCL. The coaxial collagen/PCL outperformed the coated PCL in all areas, demonstrating cell infiltration into the scaffold (Figure 2.14c), while pure collagen scaffolds experienced complete confluence across the scaffold (Figure 2.14d). The results of this *in vitro* study demonstrate the importance of collagen in the interaction between tissue engineering material and the body, with translational implications in areas such as coatings for bone replacements (hip, knee) suggesting that integrating electrospun collagen onto the surface of such devices could reduce rejection and quicken recovery periods significantly.

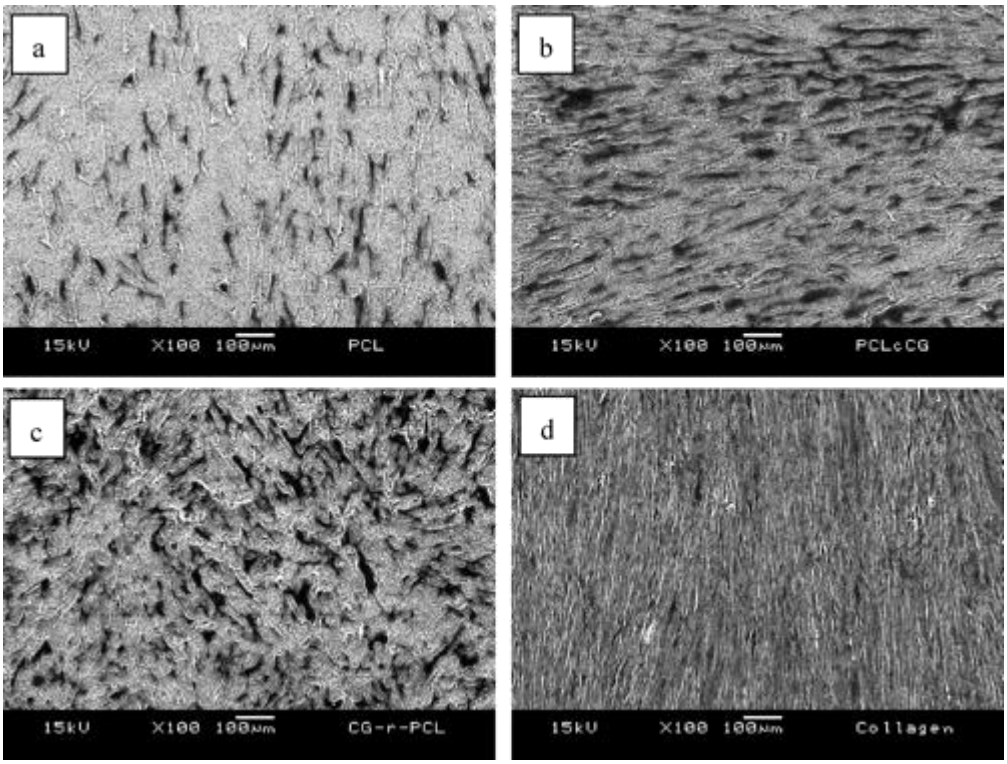

Figure 2.14 - Cell morphology of HDF at low magnification on different fibrous scaffolds: (a) pure PCL; (b) PCL with surface roughly collagen coated; (c) individually collagen-coated PCL (Coaxial Collagen/PCL); and (d) pure collagen nanofibers. Reprinted with permission from (Y. Z. Zhang et al. 2005). *Copyright 2005 American Chemical Society.*

2.6.4 Keratinocytes

As the primary cell component of the epidermis, keratinocytes have also been studied in detail. Studies on cell attachment and spreading of human oral and epidermal keratinocytes (Rho et al. 2006), immortal human keratinocytes (HaCaTs) (Zhou et al. 2016) and human dermal keratinocytes (Sadeghi-Avalshahr et al. 2017) have shown success in using electrospun collagen to mimic the native environment of keratinocytes *in vitro* and carried forward to *in vivo* research.

Rho *et al.* found that cells seeded onto collagen electrospun fibres formed from HFP and crosslinked with glutaraldehyde vapour showed poor adhesion from keratinocytes, even when compared with tissue culture polystyrene, suggesting the

structure of the collagen had been altered sufficiently to retard cell growth significantly (Rho et al. 2006).

Zhou *et al*. found significant proliferation of HaCaTs as well as stimulation of epidermal differentiation with the upregulation of involucrin, filaggrin and type I transglutaminase on their electrospun nanofibres using collagen extracted from tilapia fish (Zhou et al. 2016). The study didn't demonstrate a sufficiently high denaturation temperature from the marine derived collagen, despite evidence from (S. Chen et al. 2011) who showed a denaturation temperature of 48°C (62°C with EDC crosslinking) and furthermore did not take into consideration the damaging and harmful effects which are well documented with HFP and glutaraldehyde.

2.6.5 Neuronal

The use of collagen in the assistance of neural regrowth has been studied, particularly surrounding recovery from spinal cord injury (SCI). Collagen has been electrospun from HFP in combination with PCL to aid the growth of neural stem cells (NSC) on scaffolds which have been manipulated to produce tubular structures (Hackett et al. 2010). This allowed the group to also assess the controlled release of growth factors (fibroblast growth factor 2 and nerve growth factor) to stimulate differentiation into oligodendrocyte lineages and large primary neurosphere proliferation. The release of growth factors in a controllable manner was observed and provides good evidence of the useful application of co-electrospun collagen/PCL in the controlled release of bioactive molecules *in vitro* as seen in Figure 2.15.

Research surrounding the use of neuronal cells in electrospun scaffolds containing collagen have demonstrated the importance of alignment of fibres in the future regeneration of nerve tissues. The growth of pheochromocytoma derived cell line (PC12) cells on electrospun scaffolds of Poly (3-hydroxybutyrate-co-3-hydroxyvalerate) (PHBV) alone or in combination with 25% or 50% collagen were assessed for cell phenotype and neurite extension on the electrospun scaffolds (Prabhakaran, Vatankhah, and Ramakrishna 2013). The results clearly display the advantage of the inclusion of collagen within the scaffolds, significantly enhancing

cell proliferation, and alignment of the nanofibres led to neurite extension in the direction of scaffold alignment.

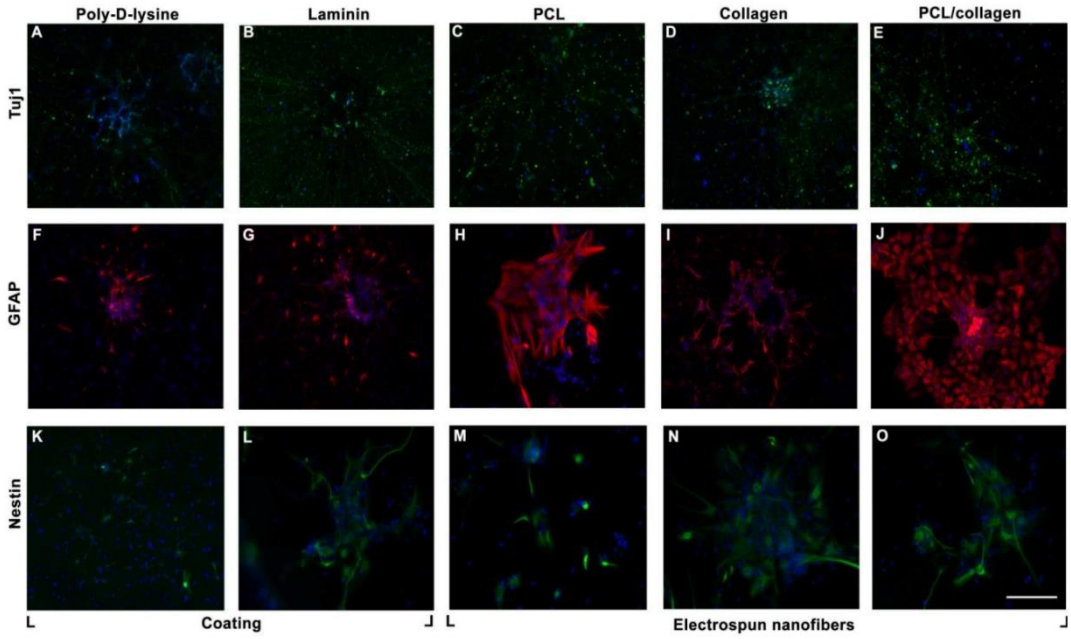

Figure 2.15 - Immunofluorescence analysis of NSCs cultured on various treatments. Representative images of cells on each substrate were stained for Tuj1 (A-E), GFAP (F-J), and Nestin (K-O). Cell nuclei (blue) were counterstained using DAPI. All cells were imaged at 20X; scale bar = 100 μm. Reprinted from (Hackett et al. 2010) Distributed under ("Creative Commons — Attribution 3.0 International" 2018)

Finally, by creating a gradient of stromal cell-derived factor-1α (SDF1α) which is bound to electrospun collagen scaffolds through a collagen binding domain, it is possible to direct cell migration and polarise morphology towards the area of higher SDF1α concentration (Li et al. 2015). This experiment displays another useful quality of collagen when influencing cell interactions, where collagen's native presence in the ECM has evolutionary and secondary attributes which influence cell behaviours, rather than simply acting as structural support, with collagen binding domains serving as but one example.

2.7 Conclusions.

The preceding decade has presented many limitations in the electrospinning of collagen membranes, with many of the traditionally accepted methods for the fabrication and stabilisation of these membranes called into question. Their efficacy has been shown to be greatly reduced by the use of fluorinated alcohols, and the use of glutaraldehyde as the 'gold standard' crosslinking agent has caused calcification of surrounding tissues, lowering the efficacy of the scaffold in medically relevant settings.

The move away from these aggressive methods in recent years, though slow, has further exhibited the need for collagen in medical scaffolds, and the desire to see the body's most abundant protein utilised for its structural and chemical nuances. There remains a great deal of interest, and this has led to several research groups exploring novel methods to preserve the collagen during electrospinning and to use a crosslinker which is much more biocompatible.

As the techniques for electrospinning continue to improve and the fundamental understandings of control parameters advance, the technology will allow for increased control and variety of collagen based electrospun scaffolds to be produced, both at bench and commercial scale. Even with the ongoing debate over the denaturation of collagen when electrospun, the biomaterial has shown itself to be extremely useful when interacting with cellular systems, and with slight modification, the increased control gained from modern electrospinning setups has shown that collagen has many desirable qualities which current synthetic polymers are unable to mimic. As new techniques enable a more native collagen to be electrospun, the potential improved clinical results may cement electrospun collagen's place as the polymer of choice for clinical applications, including wound, vascular, nervous, bone and dental.

This work aims to refine the production of collagen from jellyfish, permitting the use of this material in tissue engineering without experiencing the denaturing effects seen in the literature presented. The work aims to create a scalable system for the extraction of high-quality collagen to reduce the cost to market and enable better uptake of this material. The aim is for the material to retain the native features of triple helical collagen that is essential for tissue engineering, while ensuring the material is suitable for electrospinning.

The work further aims to remove the need for denaturing solvents in the electrospinning of nanofibrous collagen membranes, while ensuring the retention of the native properties of collagen that distinguish the material from gelatin. The achievement of this would present a novel solution that would permit the electrospinning of collagen for regenerative medicine and tissue engineering.

3 Materials and Methods

3.1 Materials

Unless otherwise stated, all chemicals were purchased from ThermoFisher Scientific, United Kingdom).

The crosslinking agent Genipin was supplied by Sigma Aldrich, United Kingdom or Challenge Biosciences, Taiwan.

The crosslinking agent EDC was supplied by Sigma Aldrich, United Kingdom.

All water used in extractions was produced using a reverse osmosis membrane with a conductivity of 2.0µS or lower.

All water used for characterisation was ultrapure deionised water, with a resistivity of 18MΩ.

pH was measured using an electronic pH probe, Jencons, United Kingdom.

Insoluble collagen from bovine was purchased from Sigma Aldrich, United Kingdom.

Jellyfish (Rhizostomas pulmo) were supplied by Jellagen PTY LTD.

A 50,000 NMWCO hollow fibre membrane (model number UFP-50-C-8A) of surface area 5300cm^2 was purchased from GE Healthcare.

A 0.2 µm hollow fibre membrane (model number CFP-2-E-35A) of surface area 9200 cm^2 was purchased from A/G Technology Corporation.

10,000 & (50,000) NMWCO hollow fibre membranes (model numbers Romicon CTG, 3" HF25-43-PM10(50)) were purchased from Koch Membrane Systems.

3.2 Extraction Methods

Collagen was extracted using various techniques, building on previous work on the extraction of collagen from the Rhizostomas jellyfish by other groups such as (Nagai et al. 2000). Initial experiments utilised the same techniques as those well known to the art, using dialysis tubing, centrifugation and bench-scale stirring to aid with acid solubilisation.

The advancement of the acid soluble technique focused on the design and implementation of hollow fibre membrane technology integrated into a series of circulation loops, which allow for the processing of the raw material into collagen at scale; This is explored in detail in chapter 4 of this thesis.

3.3 Characterisation of Extraction Methods

3.3.1 Flow Rate Analysis

In order to assess and obtain the optimum flow rate for the collagen batch extraction, several variables were recorded and monitored in respect of permeate flow rate. These include measurements at different collagen concentrations, membrane areas, pore sizes, solution compositions as well as retentate flow rates. 5 measurements were taken at 0, 1, 10, 60- and 120-minute intervals which allowed for the assessment and improvement of extractions in subsequent batches. The volume of liquid was measured in litres per minute (LPM) using graduated measuring cylinders on the permeate side of the membrane. Each measurement was repeated 3 times to ensure consistency and the change of each parameter and its effect on permeate flow was assessed.

Retentate cycle flow rate measurements were taken using a flow meter on the retentate line of the setup, and speed was controlled by 2 centrifugal pumps controlled by 3-phase potentiometer and inverter setups mounted within the control box.

3.3.2 Pressure Variables

In order to assess the effects of pressure in both forward (pump driven) and restrictive (valve restriction) types, measurements were taken between 0 and 1.0 bar for pump pressure and 0 and 1.5 for back-pressure. The effect on permeate flow was measured at 0, 1, 10, 60- and 120-minute intervals using graduated measuring cylinders measuring for 1 minute.

3.3.3 Collagen Concentration

In order to give an estimate of collagen concentration to signal the end of the batch run, visual observations were made by sampling 100mL of solution and comparing against standard concentrations of collagen solutions from previous batches. Once turbidity was approximately equal to a 6mg/mL stock solution if used for liquid experiments or 12mg/mL if solution is to undergo lyophilisation, then the samples were tested against known concentrations using the Lowry assay for total protein concentration and dry weight measurements as described by (Lowry et al. 1951).

3.3.4 Pore Size

Membrane pore sizes were used to determine the optimum for purity of product. Initial tests were carried out on a 5,000 NMWCO membrane, based upon the 3-5 kDa regenerated cellulose diafiltration membranes used previously by the research group and scaled up iterations were tested with 10,000 NMWCO and 50,000 NMWCO hollow fibre membranes. Each membrane extraction was examined using SDS PAGE as described in Chapter 3.6 and yield calculations, as well as visual observations of the solution and dry sponge material.

3.3.5 Source Comparisons

In order to examine any differences in collagen source, as well as to assess the universal potential for this extraction process, batches of collagen were extracted from various sources including jellyfish and bovine under optimum extraction conditions which were previously examined. Any variance in extraction characteristics were examined and re-optimised according to need.

3.3.6 Solution Compositions

In order to assess the effectiveness of different concentrations of base and acid used in the extraction of collagen, concentrations at 0.1M, 0.25M and 0.5M were assessed independently. Initial extractions examined the published techniques of (Song et al. 2006; Nagai et al. 2000; Barzideh et al. 2014a), which utilised 0.5M NaOH and 0.1M AcOH, these were varied in order to improve the quality of the collagen and remove contaminants, as well as ensuring the membranes in use were not damaged during processing by strong concentrations of base. The final fill solution was also examined to assess effectiveness during long term storage (up to 6 months), which included AcOH at concentrations of 0.1-0.5M as well as PBS and RO water for neutral solution compositions.

3.4 Reactor Design

Reactor design and process flow diagrams (PFD) were carried out using Microsoft Visio 2013 using process engineering shapes. These were then translated into either 1.5inch or 1inch 304 stainless steel piping with tri-clamp sanitary fittings and silicone flanged gaskets. For 20L reactor design, a single 1 phase centrifugal pump was used, while larger applications employed two separate 3 phase pumps for greater speed and pressure control. Either butterfly valves or PTFE diaphragm valves were used, depending on location requirements.

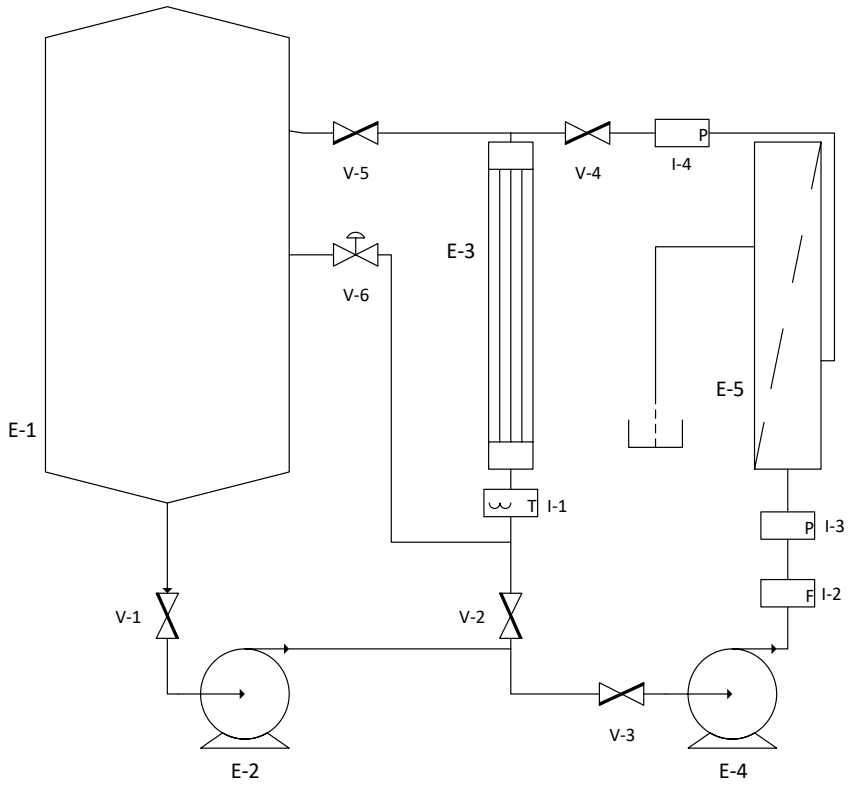

Equipment List	
Equipment Number	**Description**
E-1	100L Vessel
E-2	Pump 1
E-3	Heat Exchanger
E-4	Pump 2
E-5	50,000 NMWCO Hollow Fibre Membrane

Instrument List	
Instrument Number	**Description**
I-1	Temperature Sensor
I-2	Flow Meter
I-3	Pressure Sensor - Pre-membrane
I-4	Pressure Sensor - Post Membrane

Valve List		
Valve Number	**Description**	**Valve Type**
V-1	Tank Cutoff	Butterfly
V-2	Loop 1 - Loop 2 Switching	Butterfly
V-3	Loop 2 Isolating - Pre Membrane	Butterfly
V-4	Loop 2 Isolating - Post Membrane	Butterfly
V-5	Loop 1 Return Line Isolator	Butterfly
V-6	Loop 2 Return Line & Backpressure	Diaphragm

Figure 3.1 Example Process Flow Diagram for 100L Collagen Extraction Process with equipment, instruments and valves listed and described.

3.5 Freeze Drying

Freeze drying is a dehydration process which allows for the removal of liquid from a solution through the use of low temperature and low pressure, without harming the product through heating or evaporative shear forces (Prosapio, Norton, and De Marco 2017). This process facilitates the sublimation of ice to gas as shown in Figure 3.1.

One of the major benefits of freeze drying is the retention of the original shape of the product, without sacrificing product quality (Ratti 2001). The process is commonly applied to the drying of proteins and other biologics due to its preservative nature (Rey and May 2010).

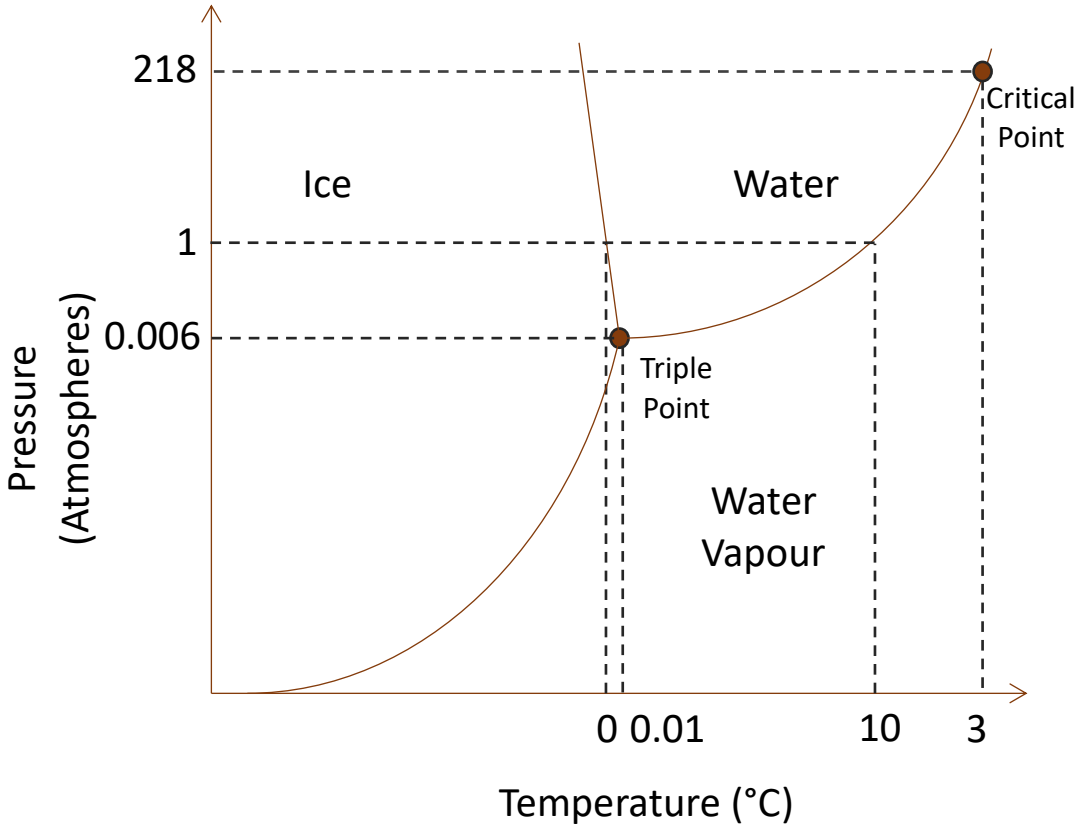

Figure 3.2 Chart of conditions relating temperature and pressure to the freeze-drying process.

For lyophilisation of collagen samples, an optimisation of drying was first performed under different freezing gradients, temperature gradients and chamber

pressures to ensure the collagen sponge structure formed was not deformed and to ensure the collagen material was not denatured by shear forces. After optimisation, freeze drying was carried out by first aliquoting 30mL of collagen solution at between 3 and 6 mg/mL into flat bottomed centrifuge tubes and allowing the samples to freeze at -20^{o}C overnight. The samples were then weighed to allow calculation of concentration against chemical assays such as the Lowry assay to aid calculation of purity, yield and to ensure residual ice is completely removed at the end of the drying cycle. These were then transferred into a -80°C deep freezer and allowed to freeze overnight. Once completely frozen, the samples' lids were removed and replaced with paraffin film that was speared to allow liquid vapour to escape during sublimation. These samples were then placed back into the -80°C for 30 minutes to ensure all samples remained frozen. The freeze-drying pump and condenser were powered up and allowed to acclimatise for 20-30 minutes until the desired temperature was achieved, ensuring the vacuum pump has sufficient oil which is free of contaminants. The samples were then placed upright on trays and placed in the chamber of the freeze dryer. The unit was then sealed, and the chamber brought under vacuum to begin primary drying.

The samples were then allowed to dry for a minimum of 60 hours and a maximum of 200 hours depending on composition, concentration and number of samples being dried. Once lyophilisation was complete, the chamber was brought to atmospheric pressure and samples were removed and weighed again using a 4-point scale and the values for each sample were recorded, and a sample with an abnormally high weight would signify that some residual ice in the centre of the sponge remains and drying must continue to prevent the sample from being dissolved upon melting.

3.6 Sodium Dodecyl Sulphate Poly Acrylamide Gel Electrophoresis

Sodium Dodecyl Sulphate Poly Acrylamide Gel Electrophoresis (SDS-PAGE) is a well-known technique for the separation and examination of proteins based on their molecular weight. First described in 1970 by (Laemmli 1970), the process can assess both the purity of a protein extract as well as the bulk presence of protein contaminants. When combined with Western Blot analysis the protein of interest can

be confirmed using antibody detection to as little as 5µg of protein (Mruk and Cheng 2011).

3.6.1 Running of Gel

SDS PAGE analysis was carried out on samples from each batch extraction and after each manipulation, including before and after electrospinning to monitor for any changes to the presence or absence of particular chains of collagen alpha helix molecules. Samples to be run were first centrifuged to remove any large contaminants at 4000 rpm. 7.5µL of collagen (3 mg/mL) dissolved in Acetic acid at 4^{o}C was mixed with 2.5µL NuPAGE ® LDS Sample Buffer (4X). This mixture was then heated at 70^{o}C in an incubator to reduce the collagen.

Running buffer was prepared using 50mL 20X NuPAGE® Tris-Acetate SDS Running Buffer added to 950mL deionized water. NuPAGE® Tris Acetate Mini Gels were loaded into the holding clamp frame (Jencons, UK) and the running buffer added accordingly: 200mL inner chamber, 600mL outer chamber. The samples were then loaded alongside repeats of Benchmark™ Unstained Protein Ladder (Novex, UK) and the gel ran at 150V using a concord power pack. Observed current ran from starting 45mA to final 27mA. After running, the gel was removed from the setup and placed into a tray for staining.

3.6.2 Staining (Coomassie)

The gel was stained using Colloidal Blue staining kit (Invitrogen) based on work described by (Neuhoff et al. 1988). Briefly, the gel was initially stained using a mixture of Stainer A, composed of ammonium sulphate in a phosphoric acid solution, and Stainer B containing the Coomassie Brilliant Blue (CBB) G-250 Stain, with further addition of ultra-pure water and methanol. This mixture forms particles of colloidal dye which in combination with the methanol, shifts the equilibrium of the CBB G-250 stain from the colloidal form to a molecularly dispersed dye, allowing complete diffusion into the dye. This solution is left to shake for a minimum of 3 hours and is then decanted and replaced with ultra-pure water overnight to remove any dye not

bound to the protein bands. The stained gels were then imaged using a UV and white light box and examined using ImageJ software.

3.6.3 Staining (Silver Stain)

The gel was stained using the SilverXpress® Silver Staining kit (Invitrogen, UK) in the following stages. The gel was initially fixed using 90ml ultra-pure water, 100ml Methanol and 20ml Acetic Acid for 10 minutes, followed by two repeated sensitising stages for 10 minutes, containing 105ml ultra-pure water, 100ml methanol and 5 ml sensitizing solution. The gel was then washed twice for 5 minutes using 200ml ultra-pure water.

The gel was stained using a mixture of Stainer A and Stainer B at 5ml each, with 90ml of ultra-pure water and left for 15 minutes to allow staining to occur. This was then washed twice with 200ml ultra-pure water each for 5 minutes to remove excess stain. The developing solution of 5ml developer and 95ml ultra-pure water was added and left until sufficient development of bands could be seen. The reaction was then stopped by adding 5ml of stopping solution to the developing mixture. The gel was finally washed 3 times using 200ml ultra-pure water for 10 minutes each time.

The gels were imaged using a light box and examined using ImageJ software. Gels were stored at $4^{o}C$ in sealed containers in a 20% ammonium sulphate solution to allow future comparison of gel information.

3.7 Fourier Transform Infrared Analysis

Fourier-transform infrared spectroscopy (FTIR) allows for the analysis of the wide spectral range of absorption seen with proteins with sufficient resolution to clarify differences in secondary and tertiary structure changes. This is of particular interest in this project for the differentiation between collagen samples, with a large focus on the retention of native secondary structure in the single alpha chain collagen, despite separation of the three α-helical chains into individual monomers. This also allows us to assess changes to these structures both before and after electrospinning of the collagen samples.

Collagen samples were examined using a Perkin Elmer FTIR/ATR device using a soft tip. For liquid samples 5µL of solution was placed on the diamond stage and allowed to dry. The samples were then tested using a scan range from 4000–400 cm^{-1}. Internal background correction was carried out to reduce noise using the Spectrum 10 software. The data was normalised and was analysed using the Spectrum software and compared between samples to give a percentage similarity. This data was then exported and analysed for changes to secondary structure elements, as well as triple helix abundance, according to previous research (Petibois et al. 2006). For Solid samples, such as electrospun samples, the samples were tested dry and by dissolving in mild AcOH (0.1M) and tested as above.

3.8 Electrospinning

Electrospinning of soluble collagens provides a suitable way of producing scaffolds which closely mimic the ECM, although due to the denaturing effects presented in Chapter 2.5.1 it is essential that alternative methods are developed. Electrospinning was developed in the first half of the 20th century (Formhals 1934), and further investigated with added detail (Reneker and Chun 1996; Reneker et al. 2000). The process of electrospinning involves a simple process detailed in Figure 2.4, which consists of a high voltage power supply that supplies positive charge to an electrospinning needle and a grounding electrode coupled to the collector plate. The electrospinning needle is supplied by a syringe loaded with polymer and solvent which is fed at a controlled rate using a syringe pump. The voltage applied to the solution causes the charges within the polymer to oppose surface tension. This leads to an elongation of the polymer droplet, termed the Taylor cone (Taylor 1964). Once the solution reaches its critical voltage it is then ejected from the cone as a single stream, due to the electrostatic attractive force between the solution and grounding plate. This jet then undergoes elongation and whipping instability, causing the polymer to dry in flight, before depositing upon the collector as fibres in either micrometre or nanometre scale (Bhardwaj and Kundu 2010). Electrospinning setups can be either horizontal or vertical depending on solution properties, such as low viscosity liquids which may use gravity to assist and prevent spraying of material onto the mat.

3.8.1 Needle Based Electrospinning

The electrospinning apparatus was set up using aluminium foil wrapped around the collector plate to act as the grounding target and was connected to earth. The syringe pump was set up to the correct diameter for a BD Plastipak® 10ml needle and an 18G blunt tipped needle was used. The solution was then taken into the syringe and any air cleared before loading onto the syringe pump.

The syringe pump was set to use the designated flow rate measured in mL per hour. The distance from needle tip to collector was optimised and a voltage of between 10 and 25kV was used. Voltage was applied when a droplet had formed at the tip of the needle and flow was maintained so volume of the droplet did not increase or reduce. Taylor cone formation and electrospinning was observed using a camera and laser and an AcOH bath was placed in the electrospinning unit to prevent gelation of the droplet during periods of prolonged electrospinning.

After electrospinning, the voltage was stopped, and the equipment made safe, any remaining collagen was stored at 4°C for characterisation. The mat produced was then sampled and coated in a 5nm layer of chromium before being examined by scanning electron microscopy (SEM) using a Hitachi S4800 FEG-SEM at an acceleration voltage of 10kV and emission current of 9µA. Micrographs were taken with a magnification of 1500X for fibre diameter measurements which were analysed using ImageJ software.

3.8.2 Needle-Less Electrospinning

Needle-less electrospinning describes the electrospinning process which has been previously described by (Burke et al. 2017). The setup adapts the standard electrospinning approach to allow the formation of several polymer jets simultaneously in order to allow for scalable fibre production (Thoppey et al. 2011). For these experiments, the Nanospider NS Lab 200 System (Elmarco, Czech Republic) was used.

The process begins as seen in Figure 3.3 by applying a high voltage to a polymer bath which is continuously coating a 6-wire mandrel with droplets of polymer

solution, which when exposed to the high voltage becomes elongated and Taylor cone formation occurs, forming multiple ejection points across the wire. The solution then undergoes rapid drying before being deposited on the collector. The material setup used a mandrel rotation speed at 10 revolutions per minute, a distance from mandrel tip to stationary collector of 30cm and a mandrel to collector voltage of 80kV. Using these conditions, the current from mandrel to collector was observed to remain between 100 and 120µA, signalling consistent fibre formation to be occurring. The process was carried out for 1 hour before being removed and samples taken for SEM imaging and characterisation as described above. Any remaining collagen solution was removed and stored at 4°C for further solution testing, and the mat was sealed with silica packs to prevent excess moisture and kept at 4°C.

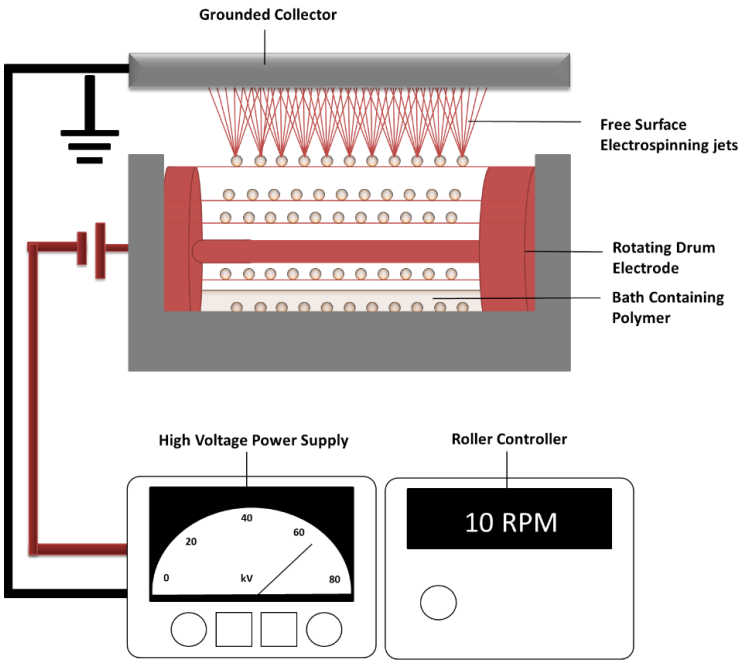

Figure 3.3 Nanospider (Elmarco, CZ) needle-less electrospinning setup using a rotating mandrel with wire electrodes that permit multiple initiation sites for electrospinning to occur. Continuous spinning is achieved by optimising mandrel rotation to polymer usage rate while voltage is typically significantly higher than with single needle electrospinning.

3.8.3 Co-axial Electrospinning

Coaxial electrospinning is a technique which allows materials which would not traditionally be capable of forming electrospun fibres to be incorporated into a scaffold. This technique has been successfully used for various applications, with drug delivery and tissue engineering being the key beneficiaries of the technology (Sill and von Recum 2008).

The technique involves the use of a coaxial needle, one which has inner (core) and outer (sheath) orifices, allowing two different solutions to be combined in the final scaffold as seen in Figure 3.2. The electric current acts primarily on the sheath solution, causing a viscous drag upon the core solution which undergoes the same fundamental processes such as the whipping region without the shear created by the high voltage. This process created fibres which contain a core composed of one material and the sheath, which can either be another polymer, or in some cases, a buffer solution which does not remain in the final electrospun mesh. The setup remains entirely the same in all other regards, besides an extra syringe pump required to supply the extra solution, though depending on the parameters required, a dual head syringe pump may be used if the flow rates are equal for both solutions.

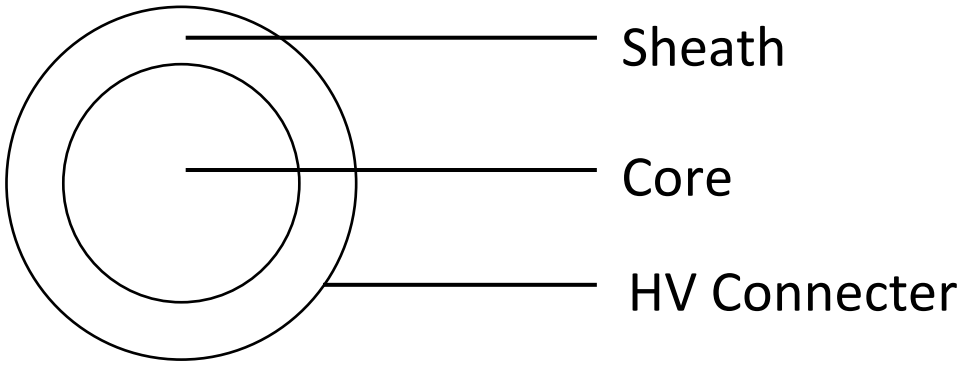

Figure 3.4 Diagram of Coaxial Needle, with core and sheath configuration.

3.9 Crosslinking

Collagen nanofiber mats were crosslinked for use in applications where stability in water or media was required. This was essential due to the water solubility of collagen after electrospinning. For these tests, 1-ethyl-3-(3-dimethyl amino-propyl) carbodiimide (EDC) and genipin (GP) were tested for their ability to reduce collagen solubility post-electrospinning.

3.9.1 EDC Crosslinking

EDC is a zero length crosslinker which reacts with adjacent collagen molecules creating amine bonds between collagen chains as seen in Figure 3.3.

For crosslinking with EDC, a 1% solution of EDC in ethanol (w/v) was prepared and chilled to 4°C. Initially this was used by covering the electrospun collagen until submerged, however later work injected the solution onto the electrospun collagen while compressed using petri-dishes with the base compressing against the lid as seen in Figure 3.4.

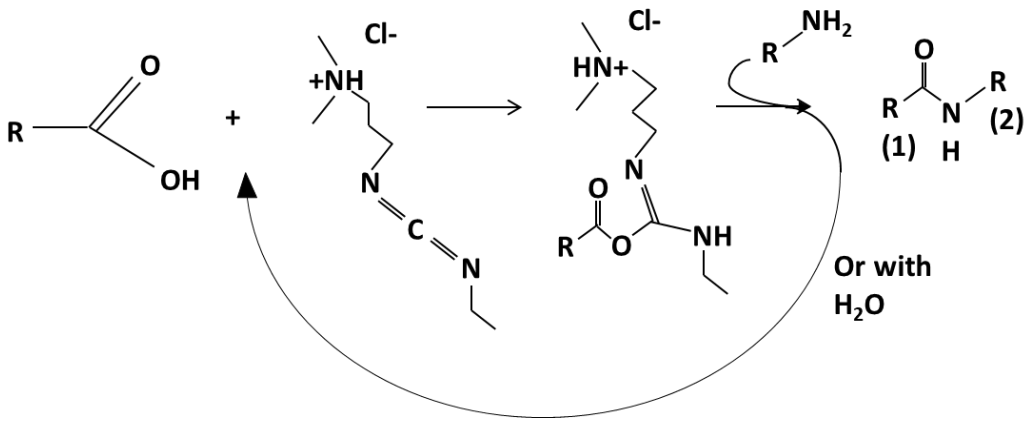

Figure 3.5 EDC crosslinking mechanism producing either a stable amide bond or in the presence of water reverting to uncrosslinked form.

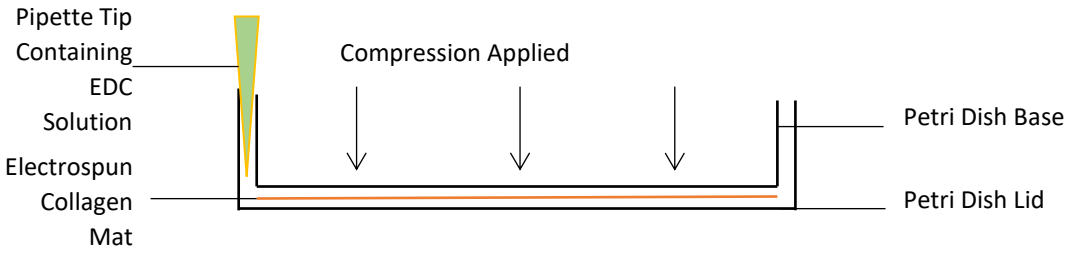

Figure 3.6 Setup for the crosslinking of collagen electrospun fibres to prevent swelling and merging of fibres, which would otherwise lose their fibrous nature. Compression applied must be >1kg per 50cm^2.

Once applied, the electrospun collagen material was left immersed in the EDC solution for 4 hours. After this, the EDC was removed, the scaffold washed to remove any residual EDC, and left to soak in ultrapure water (18MΩ) overnight. The following day the water was replaced with fresh ultrapure water, and either frozen and lyophilised or sealed and left moist.

3.9.2 Genipin Crosslinking

Genipin (GP) is a non-zero length crosslinker which forms bonding bridges between adjacent collagen molecules, as seen in Figure 3.5. As a result of this inclusion, the final crosslinked collagen is dark blue in colour as seen in Figure 3.6.

For crosslinking with GP, a 1% stock solution of GP in ethanol (w/v) was prepared and stored at 4°C. This was applied to the collagen using the same process shown in Figure 3.6 for electrospun fibres, or by dissolving the solution at 1% within 10X PBS for use in bioprinting. It was required that the injected solution is applied onto the electrospun collagen while being compressed as with EDC. This was again achieved by compression as in Figure 3.4. Once applied, the collagen material was left immersed in the GP solution for 4 hours. After this, the GP was removed, the scaffold washed to remove any unreacted GP, and left to soak in ultrapure water (18MΩ) overnight. The following day the water was replaced with fresh ultrapure water, and either frozen and lyophilised or sealed and left moist.

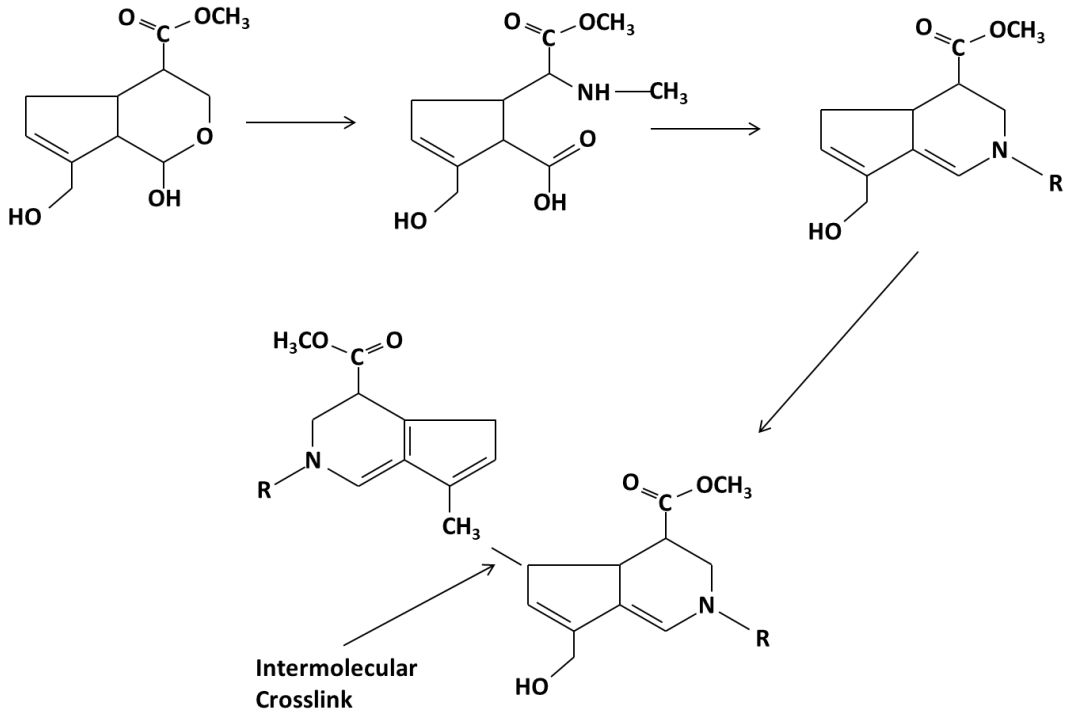

Figure 3.7 Genipin crosslinking reaction

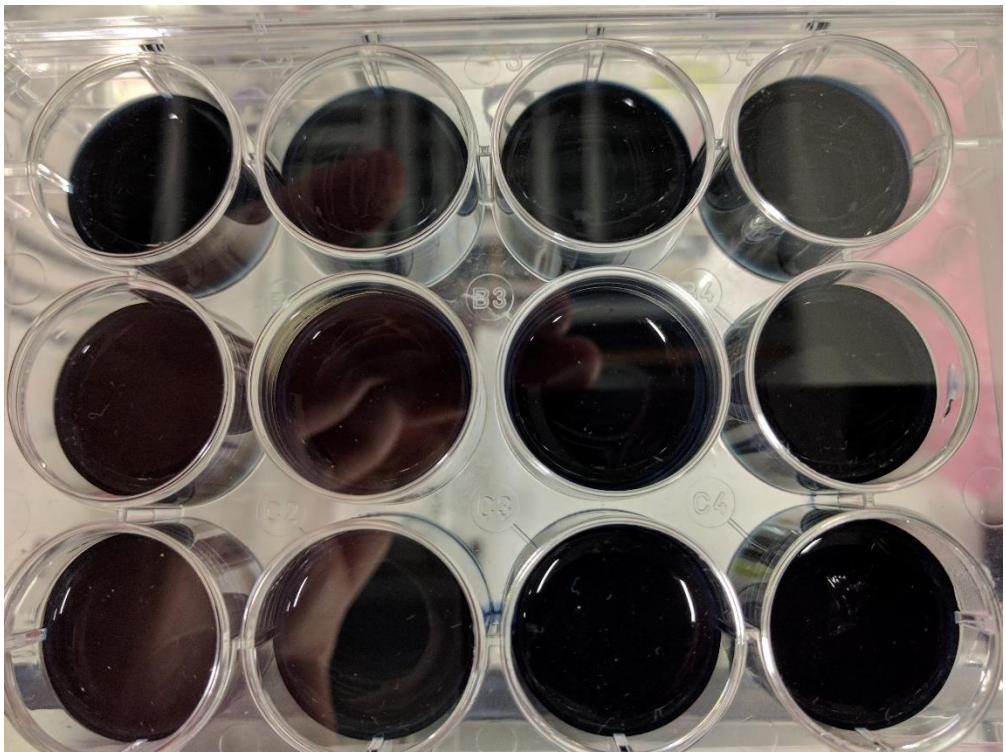

Figure 3.8 Genipin crosslinked collagen gels displaying the dark blue discolouration caused by the genipin crosslinking reaction.

3.10 Scanning Electron Microscopy

In order to examine the nanometre scale features present in samples, scanning electron microscopy (SEM) was used. The Hitachi S4800 FEG-SEM used in these experiments has a resolution of between 1.0nm and 2.0nm for conditions used between 1kV and 15kV, at a working distance of 1.5mm and 4mm respectively. Due to the insulating properties of collagen and many other biological molecules, it was necessary to coat the samples in a conductive material to prevent charging, which occurs when high-energy electrons contact insulator samples' surfaces leading to a build-up of charge due to the lack of a grounding path (Sim et al. 2010). This leads to image distortion when examining samples and is undesirable. To prevent this, samples were coated with a 5nm thick layer of chromium using a sputter coater (Quorum, UK), which achieves vacuum prior to chromium target excitation, coating the sample before venting and allowing the sample to be removed.

Once coated, the sample is adhered to the stage using carbon sticky tape and held using the stage clamp arms. The sample is then loaded into the sample transfer chamber of the Hitachi S4800 FEG-SEM and locked onto the loading arm. The transfer chamber is then sealed and vacuumed before the sample stage is loaded into the main chamber and locked into position. The stage is electronically homed into its correct position before the beam is activated, and voltage is applied. Once the sample has been located and voltage applied, it is focused and any errors in the astigmatism are corrected before imaging proceeds, as per standard operating practice. High magnification images are taken using both upper and lower detectors at an acceleration voltage of between 2 and 10kV and emission current of 9µA with working distance modified to ensure sufficient resolution. Micrographs were taken with a magnification of between 100X and 1500X magnification for representative imaging and at 1500X magnification for fibre diameter measurements. Measurements were taken and were analysed using ImageJ software.

3.11 Collagen Gel Formation

In order to achieve gelling of the collagen, the samples were first diluted to the appropriate concentration of collagen using ultrapure water, varying between 3.0 and 15.0 mg/ml. The stock crosslinking solution was produced by dissolving 10 PBS tablets (0.01M phosphate, 0.0027M KCl, and 0.137M NaCl per tablet, pH 7.4 at 25°C) in 200mL ultrapure water then dissolving either 1g or 2g of genipin into the 10 X PBS solutions. Once dissolved completely, the crosslinking solution was cooled to 4°C before use. 1mL of the above crosslinking solution was added per 9mL of collagen solution to achieve a final crosslinker concentration of 0.05 or 0.1% in 1X PBS. Following this, the pH of the acidic collagen solution was raised to between 6.0 and 9.5 using 1% (0.25M) and 20% (5M) solutions of NaOH which were prepared by dissolving 0.5g and 10g in 50mL of ultrapure water. Once the solution had reached its desired pH it was placed at 4°C, room temperature (25°C) or 37°C and gelling time was monitored until the gel had set enough that it could be inverted.

3.12 3D Bio-printing

In order to assess the application of ASC and other polymers, the conversion of a standard 3D printer costing under £1000 was carried out. This involved the replacement of the head module by retrofitting the unit with a series of 3D printed parts to enable the use of syringes containing collagen solution to be printed. The process began by recreating the work carried out by (Hinton et al. 2015) into freeform reversible embedding of suspended hydrogels (FRESH) printing which allows for the supporting of a hydrogel in three dimensions using fused filament fabrication (FFF) technologies for the application of bio-printing.

3.12.1 Design and Build

To begin, the Creator Pro 3D printer (Flashforge, China) was setup in standard format and the parts required for conversion were printed based on the work of (Hinton et al. 2015). These can be seen in Figure 3.7.

Figure 3.9 Replistruder adapted from the updated version produced as published in (Hinton et al. 2015) which allows for the printing of solutions on standard 3D fused filament fabrication (FFF) printers.

In order to further enable this setup for use on the Creator Pro 3D printer, a rail plate attachment was designed using Solid works to create a CAD model and a stand to hold the syringe extruder in place on the rail plate. These can be seen in Figure 3.8.

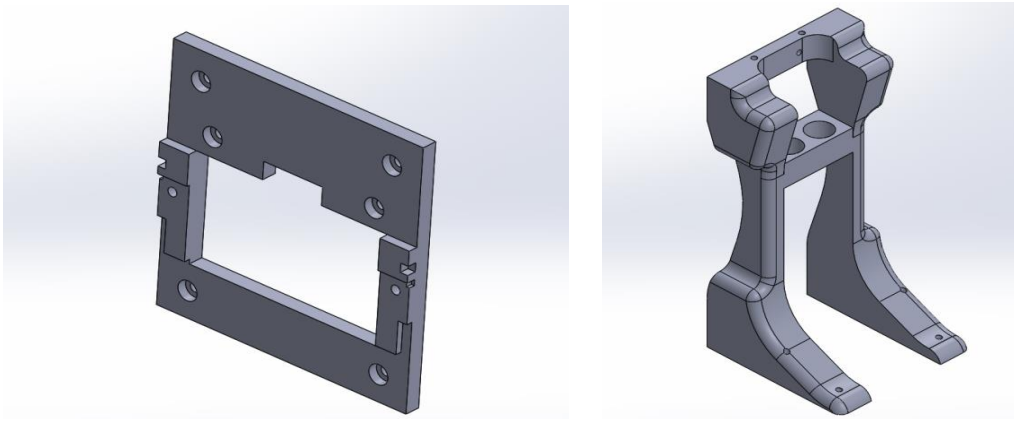

Figure 3.10 Rail plate and stand to adapt the printer to support bioprinting setups.

Once assembled, the syringe extrusion was optimised by changing the parameters of the printing Flashprint software (Flashforge, China) to match the nozzle diameter with the diameter of needle being used. As the existing stepper motor was being used in the syringe extruder, filament diameter was set to match the internal diameter of the 10mL syringe (BD, USA). Once successfully installed, the extrusion rate was optimised accordingly to achieve the correct volume throughput.

Testing with Collagen was carried out by first optimising gelling in the collagen in order to achieve gelation after printing was complete, as gelation occurring before printing had finished would block the syringe and printing would fail. Once optimum conditions were met, the printing was carried out by loading the gelling solution (3-10mg/mL ASC, pH 6.0-9.5, 0.1% GP, 1X PBS) into a 10mL syringe and loading the syringe into the extrusion setup.

3.12.2 Production of gelatin slurry

For the solution to be supported while still undergoing gelling and for the structure to be supported in three dimensions as each layer is sequentially printed, a gelatin slurry was prepared following the methods of (Hinton et al. 2015). To prepare the gelatin slurry, 150mL of 4.5% (w/v) type A porcine gelatin was mixed with 11mM $CaCl_2$ and left to gel at 4°C overnight in a 1L glass bottle. Once gelled, a further 350ml of 11mM $CaCl_2$, precooled to 4°C was added and the entire solution was blended for 120 seconds using a domestic blender (Kenwood, UK). The slurry was aliquoted into

50ml centrifuge tubes and centrifuged at 2000 RCFfor 2 minutes. This caused the separation of slurry particles (pellet) from the $CaCl_2$ and soluble gelatin (supernatant). The supernatant was removed and replaced with fresh $CaCl_2$, vortexed back into solution and centrifuged again. This was repeated until no bubbles were observed at the top of the supernatant, signalling that all soluble gelatin had been removed. The resulting slurry pellets were then pooled and stored at 4°C until required for printing.

3.12.3 Statistical Methods

For all experiments where changes to conditions were assessed for significance, samples were taken in triplicate and analysed using the students t-test. For changes between extract stages, the mean values of each stage were used with batches 6-10 providing n=5 for each t-test. Where significance was shown, the p-value is indicated.

Each measurement was taken in triplicate for each batch, with the mean average being taken for each measurement, such as permeate flow rate. These mean averages for extractions were then taken to compare between stages of extraction. Where error bars are displayed on graphs, these are representative of the standard error of the mean. Where statistical analysis is carried out, this is indicated on the graph.

3.12.4 Total Error Estimate

In order to compensate for errors in the measurement of variables, an estimate of total error was carried out for the extraction of acid soluble collagen. The assumed errors in measurement relate to flow rates of permeate and retentate solutions, as well as in the aliquoting of solutions for lyophilisation and weight of final extracts for yield determination. The error was calculated by taking the difference between expected values and the measured values where possible, and dividing this by the measured value, multiplied by 100 to give the % difference. Where this could not be carried out, a 5% error was assumed. The mean of these values was then calculated to give the average error as a representation of the total error within the extraction.

4 The Extraction, Scale Up & Characterisation of Acid Soluble Collagen

4.1 Introduction

The use of dilute acid in the extraction of collagen has changed methodically since being first described in the 1920s (Nageotte 1927). This process has introduced the use of sodium hydroxide or other base added to disrupt and remove cells and to aid the breakdown of non-collagenous materials. The use of pepsin was introduced in order to digest collagen that would traditionally be insoluble, allowing sources such as cartilage to be digested to produce type II collagen. The use of pepsins, by aiding the removal of non-helical ends of the collagen chains, is able to increase yield whilst not disrupting the α-helical structure of collagen (Miller 1972). The extraction of collagen has been examined in detail, with many minor changes being implemented to increase the yield of extractions. Typical maximum yield is consistently below 2% of the wet weight of starting material and is often below 5% of the dry weight basis in many cases (Nalinanon et al. 2007; Krishnamoorthi et al. 2017).

The extraction of collagen has been carried out from many sources, but is commonly obtained from bovine, porcine and equine sources for *in vivo* use (Silvipriya et al. 2015). Differing animal by-products are utilised in order to obtain specific collagen types, for example, bovine hide is often used to extract type I collagen, which often contains type III collagen as an impurity. Rat tail collagen is popular among research groups for in-house extraction of type I collagen, while bovine cartilage is often used to obtain type II collagen for chondrogenic *in vitro* studies. The use of mammalian sources, despite their greater use, have potential problems with the risk of BSE and other TSEs. Viral vectors are also of concern for their transmissibility to humans (Asher 1999; Lupi 2002) and many suppliers carry out expensive and involved viral inactivation studies to ensure their process does not carry an active viral load.

More recently, jellyfish and other marine animals have emerged as a plausible alternative source of collagen owing to a plentiful supply (Williams 2015) and offer a

safer source through their inherent lack of BSE risk and potential viral vectors (Song et al. 2006). The low denaturation temperatures seen with marine collagens (Addad et al. 2011; Kittiphattanabawon et al. 2010; Bae et al. 2008; Sadowska, Kołodziejska, and Niecikowska 2003) remain the major weakness for these sources, particularly surrounding their use for *in vitro* or *in vivo* testing.

The currently available extraction techniques are not well suited to industrial production, causing a high cost to the research market at ~£1800 per gram of type I collagen (Sigma Aldrich, UK, 2018). The process of acid extracting collagen from animal sources typically produces collagen peptide fragments, which survive extraction and reduce collagen purity, which is typically defined in specifications as > 90% of protein within α, β and γ regions. Endotoxin content, product clarity, and small batch sizes are all concerns with current extractions that usually result in high batch-batch variation, causing reliability problems for end users.

This chapter will focus on the design and implementation of a scalable process for the extraction of type I like collagen from the *Rhizostomas pulmo* jellyfish. The chapter will first examine the traditional processes used by others at bench scale, where yield will be examined, and potential issues can be dealt with prior to scale up. The application of drying the jellyfish prior to extraction was devised in collaboration with the KESS sponsor company Jellagen PTY LTD, in order to aid their aims of shipping the raw material from South Wales to Glasgow for processing within a GMP accredited facility. The ability to preserve collagen quality while allowing for significant financial savings in shipping costs gave rise for a need to explore the possibility of this. This chapter will explore a system that uses the qualities of hollow fibre filtration in a tangential flow filtration set up to remove constraining stages of collagen extraction, which are specifically the addition of salt and high-speed centrifugation to purify the extract. Here the successful implementation of the system at up to 100L scale is demonstrated, removing the need for low volume centrifugation stages that often result in lower than expected yield outcomes.

The collagen that is extracted using the various scales will be analysed for protein purity and yield, while pilot scale extractions will further characterise the resulting collagen extracts for their nativity, as well as their conformation to known spectral positions with FTIR. Various optimisations will be implemented throughout the process in order to increase yield, purity and improve the quality of the extracts for

their use in research and medical device applications. The effective removal of collagen peptides within the extract, whilst carefully preserving higher molecular weight collagens that can produce fibrils will be controlled, an essential part for gel formation *in vitro* that is unreliable with current collagen suppliers.

4.2 Traditional Acid Solubilisation of Freeze-Dried Jellyfish Material

For the extraction of collagen from jellyfish, traditional methods similar to (Nagai et al. 2000) were used. For this, freeze dried or vacuum dried material from the jellyfish (*Rhizostomas pulmo*) was thawed at 4°C overnight. This was then cut into pieces of 0.5cm^2 to increase the surface area: volume ratio of jellyfish to base. This was then washed with reverse osmosis (RO) water (1.5-3µS) to remove large impurities and rehydrate the specimen.

The samples were then treated with 0.1M NaOH at a sample/solution ratio of 1:10 (w/v). This was then stirred using a magnetic stirrer) for 2 days at 4ºC. The solution was then filtered through cheesecloth, followed by glass wool to collect any insoluble material.

The insoluble materials were then hydrated with RO water at a sample/solution ratio of 1:10 (w/v) which was then poured into dialysis tubing and dialyzed against 0.02M Na2HPO4 (dialysis buffer) with a sample/solution ration of 1:50 (v/v). This was stored at 4°C that was changed once every 24 hours for 72 hours. The collagenous material remains insoluble and appears as a white solid.

The collagen containing solution was then centrifuged at 10 000rpm / 16 000g for 10 minutes at 4ºC using a fixed rotor centrifuge. The collagenous pellet material was then suspended in 500ml 0.15M acetic acid (Acros Organics, UK) for 48h at 4°C to purify and solubilise the collagen. After this period, 25g of solid NaCl (Fisher, UK) was then added to give a concentration of 5% and overnight incubation at 4ºC dissolved the salt, causing the displacement and precipitation of the collagen. This solution was then centrifuged as before, and the pellet collected and re-suspended in 0.15M acetic acid. The process from salting out, centrifugation and resuspension was repeated twice more to further purify the collagen, followed by a final salting out and centrifugation at 10 000rpm for 10 minutes at 4ºC. The final pellet was dissolved in

500mL of 0.15 M Acetic Acid at 4°C and dialyzed against Dialysis Buffer as before for 5 consecutive days, with changes once every 24 hours for 5 days at 4°C to remove all traces of NaCl. The solution was then centrifuged at 10 000rpm / 16 000g for 10 minutes at 4°C and the pellet suspended in 70% Ethanol (Absolute Stock) to sterilize the collagen. This solution was placed on a magnetic stirrer at 4°C for 48 hr and collected by centrifugation (10,000 rpm for 10 min at 4°C). The collagen solution was then transferred in a laminar flow hood to sterile, pre-weighed 50 ml tubes. This was then either frozen at -80°C overnight and lyophilised the following day using a freeze drier or stored at 4°C. The tubes were weighed prior to use and compared to their weight post lyophilisation using a 4-decimal scale (Sartorius, UK) and the weight of the collagen determined. Sterile 0.15 M Acetic Acid was added to give a final concentration of collagen of 3 or 6 mg/ml or stored dry at 4°C.

4.3 Traditional Acid Solubilisation of Whole Jellyfish Material

Separated jellyfish bells or tentacles were thawed overnight at 4°C and drained of any residual liquid. Weight was recorded for comparison to catch weight and final yield calculations.

The samples were washed with RO water, precooled to 4°C, in order to remove any foreign bodies and continued until the bell or tentacles were almost clear. These were then blended roughly to produce a slush consistency of material ready for processing.

The samples were then treated with 0.1M NaOH (1M Stock) at a sample/solution ratio of 1:10 (w/v). This was then stirred using a magnetic stirrer for 2 days at 4°C. The solution was then filtered through cheesecloth, followed by glass wool to collect any insoluble material.

The insoluble materials were then hydrated with RO water at a sample/solution ratio of 1:10 (w/v) which was then poured into dialysis tubing and dialyzed against Dialysis Buffer with a sample/solution ration of 1:50 (v/v). This was then stored at 4°C which was changed once every 24 hours for 72 hours. The collagenous material remains insoluble and appears as a white solid.

The collagen containing solution was then centrifuged at 10 000rpm / 16 000g for 10 minutes at 4ºC using a fixed rotor centrifuge. The collagenous pellet material was then suspended in 500ml 0.15M acetic acid for 48h at 4°C to purify and solubilise the collagen. 25g of solid NaCl was then added to give a concentration of 5% and overnight incubation at 4ºC dissolved the salt, causing the displacement and precipitation of the collagen. This solution was then centrifuged, and the pellet re-suspended in 0.15M acetic acid. The process from salting out, centrifugation and resuspension was repeated twice more to further purify the collagen, followed by a final salting out and centrifugation at 10 000rpm for 10 minutes at 4ºC. The final pellet was dissolved in 500mL of 4ºC 0.15 M Acetic Acid and dialyzed against Dialysis Buffer for 5 consecutive days at 4°C to remove all traces of NaCl, ensuring the Dialysis Buffer was changed daily. The solution was then centrifuged at 10 000rpm / 16,000g for 10 minutes at 4ºC and the pellet suspended in 70% Ethanol (Absolute Stock) to sterilize the collagen. This solution was stirred at 4°C for 48 hr and collected by centrifugation at 10,000 rpm for 10 min at 4ºC. The collagen solution was then transferred in a laminar flow hood to sterile, pre-weighed 50 ml tubes. This was then frozen at -20°C, then transferred to -80ºC overnight and lyophilised the following day using a freeze drier. The tubes were weighed prior to use and compared to their weight post lyophilisation using a 4 decimal scale and the weight of the collagen determined. 0.15 M Acetic Acid was added to give a final concentration of collagen of 3 or 6 mg/ml or stored dry at 4ºC.

4.4 Reactor Design & Scale Up

For initial reactor design, a 1L system was designed and assembled. The extract solution is contained within a sealed, jacketed glass vessel with stirring and recirculating coolant to maintain temperature at 7°C as seen in Figure 4.1. The jellyfish material was defrosted, washed and blended as above, and placed in 0.1M sodium hydroxide at a sample: solution ratio of 1:10 (w/v). The extract was stirred for 3 days, maintained at 7°C. After 3 days, the solution was then circulated by peristaltic pump (E-2), through the hollow fibre membrane (E-3) and pressure was controlled across the membrane by restriction of the return line piping. The removed permeate solution

was sampled and discarded, and the retentate solution was supplemented with deionised water to maintain a total volume of ~750 mL until a pH of < eight was achieved.

Following this, the extract solution was supplemented with acetic acid to lower the pH to approximately three with a final concentration of 0.5M. This solution was stirred for 3 days, maintaining a temperature of 7°C. After 3 days, the extract solution was again circulated as above, until a pH of greater than six was achieved. The extract solution was again acidified to 0.5M acetic acid concentration and maintained for 3 days. The above was repeated once more, giving a total of 3 acid cycles to improve purity before being concentrated and collected for drying and characterisation. Following the successful proof of concept at one litre scale, the extraction process was scaled to 20L. This included the use of stainless steel with hygienic fittings, centrifugal pump, as well as the use of a dedicated heat exchanger and bypass line to facilitate the change of scale.

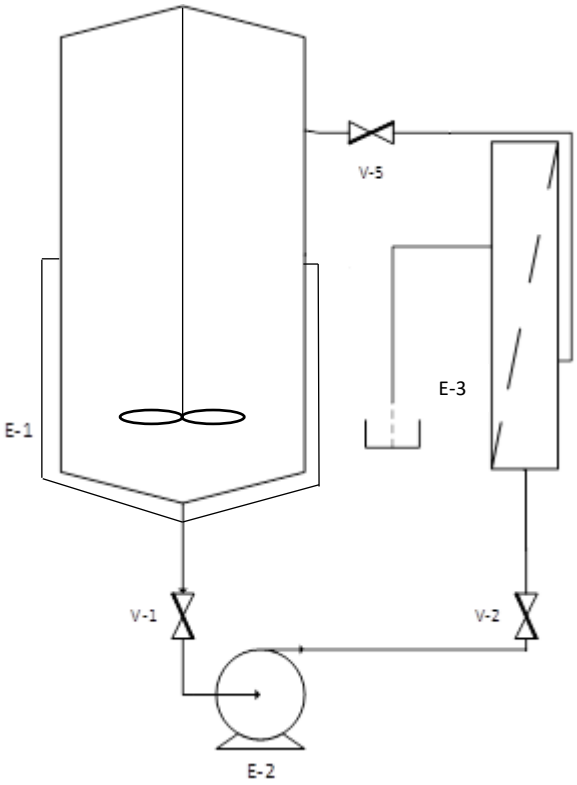

Figure 4.1 Process Flow Diagram of 1L Collagen Extraction Process, containing stirred & jacketed vessel (E-1), peristaltic pump (E-2) and hollow fibre membrane (E-3) as well as valves to create a pressure differential across the membrane.

The process flow diagram for the 20L extraction can be seen in Figure 4.2. The solution is circulated from the glass 20L vessel and gravity fed into the centrifugal pump. This then runs in loop 1 to maintain temperature <10°C. When dialysing as in loop 2, solution is pumped through the hollow fibre membrane while leaving the bypass line open. In order to increase pressure across the membrane and influence the path of least resistance, backpressure is applied on the return line (post membrane), which acts across both membrane and bypass lines. This pressure was increased to the desirable amount and maintained during dialysis. Once dialysis was completed, the backpressure was released in a controlled manner to not shock the membrane and the membrane was isolated. This was then removed, washed with RO and replaced. Retentate flow rate was measured by collecting the flow into a 5L jug and measuring with a measuring cylinder to ascertain the recirculation rate. Permeate flow rate was measured by collecting the permeate in a measuring cylinder for 1 minute.

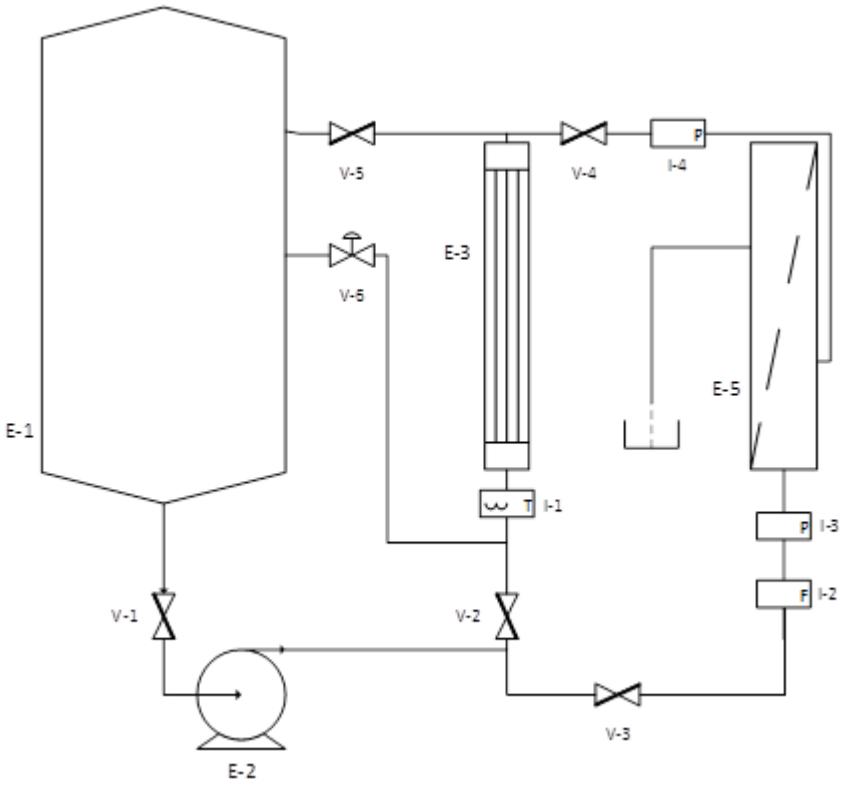

Figure 4.2 Process Flow Diagram of 20L Collagen Extraction Process, containing glass vessel (E-1), centrifugal pump (E-2), heat exchanger (E-3) and hollow fibre membrane (E-5). Valves V-3 and V-4 and V-5 are closed during loop 1 to maintain temperature and V-2 and V-5 are closed during diafiltration in loop 2. V-5 is used to create variable pressure on the system.

For the 100L system, the design is shown in Figure 4.1. The solution is circulated from the stainless 100L vessel and gravity fed with vacuum pulling into the first centrifugal pump that mostly delivers the flow for the system. This runs in loop 1 to maintain temperature <10°C. When dialysing as in loop 2, solution pumped from centrifugal pump 1 is diverted by closing the butterfly valve into the second centrifugal pump that mostly delivers the forward pressure to the system. The solution is then pumped through the flow meter and the hollow fibre membrane, then across the jacketed condenser in the reverse direction to loop 1. This then returns to the vessel. The pressure was slowly raised to ~ 1bar pre-membrane pressure with a flow rate of ~100LPM and backpressure was applied to give a cross-membrane pressure differential of ~0.5bar. These figures were varied during optimisation as appropriate. Retentate flow rate was measured using the flow meter readout, while permeate flow rate was measured for one minute using a measuring cylinder to ascertain the LPM. Samples of collagen solution were taken at 0, 1, 4, 7 and 14 days of extraction, which relate to JF material pre-treatment, JF in NaOH, JF in Neutral pH, JF Collagen in AcOH (1 cycle) and JF Collagen in AcOH (Final Product).

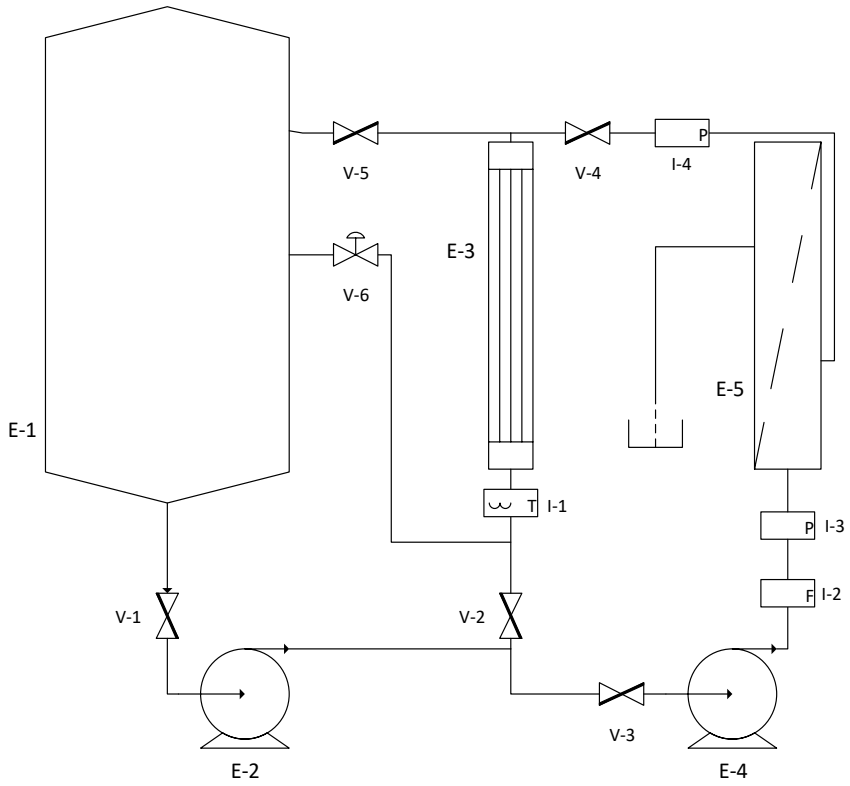

Equipment List	
Equipment Number	**Description**
E-1	100L Vessel
E-2	Pump 1
E-3	Heat Exchanger
E-4	Pump 2
E-5	50,000 NMWCO Hollow Fibre Membrane

Instrument List	
Instrument Number	**Description**
I-1	Temperature Sensor
I-2	Flow Meter
I-3	Pressure Sensor - Pre-membrane
I-4	Pressure Sensor - Post Membrane

Valve List		
Valve Number	**Description**	**Valve Type**
V-1	Tank Cutoff	Butterfly
V-2	Loop 1 - Loop 2 Switching	Butterfly
V-3	Loop 2 Isolating - Pre Membrane	Butterfly
V-4	Loop 2 Isolating - Post Membrane	Butterfly
V-5	Loop 1 Return Line Isolator	Butterfly
V-6	Loop 2 Return Line & Backpressure	Diaphragm

Figure 4.3 Process Flow Diagram of 100L Collagen Extraction Process with equipment, instruments and valves listed and described. In this diagram it is possible to observe both loops 1 and 2 in the extraction of ASC with necessary valves to ensure flow direction is appropriate for each loop.

4.5 Membrane Extraction of Collagen from Jellyfish

The frozen jellyfish material which was earlier separated into either tentacles or bells were thawed at 4°C overnight and thoroughly washed with RO water, until no foreign bodies were present, and the material was almost clear. This material was blended thoroughly until no chunks of material present were larger than 1mm in diameter. This was then pumped into the bioreactor vessel by use of a peristaltic pump and autoclaved tubing. The samples were then treated with 0.1M NaOH (1M Stock) at a sample/solution ratio of 1:10 (w/v). The solution ran under circulation loop 1 as demonstrated in Figure 4.2 for 3 days to allow cellular matter and other non-collagenous material to be destroyed and the hydrolysis of fats and proteins that can allow for their removal through the membrane system.

The solution was then dialysed using loop 2 as shown in Figure 4.3 to remove NaOH from solution using a 50,000 NMWCO hollow fibre membrane that was selected to ensure the retention of all collagen components while allowing the removal of low molecular weight impurities such as partial digests of collagen, as well as non-collagenous materials which are produced during cellular disruption with NaOH. The reduction in volume is then replaced with RO water to maintain total volume of 20% reactor capacity. The solution was filtered until a pH <8.0 were obtained. The remaining capacity of the bioreactor was then filled with the appropriate volume of acetic acid and RO water (1.5-3µS) to make a final concentration of 0.5M acetic acid. This was then cycled under loop 1 as shown in Figure 4.2 for 3 days to allow the collagen to solubilise through partial cleavage of the telomere regions.

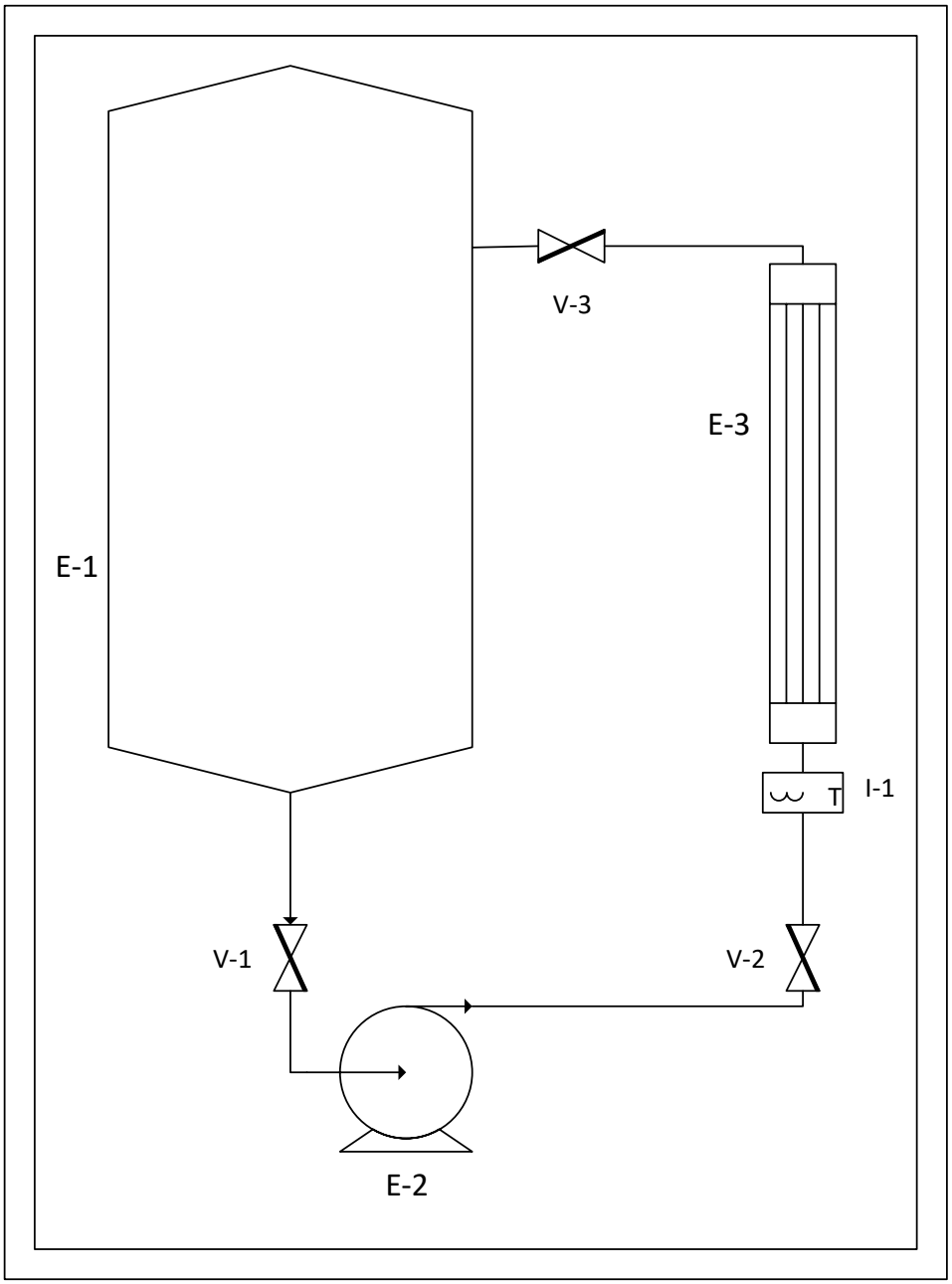

Figure 4.4 Process diagram of circulation loop 1 demonstrating the circulation of collagen solution from vessel (E-1) through pump 1 (E-2) and through the temperature sensor (I-1) and heat exchanger (E-3), before passing back to the vessel.

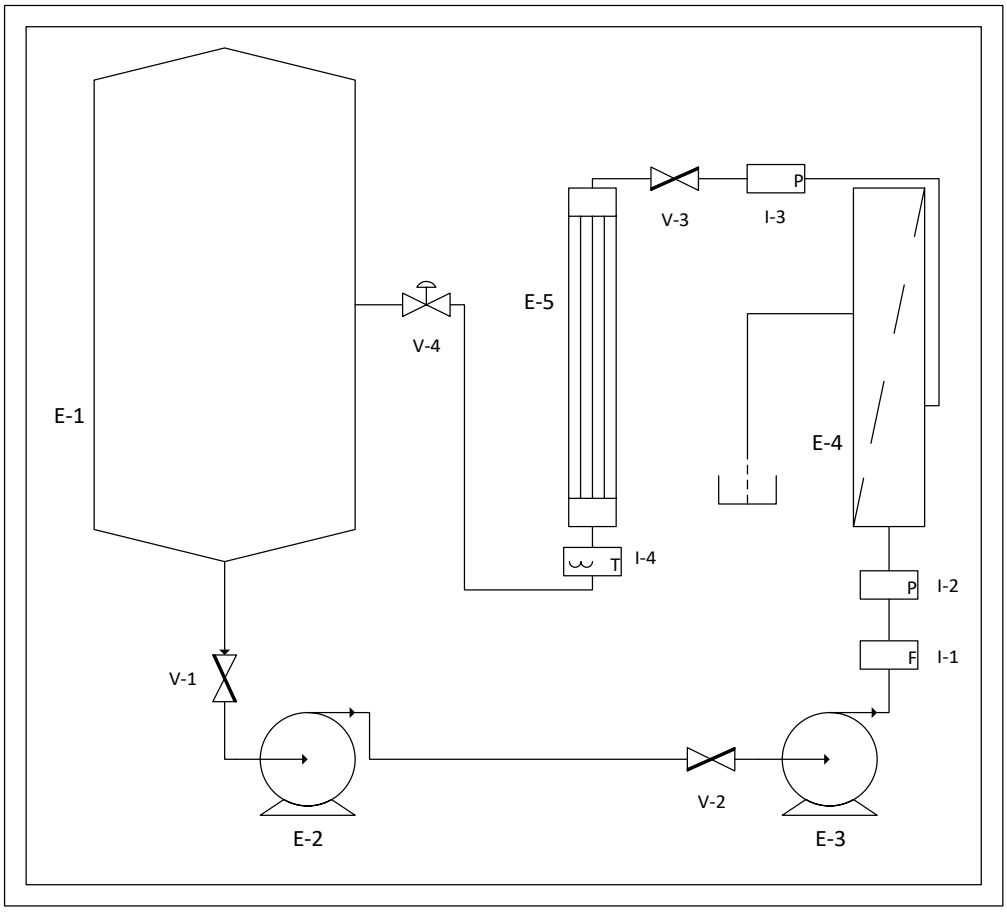

Figure 4.5 Process diagram of circulation Loop 2 demonstrating the diafiltration of the collagen solution through the 50,000 NMWCO hollow fibre membrane to alter pH and remove solution impurities <50kDa. The collagen solution passes from the vessel (E-1) through pump 1 (E-2), then pump 2 (E-3) which provides enhanced pressure control over a single pump setup; the solution passes through an inline flow meter (I-1) and pressure sensor (I-2), through the hollow fibre membrane (E-4), past the second pressure sensor (I-3), through the heat exchanger (E-5) and temperature sensor (I-4) before passing through the diaphragm valve (V-4) and back into the vessel. The diaphragm valve allows backpressure to be applied to the system by restricting flow, with enhanced control over membrane flux.

Following this, the solution was again dialysed, instead to remove the acid as in loop 2 using a 50,000 NMWCO hollow fibre membrane. The reduction in volume was again replaced with RO water to maintain a total volume of 20% of reactor capacity and the solution was filtered until a pH >6.5 was obtained and subsequently replenished to 0.5M AcOH at 100L capacity to increase yield. This was repeated 3 times in total before the volume of solution was reduced as much as possible to leave

a highly concentrated mixture ready to be dried. Once dialysed and concentrated, samples of the solution were either lyophilised to determine dry weight of the collagen or dialysed against 0.1M acetic acid for 3 days and diluted to a concentration of either 3 or 6mg/ml.

4.6 Membrane Extraction – Bovine Insoluble Collagen

400g of bovine insoluble collagen was stored at 4^{o}C until use. This insoluble material was then hydrated in RO water and blended thoroughly until no chunks of material present were larger than 1mm in diameter. This was then pumped into the bioreactor vessel by use of a peristaltic pump and autoclaved tubing. The samples were then treated with 0.1M NaOH (1M Stock) at a sample/solution ratio of 1:10 (w/v). The solution was run under circulation loop 1 as demonstrated in Figure 4.2 for 3 days to break down non-collagenous material which could be removed during membrane dialysis in order to increase collagen purity, which was indicated at ~ 60%.

The solution was then dialysed using loop 2 as shown in Figure 4.3 to remove NaOH from solution using a 50,000 NMWCO membrane. The reduction in volume is then replaced with DI to maintain total volume of 20% reactor capacity. The remaining capacity of the bioreactor was then filled with the appropriate volume of acetic acid and RO water to make a final concentration of 0.5M acetic acid. This was then cycled under loop 1 for 3 days to allow the collagen to interact and undergo partial cleavage of the telomere regions.

Following this, the solution was again dialysed, instead to remove the acid as in loop 2, and subsequently replenished to 0.5M AcOH at 100L capacity to increase yield. This was repeated 3 times in total before the volume of solution was reduced as much as possible to leave a highly concentrated mixture ready to be dried. Once dialysed and concentrated, samples of the solution were either lyophilised to determine dry weight of the collagen or dialysed against 0.1M acetic acid for 3 days and diluted to a concentration of either 3 or 6mg/ml.

4.7 Results - Whole & Freeze-Dried Jellyfish – Traditional Acid Solubilisation

The extracts of collagen obtained using the traditional solubilisation process were analysed for yield and protein purity by SDS PAGE and lyophilised weight calculated. The collagen obtained through this method was extracted from either frozen whole jellyfish or freeze-dried jellyfish which was previously blended and lyophilised. The protein extracts observed from these samples can be seen in lanes 7 and 8 of Figure 4.4. Samples extracted from freeze dried jellyfish yielded very little collagen, and visualisation by SDS PAGE and silver staining demonstrated an absence of significant quantities of collagen. Collagen obtained through this process using whole frozen jellyfish yielded collagen which was higher concentration and is easily visualised by silver staining on the tris acetate gel. Lanes 5 and 6 display the collagen extract with defined alpha 1 and 2 bands, but also contain banding at ~30kDa and 60kDa, suggesting a partial cleavage of the collagen backbone. Lanes 3 and 4 display a control sample of collagen extracted from frozen and blended jellyfish provided by Collagen Solutions Plc.

These results are in agreement with the findings of other research groups, in relation to collagen protein purity and molecular weight for collagens extracted from jellyfish and other marine animals (Zhang et al. 2014; Barzideh et al. 2014a).

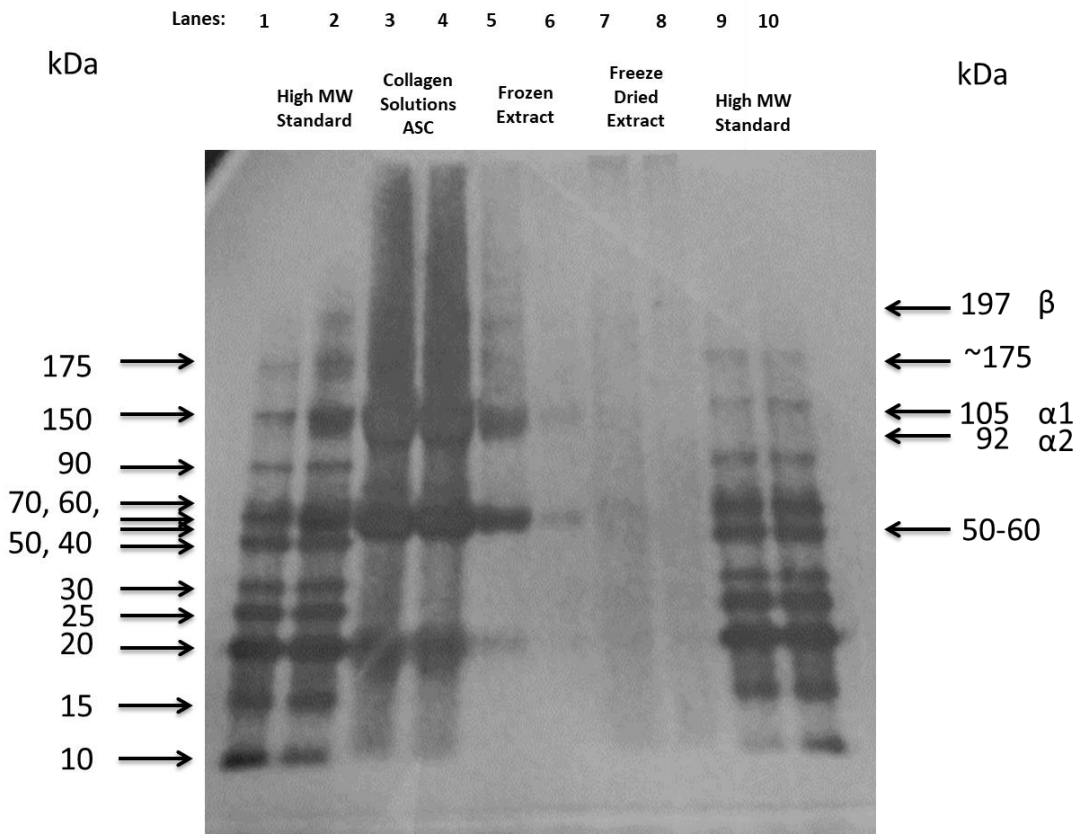

Figure 4.6 Silver stained SDS-PAGE gel. Lanes 1-2 & 9-10 Standards, 3-4 CS sample, 5-6 Frozen Extract, 7-8 FD Extract for batch 1 (n=2 per sample). Positive collagen banding can be seen in lanes 3-6.

Gel analysis consistently displayed positive banding for collagen from samples provided by CS, while these samples contain 30kDa and 60kDa impurities as well as heavy staining in the higher regions of the gel, suggesting partial conversion of the extract into gelatin.

The yields gained from either frozen or freeze-dried material can be seen in Table 4.1. As the freeze-dried material had been dried, removing the approximately 98% water content, a correction to yield estimation was applied to this sample to give a comparative yield estimation to that of other samples.

Table 4.1 Starting weight and collagen yields from extracts of jellyfish tentacles and bells which were either frozen or freeze dried. Samples 2 and 4 have been corrected to account for the decrease in water/solid ratio compared with hydrated samples (n=3).

	Average Tentacle Extract		Average Bell Extract	
	Frozen	FD	Frozen	FD
jellyfish (g)	42.2 ±2.1	25.2 ± 1.6	25.9 ±2.5	25.3 ±2.1
collagen (g)	0.1342 ±0.057	0.1542 ±0.038	0.0330 ± 0.042	0.0394 ± 0.051
yield %	0.32	0.61	0.13	0.16
Freeze Dried Weight / Yield Correction	N/A	0.012	N/A	0.0031

Due to the relative success of tentacle extracts when compared with freeze dried material, and due to the difficulties experienced with bells being used in processing, tentacles were selected to be used for future scale up activities.

4.8 Results – 1L Scale Extraction

Progression to the new method, incorporating membrane filtration to replace the continual centrifugation stages required for collagen extraction was carried out. Extracts were examined for protein purity and yield by SDS PAGE and lyophilised weight calculation. Figure 4.5 displays unconcentrated extracts of collagen using the 1L hollow fibre membrane process. Lanes 3 and 4 clearly display the characteristic pattern obtained by CS extracts, while lanes 8 and 9 have very faint bands observed at 60kDa, 92kDa and 105kDa.

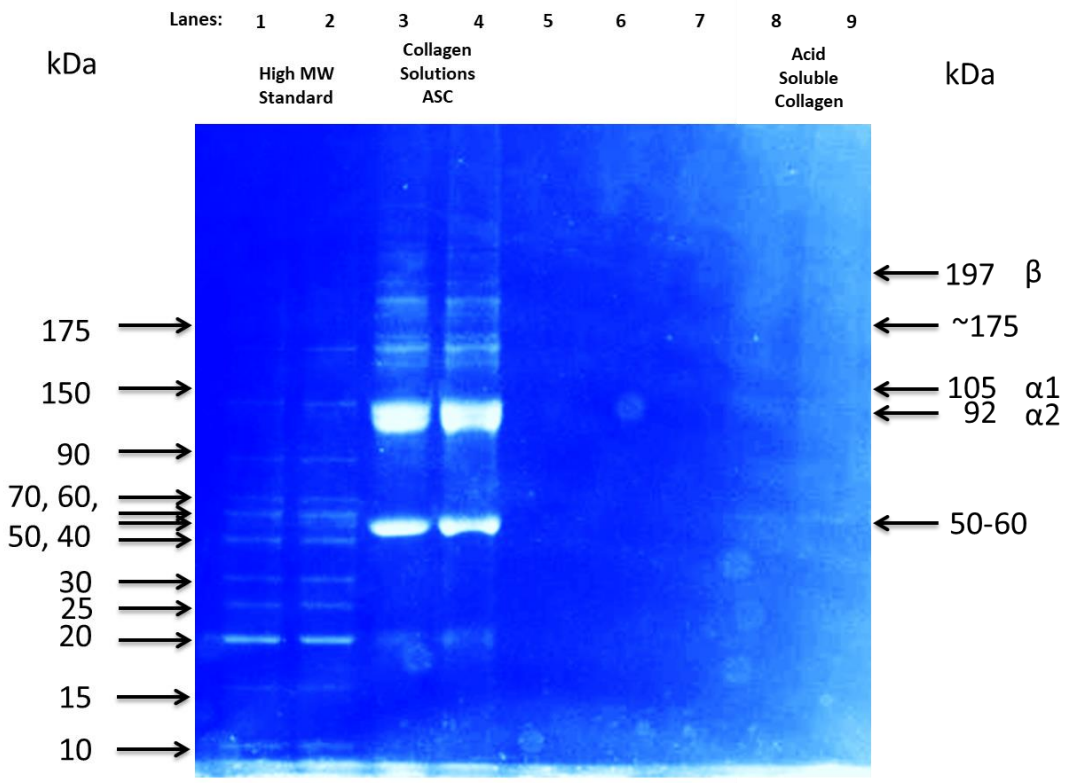

Figure 4.7 Coomassie stained SDS-PAGE gel. Lanes 1-2 High MW Standards, 3-4 CS Control Sample, 5-7 proteins passing through the membrane (negative control), 8-9 Collagen retained in extract without contamination. The presence of collagen without concentration in lanes 8-9 signifies collagen extraction was successful (n=2).

The yields from 1L extraction scale can be seen in Table 4.2 where yield of tentacle materials, in various levels of hydration were extracted. Batches 11 and 12 were pre-concentrated by filtering the blended tentacles through the hollow fibre filter prior to decellularization in NaOH solution. Yield obtained using the hollow fibre method gave rise to yields which were up to four times higher than those achieved using the centrifugation intensive methods.

Table 4.2 Membrane extract batch yields, from standardised starting weights with differing concentrations. For batches where pre-extract concentration was carried out, a yield correction factor was used, to account for the weight of water removed from the system prior to extraction (n=5).

Batch	**9**	**10**	**11**	**12**
	Membrane Extract Batches			
	solid	liquids	Concentrated solid	Whole Mix
Jellyfish (g)	25 ±0.1	25 ±0.1	25 ±0.1	25 ±0.1
Collagen (g)	0.2259 ±0.06	0.1691 ±0.07	1.0611 ±0.15	1.4562 ±0.09
Yield %	0.90	0.67	4.24	5.82
Concentration Corrected Yield %	N/A	N/A	0.85	1.16

The application of hollow fibre filtration allowed for the removal of lengthy centrifugation steps, the requirement for salting out stages, while sufficiently removing non-collagenous proteins from the extract, while due to the retention of the 50,000 NMWCO membrane, negligible collagen was lost, giving rise to high yields when compared with the traditional process.

4.9 Results – 20L Scale Extraction

In order to extract sufficient quantities of collagen for electrospinning and other device formulations to be established, the extraction was scaled from benchtop 1L to 20L capability. Extracts from 20L were analysed using SDS PAGE, yield analysis and were of sufficient quantity for visual assessments, such as colour, clarity and viscosity to be assessed.

The effects of scale up are seen in Figure 4.6 where 30kDa bands are effectively removed from the system, while larger fragments are caused by the use of one phase, non-regulated centrifugal pump systems over the peristaltic system used in the 1L system. The use of non-speed controlled centrifugal pumps within the 20L system also causes the effective removal of the higher chain gamma collagen bands which are seen in later extracts. Despite this, banding for alpha 1 and alpha 2 chains at 105kDa and 92kDa, as well as beta chain at ~200kDa are present confirming the presence of acid soluble collagen within the extracts.

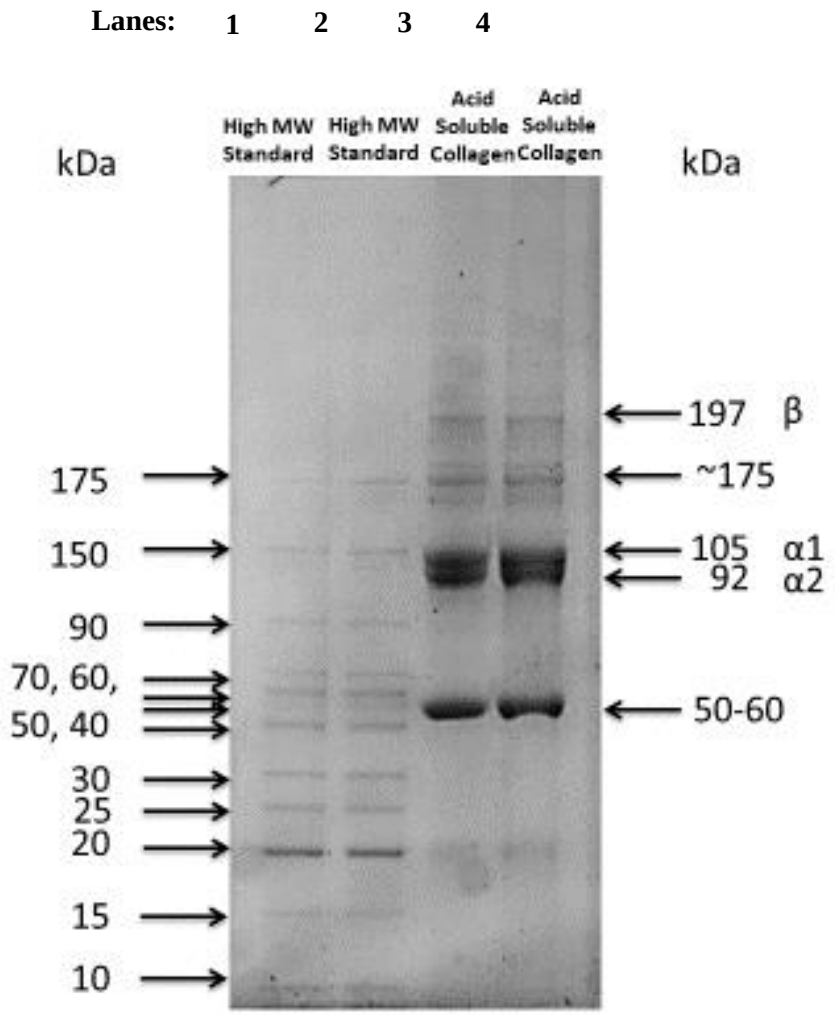

Figure 4.8 SDS PAGE for batch 15 (20L Membrane batch 2) displaying characteristic α- chains and β-chain, as well as partial collagen backbone digests at 50-60kDa and 175kDa (n=2).

The yields of collagen extraction for 20L batches are seen in Table 4.3 below, where a yield of approximately 1.5% of starting weight is now being consistently achieved. At 20L scale, one tub of jellyfish tentacles equates to one batch, which prevented the need for material to be re-frozen, possibly raising yield by removing the instances where collagen breakdown through protease release or crystal formation disrupting cell walls could occur.

Table 4.3 Batch results for the 20L system. Collagen yields demonstrate the success of the hollow fibre membrane system, where yields are consistently at 1.5% ± 0.1%.

20L System Batches

Batch	1	2	3	4	5	Average
Tub Weight (Kg)	22.74	21.93	23.18	19.79	21.54	21.84 ±1.18
jellyfish (g)	2060	2120	1980	2040	2160	2072 ±62.74
collagen (g)	30.6	31.4	29.2	30.1	32.64	30.79 ±1.17
yield %	1.485	1.481	1.475	1.475	1.511	1.49 ±0.01

The flow rate and permeate rates for each stage were monitored and recorded. Flow rates for each batch showed a gradual increase of recirculating retentate, due to the breakdown of non-collagenous materials that were removed through cross-flow diafiltration, as well as the subsequent solubilisation of the collagenous solution in acetic acid, leading to a reduction in overall solution viscosity. This trend is seen in Figure 4.7, where flow rate was significantly increased between stages two (NaOH processing) and eight (Final acid solubilisation) ($P < .05$). Each stage represents a crucial point within the extraction procedure, where a solvent change has occurred. Average permeate flow rate is significantly increased from stage 2 to 8 ($P < .05$), as the solution appears to becomes less viscous when the collagen solution is purified and solubilised as can be seen in Figure 4.8 and Figure 4.9. The reduction in viscosity is visualised by eye when pipetting the sample as well as through the increase in flow rate at the equivalent pump speed.

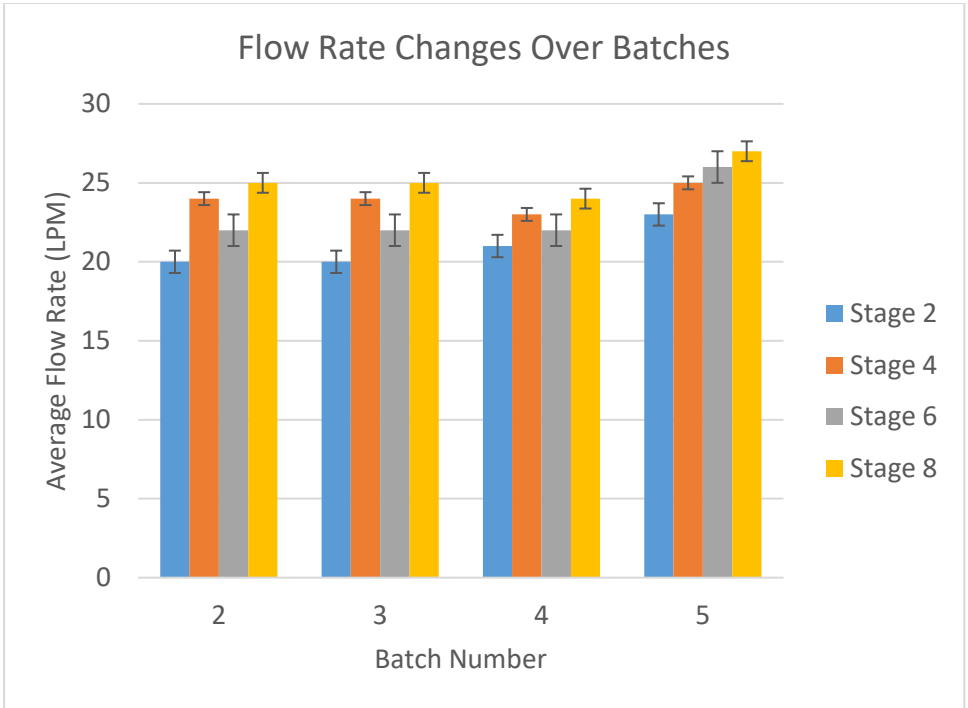

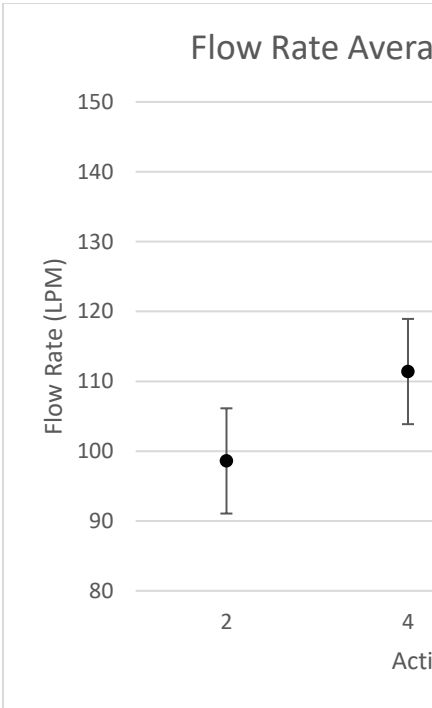

Figure 4.9 (a) Graph displaying average flow rates for batches 2-5 of the 20L scale extraction increased flow rates from stages 2 to 8 indicates a lower viscosity of retentate solution. (b) Gr for extracts 2-5 (n=4). Flow rate was significantly increased between stages two and eight (P standard error of the mean.

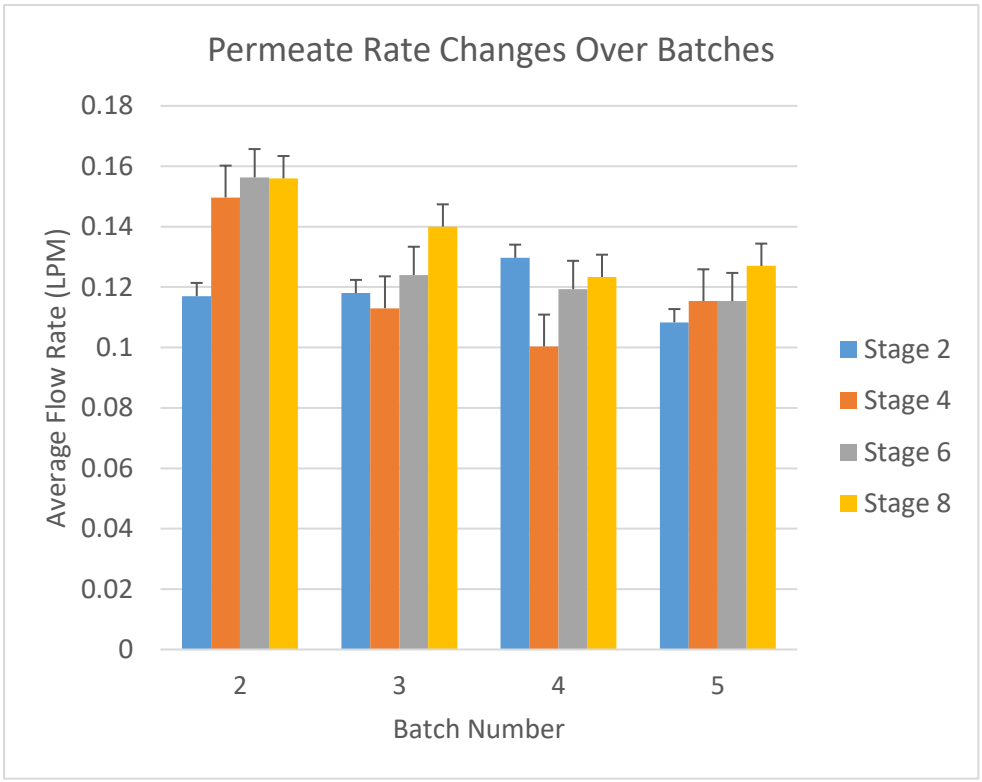

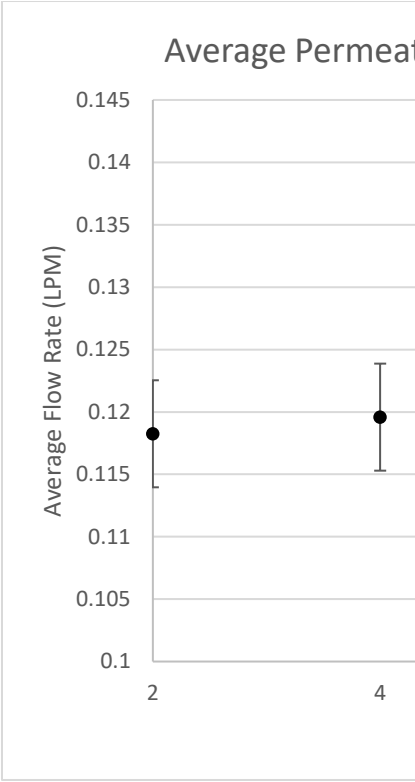

Figure 4.10 (a) Graph displaying average permeate rate changes for batches 2-5 of the 20L sc Graph displaying mean permeate rate for extracts 2-5 (n=4). Acid based stages (4-8) showed c permeate rate (P < .05) as non-collagenous material is removed from the system, leading to le membranes. Error bars represent standard error of the mean

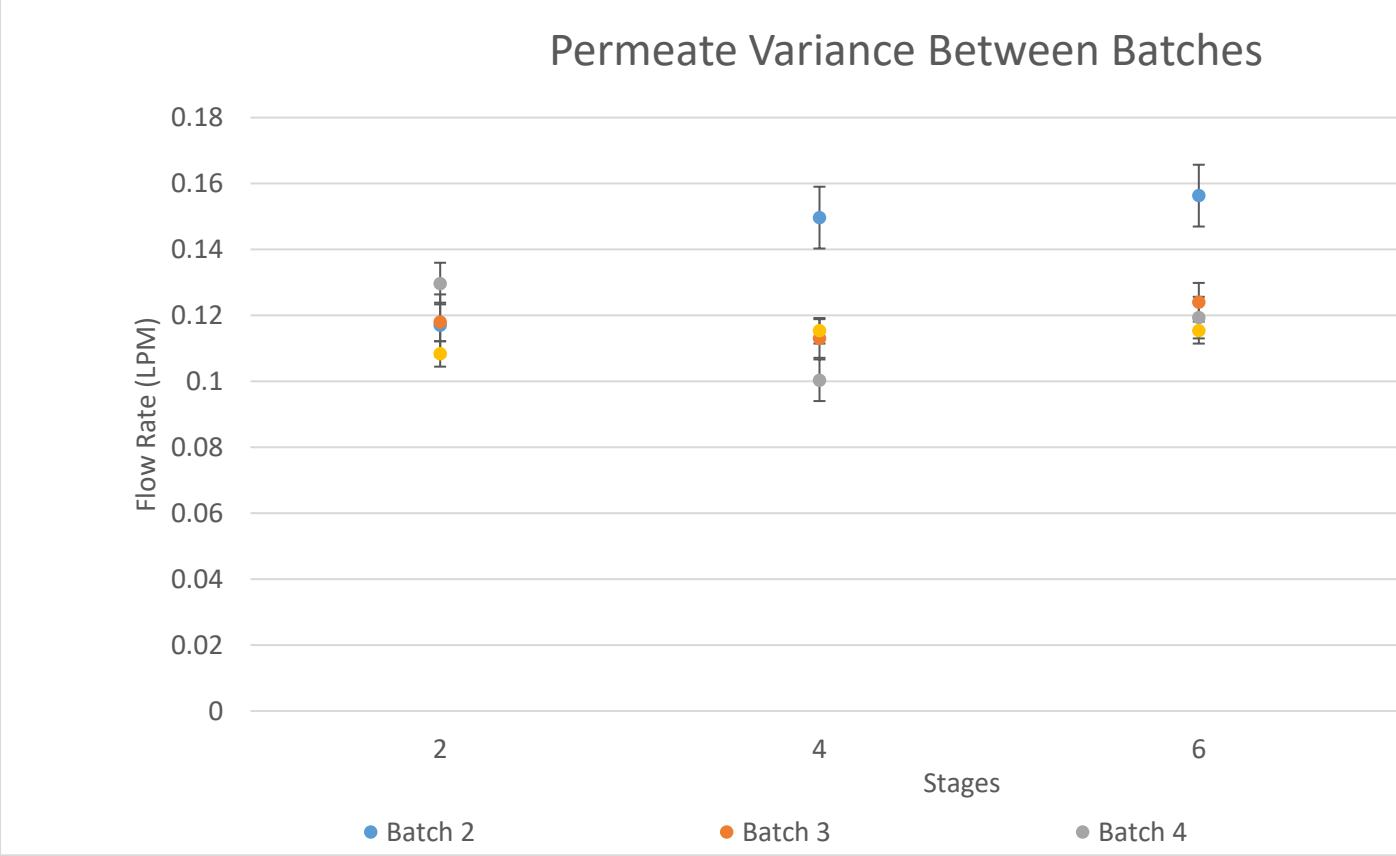

Figure 4.11 Graph displaying permeate variance for batches 2-5 of the 20L scale extractions (
standard error of the mean.

4.10 Results - 100L Scale Extraction

The extraction of collagen was scaled from 20L to 100L for pilot scale testing to ensure any barriers to large scale production could be overcome. Extracts from the 100L system were analysed using SDS PAGE, FTIR, yield and visual analysis. Lowry assays were optimised for collagen using extracts from 100L batches, due to the known affinity issues with the Folin-Ciocalteu reagent (López et al. 1993). To tackle this, gelatin standards of known concentration were used alongside BSA standards. The 100L process also permitted sufficient volume of collagen to proceed with thorough testing of medical device formulations. This included techniques such as electrospinning and bio printing that will be covered in chapter 6.

SDS PAGE analysis of batches 19 – 23 (Scale-up batches 6-10) displayed the typical banding for collagen, with alpha and beta present. However due to the introduction of two three-phase centrifugal pumps, it was now possible to reduce shear to the collagen solution by creating slower ramps at the onset and termination of TFF stages. This led to reduced quantities of 30 and 60kDa peptides apparent in the SDS PAGE analysis and allowed for the retention of gamma chains within the extract. These can be seen in Figure 4.10.

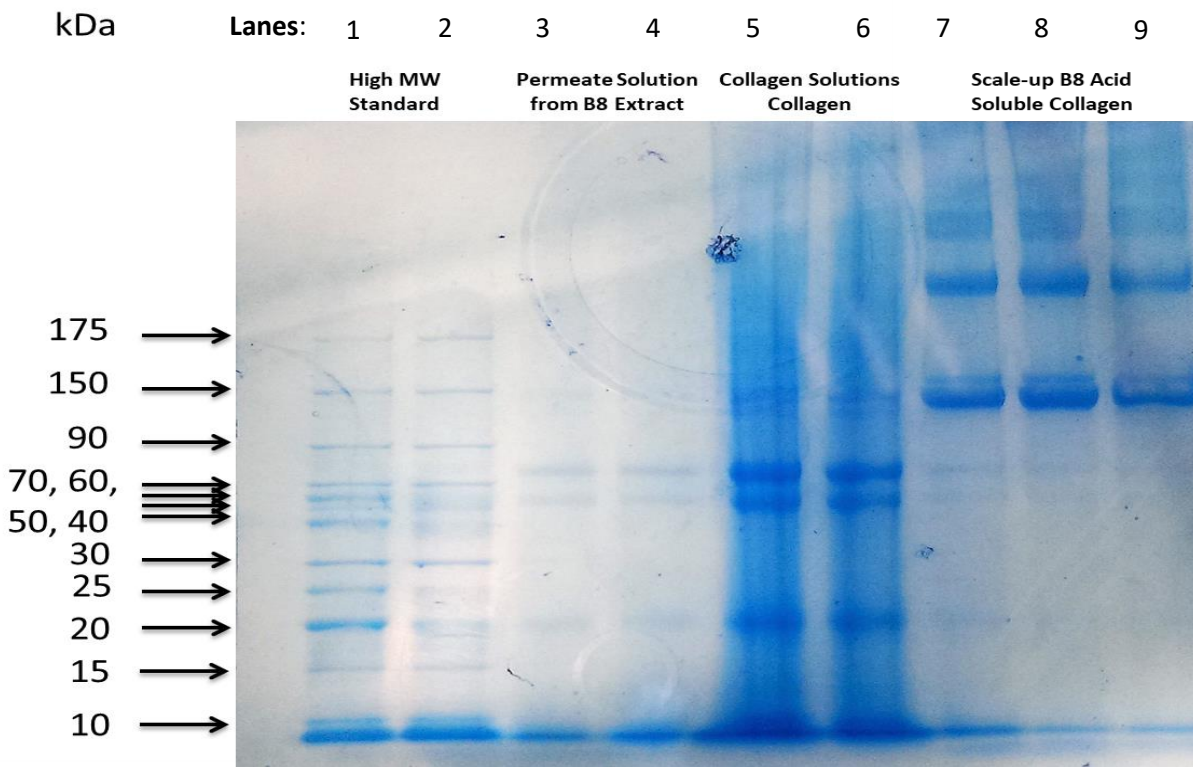

Figure 4.12 SDS PAGE displaying scale-up B8 extract (Lanes 7-9) containing alpha, beta and lower residual 30 and 60kDa peptides. Lanes 5-6 display collagen solutions collagen, which h and 30kDa peptides with relatively little alpha or beta collagen remaining. Lanes 3-4 display was removed from B8 during TFF processing (n=2 for permeate solution and collagen solution

SDS PAGE analysis of the 100L batches was used primarily to refine the process, permitting the removal of lower molecular weight, partially digested collagen impurities. Impurities in collagen solutions are generally defined by the percentage of protein which resides outside of the alpha, beta and gamma regions, and typically a protein purity of 90% or higher is expected in research grade materials.

The SDS PAGE result for batch 9 of the scale up extractions can be seen in Figure 4.11 below. It is possible to observe here that the 30kDa and 60kDa impurities have been further reduced, and undigested fibril content within the solution has been further reduced, leading to a more soluble collagen solution which is less opaque and of lower viscosity than seen in batch 8. The minimum detection for Coomassie staining is quoted at 0.1µg of protein. This would equate to 10µg/mL in the collagen solution. The 30kDa impurity was very difficult to image, and is likely close to this quantity, the 60kDa impurity is double the content, at around 20µg/mL within the collagen solution. Figure 4.12 is the expanded gel which demonstrates the increased level of impurities seen in samples obtained from collagen solutions, which have further degraded, due to uncontrolled processing parameters and shipping temperature issues.

Overall success was obtained in the use of hollow fibre filtration in order to increase protein purity to equal to or above those possible using the traditional extraction processes, with the added benefit of successful demonstration at pilot scale. These results appear to offer better preservation of higher molecular weight chains, with less fragments produced by over or under-digestion. The use of tris acetate gels also offers better separation of these high molecular weight proteins than is commonly seen by other groups (Zhang et al. 2014; Barzideh et al. 2014a).

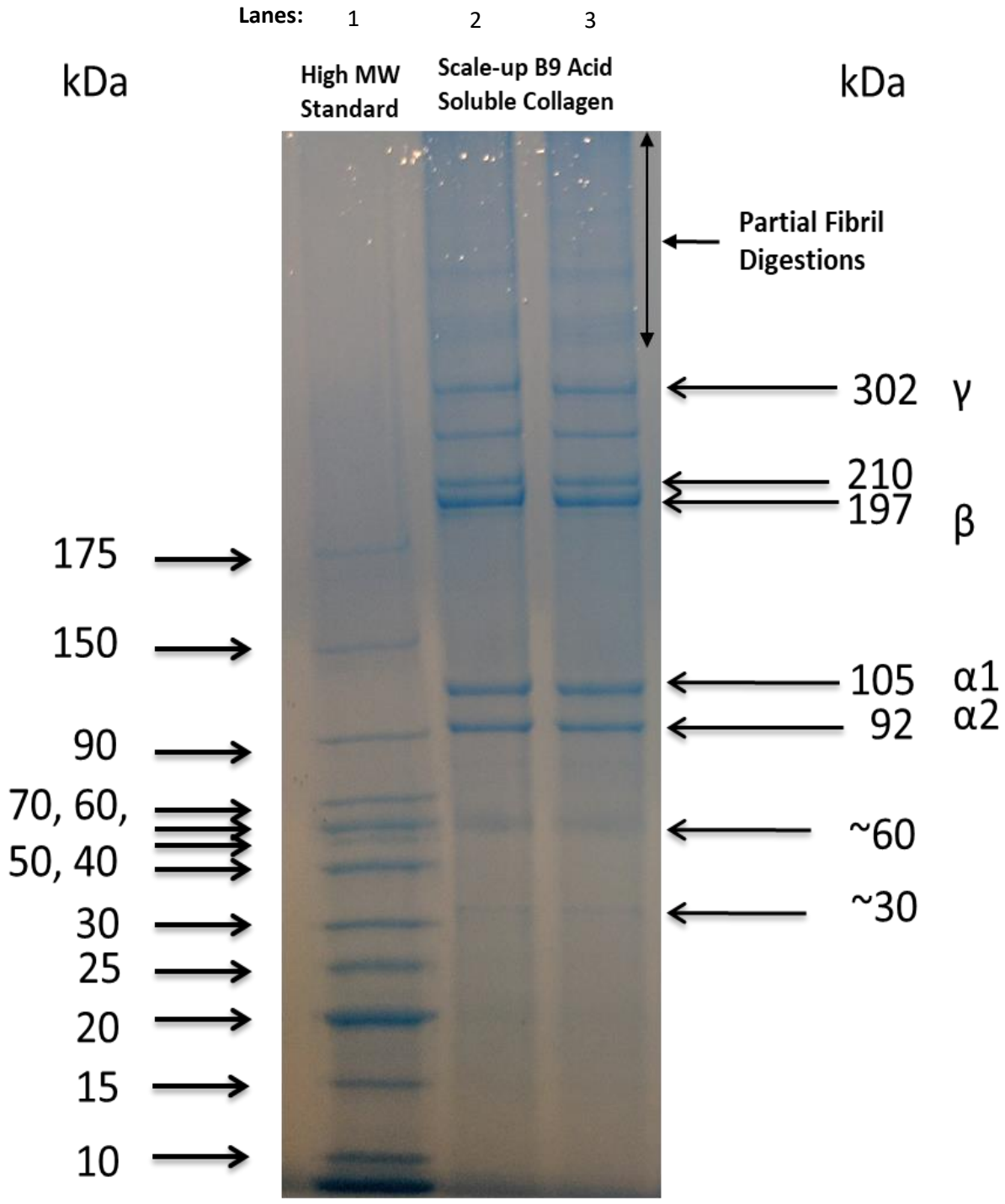

Figure 4.13 SDS PAGE displaying scale-up B9 extract (Lanes 2-3) containing alpha, beta and gamma collagen chains, with very little residual 30 and 60kDa peptides (n=2).

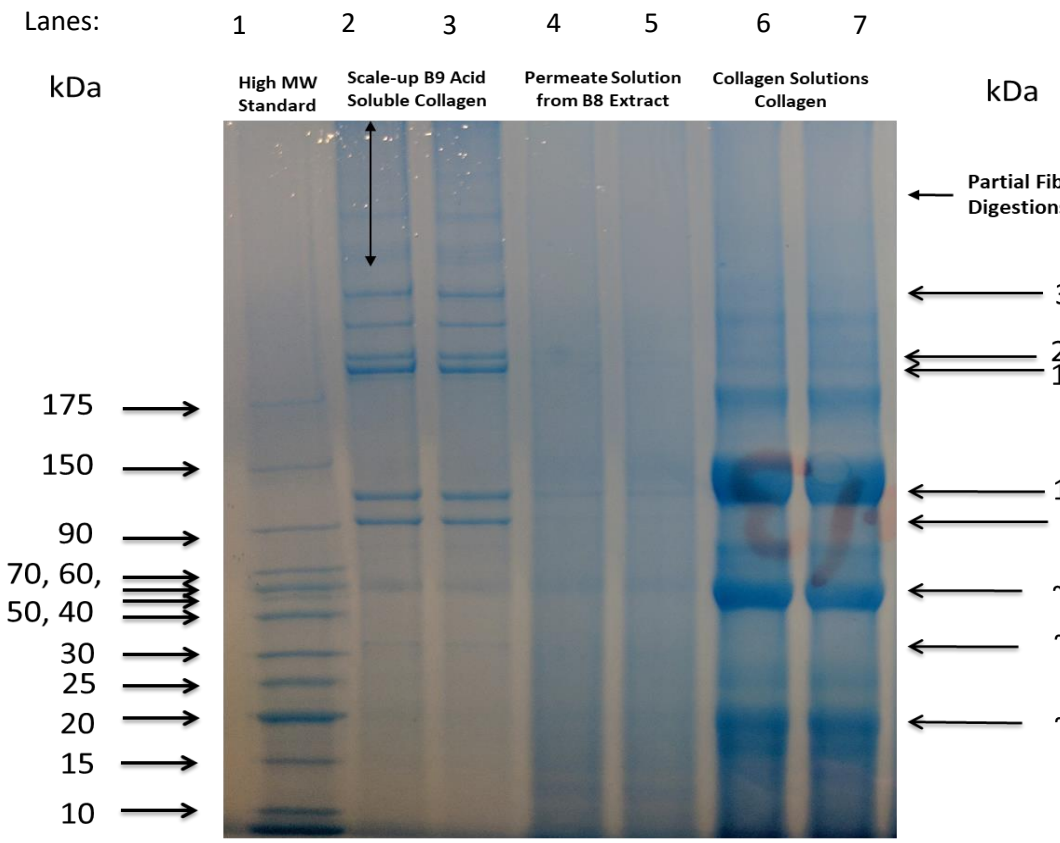

Figure 4.14 Expanded SDS PAGE comparing the residual impurities present within scale-up B supplied by Collagen Solutions PLC (n=2).

The average flow rate for the 100L scale up batches, as seen in Figure 4.13 and Figure 4.14 was assessed and found a significant increase in flow rate between initial NaOH diafiltration in stage 2 and the final diafiltration of acid solubilised collagen in stage 8 by t-test ($P < .05$) (Excel analysis ToolPak) as seen in Table 4.4. This hints to a reduction in membrane caking, and easier pump action due to large quantities of impurities within the sample being removed that allows filtration to occur with higher flow rates for each progressive stage despite equal or higher pressures being used.

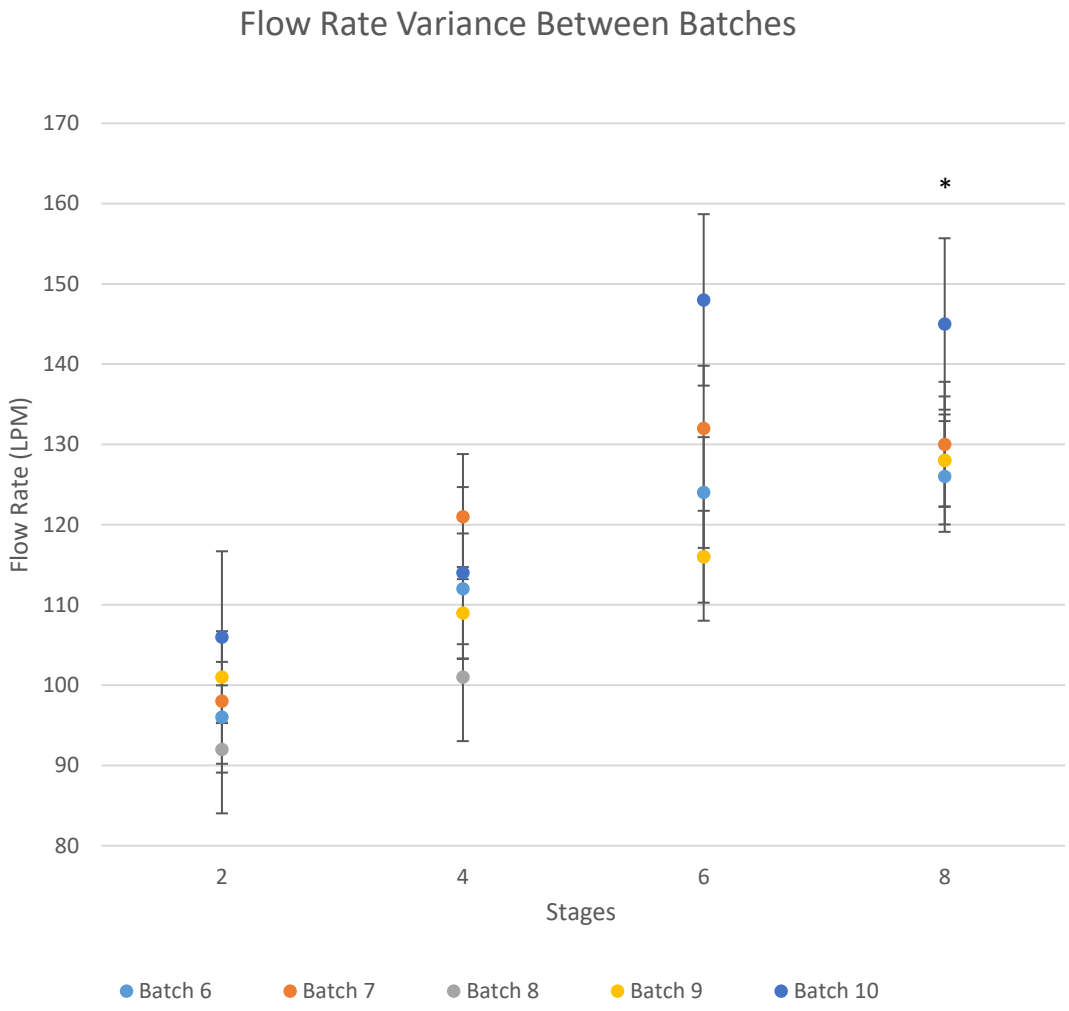

Figure 4.15 Graph comparing the flow rates at different active stages for scale up batches 6-10. Flow rate was shown to significantly increase ($P < .05$) between NaOH diafiltration (stage 2) and the third acid extract diafiltration cycle (stage 8). Error bars represent standard error of the mean (n=3).

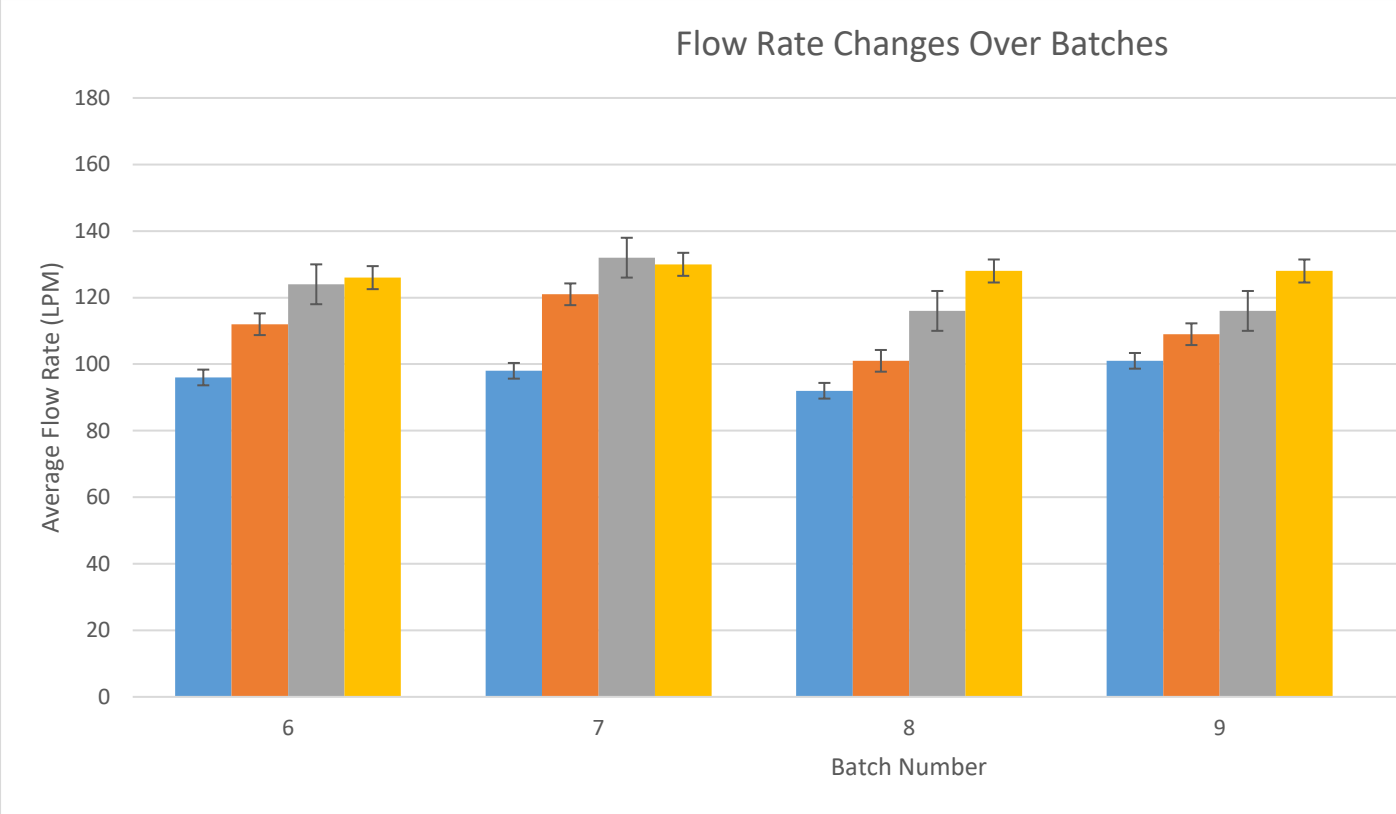

Figure 4.16 Chart comparing the flow rates at different active stages for scale up batches 6-10 standard error of the mean (n=3).

Table 4.4 t-test comparing change in flow rate for scale up batches 6-10 between stage 2 and stage 8.

Stage 2 Flow Rate	**Stage 8 Flow Rate**	
96	126	
98	130	
92	128	
101	128	
106	145	
t-Test: Two-Sample Assuming Unequal Variances		
	Variable 1	Variable 2
Mean	98.6	131.4
Variance	27.8	59.8
Observations	5	5
Hypothesized Mean Difference	0	
df	7	
t Stat	-7.836223114	
P(T<=t) one-tail	4.97825E-05	
t Critical one-tail	1.894578605	
P(T<=t) two-tail	0.000103994	
t Critical two-tail	2.364624252	

Permeate rate was examined for changes across active stages for 100L scale up batches 6-10, the results are presented in Figure 4.17 where permeate rate was shown to significantly increase in both 50kDa (6-7) and 0.2µm (8-10) setups when examined by students t-test ($P < .05$). Finally, yield was assessed across the 10 scale-up extractions and was shown to significantly increase when moving from the 20L scale to the 100L scale ($P < .05$, n=5), as seen in Figure 4.16.

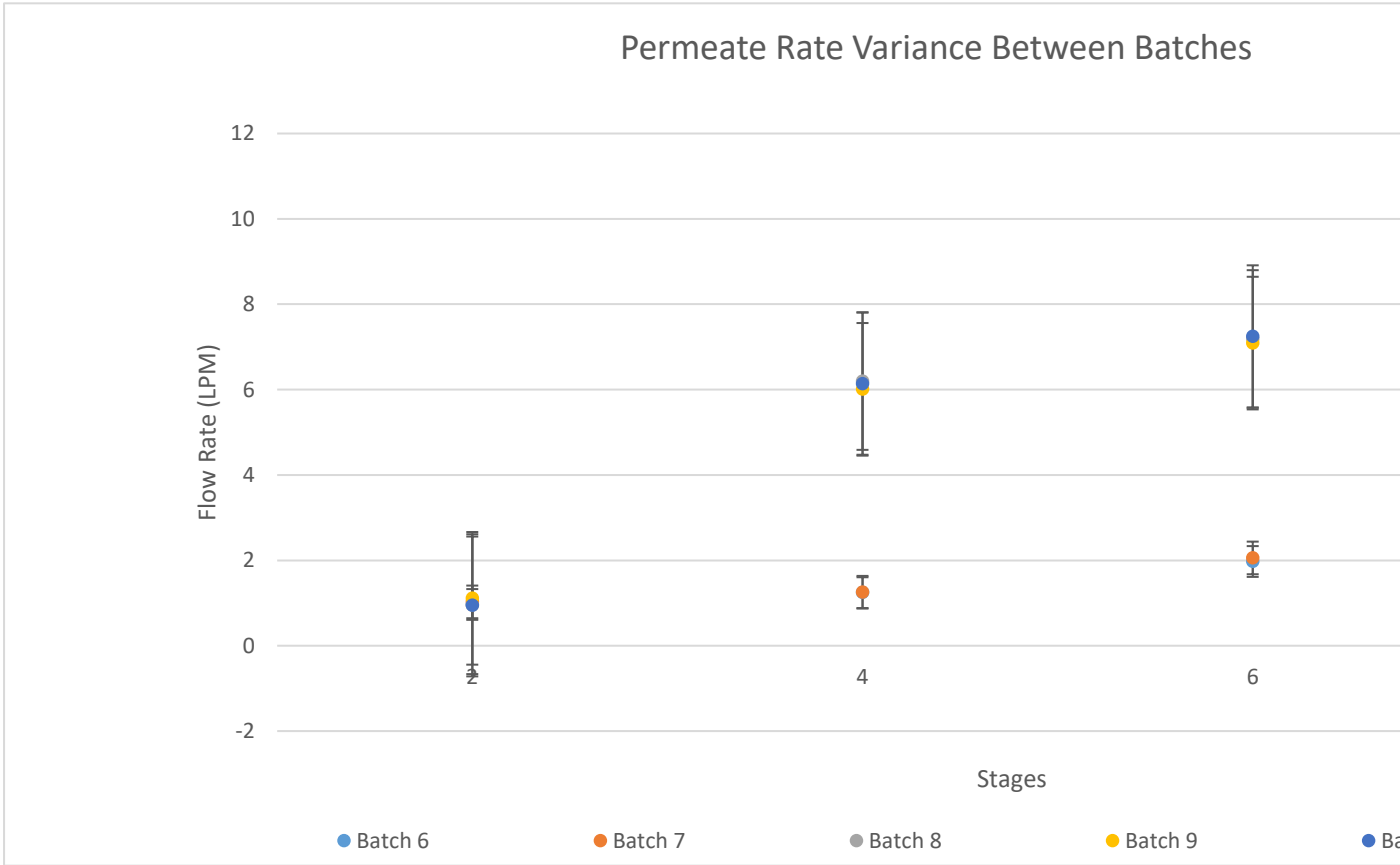

Figure 4.17 Graph displaying change of permeate rate between active stages of scale up batch 0.2µm setups showed a significant increase in flow rate between stage 2 and 8 (P < .05 for ba batches 7-10 and P < .05 for batches 6-10 combined). Error bars represent standard error of t

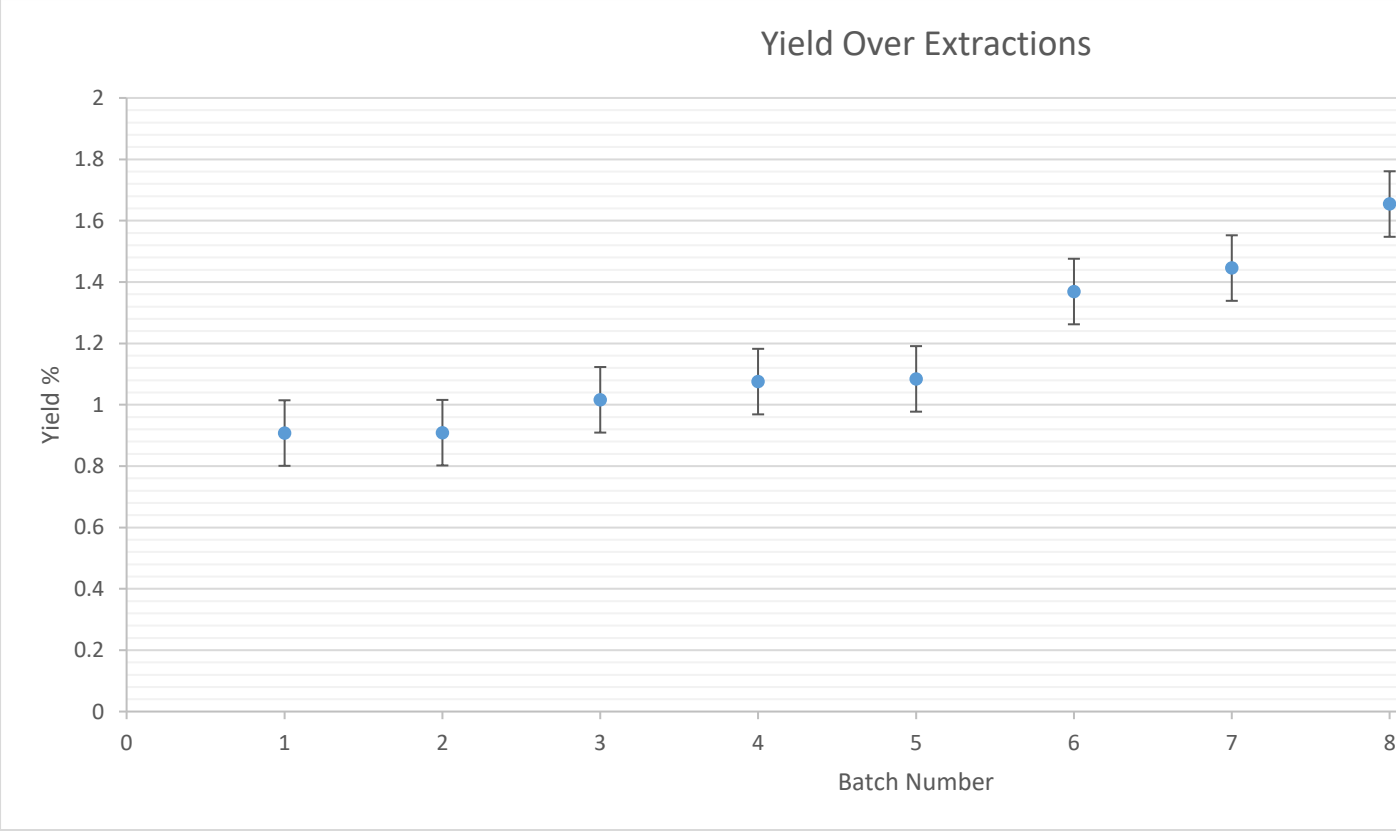

Figure 4.18 Graph displaying yield % over scale up batches 1-10. Collagen yield is shown to s
20L (1-5) and 100L (6-10) systems (P < .05, n=10). Error Bars represent standard error of the

4.11 Total Error

For the starting weights of raw jellyfish, each bucket was expected to have a weight of 20 kg. The average starting weight was 21.35 kg. This gave an error of 6.3%. For the flow rate of 20L batches, an average retentate flow rate of 40 LPM was expected. The average across 20L batches was 35 LPM. This gave an error of 14.3 %. For the permeate rate of batches 20L batches, a flow rate of 0.12 LPM was expected. The average permeate rate was 0.126 LPM, giving an error of 4.6 %.

For the flow rate of 100L batches, an average flow rate of 100 LPM was expected. The average across the batches was 117 LPM. This gave an error of 14.6%.
For the permeate rate of 50kDa 100L batches, an average permeate rate of 1.5 LPM was expected. The average across the batches was 1.7 LPM. This gave an error of 12.9%.
For liquid aliquots an estimated 5% error was assumed.
For weight determination, a 5% error was assumed.

The average error for these variables was 9%, giving a total error estimate for 100L batches of 9.0%. This value should be considered when examining the statistical significance of extraction yields. A 9% error variance in the yield determination would support the above data showing statistical significance ($p < .05$).

4.12 FTIR

Samples from scale up were assessed by FTIR and compared to samples of acid soluble collagen from other sources. This included type 1 rat tail collagen purchased from Sigma Aldrich, UK, jellyfish collagen provided by Collagen Solutions Plc and bovine insoluble collagen which was processed into acid soluble collagen in-house. Comparisons between batches were carried out and analysed for their similarity values. In FTIR for pharmacopeia, similarity values >95% are generally considered identical (PASS) (Gallignani et al. 2015). Values of >90% can be considered the same, although there are several differences between these, in this case it is essential to

compare peak maxima and shape to elucidate similarities and differences in content (Smith 2015).

Figure 4.17 compares the spectra obtained from jellyfish collagen that was produced using the scale-up membrane filtration method, batch 9 with jellyfish collagen supplied by Collagen Solutions Plc. The highest level of absorbance was in the amide 1 region (1658cm^{-1}) for both samples as expected. Peak picking with values at 1638cm^{-1}, which is representative of the presence of triple helix were 2.9231 and 2.8393 for membrane extracted and tradition extract respectively. Values for 1658cm^{-1}, representative of α-helices were 2.9415 and 3.5339 respectively. These are summarised in Table 4.5. This corresponds well to the SDS PAGE data presented in Figure 4.11 and Figure 4.12 for collagen solutions samples, where there was a reduction in gamma chain collagen (including alpha and beta strands which have been reduced), but a large content of helical peptides at ~30kDa and ~60kDa. Percentage homology between CS supplied collagen and B9 was 90.4403%. This figure is below 95% signifying the two samples are not identical by pharmacopeia standards, but is above 90%, showing similarities between the two samples. Interestingly, the pellet of batch 7, which was highly impure, and was subsequently centrifuged at 15,000g for one hour in an attempt to remove brown discolouration from zooplankton, scored a homology of 96.49% against commercially available collagens, further demonstrating the purity issues with the traditional extraction, and the graph can be seen in Figure 4.18.

Figure 4.19 compares the spectra obtained from scale-up jellyfish derived collagen (Batch 9) with collagen supplied by Merck Millipore, UK. The highest level of absorbance was again within the amide 1 region for both samples as expected. Peak picking values for comparative rat tail (Merck), rat tail (Sigma) or bovine samples can be seen in Table 4.5. Percentage homology between B9 jellyfish collagen and rat tail (Merck) was 56.2191%. This figure is far below the 90% threshold for similarity and is mainly due to a peak shift throughout the spectra for the Merck sample that could be caused by tensile bond strength differences, as well as an increased mass of the collagen molecule within the sample, which would signal a lower degree of solubilisation, while temperature and concentration can also contribute to this shift (Ryu, Noda, and Jung 2011).

Figure 4.20 compares the spectra obtained from scale-up jellyfish derived collagen (Batch 9) with collagen supplied by Sigma Aldrich, UK. The highest level of absorbance was within the amide 1 region for both samples as expected. % Homology between these samples was 54.4772%, signifying a large degree of variance between both rat tail samples and the scale-up batch process jellyfish derived collagens. Similarity between Sigma and Merck samples was 74.3433%. These large variances show the disparity in the consistency of collagen products that are currently available.

Figure 4.21 compares the spectra obtained from scale-up jellyfish derived collagen (Batch 9) with bovine acid soluble collagen that was processed using the membrane filtration system from insoluble collagen purchased from Sigma Aldrich, UK. Both samples have their highest peak absorbance within the amide 1 region. Homology between these samples was 62.3408%, again signifying the large variance between sources, and demonstrating the level of selectivity that FTIR expresses.

Table 4.5 Peak picking of wavenumbers which correspond to specific features of interest in collagen comparison. The content of triple helix within a sample and α-helix abundance can aid in gauging the abundance of impurities within a sample.

Expected

Wavenumber (±2cm^{-1})	B9 MCOL	B8 MCOL	Bovine ASC MCOL	Collagen Solutions Jellyfish	Sigma Rat Tail	Millipore Rat Tail	Mode & Corresponding Vibration
1658	2.9381	2.9415	2.7337	3.5339	2.7074	2.6243	A-Helix & Amide I Absorption
1647	3.0707	3.0811	2.9455	3.2818	2.8695	2.9331	Unordered
1638	2.9260	2.9231	2.9599	2.8393	3.0868	3.0256	Triple Helix (Wetzel, Post, and Lodder 2005)
1555	2.55	2.7191	2.5772	1.7628	2.5186	2.3338	Amide II Absorption

There is a noticeable increase in unordered structure from jellyfish derived sources, which supports research conducted previously that jellyfish collagen is less highly ordered with Gly-Pro-Hyp repeats, leading to a lower denaturation temperature for the marine collagen when compared with mammalian sources (Addad et al. 2011).

For all sources, amide I and triple helix modes represent the bulk of the sample, with amide II absorption lower in each collagen sample, representing a retention of gamma chain triple helix within the samples.

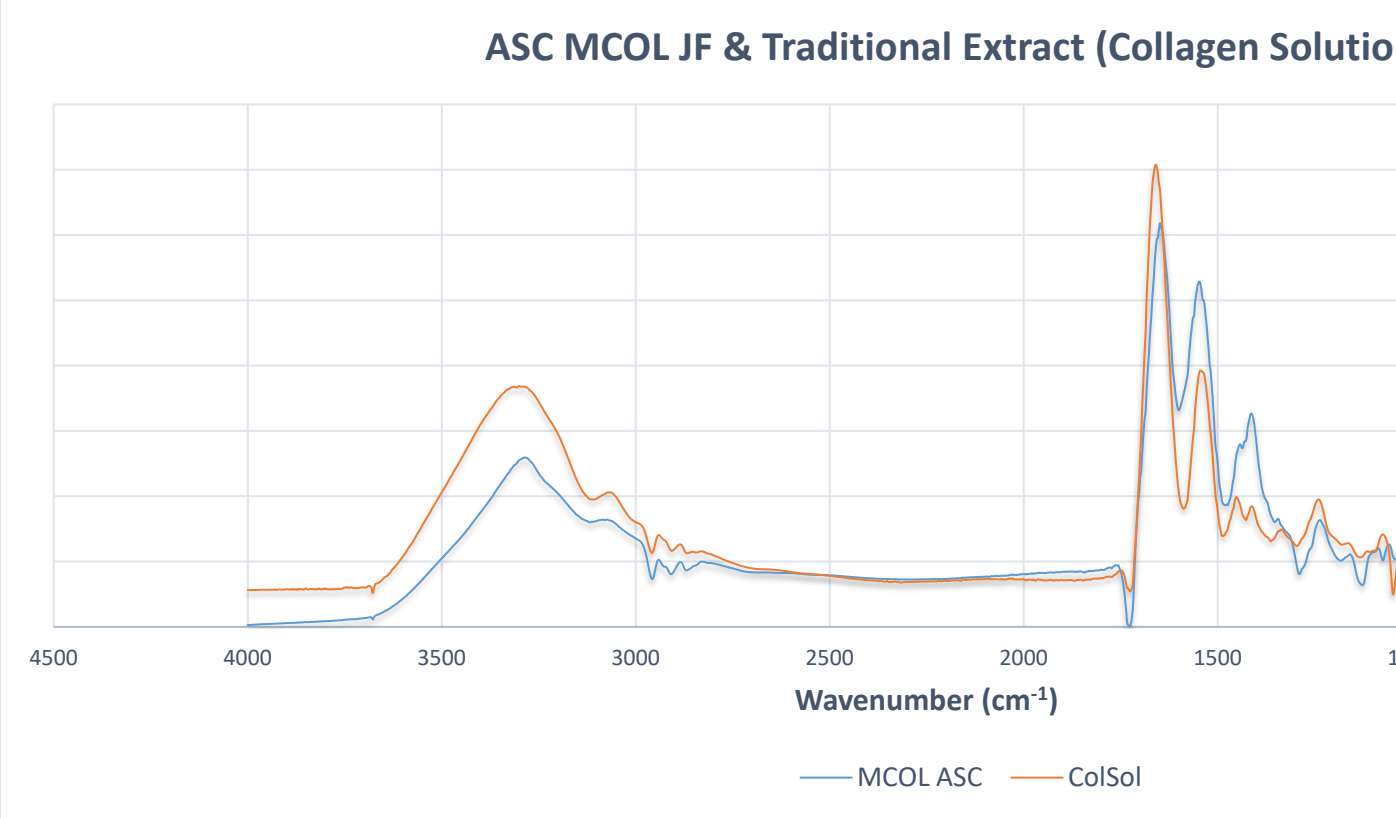

Figure 4.19 Spectral comparison of traditional extract of jellyfish derived collagen from Colla membrane filtration extracted jellyfish collagen (Scale-up batch 9) (n=2).

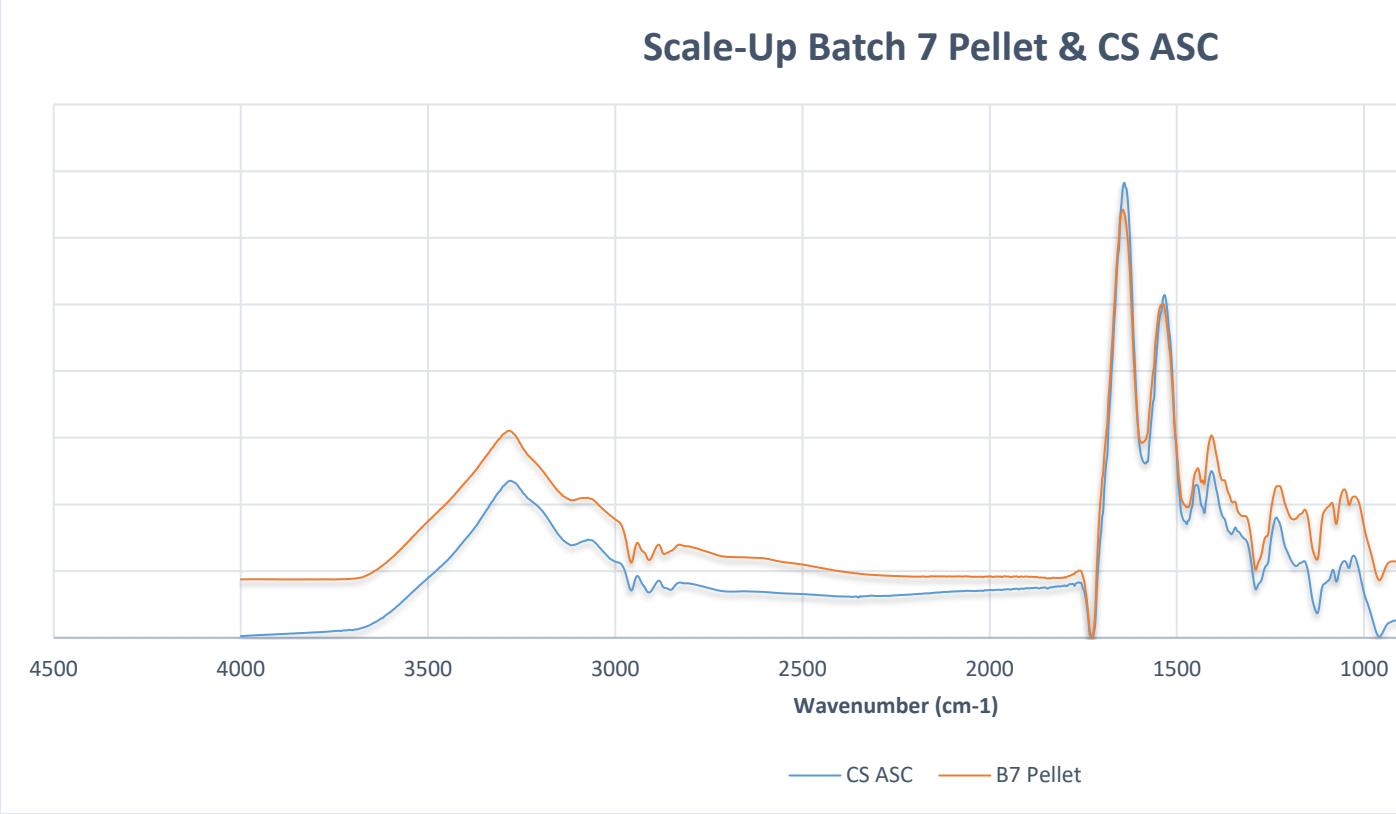

Figure 4.20 Spectral comparison of traditional extract of jellyfish derived collagen from Colla centrifuged pellet from membrane filtration extracted jellyfish collagen (Scale-up batch 7). Ho

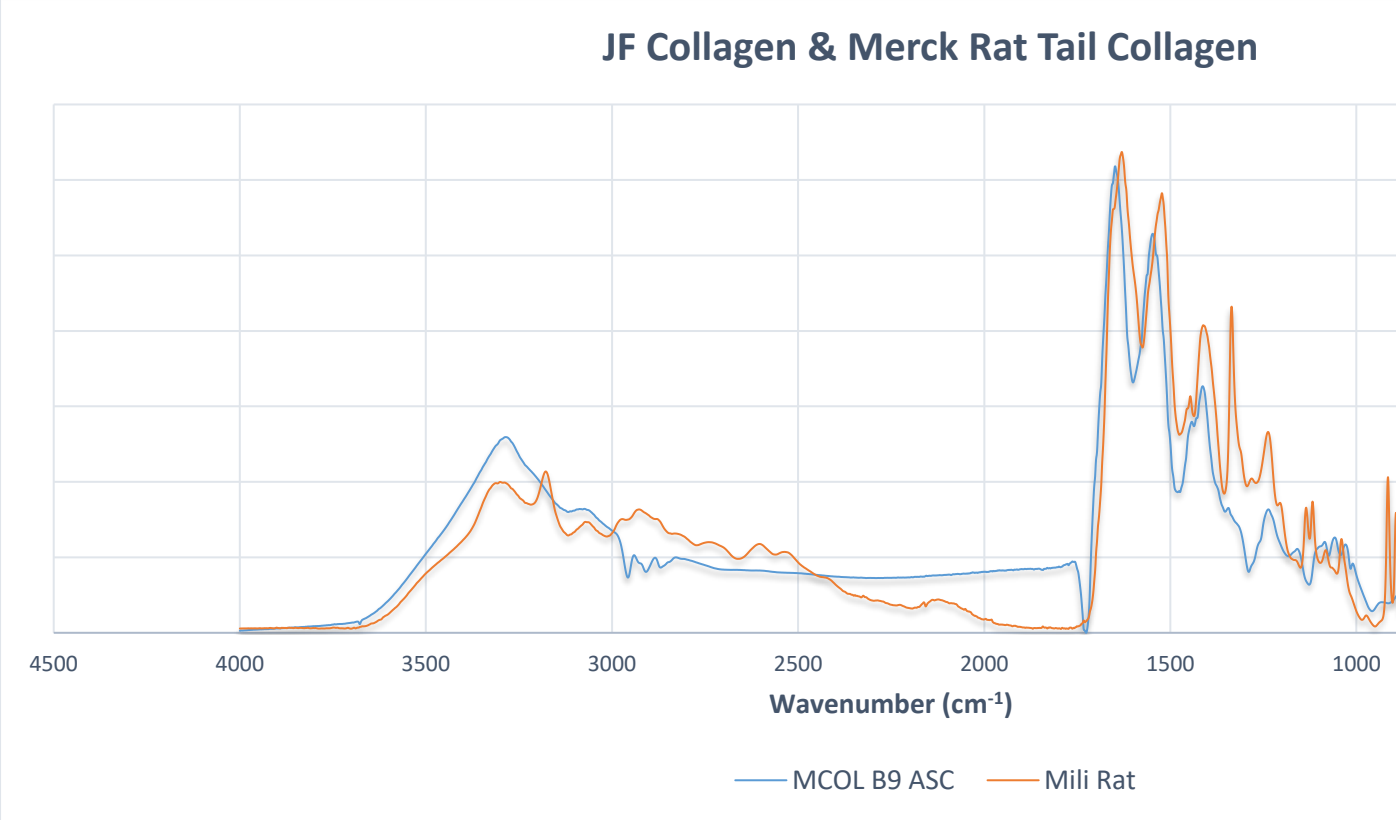

Figure 4.21 Spectral comparison of membrane filtration extracted jellyfish collagen (Scale-up purchased from Millipore, UK (n=2).

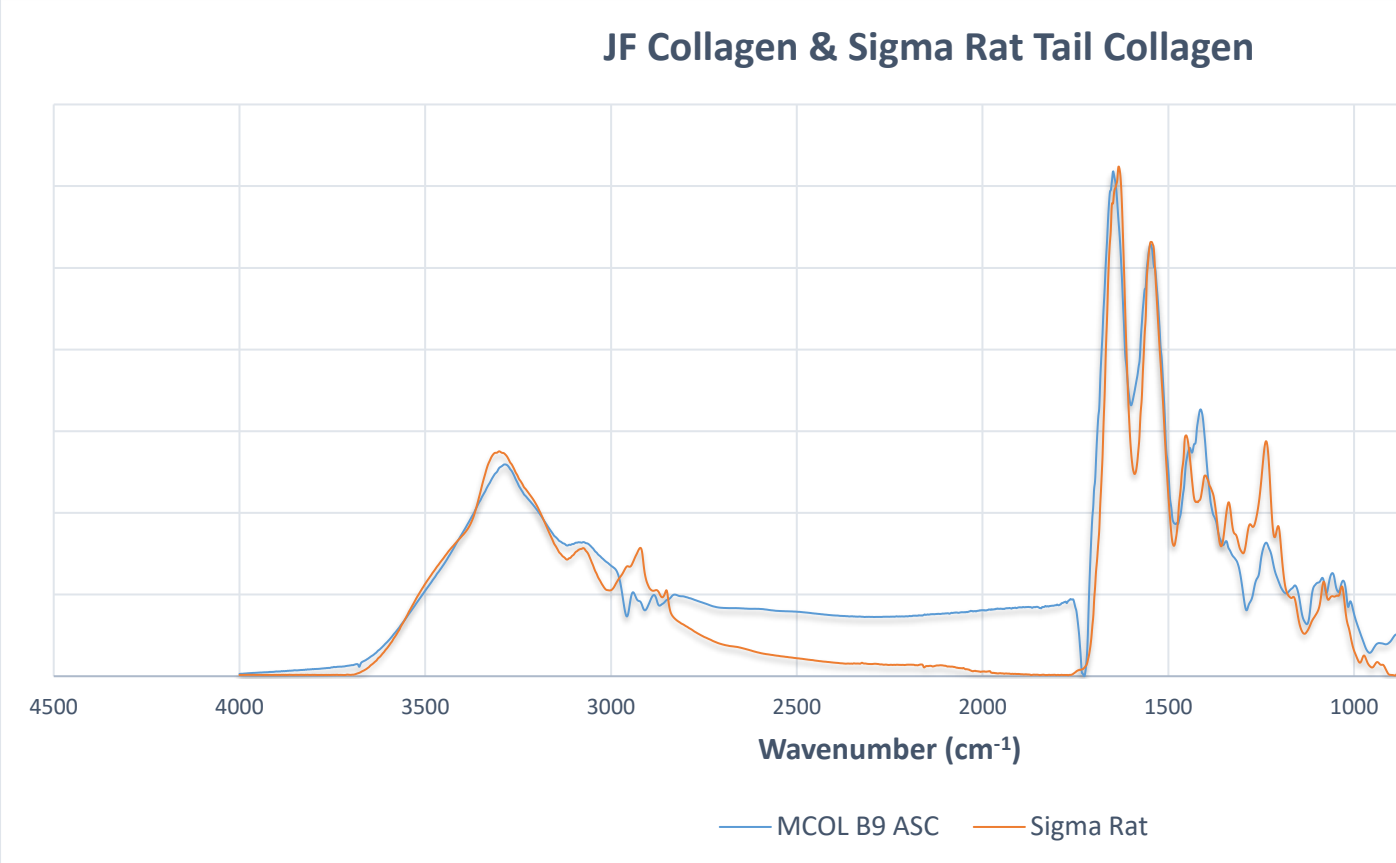

Figure 4.22 Spectral comparison of membrane filtration extracted jellyfish collagen (Scale-up purchased from Sigma Aldrich, UK (n=2).

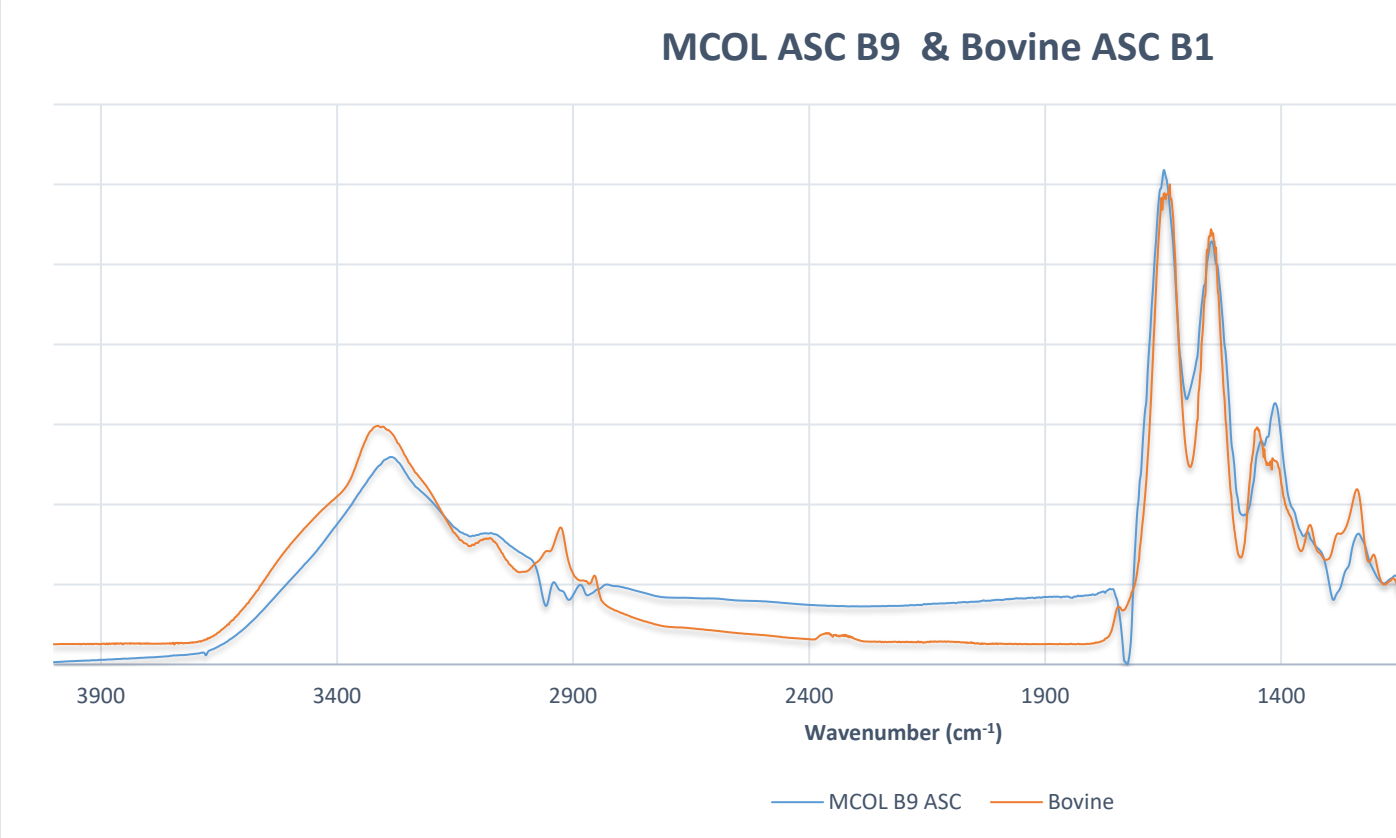

Figure 4.23 Spectral comparison of membrane filtration extracted acid soluble jellyfish collag
membrane filtration extracted acid soluble bovine collagen, processed from insoluble collagen

4.13 Operational Quality Management Considerations to Improve Collagen Purity

In order to remove colour impurities from the final collagen solutions, it was necessary to carry out significant alterations to the cleaning protocols for the starting jellyfish material. The jellyfish uses its skirt of light sensing nerves as seen in Figure 4.22 to detect bright rays, signalling a rise to the surface where it consumes zooplankton.

Figure 4.24 Rhizostomas pulmo jellyfish have a light sensing nervous system at the skirt of the bell, as seen in purple, in order to rise to the surface to feed on zooplankton.

Due to the nature of capture, the jellyfish used to extract collagen in this thesis were in the process of consuming when caught, leading to a yellow tinge in the mesoglea of tentacles during processing as seen in Figure 4.23. It was necessary to remove this material prior to processing, in order to increase the purity of the extracted collagen solutions. As it is unknown as the origin or species of each zooplankton on

the surface of the material, a lack of treatment would render the final product unsuitable for the intended applications in medical devices, so needed to be removed.

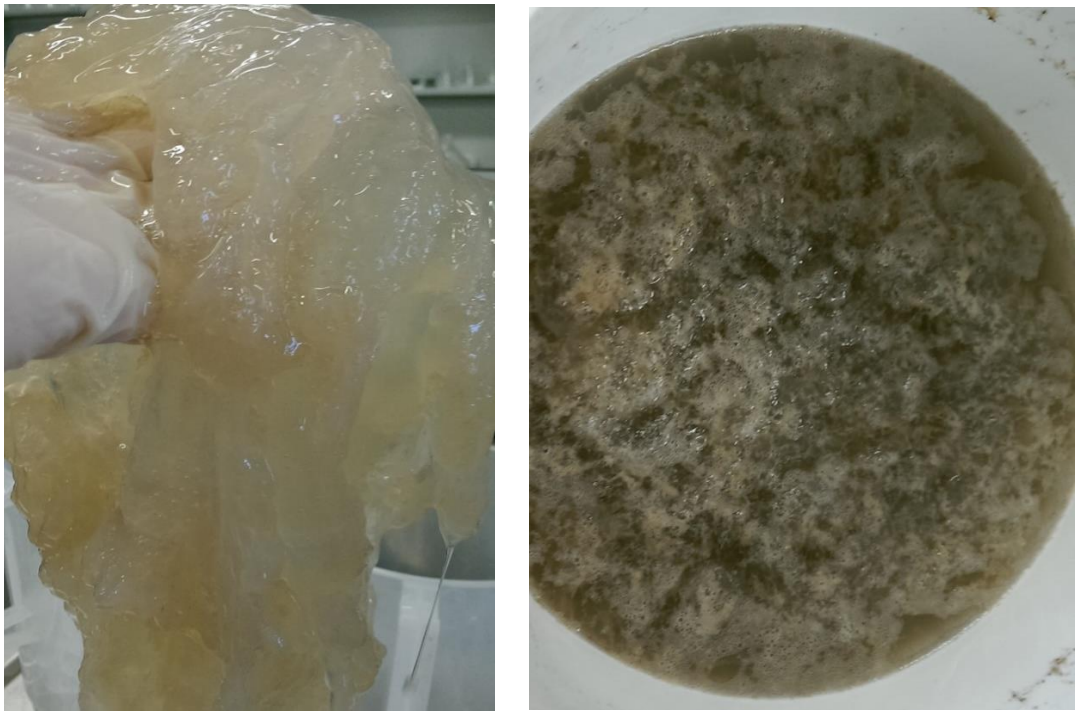

Figure 4.25 Jellyfish tentacles were covered in zooplankton prior to processing, causing a yellow / brown colour in the final product.

In order to remove the zooplankton contaminant from the starting material, it was necessary to wash each set of tentacles extensively in water. The water was required to be maintained at 10°C as higher temperatures caused the jellyfish structure to disintegrate completely within the washing solution, leaving very little solid material for processing. It was often not possible to completely remove the zooplankton from the tentacles without also losing all starting material, so a balance between cleanliness and yield was established, with final levels similar to those seen in Figure 4.24a. Once the tentacles were sufficiently cleaned, it was possible to observe the fibrils of collagen within sections of the tentacles as striations when using a digital camera microscope as in Figure 4.24b.

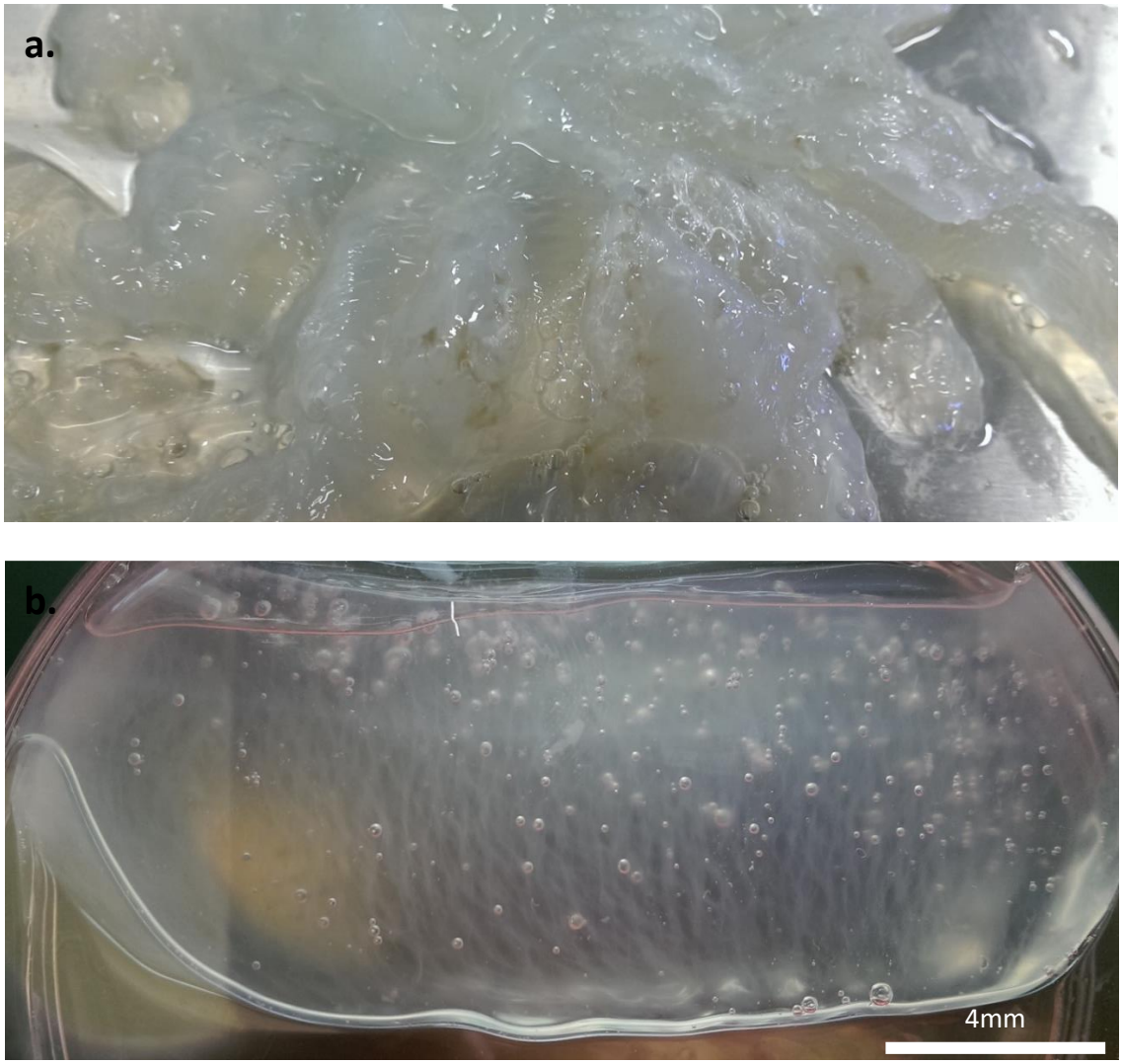

Figure 4.26 a) Remaining zooplankton on jellyfish tentacles was sufficiently low that any remaining impurities would be destroyed and removed during sodium hydroxide and acetic acid stages. b) Striations within the tentacle can be observed using a digital microscope camera once all zooplankton have been removed, signalling bundles of collagen fibres within the structure. Scale bar = 4mm.

Other methods for the removal of contaminant solids were attempted during the optimisation of scale up, including manual filtering of the NaOH stage collagen solution through cheesecloth or muslin, in similar manner to the traditional extraction. These methods were unsuccessful due to the rate of clogging that was experienced, and the loss of extract solution when the cloth required changing. It was therefore a critical point that contaminants were removed prior to blending, to ensure product quality and purity was reached.

The outcome of these extensive cleaning procedures was evident from the colour and purity of the collagen which was extracted. Figure 4.25a displays the collagen resulting from improper removal of zooplankton from the jellyfish tentacles prior to extraction, while Figure 4.25b demonstrates the purity obtained once the contaminants have been removed. Interestingly, it was not possible to remove the colour from the collagen solution after extraction was complete. Centrifugation at 18,000G was carried out in multiple passes but the pigment was retained alongside the collagen within the supernatant.

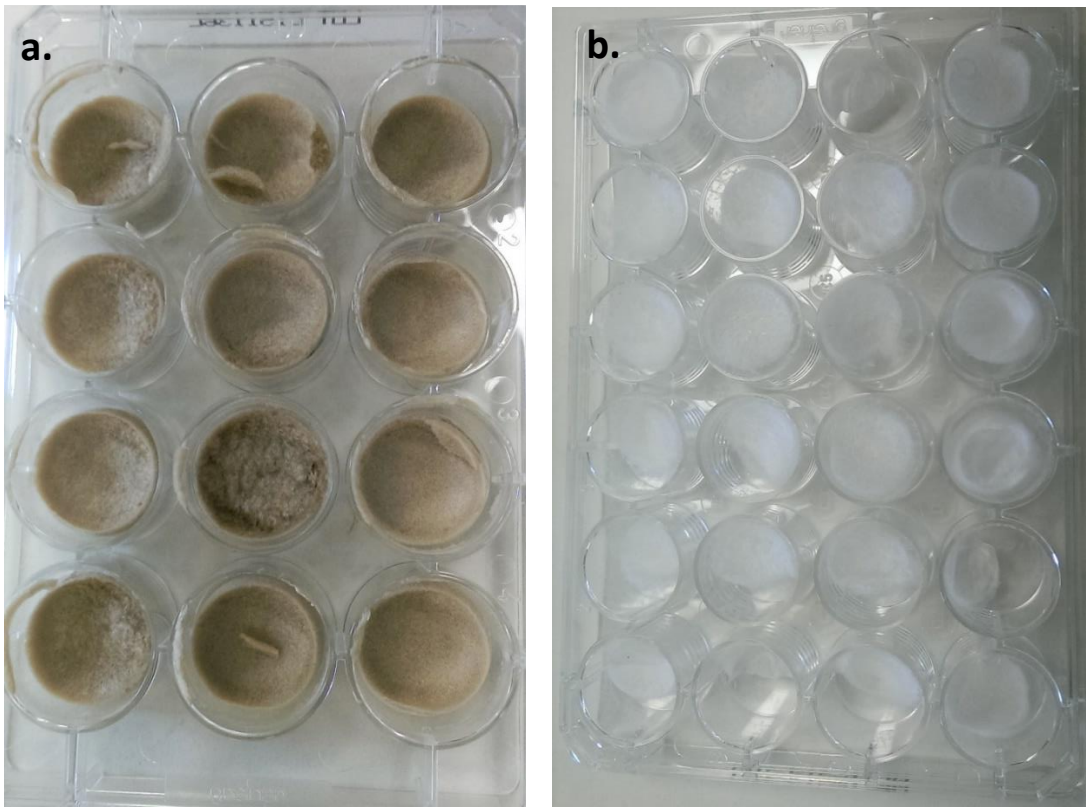

Figure 4.27 a) Batch 6 jellyfish did not undergo zooplankton removal, leading to collagen that was brown in colour, which could not be removed through centrifugation. b) Batch 7 jellyfish underwent zooplankton removal, leading to collagen which was white in colour.

4.14 Conclusions

Throughout this chapter, a novel method for the scalable extraction of collagen from the Rhizostomas pulmo jellyfish was designed, constructed and tested for its ability to produce high purity, native acid soluble collagen. The chapter compared the traditional extraction process which has been used by others (Barzideh et al. 2014a; Song et al. 2006; Addad et al. 2011), with a process which is based upon the use of hollow fibre membrane systems in a tangential flow filtration setup. The collagen produced was quantitatively assessed for purity and yield through characterisation techniques including SDS PAGE, FTIR and common protein assays such as Lowry. Qualitative assessments for colour, clarity and viscosity were used to optimise the process, with a particular focus on the use of pre-processing stages to remove contaminant zooplankton from the jellyfish tentacles.

The scale-up membrane system utilised the qualities of the 50,000 NMWCO hollow fibre membranes in order to effectively retain the alpha, beta and gamma chains of solubilised collagen, while allowing the effective removal of peptide fragments which often contaminate jellyfish collagen extracts, which are not easily removed by centrifugation at high speed. The use of this membrane allowed for very little loss of protein despite thousands of passes per extract, as can be seen in the various concentrated permeates throughout the scale up process. It was because of the retentive abilities of the membrane system that a yield of around 1.5% was consistently obtained, with the removal of the need for cheesecloth or muslin filtration allowing for yields above 1.75% to be achieved without the use of pepsin. These yields are approaching the theoretical maximum which can be achieved using partially dehydrated jellyfish which have a maximum collagen quantity of ~330g / 10kg of starting material, equivalent to 330g / 20kg of fresh caught jellyfish, due to natural water loss during freeze-thaw.

The use of pre-processing stages allowed for the contaminant removal which was reducing solution clarity and giving a brown discolouration to the material which could not be removed by centrifugation.

SDS PAGE analysis of extracts revealed that the use of speed-controlled pump systems allowed for a gentle ramp, which aided in the prevention of peptide formation, as well as enabling the retention of high MW collagen gamma chains, and in many

instances (Scale-up batches 8-10), the retention of fibrillar collagen within the extract. The protein purity of collagen solutions was shown to increase significantly, with the levels of protein which was not within alpha, beta or gamma regions being reduced to minimum detection levels (~10µg/mL), which equates to less than 0.5% of the extract. With a collagen protein purity of > 99%, this would represent a highly pure animal derived type I acid soluble collagen, further confirmed with chromogenic Limulus amoebocyte lysate tests, where endotoxin levels were at < 0.5 EU / mL when testing as described by .

FTIR comparisons of commercially available collagens revealed the current market problems with the reliability of collagen from different sources, where samples are often <75% in similarity, far below the pharmacopeia standard of 95% similarity to be deemed chemically acceptable. Internal extracts showed >95%, signifying the repeatability of the membrane process.

Peak picking of FTIR results demonstrated elevated levels of unordered structure within jellyfish derived collagen samples, in consensus with previous research into the amino acid structure of marine collagens, and its relation to temperature stability as demonstrated by (Addad et al. 2011).

The membrane extraction process has proven to be a viable system for the scalable extraction of collagen from jellyfish, with yield, purity and repeatability showing great promise, especially when applied to medical device environments, where standards conformity to ISO-13485 for repeatability and standardisation of processing are essential. The results of this chapter are supported by similar findings for the traditional extract (Barzideh et al. 2014a; Zhang et al. 2014), as well as those using membrane processed to purify collagen as in (Chang et al. 2017; Catalina et al. 2009). This work demonstrates that the extraction of intact, native collagen chains can be achieved using a membrane-based system. This system allows for the extraction of kilogram levels of collagen, with a single operator required, while ensuring the produced material meets the purity and repeatability levels required for application in medical device use. Collagen materials are typically categorised as class III devices under ISO 13485, and as such it is essential that the material be sufficiently pure and consistent for applications in this area. The work conducted in this chapter serves as a pilot scale demonstration for the technology to be utilised in industry for the large-scale production of acid soluble collagen.

5 Single Alpha Chain Collagen – Extraction & Characterisation

5.1 Introduction

In the previous chapter a new method for the scalable production of acid soluble collagen was discussed. The previous chapter demonstrated the improved quality control placed upon the material. This material showed consistent purity while demonstrating the scalability of the process. The process created in chapter 4 produced an acid soluble collagen with intact native gamma chains. With the retention of these chains, a robust extract is obtained, improving the function of collagen for structural applications. It is hypothesised that the retention of the gamma chains in the extract causes a rigidity of the chains in solution, preventing chain entanglement from occurring. The entanglement of chains is considered crucial for processes such as electrospinning to occur. Traditionally, the use of solvents such as HFP have been used to solubilise the acid soluble collagen to permit electrospinning to occur. This has been shown to denature the collagen and is presented as a fundamental problem within the literature (Zeugolis et al. 2008a).

The material contained within this chapter introduces a new collagen-based material, termed single alpha chain collagen (SACC) and examines its isolation, purification and subsequent characterisation. This material displays enhanced solubility characteristics, without undergoing conversion to random coil as seen with gelatin extracts. It further embodies the unique ability to self-assemble, or refibrillise into the full chain extract (γ-chains) in physiological conditions.

In order to address the characteristics of this novel protein, this chapter describes the isolation of this material, followed by SDS PAGE analysis and FTIR examination to observe the unique ‘fingerprints’ of this material. This will be followed by the examination of solubility and examples of potential applications. The variance between this material and precursor acid soluble collagen from both jellyfish and bovine sources is compared.

5.2 Single Alpha Chain Isolation

The collagens produced using the extraction protocols detailed in chapter 4 were diluted accordingly to maximum reactor volume at an AcOH concentration of 0.5M in preparation for α-chain isolation. These materials were allowed to fully disperse overnight at 4°C while run under circulation loop 1 as shown in Figure 4.2 then subjected to loop 3 as shown in Figure 5.1 that comprised the inclusion of a 0.2µm hollow fibre membrane as the first filtration step. The retentate was recycled and kept at 100L with input of fresh 0.5M AcOH using a peristaltic pump and autoclaved tubing. The permeate of the system was collected aseptically into a secondary vessel that acted as a feed tank for loop 4 also shown in Figure 5.1. This permeate solution was then pumped across a 50,000 NMWCO hollow fibre membrane to concentrate the solution and allow the removal of the ~40kDa protein present in jellyfish collagen extracts.

The single α-chain collagen solution was concentrated to < 1L in all scales and collected aseptically by pumping from the sealed container using a peristaltic pump and autoclaved tubing, ready for bottling in a class II biological cabinet which was sterilised under standard cell culture practice. Namely, the use of UV irradiation and 70% ethanol spraying which was wiped down and reapplied before being left to air-dry. The subsequent material containing either pure α-chains (α1 & α2 collagen fibres) or a mixture of α-chains and β-collagen chains was then stored at 4°C for use in further characterisation or frozen at -80°C overnight and lyophilised, then stored as a dry sponge or blended into powder. The retentate from the 0.2µm filtration was concentrated to the minimum system volume (10L for 100L system) and stored at 4°C for further characterisation.

This process was followed for all extracts of SACC, which included scale up batches 7-10 and bovine insoluble collagen conversion batch 1. The use of the 0.2µm filtration system simultaneously creates a sterilised product, which acts as a further benefit to the SACC product, while many collagen products are non-sterile due to the caking effect experienced in membrane systems (Blatt et al. 1970).

The production of the novel single alpha chain collagen material, as well as its characteristics, as discussed within this chapter are subject to patent filing at the time of writing, with patent cooperation treaty (PCT) stage currently underway to protect

the information disclosed within this thesis (Filing No. GB1717134.9). Through this filing, the identification of similar but fundamentally different materials was discovered, namely the work of (Chandrakasan, Torchia, and Piez 1976) which discusses the extraction of monomeric collagen, where purified extracts of ASC were produced with up to 60% alpha chains through the process of salt precipitation to fractionate the removal of 'polymeric materials' which refer to the γ-chain content. This work, while creating an enriched alpha chain product, does not succeed in the effective removal of gamma chains or beta chains, with a further disadvantage in its lack of scalability, requiring a minimum of 3% NaCl addition in order to achieve sufficient fractionation, followed by high speed centrifugation and exhaustive dialysis. This method, while describing enriched alpha chain streams of collagen, does not significantly differ from that of other researchers such as (Senaratne, Park, and Kim 2006; Song et al. 2006; Barzideh et al. 2014b; Mocan, Tagadiuc, and Nacu 2011). Confirmation of novelty and significant difference between the SACC characteristics and methods to those of (Chandrakasan, Torchia, and Piez 1976) and other prior art has been confirmed with the filing of a patent application in relation to the material described within this chapter.

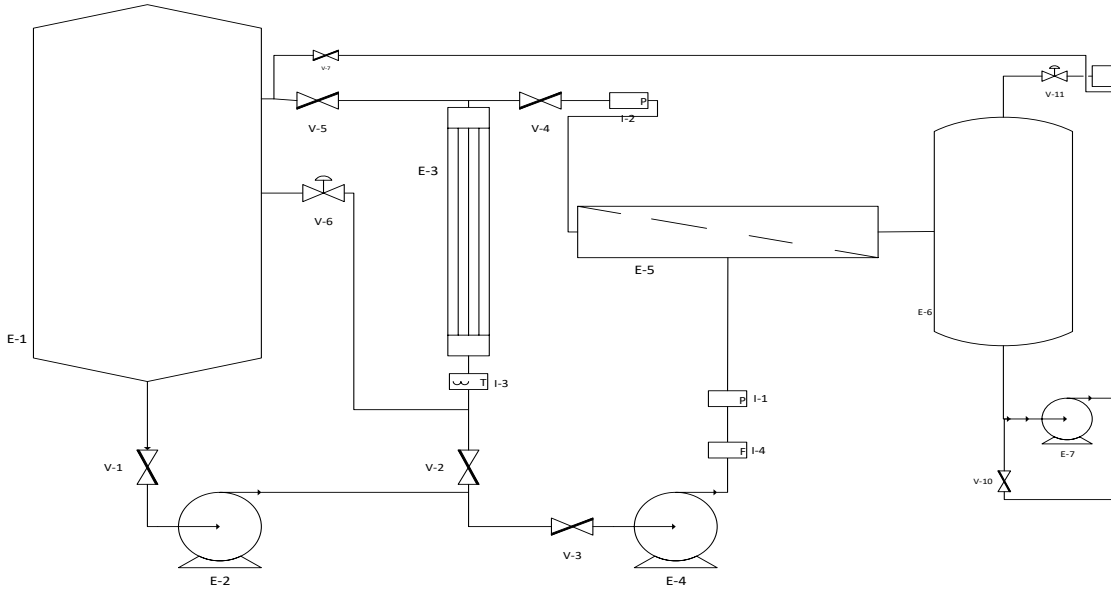

Valve List		
Valve Number	**Description**	**Valve Type**
V-1	100L Tank Isolator	Butterfly
V-2	Loop 1 / 2 Switching Point	Butterfly
V-3	Loop 2 Isolation Pre-Membrane	Butterfly
V-4	Loop 2 Isolation Post-Membrane	Butterfly
V-5	Loop 1 Return Line Isolation	Butterfly
V-6	Loop 2 Return Line Backpressure	Diaphragm
V-7	Drain Isolation / Collection / Cleaning	Butterfly
V-8	100L Drain Isolation	Butterfly
V-9	SACC Drain Isolation / Backwashing	Butterfly
V-10	SACC Collection Line Isolator	Butterfly
V-11	Backpressure Regulation	Butterfly

Equipment List	
Equipment Number	**Description**
E-1	100L Stainless Steel Tank
E-2	Centrifugal Pump
E-3	Tubular Cooler
E-4	Centrifugal Pump
E-5	0.2µm Hollow Fibre Membrane
E-6	50L SACC Collection Tank
E-7	Centrifugal Pump
E-8	50,000 NMWCO Hollow Fibre Membrane
E-9	SACC Concentrate Collection Vessel

Instrument Number	
I-1	P
I-2	P
I-3	
I-4	
I-5	

Figure 5.1 Setup for the separation of single alpha chain collagen from acid soluble collagen.

5.3 SDS PAGE Analysis

The isolated solution of alpha chain collagen was examined against both protein ladder and collagen extracts to act as standards. Figure 5.2 reveals the initial results of batch 8, where low molecular weight contaminants were present in significant quantities and partial digests were not fully removed from the solution.

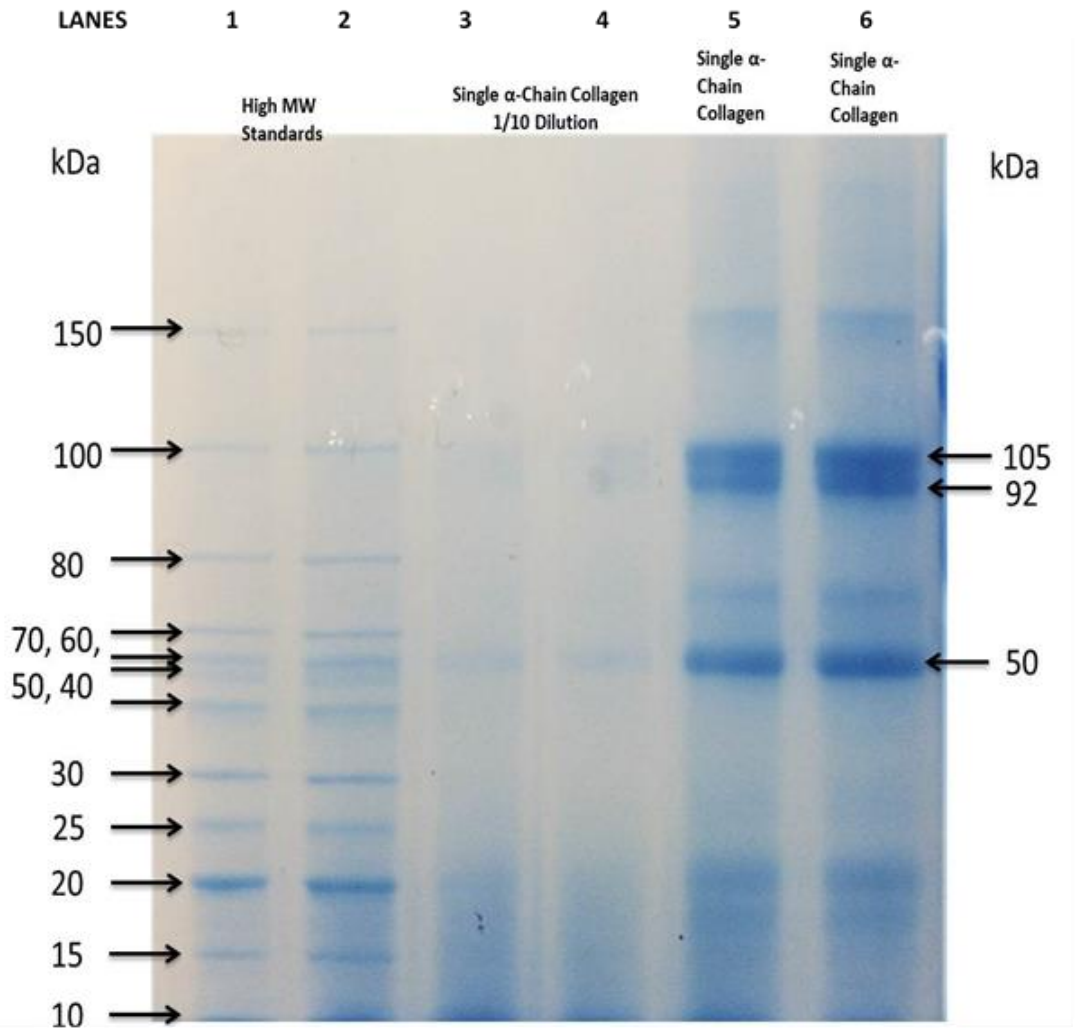

Figure 5.2 SDS PAGE of Single Alpha Chain Collagen extract from scale up batch 8. Lanes 1-2, High Molecular Weight Standard. Lanes 3-4, 1 in 10 dilution of B8 SACC solution. Lanes 5-6, Single Alpha Chain Collagen extract with impurities <20kDa which have not been removed, further partial digests at ~50kDa and 75kDa (n=2).

In order to remove the impurities from the system more effectively, further flushing of the solution with fresh 0.5M AcOH was used at ten times the volume in batch 9 and 10 extracts. For example, where final extract was collected and maintained at 5L then 50L of AcOH was used to remove impurities from the system. This led to a higher purity acid soluble collagen extract from the retentate of the 0.2µm system as can be seen in Figure 5.3.

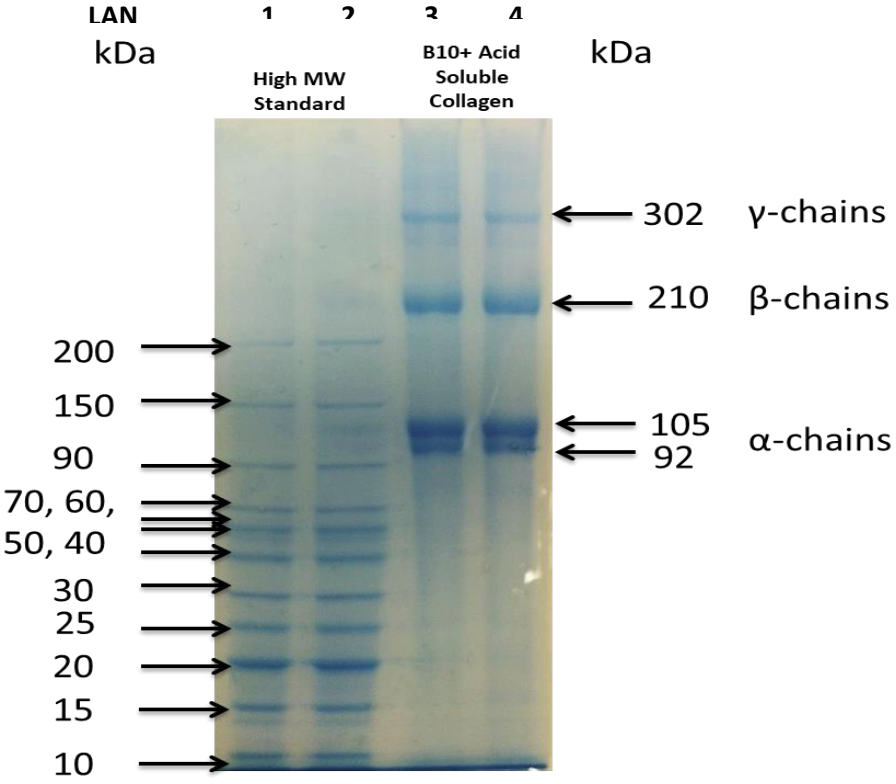

Figure 5.3 SDS PAGE displaying highly purified scale up batch 10 acid soluble collagen containing α-chains and high MW β & γ chains. α-chain quantity >60% while low molecular weight impurities have been removed (n=2).

It is clear that the use of further flushing with fresh AcOH, when combined with the operational quality management protocols described in 4.11 is able to remove the low molecular weight impurities (<90kDa) which are consistently present in jellyfish extracts seen in Figure 4.6. This led to a reduction in low molecular weight contaminants within the extract, however it was clear that the lack of regulation within

the pump system used in loop 3 as well as difficulty in controlling the temperature led to an increased quantity of low molecular weight fragments (<20kDa) within the extract during subsequent passes as also shown in 20L batch 2 (Figure 4.8), when the same pump setup was used. This can be seen in Figure 5.4 and Figure 5.5.

Overall, SACC extraction showed marked improvement in purity, where the removal of contaminant bands was possible with careful control of temperature, flow rate as well as the removal of zooplankton as with the ASC products. In order to further increase the protein purity of these extracts, it is important that higher quality pump control be implemented, to prevent the shear and cleavage of collagen chains into low molecular weight fragments. When control of the stages are optimised, a purity >95% of single α-chain collagens within the SACC extract is obtained and can be assessed against the background using ImageJ software.

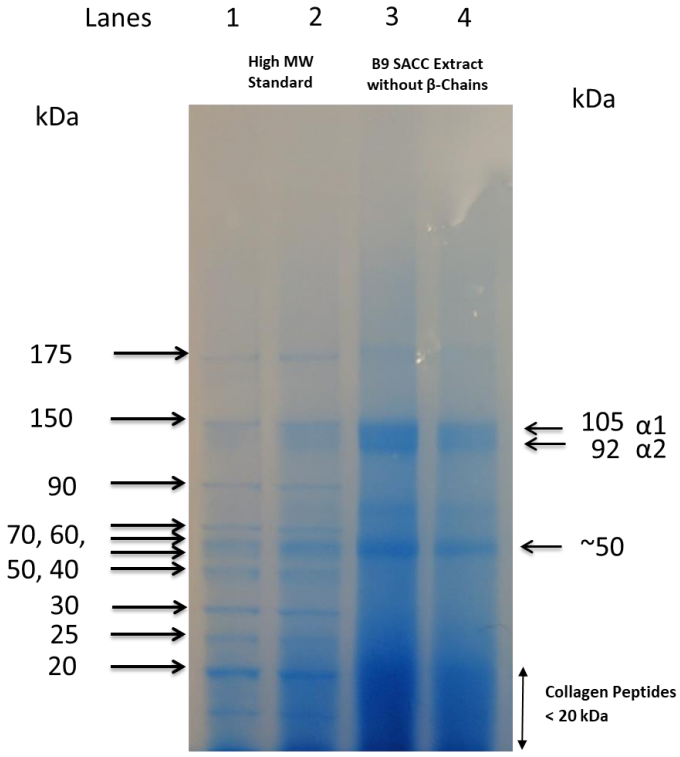

Figure 5.4 Purified SACC extract which has almost complete removal of beta chains and a distinct absence of gamma chains. The intensity of purification without specialist pumps leads to the smear of peptides <20 kDa to be produced. Lanes 1-2 High molecular weight standard. Lanes 3-4 Scale up B9 SACC extract which has been further purified to remove beta and gamma chains, but which has produced collagen peptides in the processing (n=2).

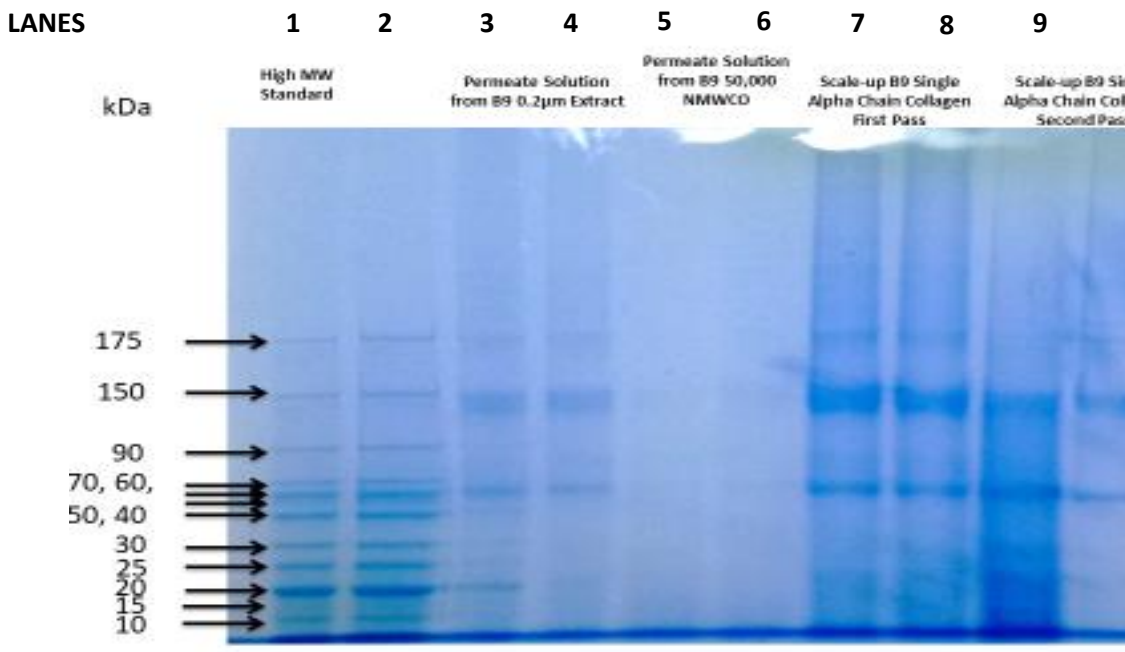

Figure 5.5 SDS PAGE of B9 Single Alpha Chain Collagen extracts, monitored during different
2, High molecular weight standard. Lanes 3-4, SACC extracts collected from permeate line du
is contaminated with lane 2 standard. Lanes 5-6, permeate from the 50,000 NMWCO membran
stage, displaying low level leaching of the protein extract at higher concentration. Lanes 7-8,
collection pass of SACC with 50L of AcOH washing. Lanes 9-10, concentrate from second coll
further 50L of AcOH washing (n-2).

5.4 FTIR

To characterise the differences between SACC extracts and ASC extracts it was necessary to carry out FTIR investigations into the structural differences. Samples were tested, background corrected and normalised as described in chapter 3.7. The association of triple helix content and absorbance at 1638 has been previously established (Petibois et al. 2006) and gives a good marker for the differentiation between ASC and SACC samples. The extracts of SACC showed a marked decrease in the amide I region at 1638 as seen in Figure 5.6. This demonstrates the lack of triple helical collagen (γ-chains) within the SACC extract, in support of the SDS PAGE findings above. By peak picking the specific values associated with each absorbance, it is possible to confirm a reduction in the quantity of triple helix within the sample, while also confirming that there was not an increase in unordered structure, suggesting the protein has not been converted to gelatin. These values can be seen in Table 5.1 and Figure 5.7 for both B10 SACC and Bovine SACC samples.

The SACC samples gave a distinct absorbance pattern which was easily differentiated from that of ASC samples, as well as gelatin samples. This shows a distinct difference between SACC and ASC, which was somewhat unexpected during the extraction of the material. Within the literature there is limited insight into this occurrence, with the work of (Chandrakasan, Torchia, and Piez 1976) describing the closest known comparison, however due to the age of the paper, techniques such as FTIR were not possible. This paper does however cite a reduction and removal of high molecular weight chains of collagen, with up to 60% monomer obtained using a salt fractionation method which as discussed above, lacks repeatability and scalability. Attempts to recreate this method were unsuccessful in yielding high levels of collagen monomers but instead yielded acid soluble collagen extracts as expected.

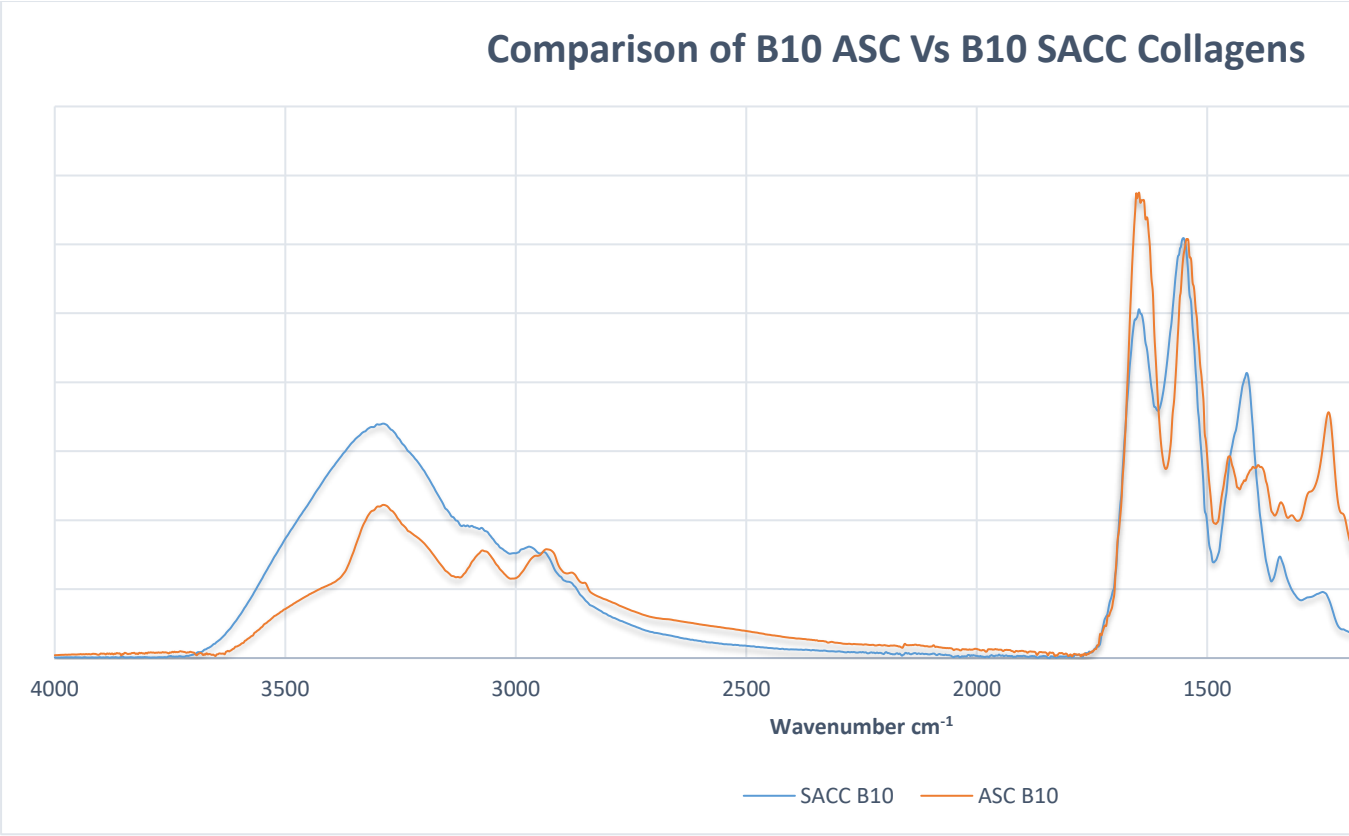

Figure 5.6 FTIR displaying a comparison between ASC and SACC extracted during scale-up b reduction in amide 1 signifying a reduction in the abundance of triple helix (γ-chains).

Table 5.1 Comparative absorbance values from acid soluble or single alpha chain collagen samples for their relative triple helix content. Defined values established in (Petibois et al. 2006).

Expected Wavenumber (±2cm^{-1})	B9 ASC	B9 SACC	B10 SACC	B10 ASC	Bovine ASC	Bovine SACC	Sigma Rat Tail	Mode & Corresponding Vibration
1690	1.658	1.803	1.056	0.981	0.998	1.253	0.820	Parallel β-Sheets
1680	2.037	2.096	1.557	1.493	1.418	1.584	1.268	Anti-Parallel β-Sheets
1668	2.569	2.520	2.125	2.447	2.158	1.959	2.170	B-Turns
1658	2.938	2.823	2.446	3.163	2.734	2.176	2.707	A-Helix
1647	3.071	3.000	2.521	3.356	2.946	2.300	2.870	Unordered
1638	2.926	2.963	2.413	3.322	2.960	2.073	3.087	Triple Helix
1625	2.580	2.799	2.074	3.007	2.558	1.846	3.108	Parallel β-Sheets
1612	2.112	2.568	1.817	2.180	1.739	1.74	2.729	B-Turns

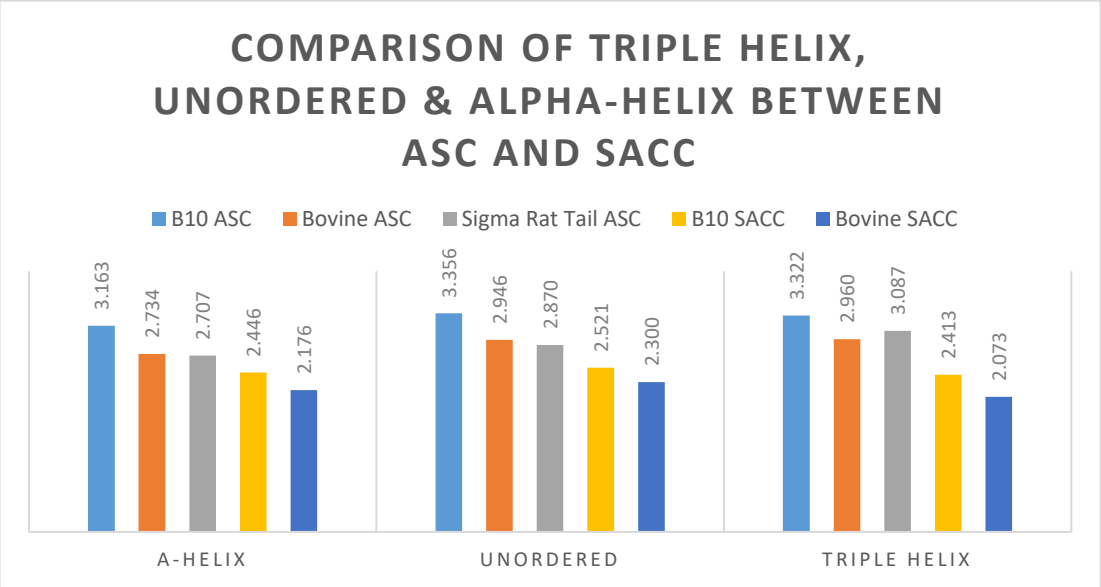

Figure 5.7 Graph displaying the reduction in triple helix content of single alpha chain collagen samples (n=3) in comparison to acid soluble collagen samples (n=3) following normalisation and background correction.

When characterising the qualities of SACC extracted from jellyfish sources, it was necessary to examine whether this same isolation procedure was possible with the bovine acid soluble extract created previously. The FTIR spectra seen in Figure 5.8 shows a large disparity in the amide 1 absorbance peak between bovine derived ASC and SACC samples, with the triple helix absorption greatly reduced. The remainder of the absorbance patterns remain relatively unchanged, in particular there was not a significant conversion to random coil at 1647 cm-1 for the bovine SACC sample, as seen in Table 5.1.

The findings of this work showed that by producing single alpha chain collagen it was possible to obtain pure α1 & α2 chains without the dimerised and trimerized forms that form the basis for collagens fibrillar structure. These chains are distinctive due to their processed nature, with the partial cleavage of non-helical ends due to acid solubilisation, enabling the maintenance of their single helix form. Their enhanced solubility raised questions as to whether the proteins had been partially denatured, however FTIR examination of vibrations relating to secondary structure has demonstrated that the only significant change is a reduction in the amide 1 region due to the absence of triple helix (γ-chain collagens). This in turn causes a change in the ratio of amide 1 and amide 2, with amide 2 becoming the more pronounced peak as seen in Figure 5.6 and Figure 5.8.

Alongside the FTIR analysis, the SDS PAGE analysis demonstrated that single alpha chain collagen possesses only α1 & α2 collagen chains, with limited β collagen chains and the absence of γ collagen chains as seen in Figure 5.4.

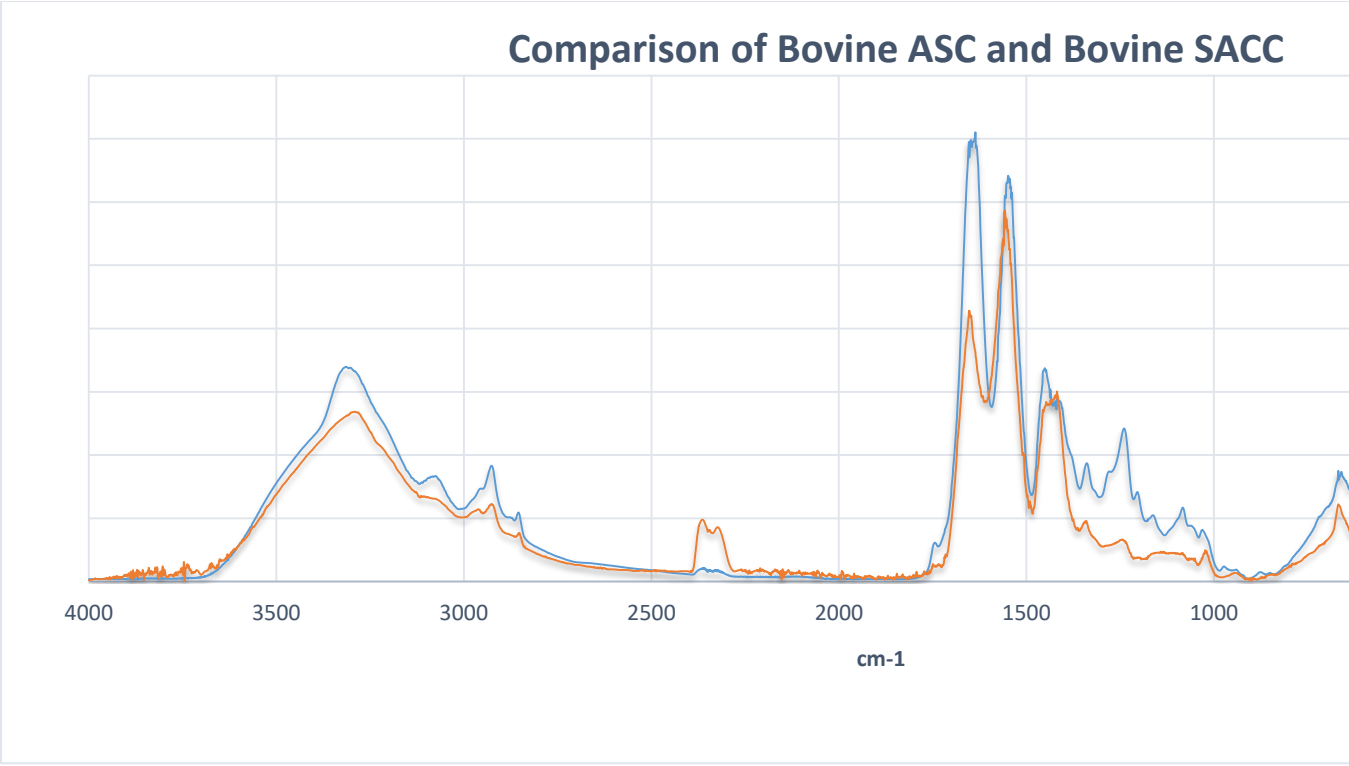

Figure 5.8 Graph displaying the FTIR Spectra comparing membrane bovine collagen extract w
spectra represents bovine SACC batch 1, blue spectra represents bovine ASC batch 1. Homolo
reduction in the amide I band.

5.5 X-Ray Diffraction Analysis

In order to further characterise the differentiation of SACC from ASC samples, x-ray diffraction (XRD) analysis was carried out to examine the presence or absence of a peak at 11Å, which has been shown to represent the presence of triple helix within a sample (Tronci, Russell, and Wood 2013; Fiorani et al. 2014; Okuyama 2008). Diffraction patterns were recorded on a Bruker D8 diffractometer in coupled θ/2θ mode using Cu k alpha (λ = 1.504 Å) radiation. kβ lines were stripped using a göbel mirror and intensity was recorded with a Linxeye 1D detector for 2θ values between 4 ° and 28 ° with a 0.02° step size.

The findings of XRD analysis show the characteristic 1.1nm peak (11Å) representing the triple helix present within ASC samples, as well as the ~0.5nm (5Å) peak which represents the isotropic amorphous region. These can be seen in Figure 5.9, while the SACC data in Figure 5.10 shows a distinct absence of the characteristic 1.1nm triple helix (Price, Lees, and Kirschner 1997), reaffirming the absence of triple helix within the SACC samples, in agreement with the SDS PAGE and FTIR findings of chapters 5.3 and 5.4 respectively.

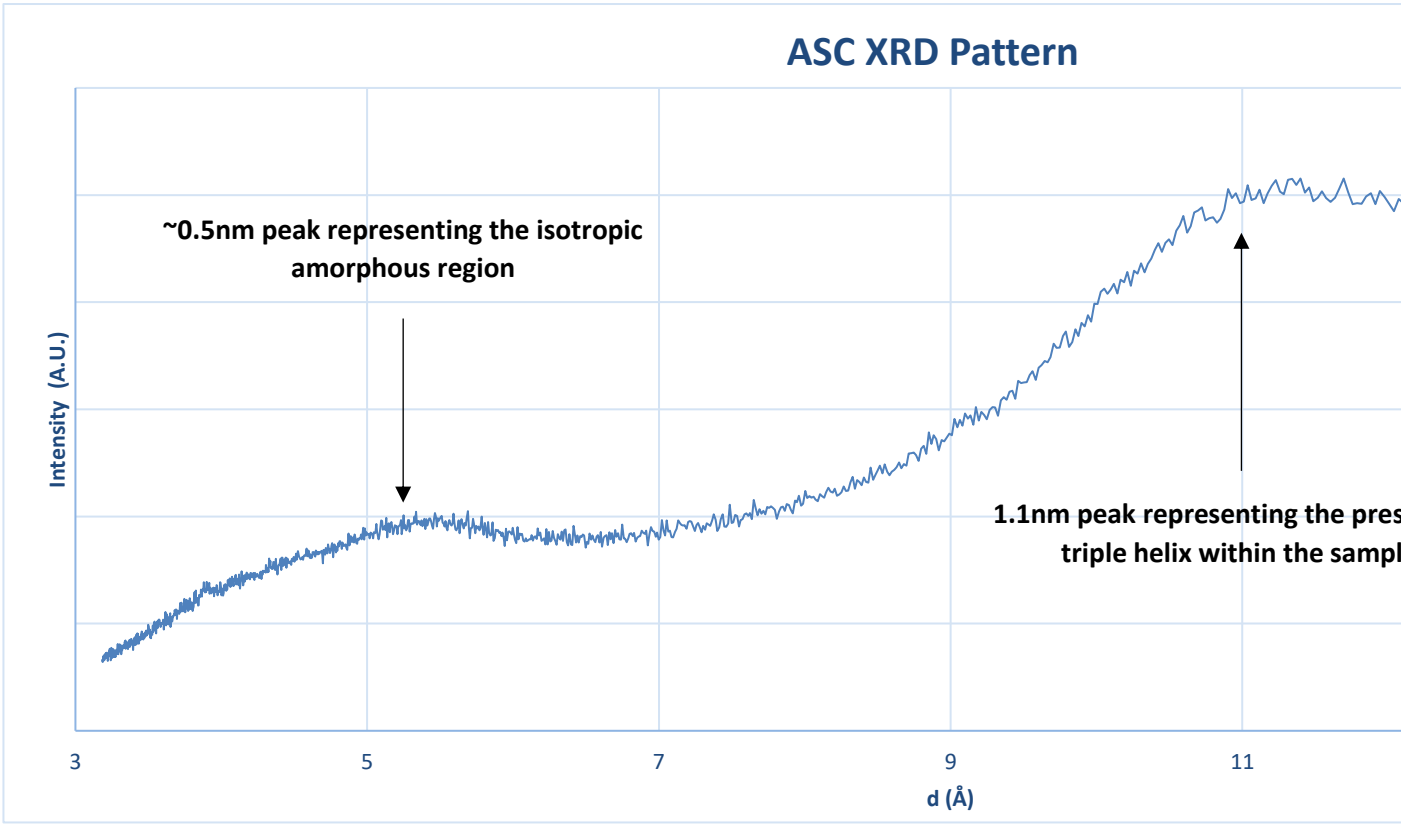

Figure 5.9 X-ray diffraction pattern for acid soluble collagen extract, showing 11Å peak, show represent the presence of triple helix within the sample (n=1).

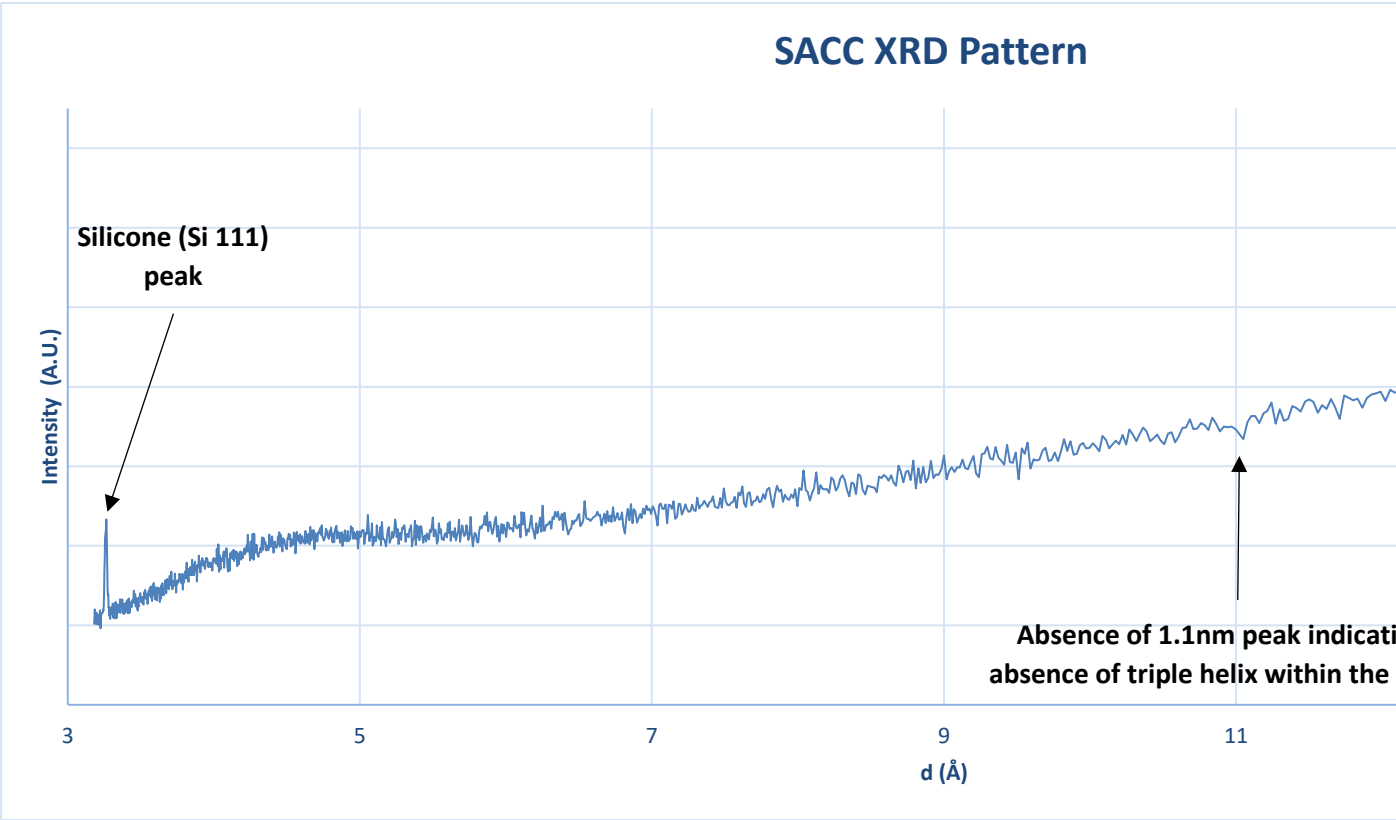

Figure 5.10 X-ray diffraction pattern for single alpha chain collagen extract, showing a distin
indicating the absence of triple helix within the sample (n=1).

5.6 Refibrillisation

During the course of the experiments, SACC was dissolved in a 1X PBS solution at a concentration of 3mg/mL and stored at 4°C. After approximately 3 months, the solution appeared to have sedimented to the bottom of the container. Upon examination by SDS PAGE it was noted that the solution, both supernatant and sediment had refibrillised to form γ-chains once more, as seen in Figure 5.11. This solution was then tested by FTIR and again, a marked increase in the amide 1 region was observed as can be seen in Figure 5.12.

The ability for SACC samples to refibrillise within physiological based conditions opens new applications for the use of SACC within medical devices, where the ability for a collagen-based material to be used in less harsh solvent systems, while retaining the ability to reform into fibrillar structures is highly desirable. The controlled use of these unique properties could open up new formulation methods such as a high-density spray which reforms when present in the wound, sealing it and providing a scaffold for the cellular processes to remodel while helping to prevent deep wound infection.

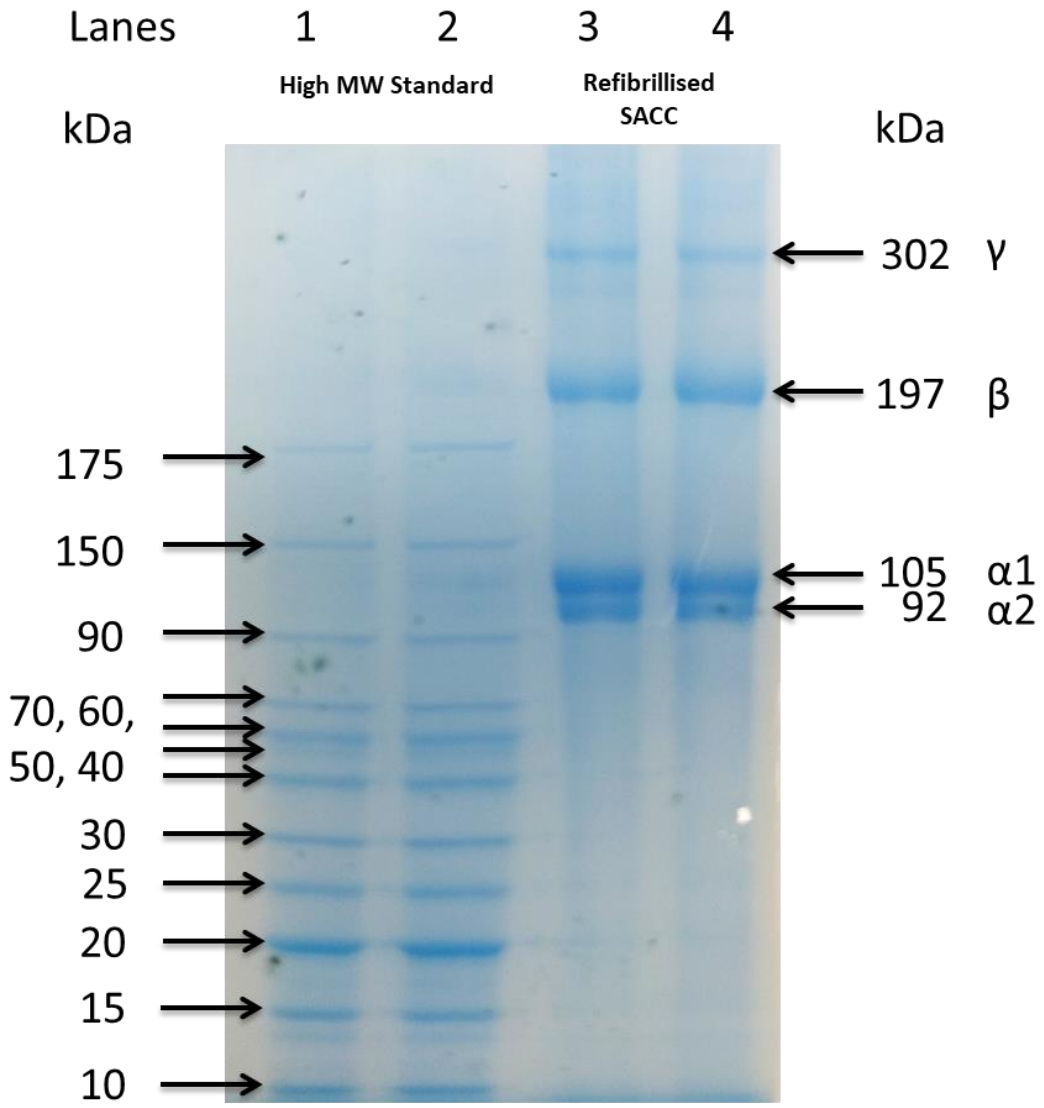

Figure 5.11 SDS PAGE of refibrillised collagen solution (liquid) where gamma chains have reformed within the extract. Extract is SACC derived from scale up batch 10. Lanes 1-2 High molecular weight ladder. Lanes 3-4 refibrillised SACC extract containing α, β and γ chains (n=2).

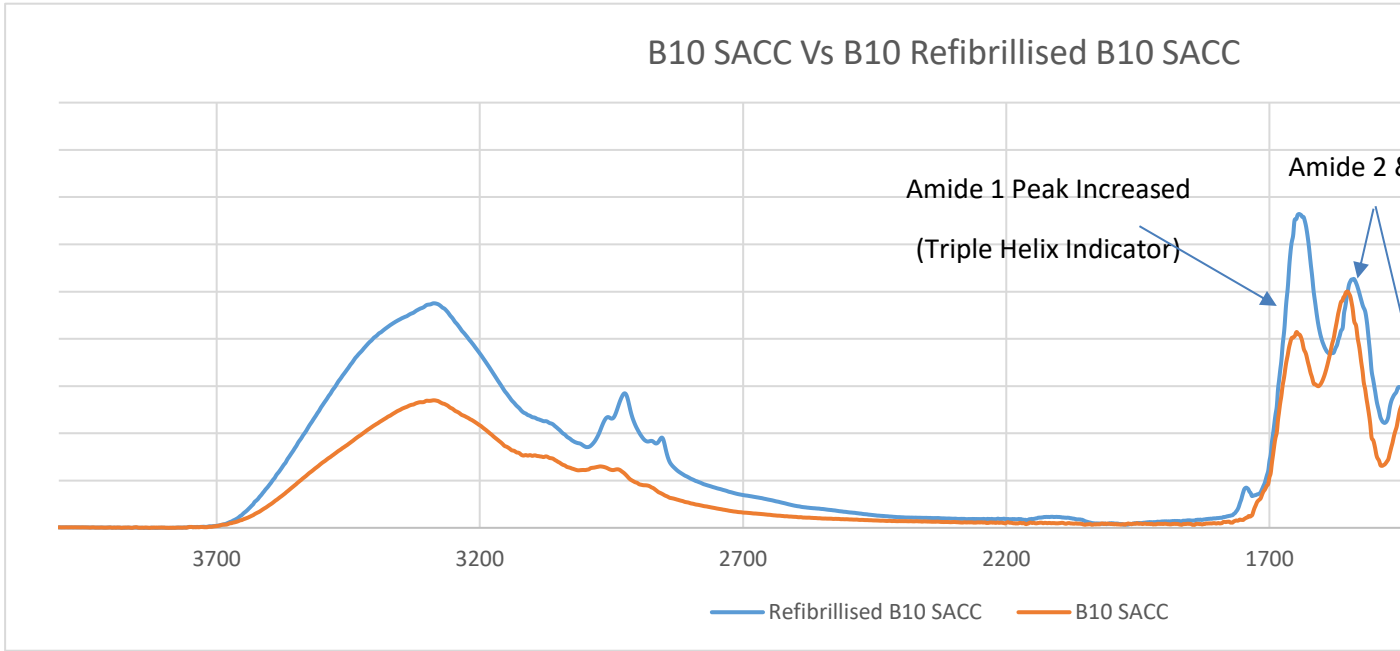

Figure 5.12 FTIR graph displaying an increase in amide 1 for refibrillised SACC samples, with remaining consistent. Extracts are SACC derived from scale up batch 10 and ASC batch 10 for

5.7 Solubility

To assess the solubility of SACC samples, dry material was dissolved in 0.5M acetic acid, 1X PBS or deionised water. In all cases it was possible to dissolve the collagen to >60% (w/v). SACC samples showed a marked increase in their solubility profile, with solutions of >95% (w/v) achieved in a solution of mild acetic acid, as well as a 1X PBS solution.

This large increase in solubility permits new fabrication methods to be explored as discussed here, where one particularly interesting application is the casting of thin films. Using SACC at concentrations > 90% (w/v) it is possible to create clear films which have medical device applications within the wound closure and dressing categories. The application of such a material would not only provide a source of collagen to the wound bed with SACC's refibrillisation profile but would also permit the sealing of the wound, whilst allowing daily observation by medical staff as is common practice (NICE 2005). It is this practice that often leads to infection within a healing wound and the ability to prevent infection whilst allowing observation would be beneficial to patient outcomes.

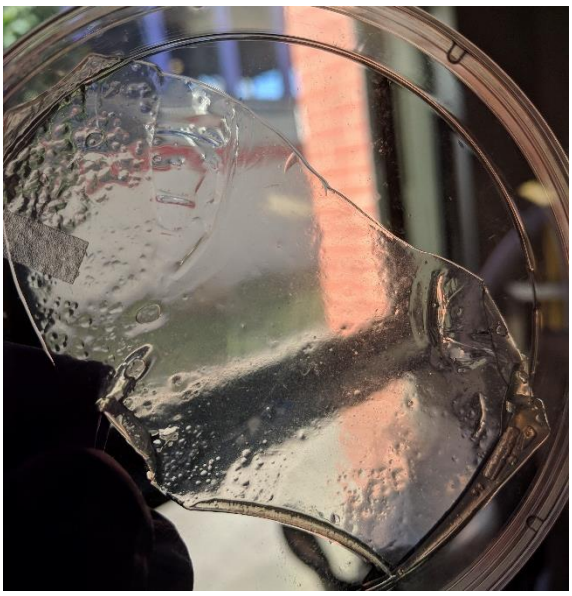

Figure 5.13 Clear film cast using SACC at a concentration of 92% (w/v) in a 1X PBS solution.

5.8 Film Casting of High Concentration SACC

The SACC solubility profile described above permitted concentrations >90% (w/v) to be obtained, which allowed the casting of clear films to be carried out. To achieve this, initial solutions were made up at 95% SACC concentration (w/v) in 50% acetic acid. 200 µL of the solution was then pipetted onto a glass slide which had been edged with Kapton polyimide tape (DuPont) of defined thickness at 0.07 mm as seen in Figure 5.14. The droplet was then spread across the surface using a utility blade to give an even layer of controlled thickness. This was then allowed to air dry within the fume hood opening for 1 hour. Thicker coatings were produced using the same process with thicker taped edges to raise the thickness of the film. Once dry, the films were either crosslinked in a 1% EDC solution in ethanol, or sealed and stored at either 4°C or 20°C.

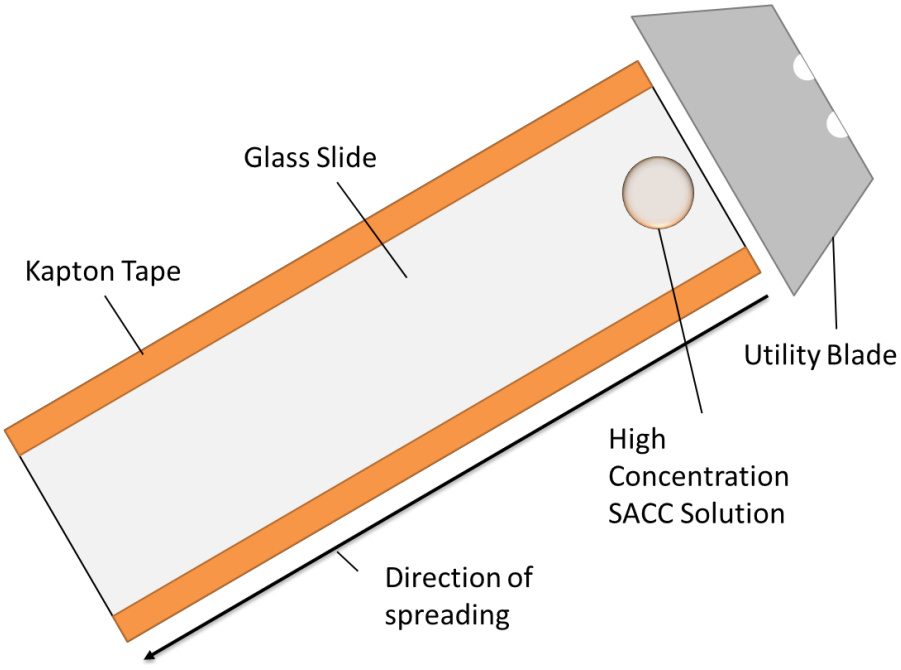

Figure 5.14 Coating of glass slide with thin film of SACC at a controlled height. Blade causes SACC solution to spread uniformly across the surface of the slide.

The casting of thin films of high concentration (>90% SACC) created scaffolds such as those seen in Figure 5.15, which could be crosslinked using EDC to produce clear, non-soluble scaffolds as seen in Figure 5.16. The scaffolds were not further

characterised and acted to demonstrate the ability of SACC to dissolve at very high concentration with applications in dressings, particularly surrounding the premise of a medical device which is able to seal a wound, maintaining sterility while allowing observation by medical staff as to the ongoing condition of the wound. The process can be easily scaled using a doctor blade setup on a conveyor with a reservoir of SACC solution using a flexible casting material.

Figure 5.15 High concentration SACC clear film cast on a glass slide.

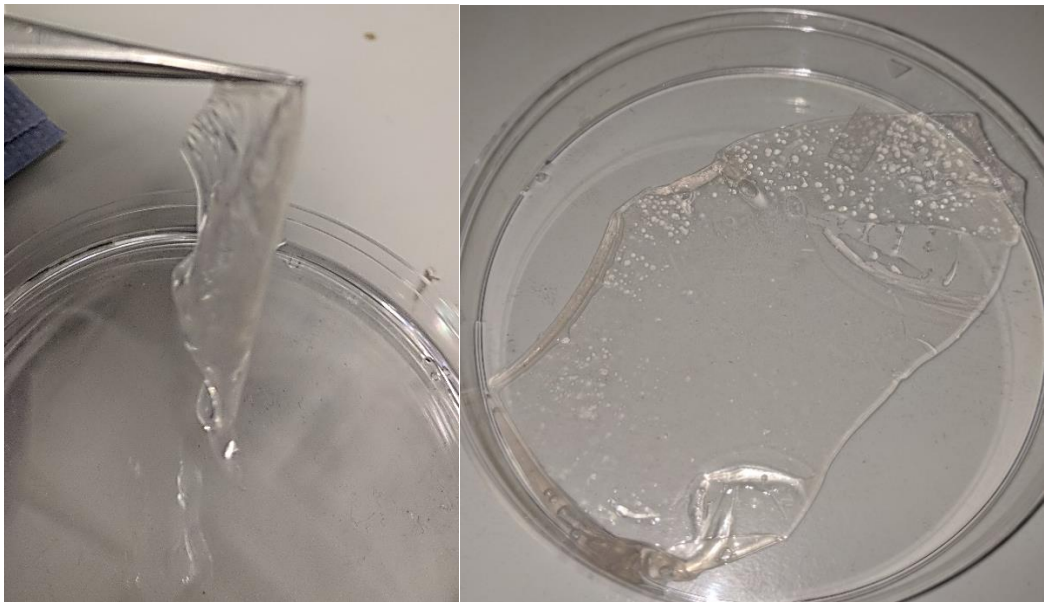

Figure 5.16 High Concentration SACC clear film crosslinked with EDC using the in-house compression method.

5.9 Molecular modelling

To investigate the reasons behind solubility increases for the single alpha chain collagen extracts in comparison to acid soluble collagen, and to give a better representation for graphical representation of the respective molecules, simple molecular modelling was carried out using Abalone (Agile Molecule 2015). As the genome of the *Rhizostomas pulmo* jellyfish has not been sequenced, the collagen structure for *Homo sapiens* was used. The chain building and folding was carried out with an assisted model building with energy refinement (AMBER03) force field that is optimised for protein simulations and defines the potential energy of the system as shown in equation 1.1. Optimisation was carried out using a hybrid Liu Storey and Conjugate Descent method provided by the software. The software was allowed to optimise until 100 iterations with a gradient of less than 0.000001 was achieved.

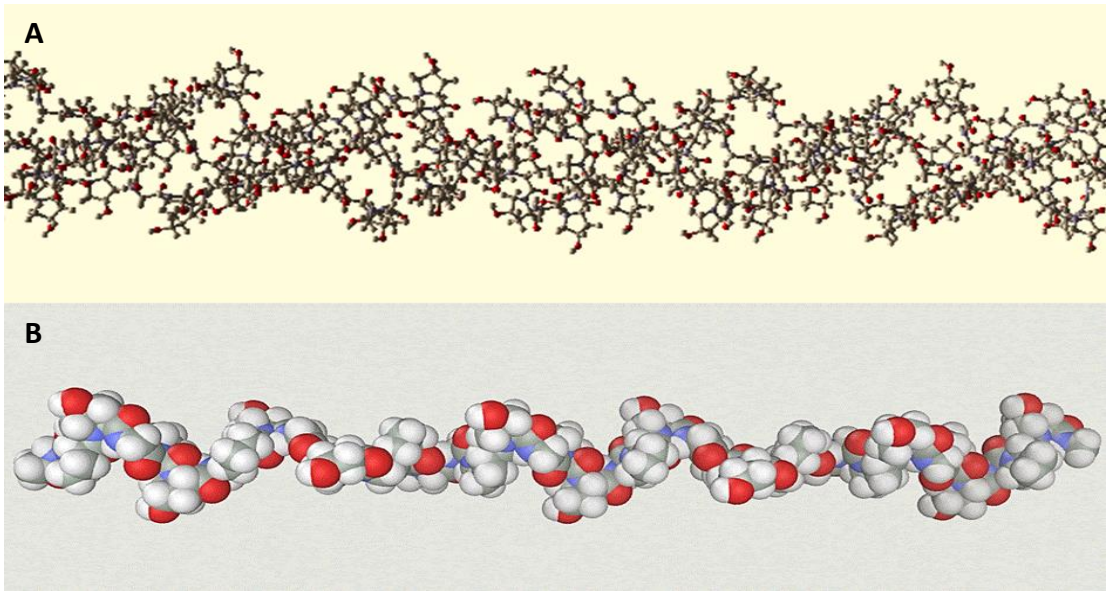

Figure 5.17 Molecular modelling of Acid Soluble Collagen (A) and Single Alpha Chain Collagen (B), displaying the α-helix formation within the Gly-X-Y repeat regions. A. The triple helix formation which creates repeating striations throughout the structure, aiding with fibril stacking order. B. The open architecture and exposed groups within the SACC molecule. Images produced using Abalone software (Agile Molecule 2015).

H-bond analysis was carried out using the Zeus molecular visualisation software (Alnasir 2017) which allowed for backbone hydrogen bonding to be elucidated and compared between SACC and ASC molecules. ASC model molecular structure for human, acid solubilised collagen was estimated to contain 708 occupied hydrogen bonds contained between the three α-helical chains with 270 total free hydrogen bonds available to external bonding. This equates to 90 free hydrogen-bonding locations per α-chain. SACC model molecular structure for human, acid solubilised collagen was shown to contain 177 occupied hydrogen bonds between the α-helix structure, with 531 unoccupied bonds per chain being available for bonding. The structures depicted from these calculations can be seen in Figure 5.18, where inter-chain bonding is highly repetitive within the structure, particularly between glycine and proline groups.

When comparing this with the literature, it became clear that collagen α-chains, while stabilised by interchain hydrogen bonds, do not undergo intrachain hydrogen bonding due to the tight packing of the Gly-X-Y formation. Instead, one hydrogen bond is formed between the amide hydrogen of glycine and the carbonyl oxygen of residue X (usually proline) in an adjacent chain (Horton et al. 2006). This difference, while not affecting the model for ASC, as this did not contain intrachain bonding, means that the SACC model must be considered, and whether it is possible that this may explain the tendency of α-chains to dimerise within the solution, making them very difficult to purify and maintain in single alpha chain configuration. While the model suggests that the relative number of interchain hydrogen bonds are as observed in Figure 5.18 a & b, it may be that the intrachain bonds seen in Figure 5.18 c & d are not present in reality, and that further hydrogen bonding is occupied with the solvent, and where possible, through partial renaturation of the chains into β-chains. This may help to explain the very high solubility levels seen with SACC samples and why further purification to remove β-chains usually lowers the overall yield significantly as seen in Figure 5.19.

Figure 5.18 Inter and intra-chain hydrogen bonding of ASC and SACC molecules. A & B, ASC inter and intra-chain hydrogen bonding than in SACC, with many bonds internalised, leading t

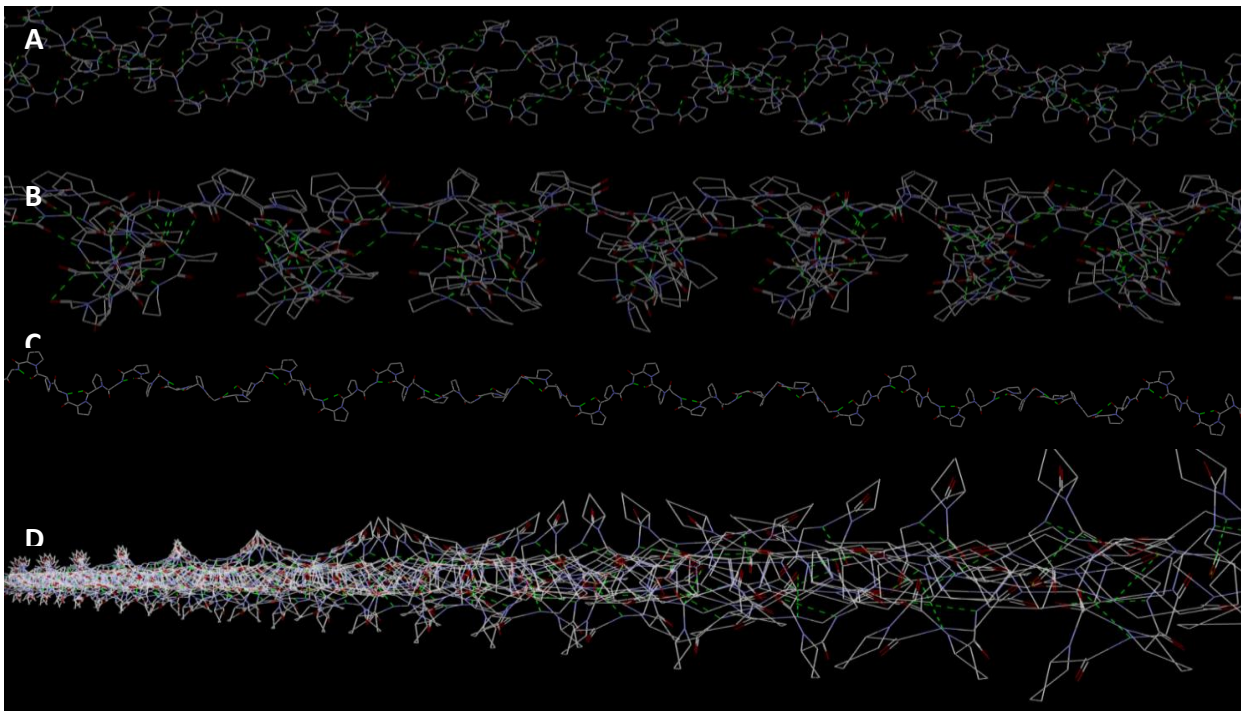

molecules and reduced solubility in aqueous solutions. C & D, SACC chains contain far fewer bonds are externalised to the surrounding aqueous solution, increasing protein solubility. Ima using Zeus PDB viewer (Alnasir 2017).

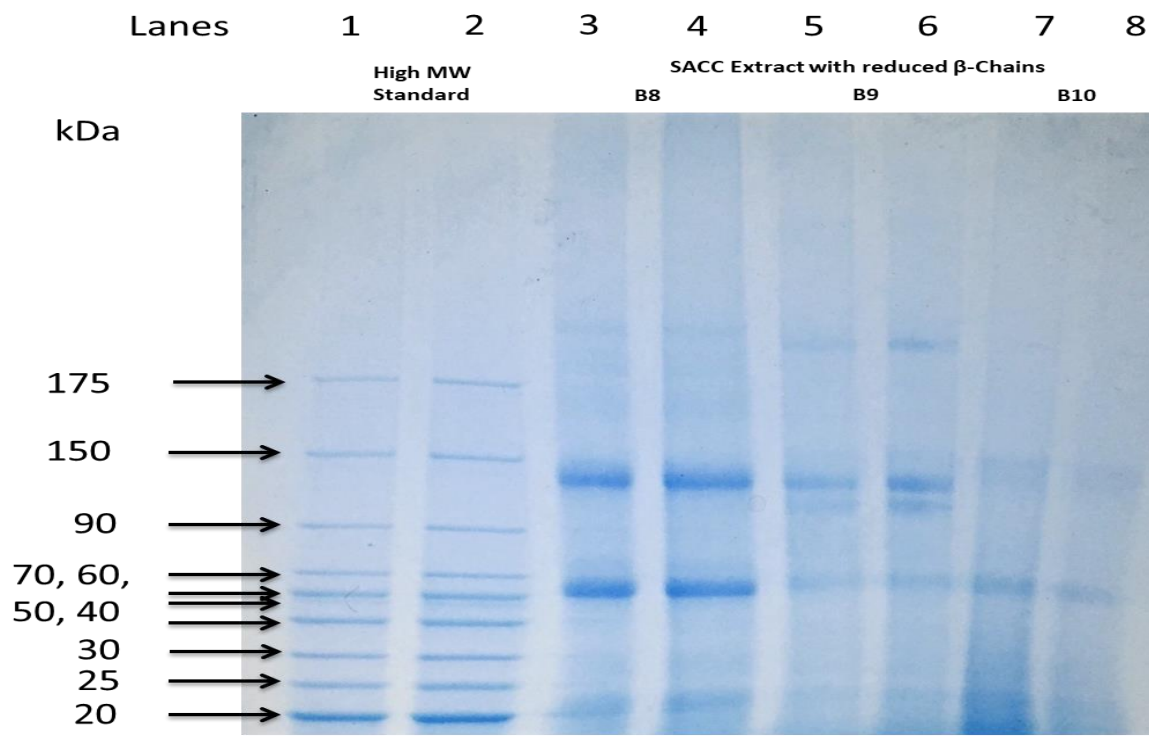

Figure 5.19 SDS PAGE displaying further attempts at purification of SACC extracts to remove reduction in alpha chain content in conjunction with β-chain removal and increase in low MW molecular weight standard. Lanes 3-4 Scale up batch 8 SACC. Lanes 5-6 Scale up batch 9 SAC SACC (n=2).

5.10 Conclusions

The isolation of single alpha chain collagen from acid soluble collagen retains the scalable processing demonstrated in chapter 4, while producing a new material with unique qualities that are needed within biomaterial tissue engineering. The material was examined for unique and differentiating qualities from ASC through SDS PAGE, XRD and FTIR analysis, all of which show a distinct lack of high molecular weight gamma chains, which are representative of the triple helix of collagen. By separating these strands, the structure gains an increased availability for hydrogen bonding, as confirmed by molecular simulations and supporting the increased solubility seen when the extract is subjected to concentrations of >95% (w/v). This increased solubility permits a range of applications which were not previously possible with acid soluble collagen, in particular the casting of clear films and electrospinning in benign / physiological solvent systems. The differentiating factor between SACC and gelatin (type A) was established with the unique ability of SACC extracts to refibrillise to produce a non-crosslinked acid soluble collagen which contains triple helical γ-chains when placed in physiological buffers such as PBS and HBSS.

SDS PAGE used in these experiments showed that SACC composed of α1 & α2 chains can be separated from the acid solubilised collagen mixture successfully; giving rise to new opportunities for the use of this physiologically soluble collagen in applications such as wound aerosol sprays, which were not previously possible because of the insoluble nature of collagen in a suitable solvent system. The method of extraction of these collagens also suits the sterility required for its applications, allowing better acceptance in immune-compromised hosts.

The applications for this new material, as well as the material produced in chapter 4, will be further examined in the next chapter, where electrospinning, bioprinting and freeze drying will be explored as methods to produce viable acellular tissue engineering scaffolds.

6 Applications of ASC and SACC in the Fabrication of Medical Devices

6.1 Introduction

The previous chapter introduced single alpha chain collagen (SACC) as a novel material with unique properties, owing to its separation of the three α-helices within the collagen structure. The separation of these strands led to a marked increase in the solubility profile of the extracts, permitting solutions >95% (w/v) of SACC in either 0.5M acetic acid or 1X PBS to be produced. It is the applications of this material that will be explored within this chapter.

This chapter will begin by exploring the electrospinning of jellyfish derived ASC from various sources in different solvents, before exploring the disparities between observed conditions for the material provided from an external source and ASC produced using the scalable manufacturing process described in chapter 4. Following this, the exploration of methods to permit the electrospinning of collagen while preventing denaturation is explored, before the discovery of SACC, which is able to undergo electrospinning while preserving the nativity and refibrillisation capabilities of the material in physiological conditions.

Electrospinning of collagen has been a controversial topic in recent years, many research findings have shown that the electrospinning of collagen solutions has led to the denaturation to gelatin (Zeugolis et al. 2008a). These findings have suggested that the main cause of this has been the use of HFP in solubilising the collagen for electrospinning. Throughout this chapter, it is shown that by using the single alpha chain collagen, it is possible to use benign solvents to solubilise the collagen for electrospinning, which do not cause further damage to the secondary helical structure present in SACC.

Following this, other applications for medical device fabrication using both ASC and SACC are explored, including 3D printing and thin film casting.

6.2 Needle Based Electrospinning Methods

Acid soluble and single alpha-chain collagens were prepared for electrospinning by freeze drying sufficient material for use. To achieve this, samples were first aliquoted and frozen at -20°C for 24 hours, and then transferred to -80°C as Lyostat analysis of the collagen solutions showed an onset of collapse at -32.5°C (Carried out by Biopharma Technologies). The samples were transferred to the Scanvac CoolSafe freeze drier for drying. Once pressure was at 100µbar, shelf temperature was measured at -30°C and the primary drying stage of the process was carried out for 100 hours. Following this, shelf temperature was raised to +20°C for 15 hrs for the secondary drying stage. Samples were then removed from the drier and weighed before being stored in sealed containers with silica pouches at 4°C until use.

A solution of 90% AcOH in DI (v/v) was produced and chilled to 4°C. Following this, the dried collagen samples were weighed and added to an appropriate amount of AcOH to produce a either a 10% solution of acid soluble collagen or gelatin (w/w), or a 25% solution of SACC (w/w). This was vortexed thoroughly until the collagen was fully dissolved and a consistent liquid was produced and was stored at 4°C to prevent the collagen from denaturing. For HFP experiments, acid soluble collagen was dissolved for 24 hours at 10% (w/v) in HFP (50mg/ml) and vortexed in order to fully dissolve the collagen. For PBS electrospinning experiments, PBS tablets (0.01M phosphate, 0.0027M KCl, and 0.137M NaCl, pH 7.4 at 25°C) were dissolved in ultrapure water (18MΩ) at 1 tablet per 200mL water to produce 1X PBS. The SACC was then dissolved in the solution using a vortex to completely dissolve the SACC, achieving a 25% solution of α-chains in 1X PBS.

The electrospinning apparatus was set up using aluminium foil as the grounding target and was connected to ground as seen in Figure 6.1. The syringe pump was set up to the correct diameter for a BD Plastipak® 10ml needle and an 18G blunt tipped needle was used. These were rinsed with DI, followed by a blank 90% AcOH solution prior to the solution being taken into the syringe and any air was cleared before loading onto the syringe pump.

The syringe pump was set to use a flow rate of 0.75mL per hour. The distance from needle tip to collector was 25cm and a voltage of 20kV was used. Voltage was applied when a droplet had formed at the tip of the needle and flow was maintained so

volume of the droplet did not increase or reduce. Taylor cone formation and electrospinning was observed using a camera and laser as shown in Figure 6.2 and an AcOH bath was placed in the electrospinning unit to prevent gelation of the droplet during periods of prolonged electrospinning.

After electrospinning, the voltage was stopped, and the equipment made safe, with any remaining collagen stored at 4°C for characterisation. The mat produced was then sampled and coated in a 5nm layer of chromium before being examined by SEM using a Hitachi S4800 FEG-SEM at an acceleration voltage of 10kV and emission current of 9µA. Micrographs were taken with a magnification of 1500X for fibre diameter measurements which were analysed using ImageJ software.

For SACC samples, SDS PAGE and FTIR analysis was carried out to examine any degradation which may have occurred during the electrospinning process.

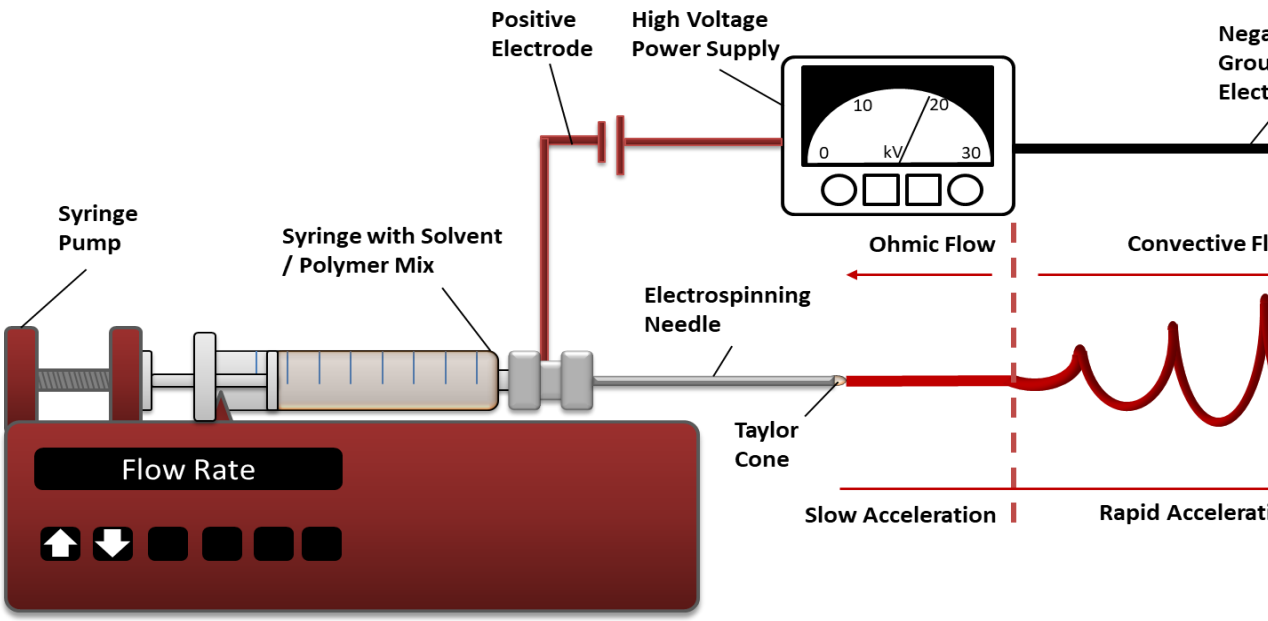

Figure 6.1 Basic electrospinning setup where a polymer solution is placed within a syringe pu connected high voltage power supply us connected to the needle, producing an electric field of conjunction with compatible parameters such as concentration and polymer choice, leads to th positive source to ground, which collects dried fibres on a conductive surface such as aluminiu can be placed in front of the ground to aid collection. Jet dispersion adapted from diagram by Zealand Institute for Plant and Food Research Ltd.

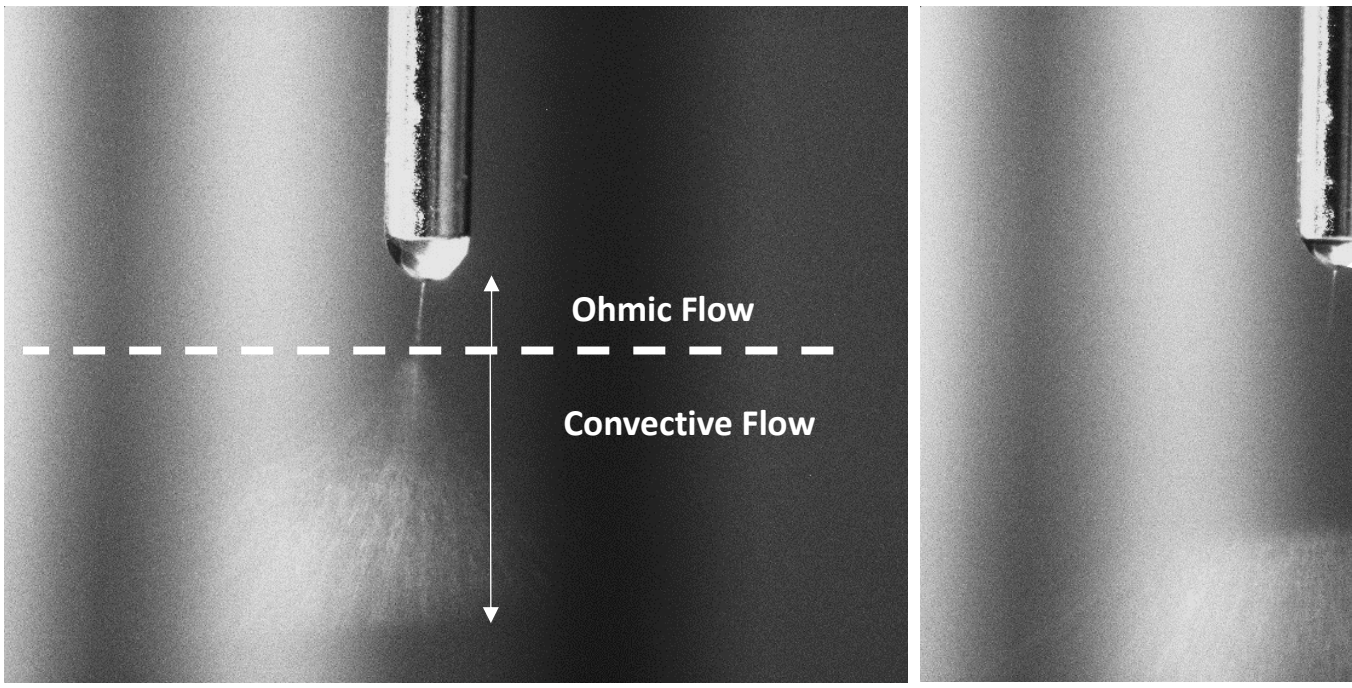

Figure 6.2 Jellyfish derived SACC collagen solution being electrospun with constant droplet b Taylor cone producing a jet of collagen solution which lands on the grounding target as collag moves from ohmic to convective as charge migration to the fibre surface occurs, leading to fib electrostatic repulsion before reaching the collector at drastically reduced fibre diameter.

6.3 Needle-Less Electrospinning Methods

For needle-less electrospinning, the roller electrospinning method was used. Samples were freeze dried using the process described in chapter 3.5 and dissolved at either 10% in AcOH (ASC) or at 25% concentration in a solution of 90% AcOH or 1X PBS in DI water (SACC). The solution was then placed in a bath and a mandrel with wires was submerged in the solution. The bath was inserted into the Nanospider NS Lab 200 System (Elmarco, Czech Republic) and a collection material placed over the grounding target.

The Needle-less electrospinning schematic shown in Figure 6.3 describes the roller electrospinning process which has been previously described by (Burke et al. 2017). Briefly, the setup adapts the standard electrospinning approach to allow the formation of several polymer jets simultaneously in order to allow for scalable fibre production (Thoppey et al. 2011). The process begins by applying a high voltage to a polymer bath which is continuously coating a 6 wire mandrel with droplets of polymer solution, which when exposed to the high voltage becomes elongated and Taylor cone formation occurs, forming multiple ejection points across the wire as seen in

Figure 6.4. The solution then undergoes rapid drying before being deposited on the collector. The material setup used a mandrel rotation speed at 10 revolutions per minute, a distance from mandrel tip to collector of 30cm and a mandrel to collector voltage of 80kV. Using these conditions, the current from mandrel to collector was observed to remain between 100 and 120μA, signalling consistent fibre formation to be occurring.

The process was carried out for 1 hour before samples were removed, taken for SEM imaging and characterisation as described above. Any remaining collagen solution was removed and stored at 4°C for further solution testing, and the mat was sealed with silica packs to prevent excess moisture and kept at 4°C.

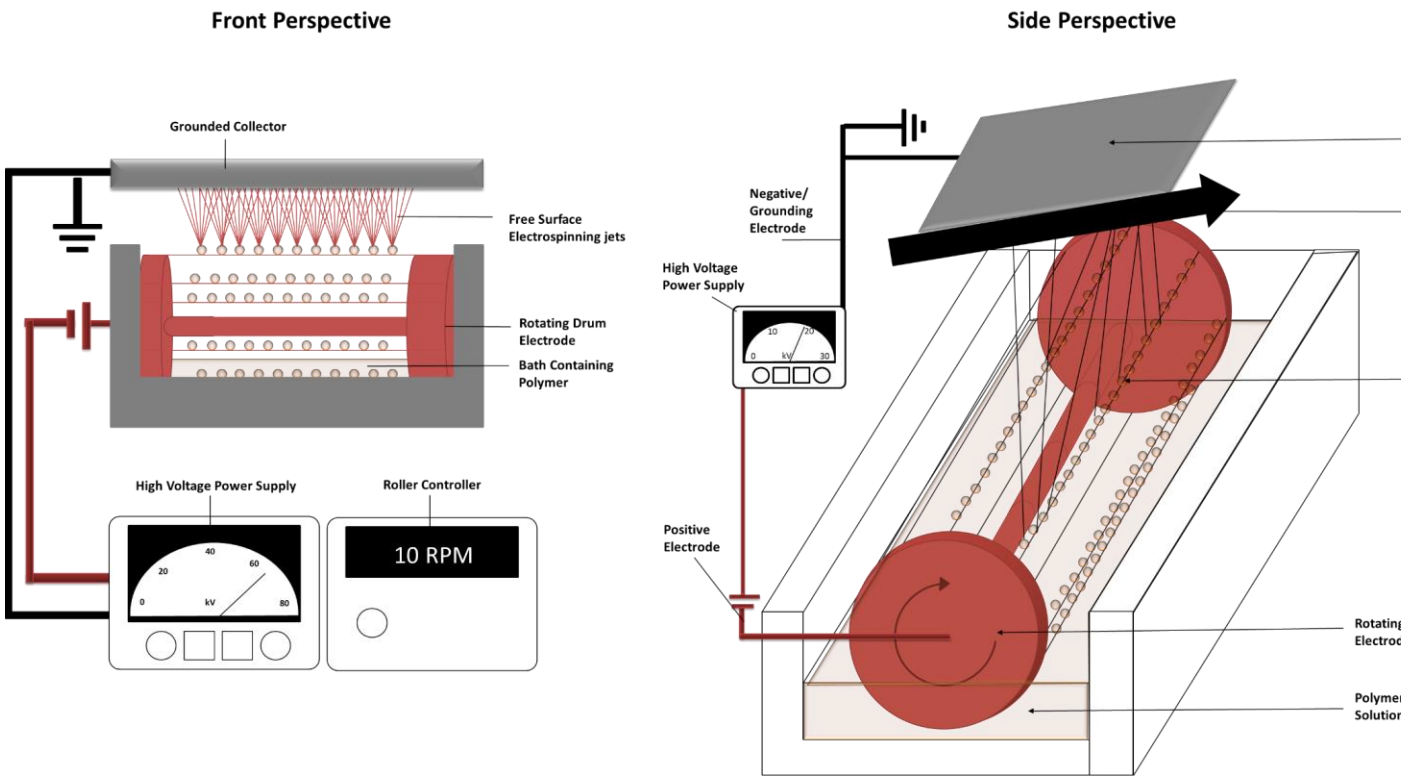

Figure 6.3 Nanospider (Elmarco, CZ) needle-less electrospinning setup using a rotating mandi permit multiple initiation sites for electrospinning to occur. Continuous spinning is achieved b to polymer usage rate while voltage is typically significantly higher than with single needle ele

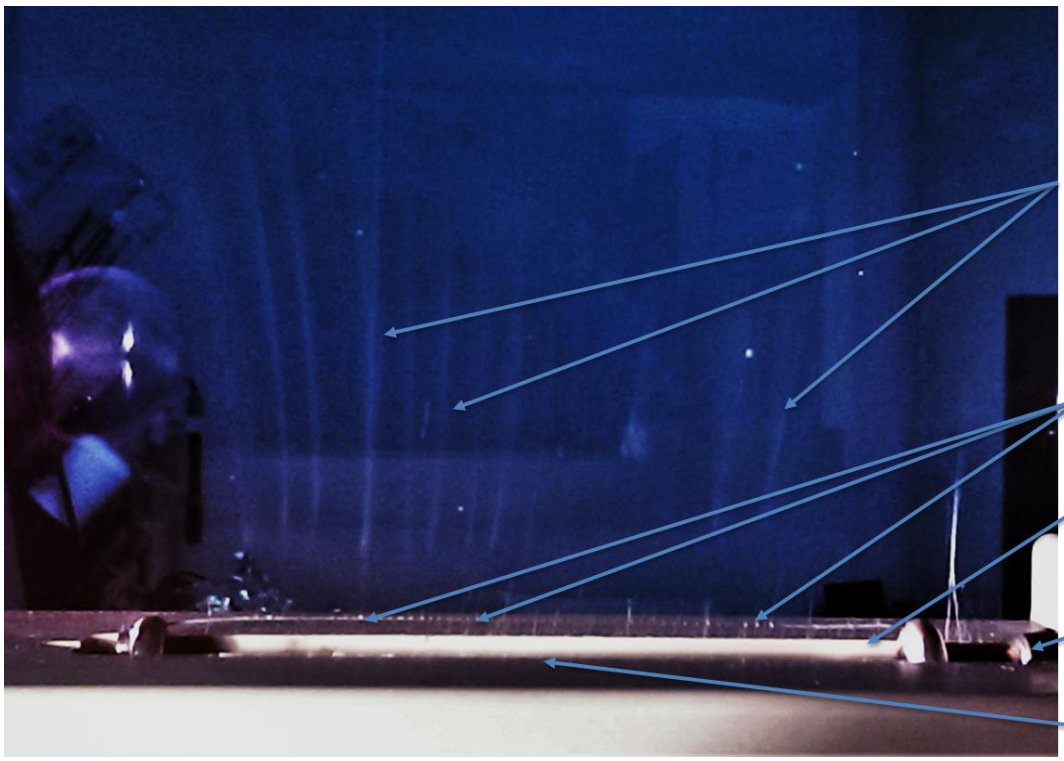

Figure 6.4 Free surface electrospinning jets of SACC being produced using the Nanospider rol are produced from the wire at multiple initiation sites on a rotating electrode which refreshes submersion within the SACC solution.

Figure 6.5 Showing external operation of Nanospider NS LAB 200.

6.4 Co-Electrospinning of Collagen & Polyethylene Oxide Methods

The combined electrospinning of collagen and polyethylene oxide (PEO) was carried out by first preparing a solution of 90% AcOH (v/v). ASC was dissolved at the desired concentration in the 90% AcOH (w/v) while a second solution of PEO at the desired concentration in 90% AcOH was also prepared. The two solutions were then blended together in a beaker and stirred using a magnetic stirrer until a homogenous solution was reached. The blended solution was loaded into a plastic syringe and the syringe added to the needle electrospinning setup as described above.

The desired voltage was applied at the tip of the needle (18G). The distance between the tip and collector was optimised and the flow rate was set. The sample was then allowed to electrospin for 10 minutes and a collection of blended fibres were created on the foil collector. Different voltages, distances, solution concentrations and flow rates were trialled in order to give the optimum results. For co-electrospun, coaxial and single needle electrospun samples, SDS PAGE and FTIR analysis was carried out to examine any degradation which may have occurred during the electrospinning process.

6.5 Single Needle Electrospinning PEO Methods

In order to compare the variance in average fibre diameter of PEO, ASC and blend, a solution of 5wt% PEO was prepared in 28.5 ml of DI water as has previously been optimised in the research group. The PEO solution was then placed into a 10 ml syringe and connected to the electrospinning apparatus. The voltage was applied at 18kV, the flowrate was set to 0.5ml/hr and the distance between the tip and the collector was 22 cm as previously optimised. The PEO solution was left to spin for 10 min until a mat was visible.

6.6 Co-Axial Electrospinning of PEO as Sheath and Collagen as Core Methods

Due to issues with the improved ASC electrospinning in benign solvents, co-axial electrospinning of ASC using PEO as the sheath polymer was trialled. This was investigated to reduce denaturation of the collagen when undergoing high voltage electrospinning as has been shown previously (Zeugolis et al. 2008a).

As the optimized parameters for co-axial electrospinning of the in-house produced ASC and PEO were unknown, optimisation experiments were carried out, adjusting parameters including flowrate of the inner and outer needle, concentration of each solution, voltage and distance from needle to collector. This allowed the optimized conditions for the electrospinning of fibres with uniform fibre diameter, lack of beading and uniform core/shell ratio.

The two solutions were seeded into two different 10 mL syringes and placed into two separate syringe pumps in the setup seen in Figure 6.6. The voltage was applied, and the apparatus was left to spin for approximately 10 minutes for each experiment. Optimised solutions were electrospun for extended periods of approximately 1 hour. Only the outer needle solution was in contact with the applied voltage; the inner solution was uncharged and was carried from needle to collector by the shell solution. Once electrospinning was completed, the samples were cut and examined by SEM as described in 3.10.

6.6.1 Freeze Fracture Method for SEM

The samples were submerged in liquid nitrogen for 30 seconds each and then immediately removed and cracked before being coated and examined by SEM to better expose the core / shell fibres.

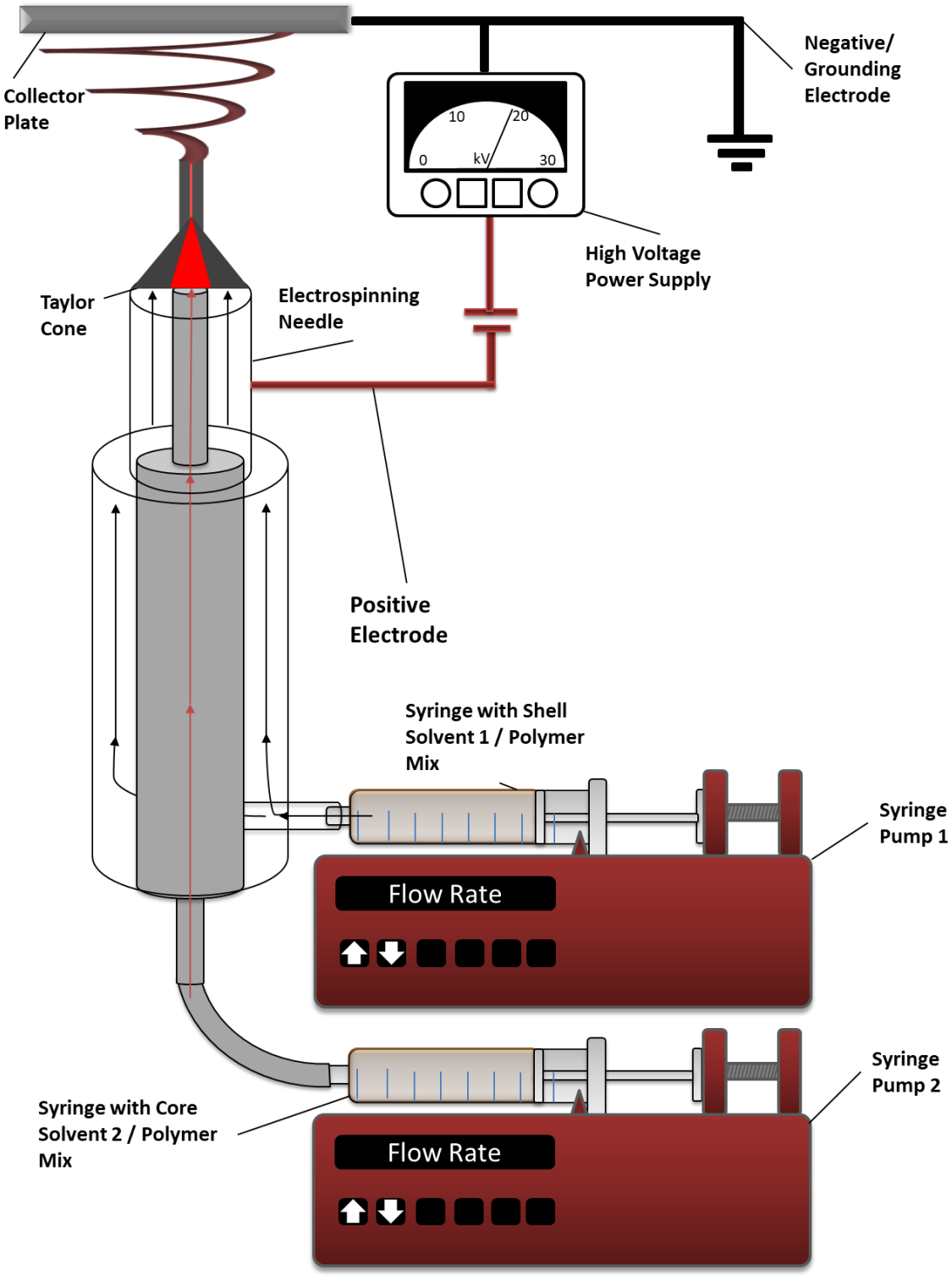

Figure 6.6 Coaxial electrospinning setup displaying coaxial needle being fed by separate syringe pumps for variable flow control of core / sheath polymer solutions. The needle is charged, causing the electrospinning of shell solution, which in turn causes viscous drag upon the core solution, creating coaxial electrospun fibres upon the grounding target.

6.7 Gelatin Electrospinning Method

To act as a comparison with collagen based electrospun fibres, a 10% gelatin solution was prepared by dissolving gelatin from porcine skin (Sigma Aldrich, USA) in 90% AcOH. The solution was placed into a 10 ml syringe and connected to the electrospinning apparatus. The voltage was set at 18kV, the flowrate was 0.3 ml/hr and the distance from the tip of the needle to the collector was 23 cm. The solution was left to spin under room temperature condition for two and a half hours until a uniform mat sufficient for experimentation was obtained.

6.8 EDC Crosslinking of Electrospun Collagen Scaffolds

For physiologically soluble polymers it is usually required that the scaffold is crosslinked. Glutaraldehyde has for many years been regarded as the standard method of crosslinking (Niu et al. 2013), particularly with proteins due to its efficiency and high degree of crosslinking across different polymers (Barbosa et al. 2014). This chemical has many limitations with regard to tissue engineering scaffolds, foremost the calcification of scaffolds and surrounding tissues which are exposed to residual crosslinking agent which may lead to device failure (Golomb et al. 1987). EDC has emerged as the favoured chemical crosslinking method for electrospun collagen scaffolds due to its efficacy and reduced residual damage to tissues. Previously, internal experimentation has been carried out through *in vivo* implantation of ASC freeze dried scaffolds to examine the efficacy of the ASC, while simultaneously assessing the method of EDC/ethanol use prior to implantation (Widdowson et al. 2017). While it was shown that residual ethanol can cause significant damage to the implanted area, the use of EDC to crosslink the scaffold, and the use of jellyfish as the source of the collagen resulted in significantly reduced histopathology scores in both crosslinked and un-crosslinked samples, whereas the bovine scaffolds' scores were not significantly reduced.

Despite this, it is necessary to crosslink electrospun collagen samples, as they are highly hygroscopic, collapsing and dissolving when subjected to water. Furthermore, the use of an Ethanol / EDC mixture causes the fibres to swell and lose their porosity,

as seen in Figure 6.7. To avoid this, when crosslinking was requires, samples were compressed using the method shown in Figure 6.8 (b) as developed in house. Others have used differing methods to avoid this problem. (Dong et al. 2009) used the method shown in Figure 6.8 (a) to prevent the collapse of the scaffold during crosslinking.

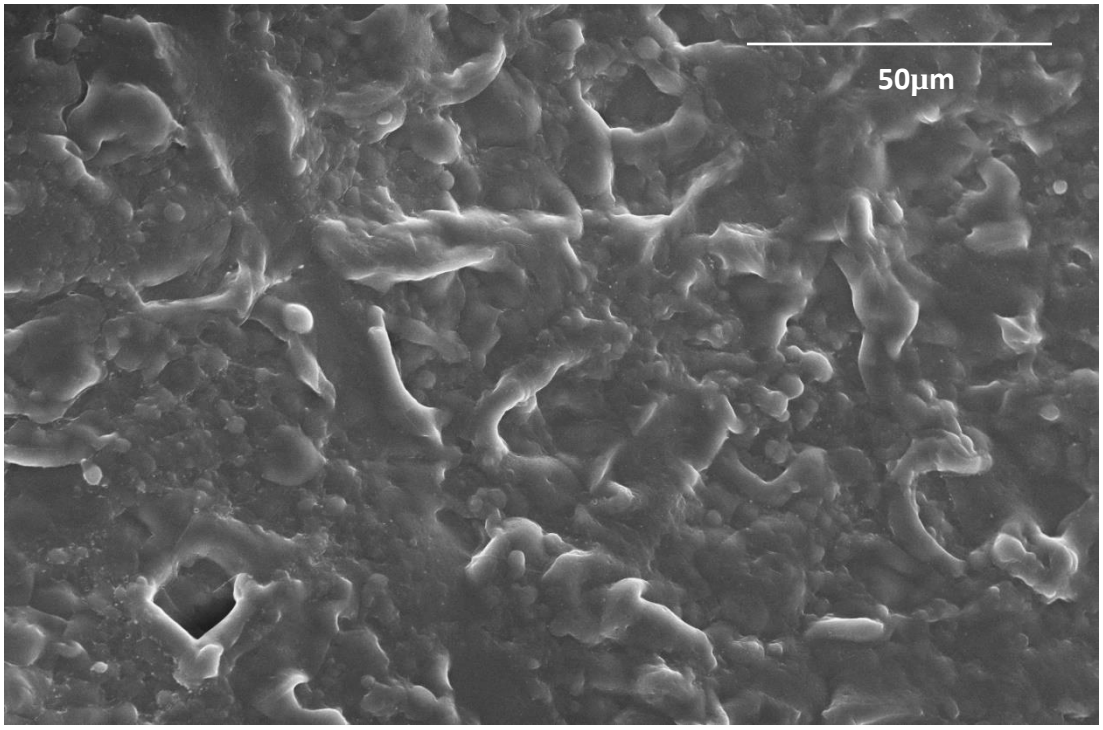

Figure 6.7 SEM micrograph of needle-less electrospun ASC crosslinked with a 1% EDC solution in ethanol. Scale bar = 50µm. Acceleration voltage = 15kV.

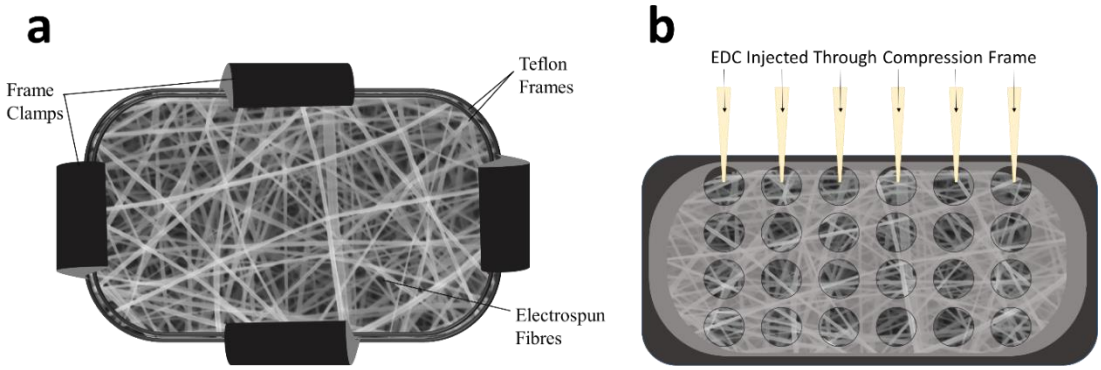

Figure 6.8 Different compression methods that have been used to prevent the swelling and loss of porosity of electrospun scaffolds crosslinked with EDC / ethanol.

6.9 FRESH Printing of ASC Hydrogel Methods

To print ASC hydrogels using the FRESH technique, the gelatin slurry prepared in 3.12.2 was added to the dish being used for printing, which was initially a petri dish, followed by the lid of cell culture plates to increase print area. The excess liquid of the slurry was removed by tamponade action using absorbent wipes, which ensures the slurry behaved similar to a Bingham plastic as described in (Hinton et al. 2015). Following this and the loading of the syringe, the .X3G program file was selected using the inbuilt menu which contains settings previously configured on a PC using the modified Flashprint program. Printing of various shapes was carried out, with optimisation of line width and consistency using cross-hatched grids as seen in Figure 6.9.

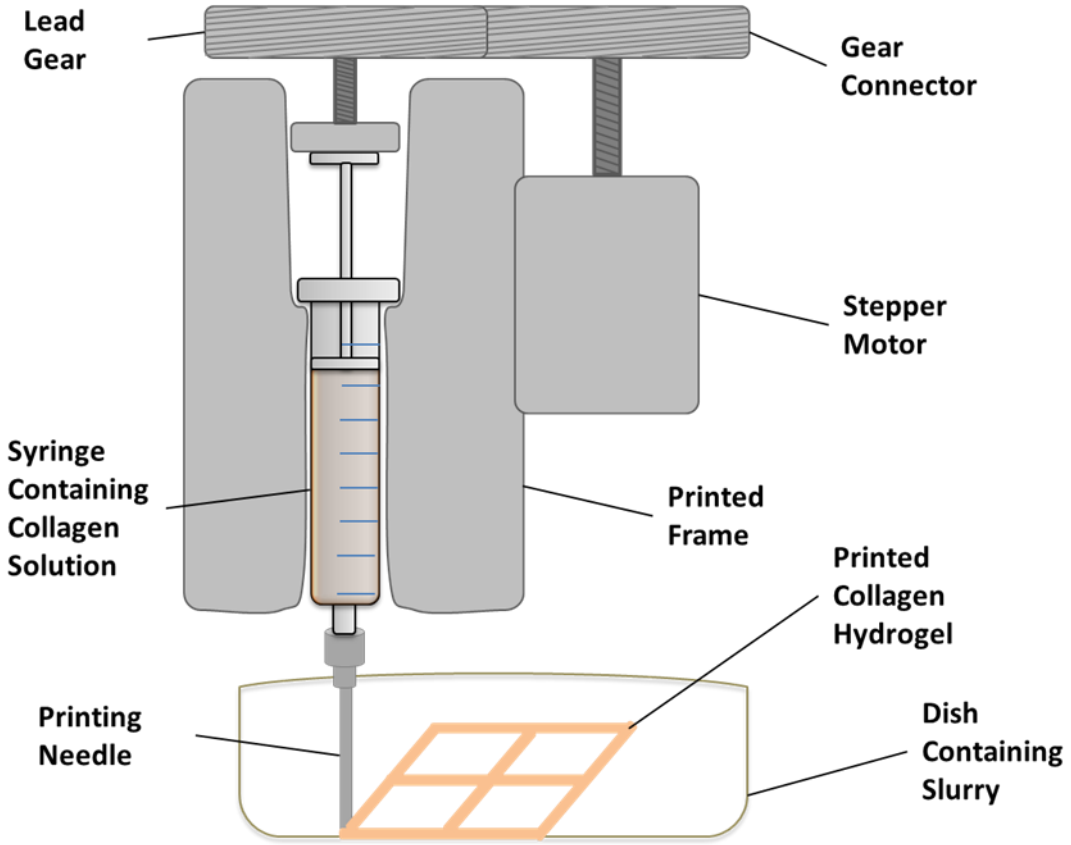

Figure 6.9 Initial FRESH printing setup used to optimise the 3D printing of ASC collagen hydrogels based on the work of (Hinton et al. 2015). *Scaffolds in a hatch formation were used to optimise the line width accuracy of the printing process.*

6.10 Testing With polycaprolactone in Acetone

To optimise the nozzle print width and height, polycaprolactone (PCL) as a commonly used polymer in research on the fabrication of artificial cartilage and bone constructs (J. M. Williams et al. 2005) was selected. PCL was dissolved at concentrations from 20% to 55% in acetone (w/v) by incubation at 40°C for between 2 and 12 hours. The dissolved solution was loaded into the syringe and printed directly onto the heated bed, without using the FRESH gelatin slurry. Optimisation of line thickness, as well as extrusion volume was deemed complete when sufficient liquid was ejected to give steady lines without dragging the printed material but without large overflows of liquid causing beads to be produced.

6.11 Coaxial FRESH Printing Methods

In order to better utilise the optimised gelation time of the improved ASC material, a modification to the printing setup was carried out, wherein genipin was not added to the printing solution but was instead kept separately by dissolving into the 10X PBS solution and loading into a syringe. The ASC was diluted to between 3.0 mg/mL and 6mg/mL and neutralised using NaOH before being loaded into the syringe. The setup was modified to use external syringe pumps which fed into a common pipeline prior to the needle, causing controlled mixing of the genipin and ASC solutions. The syringe pumps were set up to extrude where the genipin solution was set at 1/10 that of the ASC solution to give the appropriate final concentrations. This setup can be seen in Figure 6.10.

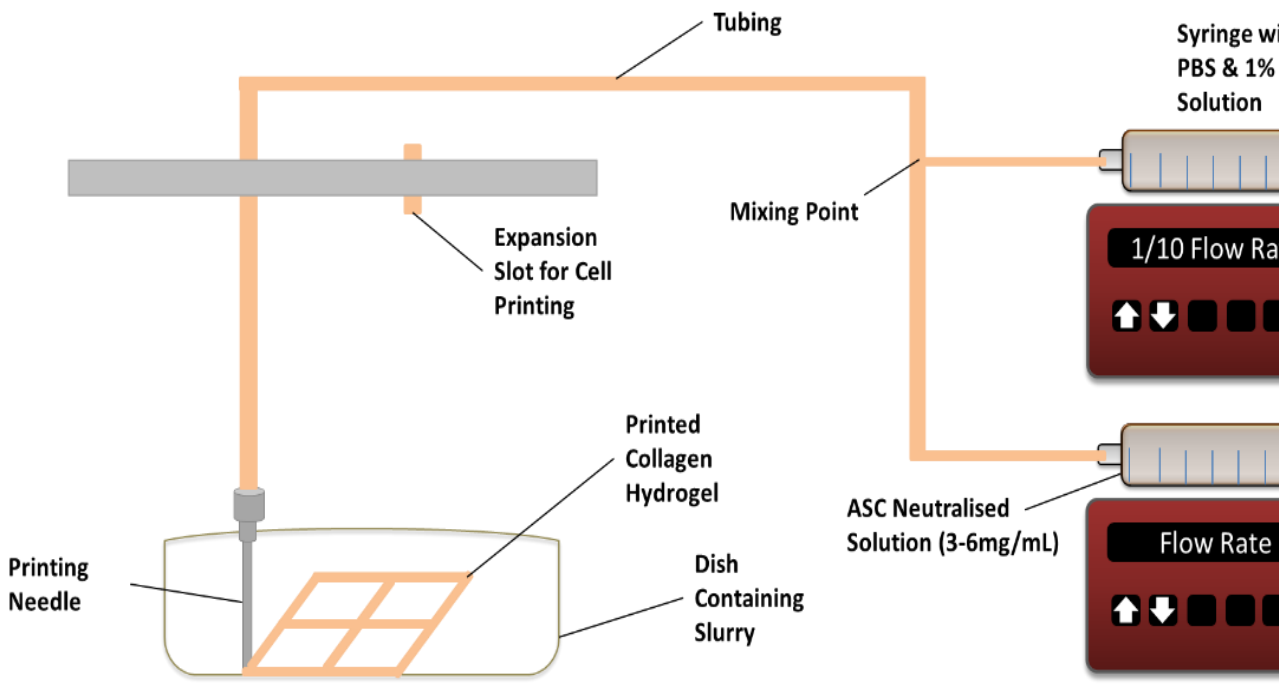

Figure 6.10 Dual pump setup for optimised FRESH printing of mixed ASC / Genipin so

6.12 Single Needle Electrospinning Results

6.12.1 Collagen Solutions ASC in AcOH

The 10% ASC samples, dissolved in 90% AcOH (w/v) were electrospun and examined by SEM, showing a mean fibre diameter of 111 nm with a standard deviation of 36 nm based on 90 fibre measurements. Micrographs of the needle electrospun fibres can be seen in Figure 6.11 (A) with frequency of range seen in Figure 6.11 (B). The fibres contained no beading suggesting electrospinning conditions were optimal at 10% CS ASC, 20 kV, 20 cm and 0.4 mL / hour.

6.12.2 Scale Up Batch ASC Solutions in AcOH

Electrospinning of the 10% Scale up ASC samples which were dissolved in 90% AcOH (w/v) was attempted and were examined by SEM. The scale up batches of jellyfish derived collagen did not electrospin but instead electrosprayed to produce microspheres of diameter 794 nm with a standard deviation of 399nm based on 90 sphere measurements. These can be seen in Figure 6.12. Despite multiple attempts it was not possible to electrospin the improved ASC. This led to a search of the literature that revealed the papers detailing both the solubility characteristics of mammalian derived collagens and the findings that the requirement for solubilisation in HFP led to denaturation of the protein (Zeugolis et al. 2008a; Zeugolis et al. 2008b). This intriguing research led me to question the nativity of the collagen that was received from collagen solutions, leading to the following sections.

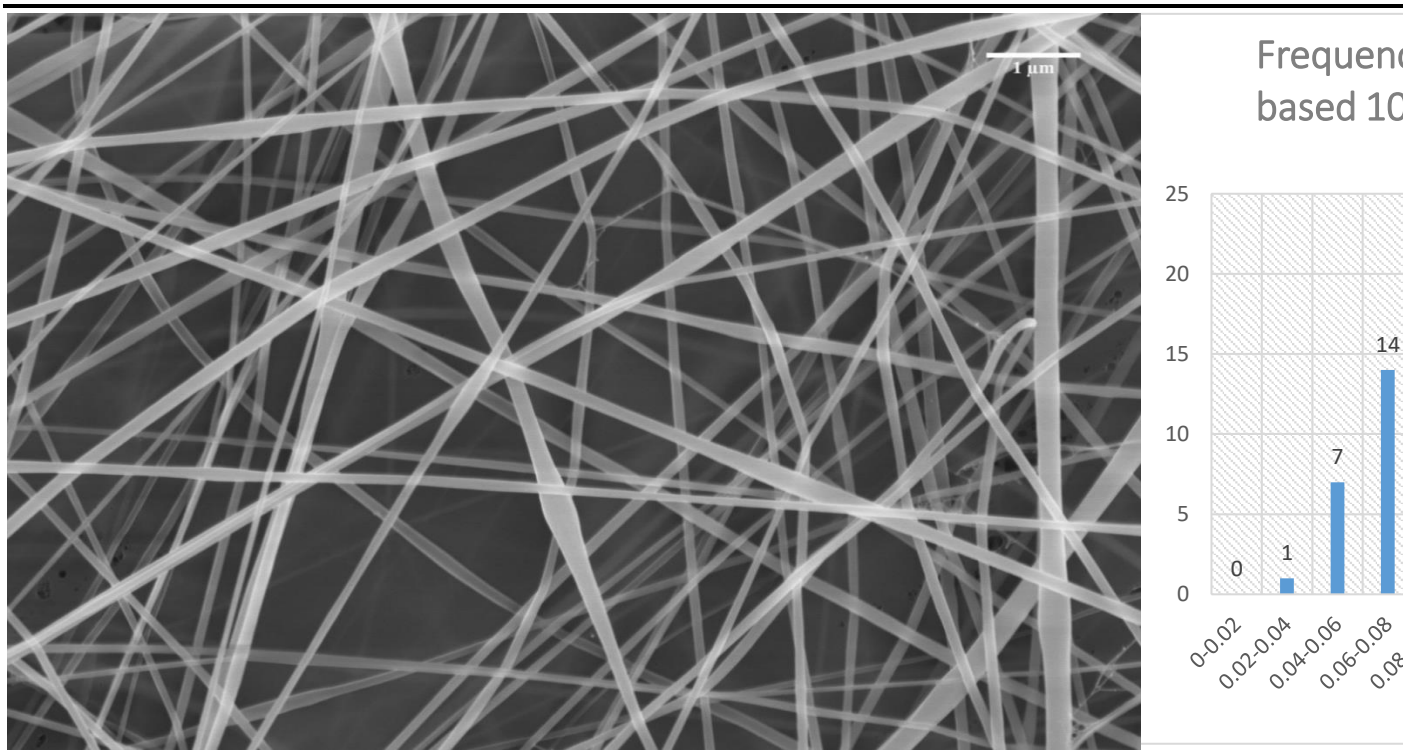

Figure 6.11 (A) SEM micrograph of Collagen Solutions ASC electrospun from a solution of 10
bar = 1 µm. Acceleration voltage = 5 kV. (B) Frequency of range of collagen fibres electrospu
AcOH (n=90).

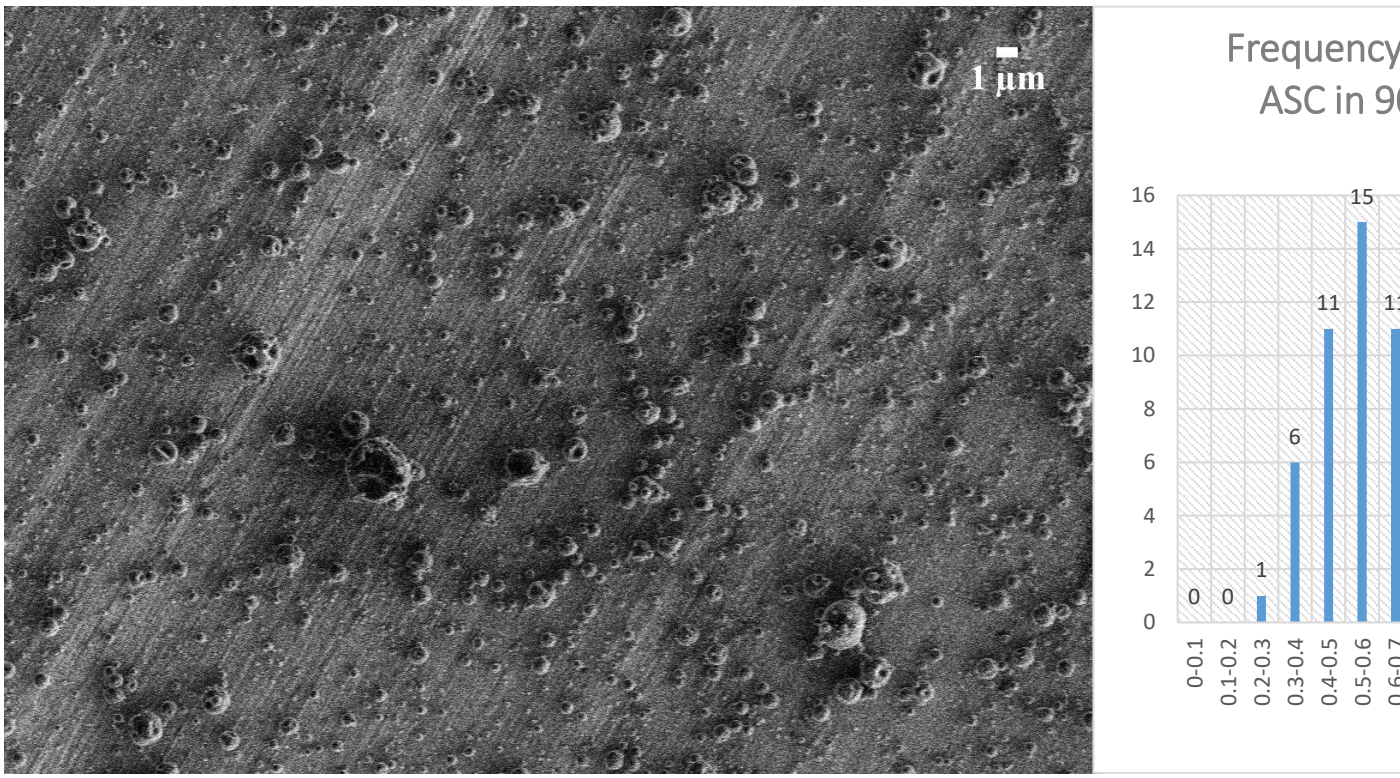

Figure 6.12 (A) SEM micrograph of scale up batch ASC electrosprayed from a solution of 10% spheres instead of fibres. Scale bar 1µm. Acceleration voltage 2kV. (B) Frequency of range of solution composed of 10% SU ASC in 90% AcOH (n=90).

6.12.3 Scale Up Batch ASC Solutions in HFP

To assess whether nativity of the ASC between collagen solutions and the in house scale up batches was the cause affecting the electrospinning of collagen, it was necessary to carry out electrospinning experiments using HFP. The scale up ASC was electrospun and examined by SEM. The results showed the ASC electrospun when dissolved in HFP, in line with mammalian collagen papers. The fibres had a mean fibre diameter of 107 nm with a standard deviation of 34 nm based on 90 fibre measurements. Micrographs of the electrospun fibres can be seen in Figure 6.13 (A) with frequency of range seen in Figure 6.13 (B). The fibres contained little beading, suggesting conditions were near optimal, however these were not further optimised as the use of HFP would not be continued.

The ongoing debate remains unclear as to whether collagen electrospun from HFP remains native or is denatured, with findings from (Jha et al. 2011) finding the characteristic 67nm banding pattern for collagen fibres within their electrospun scaffold, in contrast to (Zeugolis et al. 2008a) where 98% denaturation was shown. Most recently (Sizeland et al. 2018) found no content of fibrils within their electrospun scaffolds. Intermediaries such as (Wakuda et al. 2018) found around 30% helical structures remaining within their HFP scaffolds, suggesting HFP electrospinning may not be the only influence on denaturation of the collagen structure, further supporting the suggestions by (Zeugolis et al. 2008b) that there is a large variation in the quality of extracted collagens from different sources.

Through this work it is shown that the use of the same species, extracted and processed with different methods can lead to the denaturation of the collagen to the extent it is able to electrospin under the conditions used for gelatin as below.

6.12.4 Gelatin Solutions in AcOH

To act as a comparison to ASC samples from CS, a 10% gelatin in 90% AcOH (w/v) solution was electrospun and examined by SEM, showing a mean fibre diameter of 103 nm with a standard deviation of 33 nm based on 90 fibre measurements as in Figure 6.14 (A) with frequency of range seen in Figure 6.14 (B). The fibres contained some beading throughout, suggesting minor optimisation to the solution concentration was necessary however this was not repeated as the use of gelatin would not be continued.

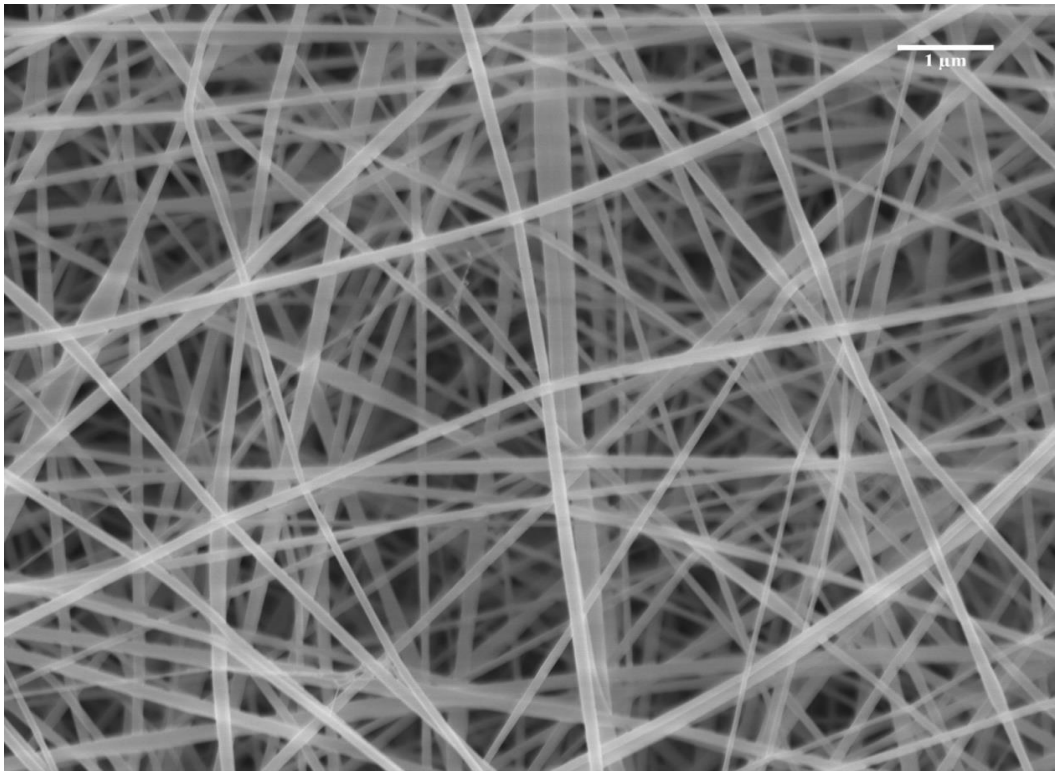

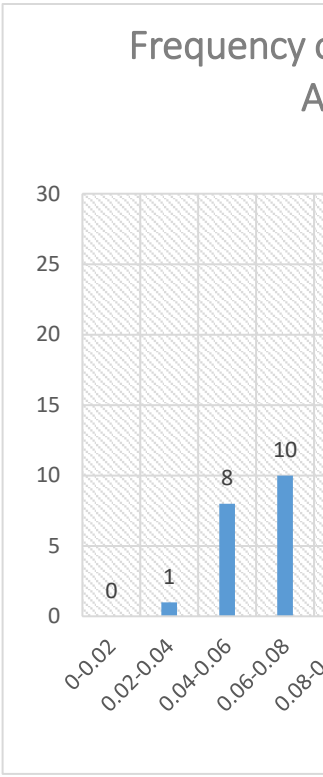

Figure 6.13 (A) SEM micrograph of scale up batch ASC electrospun from a solution of 10% AS
1 µm Acceleration voltage 5 kV. (B) Frequency of range of fibres electrospun from a solution
(n=90).

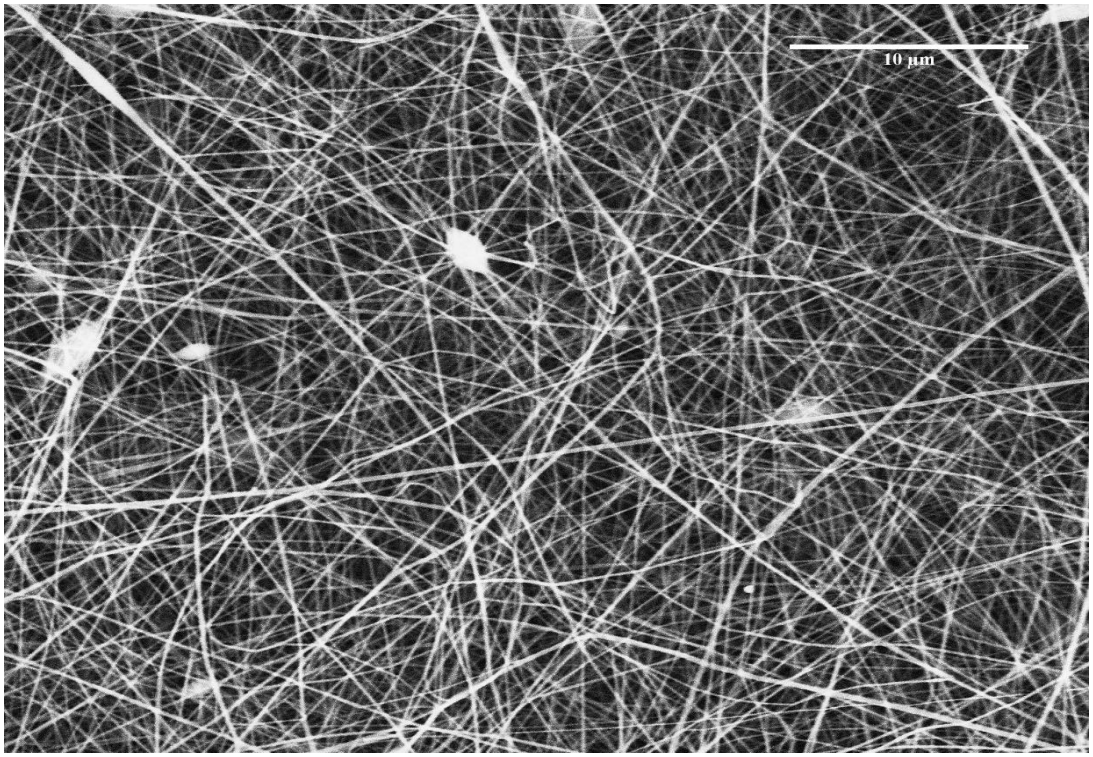

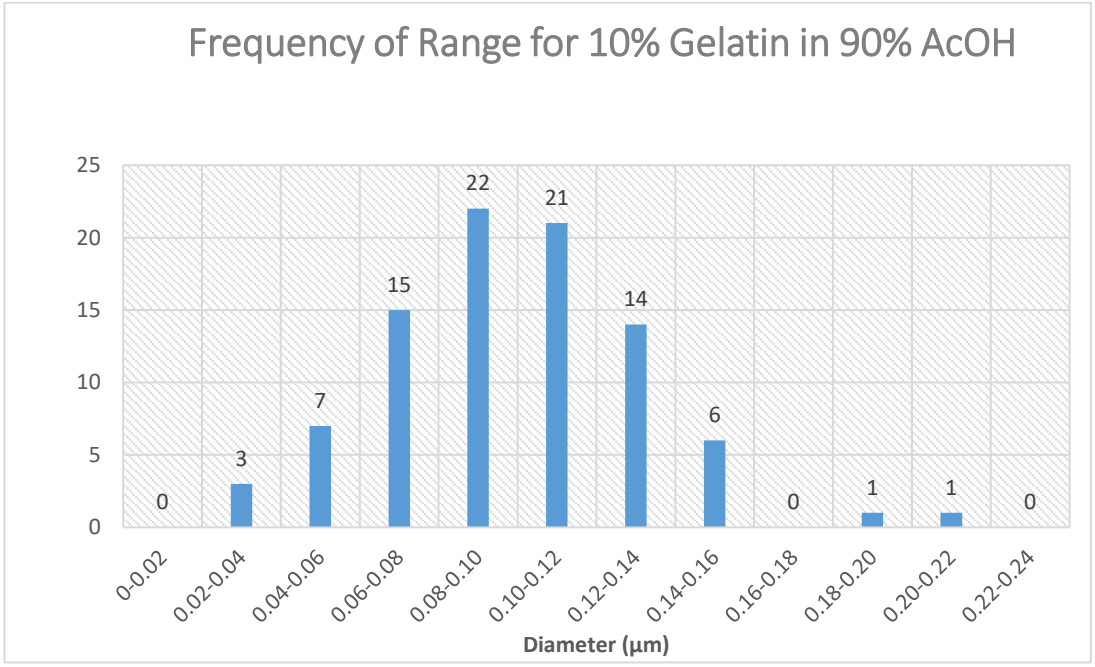

Figure 6.14 (A) SEM micrograph of gelatin electrospun fibres from a solution of 10% gelatin in 90% AcOH. Scale bar 10 µm. Acceleration voltage 10 kV. (B) Frequency of range for gelatin electrospun fibres from a solution of 10% gelatin in 90% AcOH (n=90).

6.12.5 SACC in AcOH

The 25% SACC samples dissolved in a 90% AcOH (w/v) solution were electrospun and examined by SEM, showing a mean fibre diameter of 646nm with a standard deviation of 121nm based on 90 fibre measurements. Micrographs of the fibres can be seen in Figure 6.15 with frequency of range seen in Figure 6.16. The fibres contained no beading suggesting electrospinning conditions were optimal at 25% SACC, 18 kV, 20 cm and 0.35 mL/hour. These conditions were then carried forward for experiments using 1X PBS.

The finding that it was possible to separate and electrospin the α-chain rich SACC solution occurred prior to in depth analysis of the extract by FTIR and H-bond analysis examined in 5.4 and 5.9. It was necessary to compare these findings with that of gelatin, where partial renaturations to form α-helices, as described in (Kozlov and Burdygina 1983) had been carried out to produce a SACC-like products as in (Ki et al. 2005). The possibility of these proteins being capable of electrospinning implies not only that the increased hydrogen bonding is possible, but also that greater chain entanglement is possible by reducing the rigidity of the protein. There have been several cases demonstrating that gelatin has a reduced mechanical strength when compared with fibrillar collagens due to the increased order and crosslinking in the collagen's structure (Z. Zhang, Li, and Shi 2005), further supporting this hypothesis.

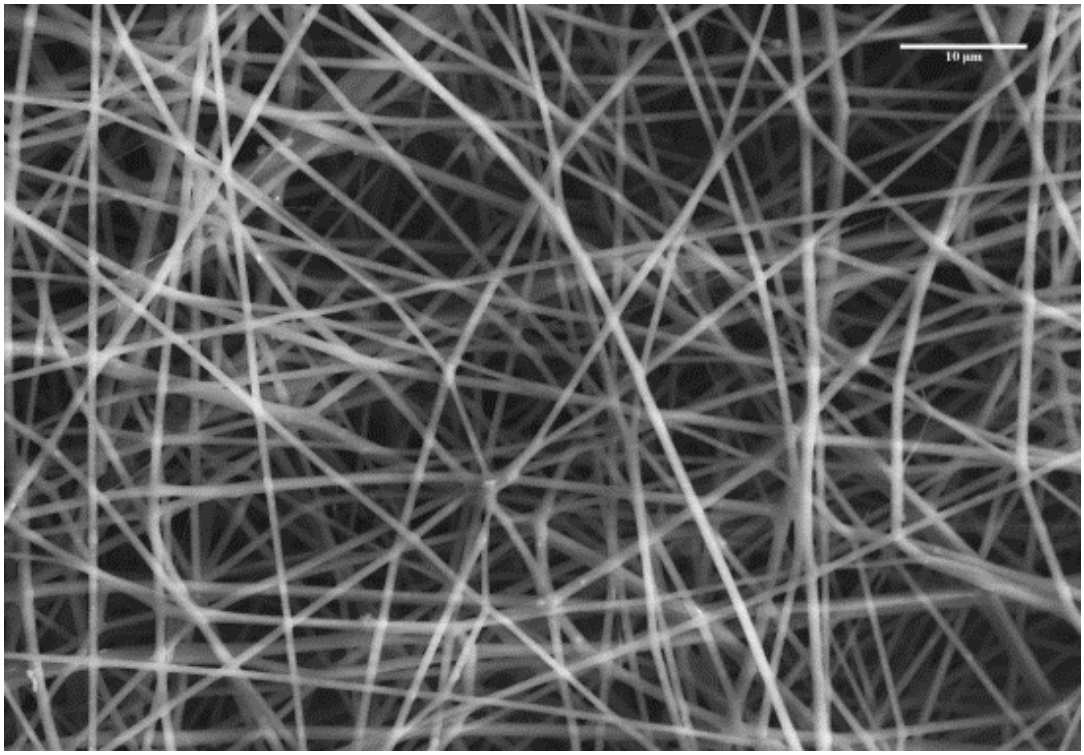

Figure 6.15 SEM Micrograph of needle electrospun jellyfish SACC fibres using a Hitachi S4800 FEG-SEM at an acceleration voltage of 10kV, emission current of 9µA and magnification of 1500X. Solution composition was 25% SACC (w/v) in a 90% AcOH solution (v/v). Fibre Diameter is shown to be 646nm ±121nm. Scale Bar = 10µm.

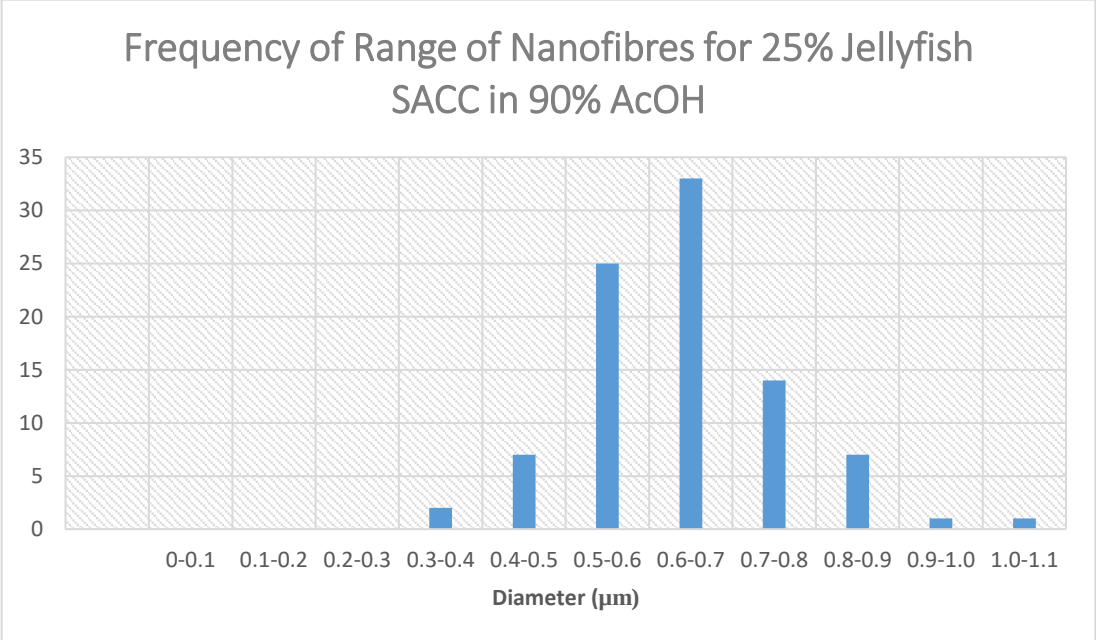

Figure 6.16 Graph representing frequency of range of single alpha chain collagen nanofibres from jellyfish sources (n=90).

6.12.6 SACC in 1X PBS

The 25% SACC samples derived from either jellyfish or bovine were dissolved in a 1X PBS (w/v) solution were electrospun and examined by SEM, showing a mean fibre diameter of 105 nm with a standard deviation of 28 nm for jellyfish derived SACC and a fibre diameter of 84 nm with a standard deviation of 27 nm for bovine derived SACC, based on 90 fibre measurements. Micrographs of the needle electrospun fibres can be seen alongside frequency of range in Figure 6.17 and Figure 6.18 respectively. The fibres contained little to no beading suggesting electrospinning conditions were optimal at 25% SACC, 18 kV, 20 cm and 0.35 mL/hour. These samples exhibited some spitting of solution onto the grounding target, due mainly to the high salt content within the solution raising the conductivity of the solution drastically. The use of PBS solution in replacement of 90% AcOH not only aids in reducing potential damage to the nativity of the SACC polymeric chain, but also produces significantly smaller diameter fibres, at 105nm for 1X PBS fibres compared with 646nm for AcOH and 107nm for HFP, meaning research findings into cell interactions with nanofibres will be more closely associated with those of HFP derived samples, of which there is an abundance of publications and reviews (Torres-Giner, Gimeno-Alcañ Iz, et al. 2009; Lu and Guo 2018; Mortimer, Widdowson, and Wright 2018).

6.13 Needle-Less Electrospinning Results

The 10% ASC samples, dissolved in 90% AcOH (w/v) were electrospun on the Nanospider system and examined by SEM, showing a mean fibre diameter of 512 nm with a standard deviation of 152 nm based on 90 fibre measurements. Micrographs of the needle-less electrospun fibres can be seen in Figure 6.19 (A) with frequency of range seen in Figure 6.19 (B). The fibres contained no beading suggesting electrospinning conditions were optimal at 10% CS ASC, 20 kV, 20 cm and 0.4 mL / hour.

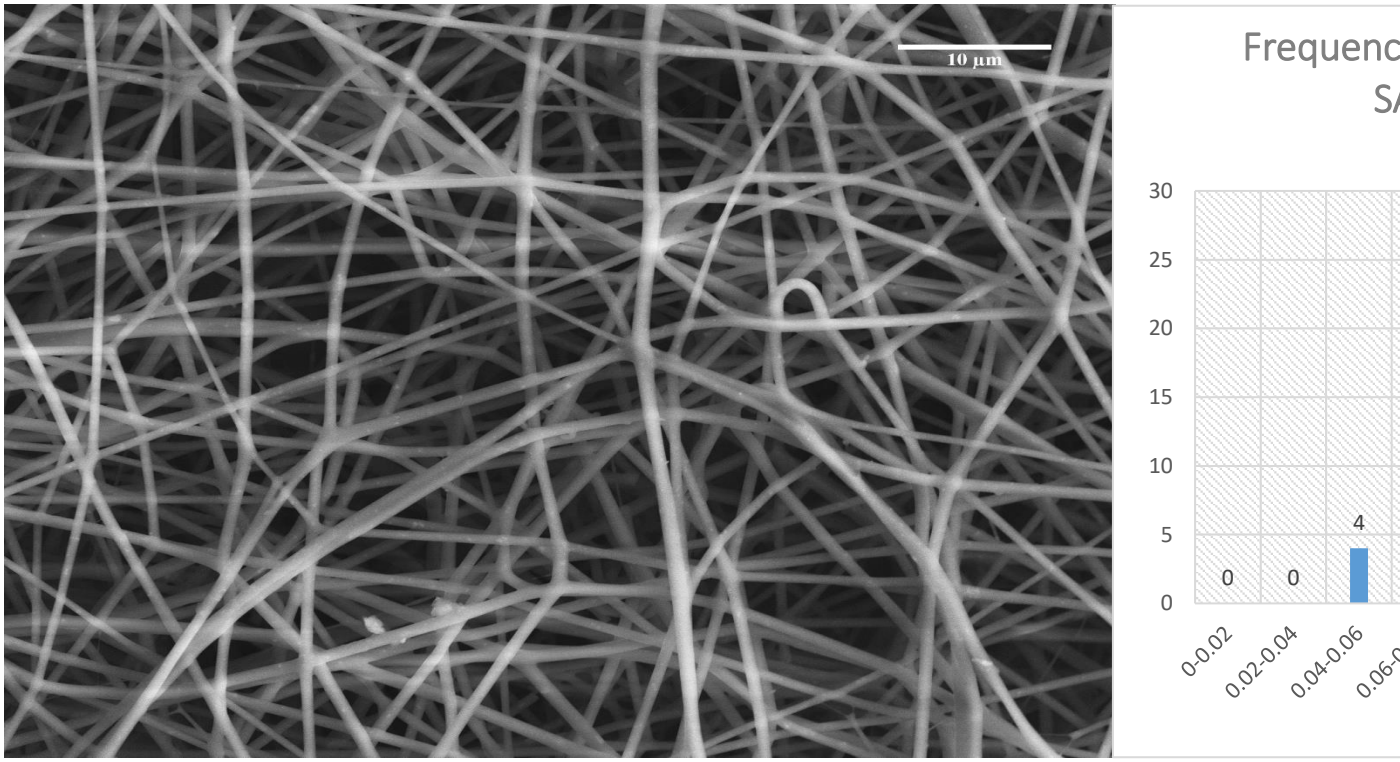

Figure 6.17 (A) SEM micrograph of JF derived SACC electrospun from a solution of 25% JF S 10µm. Acceleration voltage = 10kV. (B) Frequency of range of electrospun fibres from a soluti AcOH (n=90).

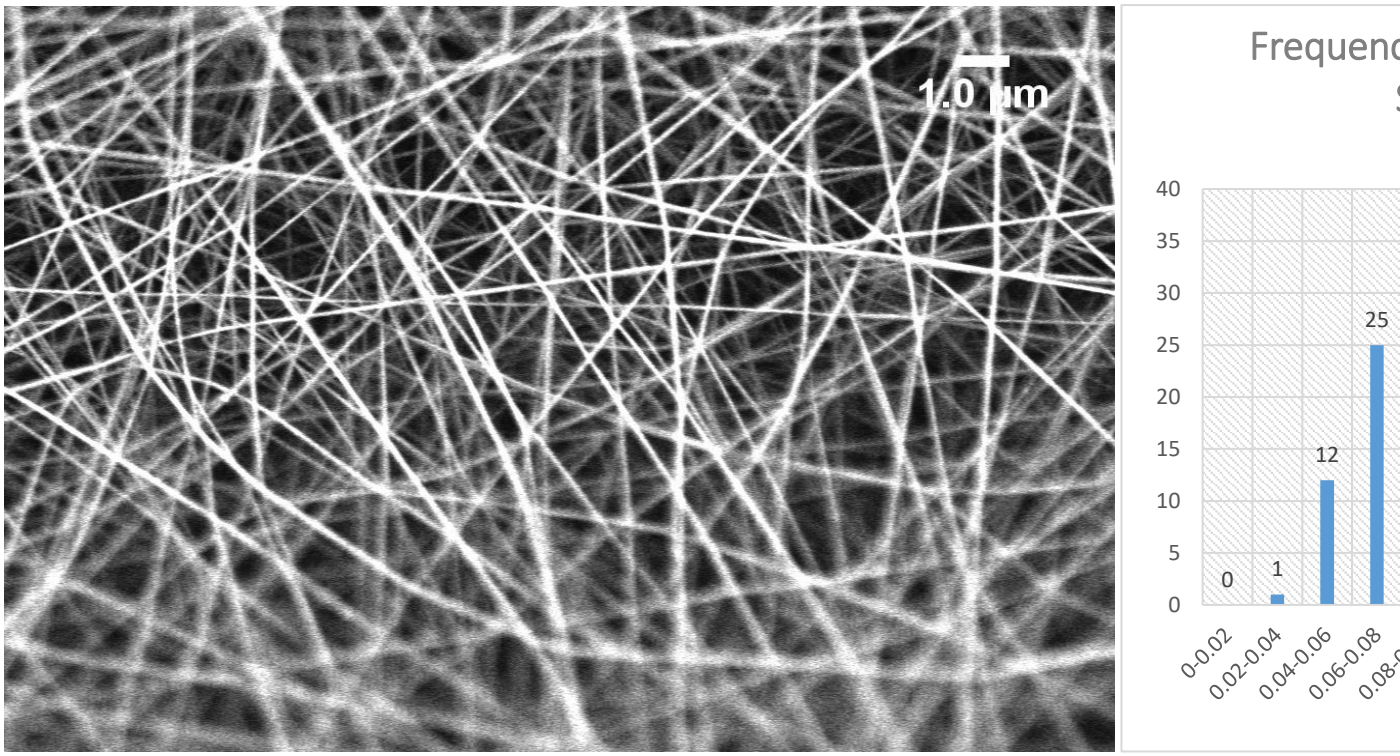

Figure 6.18 (A) SEM micrograph of bovine derived SACC electrospun from a solution of 25% b bar = 10µm. Acceleration voltage = 10kV. (B) Frequency of range of electrospun fibres from a in 90% AcOH (n=90).

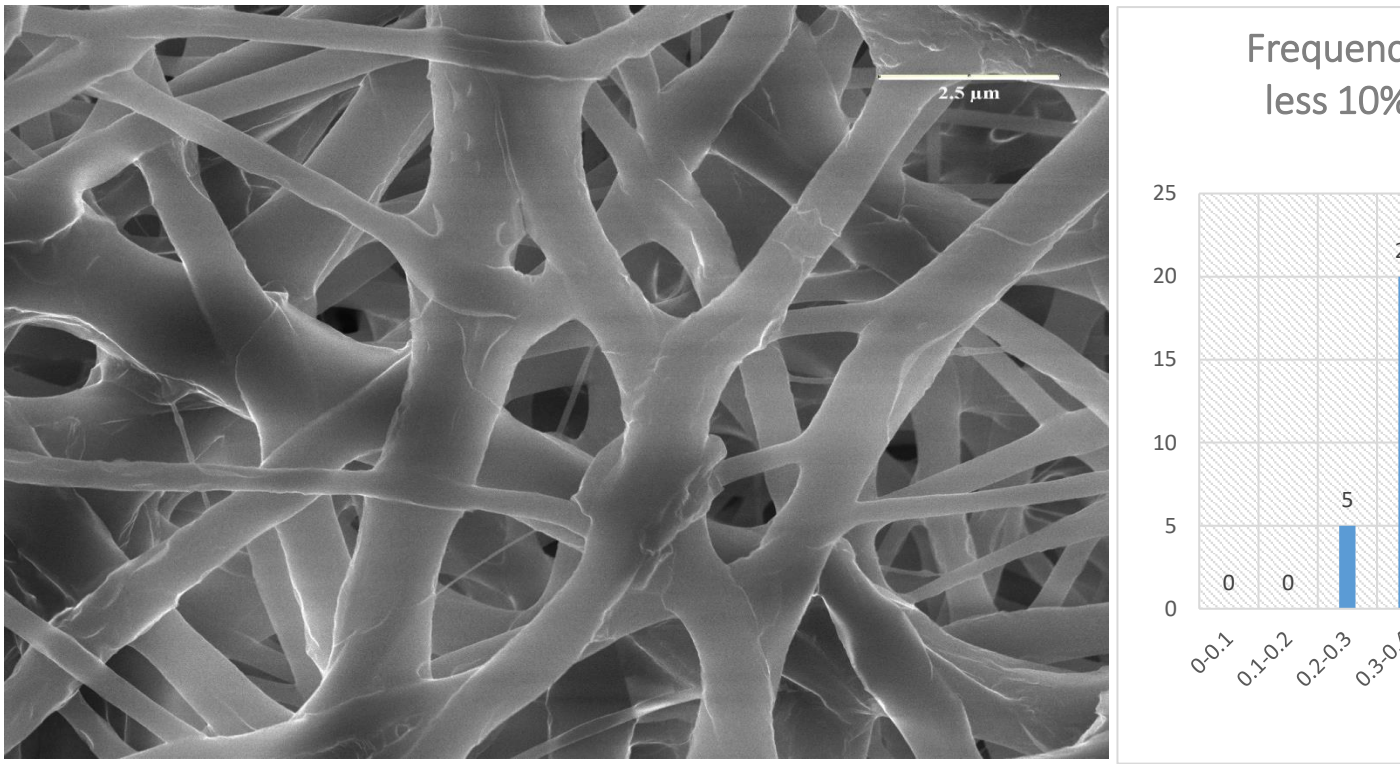

Figure 6.19 (A) SEM micrograph of needle-less electrospun CS ASC from a solution of 10% AS 2.5 µm. Acceleration voltage = 10 kV. (B) Frequency of range of needle-less electrospun fibre ASC in 90% AcOH (n=90).

It is evident from the difference in fibre diameter and standard deviation that the needle-less system, though significantly quicker in generating a dense nanofibre mat, allows for less control in fibre diameter, with a larger range of fibre diameters and larger overall fibres. This is supported by previous findings (Yener and Jirsak 2012; Burke et al. 2017) while it has been shown that the addition of salts such as tetraethylammonium bromide can control the fibre diameter to rectify this (Cengiz and Jirsak 2009).

6.14 Co-Electrospinning of Collagen & Polyethylene Oxide Methods

The solution of ASC / PEO blend was optimised at 3.214% PEO and 2.5% ASC in 90% AcOH. Electrospinning at 18kV, 20cm and 0.35mL/h were found to be optimal for an average fibre diameter of 301nm ± 51 nm, while 1.5% ASC / 1.5% PEO collagen produced dual fibre diameters where fibres of average diameter 318 nm ± 57 nm for the large fibres and 81 nm ± 26 nm were observed for the small fibres. Micrographs of the co-spun solutions and their ranges can be seen in figures Figure 6.20 and Figure 6.21.

6.15 Single Needle Electrospinning PEO Results

The 5% PEO solution produced optimal conditions, with an average fibre diameter of 134 nm, and a standard deviation of 33 nm. Micrographs for the PEO solution can be seen in Figure 6.22. The fibres were smaller than the co-spun collagen / PEO which were either 301nm or 318nm (large fibres) depending on solution concentrations.

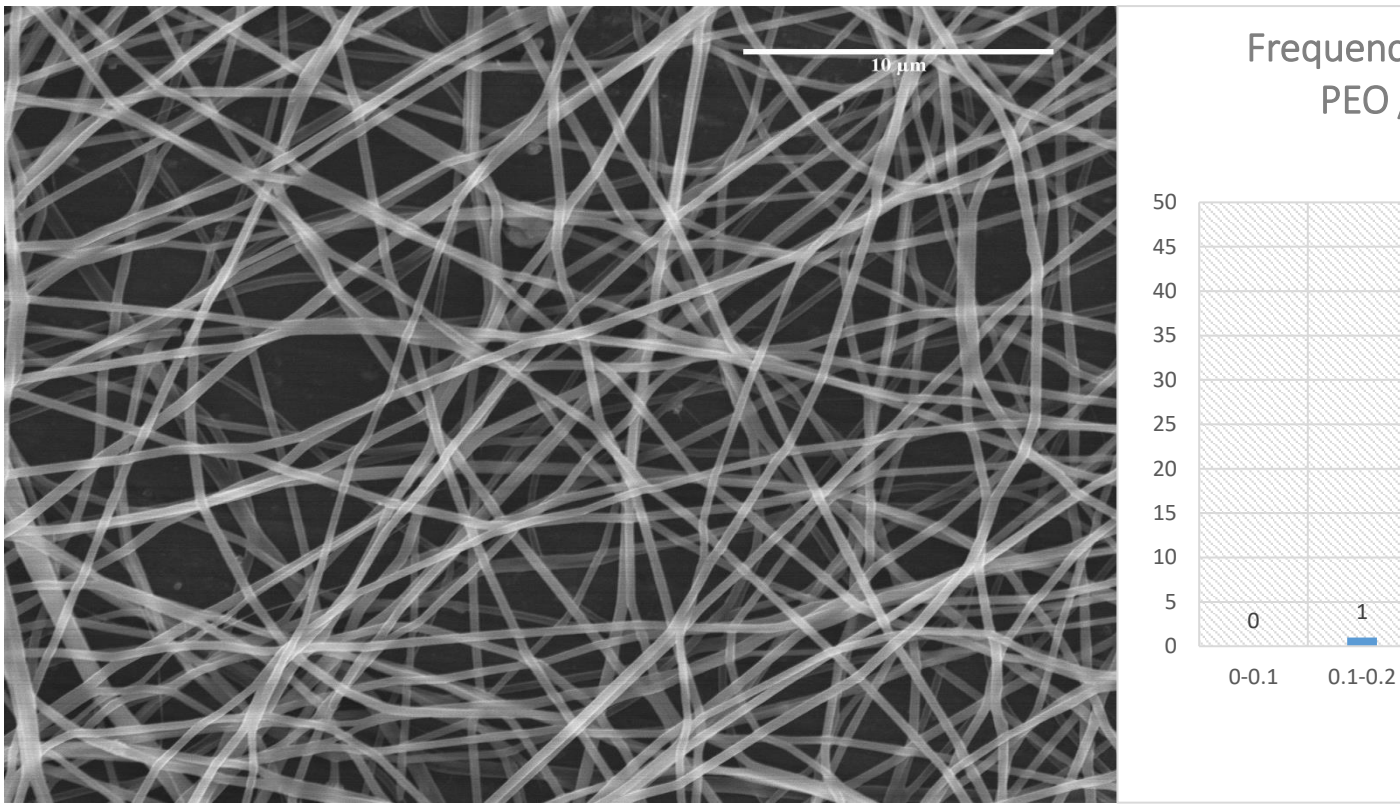

Figure 6.20 (A) Micrograph of PEO / ASC co-spun fibres at higher concentrations. Scale bar = = 10kV. (B) Frequency of Range for Co-Spun higher concentration PEO/ ASC mix (n=90).

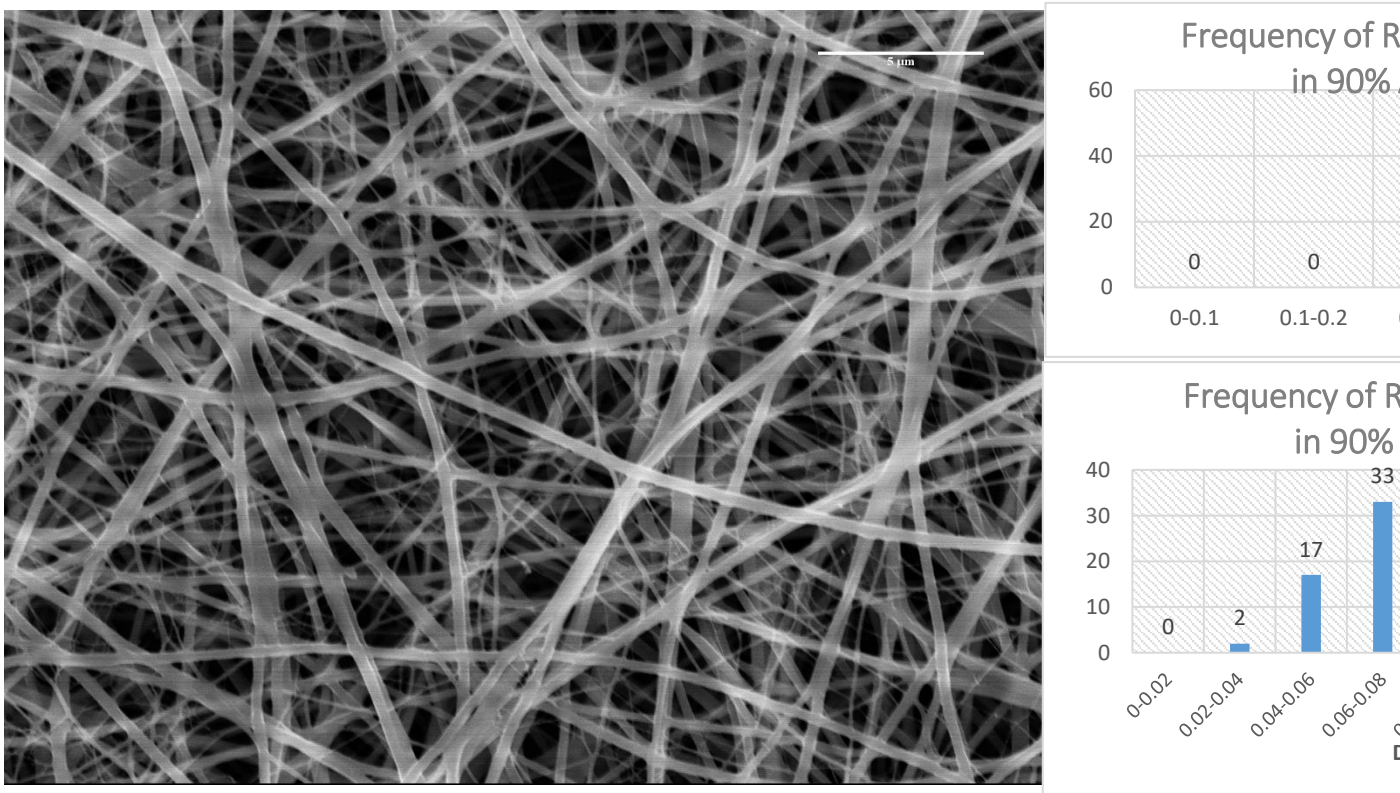

Figure 6.21 (A) SEM micrograph of electrospun blend of 1.5% PEO / 1.5% ASC in 90% AcOH. Acceleration voltage = 10kV. (B) Frequency of Range of large fibres from PEO / ASC blend (n of small fibres from PEO / ASC blend (n=90).

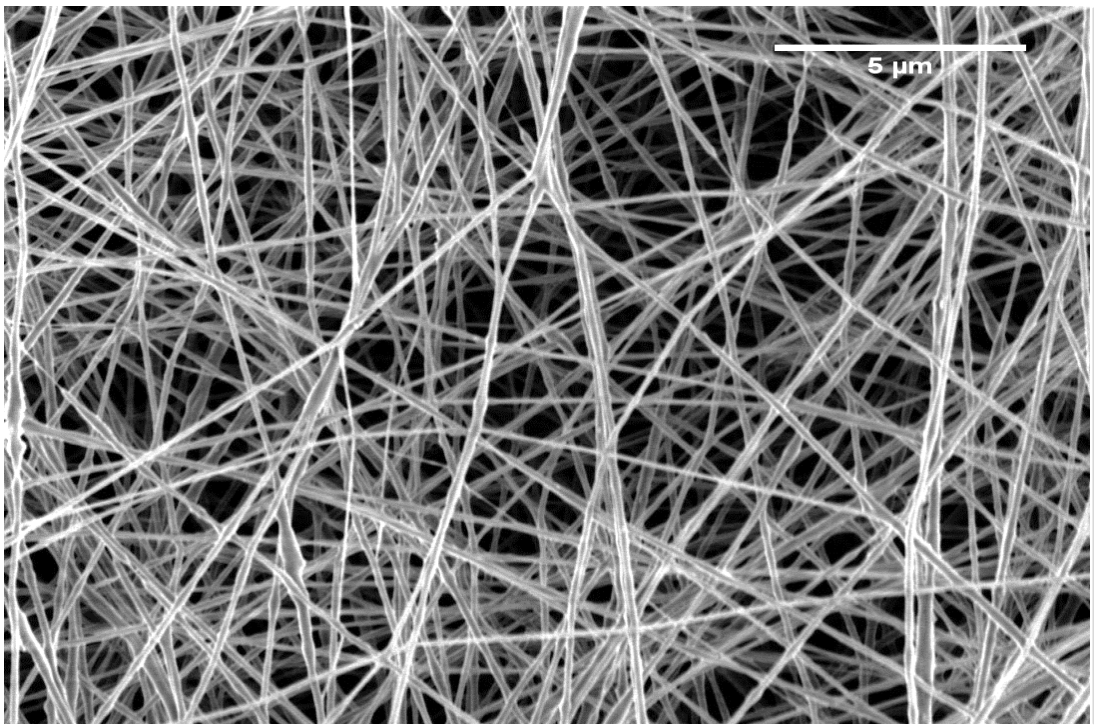

Figure 6.22 (A) SEM micrograph of electrospun PEO at 5% concentration in DI (w/v). Scale b
voltage = 2kV. (B) Frequency of range histogram for electrospun fibres of 5% PEO solution (n

6.16 Co-Axial Electrospinning of PEO as Sheath and Collagen as Core Methods

Coaxial fibres of PEO and ASC were electrospun with optimal conditions influencing the choice of concentrations used in the final optimisation, however 3.2% PEO and 2.5% ASC in 90% AcOH was unsuitable and led to beaded fibres with mixing of the polymer solutions at the coaxial needle tip. Instead the 5% PEO in DI was used in conjunction with the 10% ASC solution which led to optimum electrospun fibres using the conditions of 19kV, 18cm with syringe pumps at 0.35mL/h (PEO) and 0.2mL/h (ASC). This led to coaxial fibres of average diameter 286 nm ± 53 nm. SEM micrographs can be seen in

Figure 6.23, fibre distribution in Figure 6.24 with false colour SEM micrographs of the exposed inner ASC core obtained by freeze fracture observed in Figure 6.25.

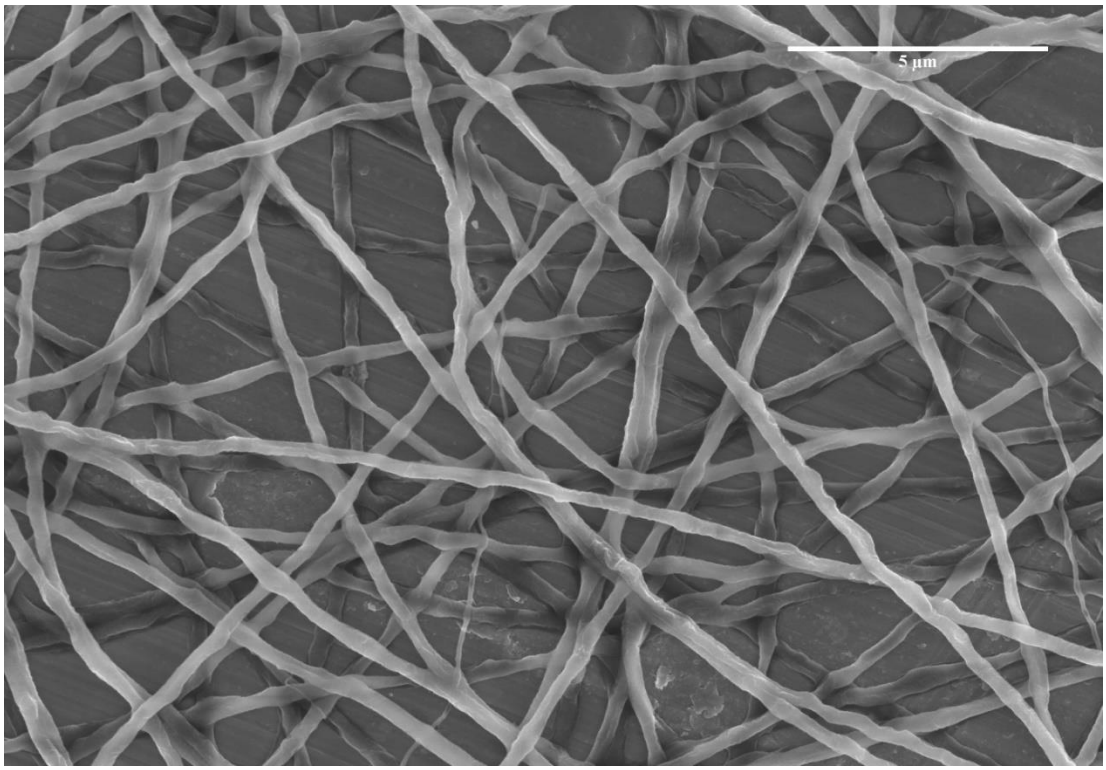

Figure 6.23 SEM micrograph of co-axial electrospun fibres of PEO / Collagen. Scale bar = 5µm. Acceleration voltage = 5kV.

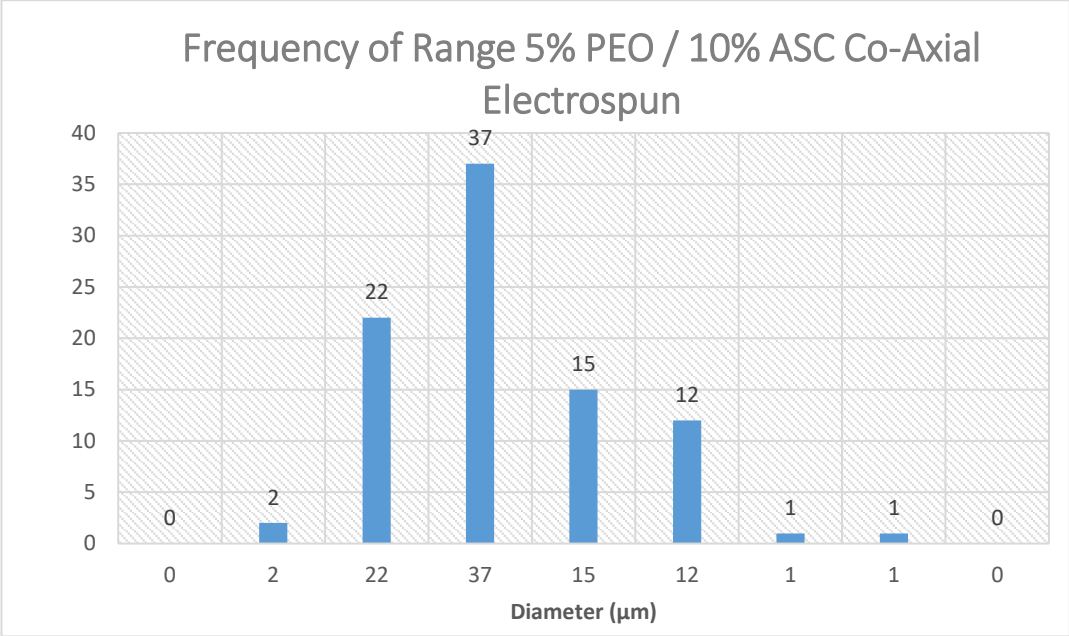

Figure 6.24 Frequency of range for co-axial electrospun PEO / collagen fibres (n=90).

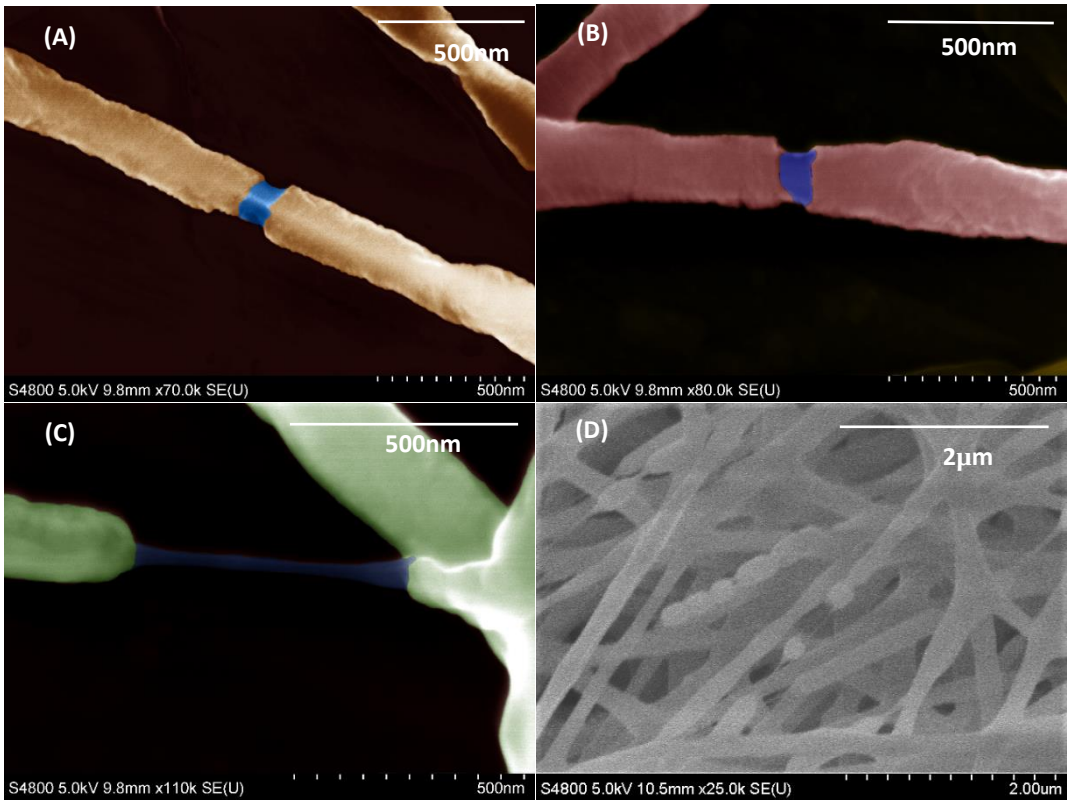

Figure 6.25 SEM micrographs of co-axial electrospun PEO / collagen fibres, freeze fractured in liquid nitrogen prior to imaging. Scale bar (A-C) = 500nm, (D) = 2µm. Acceleration voltage 5kV for all micrographs.

6.17 EDC Crosslinking of Electrospun Collagen Samples

Using the setup seen in Figure 6.8, scaffolds were crosslinked to produce insoluble fibres which retained their porous state. The use of this method was refined, where early compression was not uniform and produced poor quality scaffolds as seen in Figure 6.26, while later optimisation, using uniform compression and injection led to scaffolds which retained their original structure as seen in Figure 6.27.

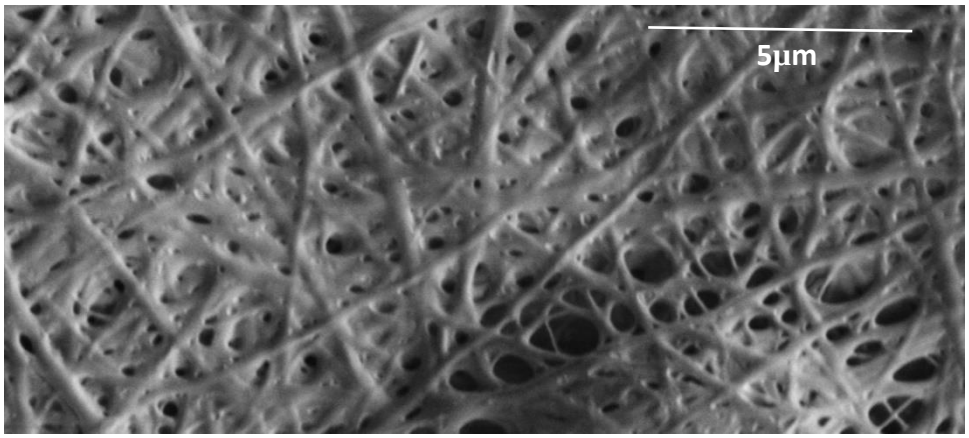

Figure 6.26 SEM micrograph of electrospun CS derived ASC crosslinked with EDC using compression method. Pores are restricted due to poor compression of the scaffold. Scale bar = 5µm. Acceleration voltage = 1kV.

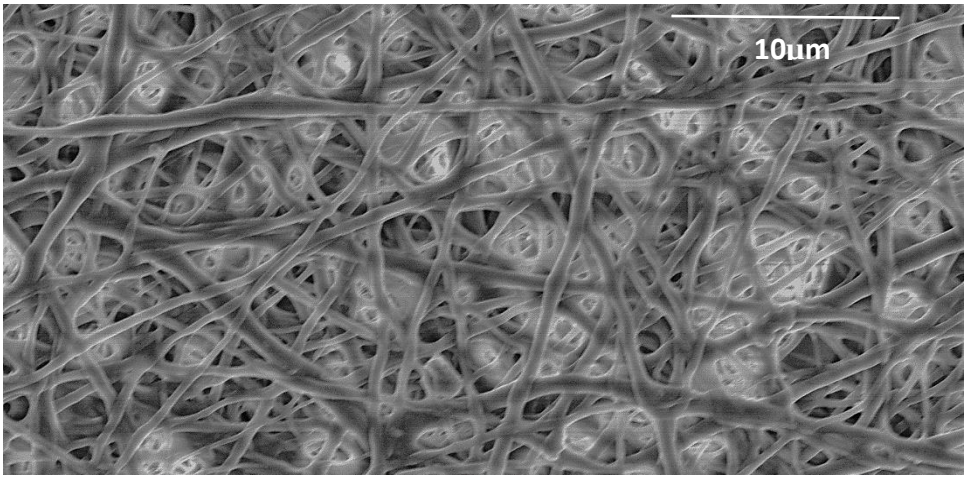

Figure 6.27 SEM micrograph of needle-less electrospun scale-up B10 SACC crosslinked with EDC using compression method. Pore access is improved due to increased compression and slower injection of EDC / ethanol solution. Scale bar = 10µm. Acceleration voltage = 5kV.

6.18 SDS PAGE of Electrospun Collagen Samples

For SACC electrospun samples, it was important to ensure that degradation had not occurred during the electrospinning process, and samples were run to test whether any chain breaks had occurred when undergoing electrospinning.

Figure 6.28 displays jellyfish derived B9 SACC prior to electrospinning in lanes 9 and 10 with lanes 3 and 4 showing the same B9 SACC solution post electrospinning when the scaffold was dissolved in DI and tested.

From this it is possible to see that some degradation has occurred from electrospinning, with a gelatin-like smear below 30kDa appearing at the bottom of the gel for lanes 3 and 4. It is noted however that lanes 9 and 10 contain a series of proteins between 10 and 25kDa due to poor purification, and it may be that the smearing of these bands as seen in lanes 3 and 4 is simply an artefact of pure stain binding. With consideration of the 1:10 dilutions in lanes 5-8, it is clearer that there is an increase in these lower molecular weight bands for electrospun SACC as can be examined using ImageJ software. This is supported by the findings of (Zeugolis et al., 2008a) where further degradation is seen from the electrospinning process than simply dissolving in HFP alone.

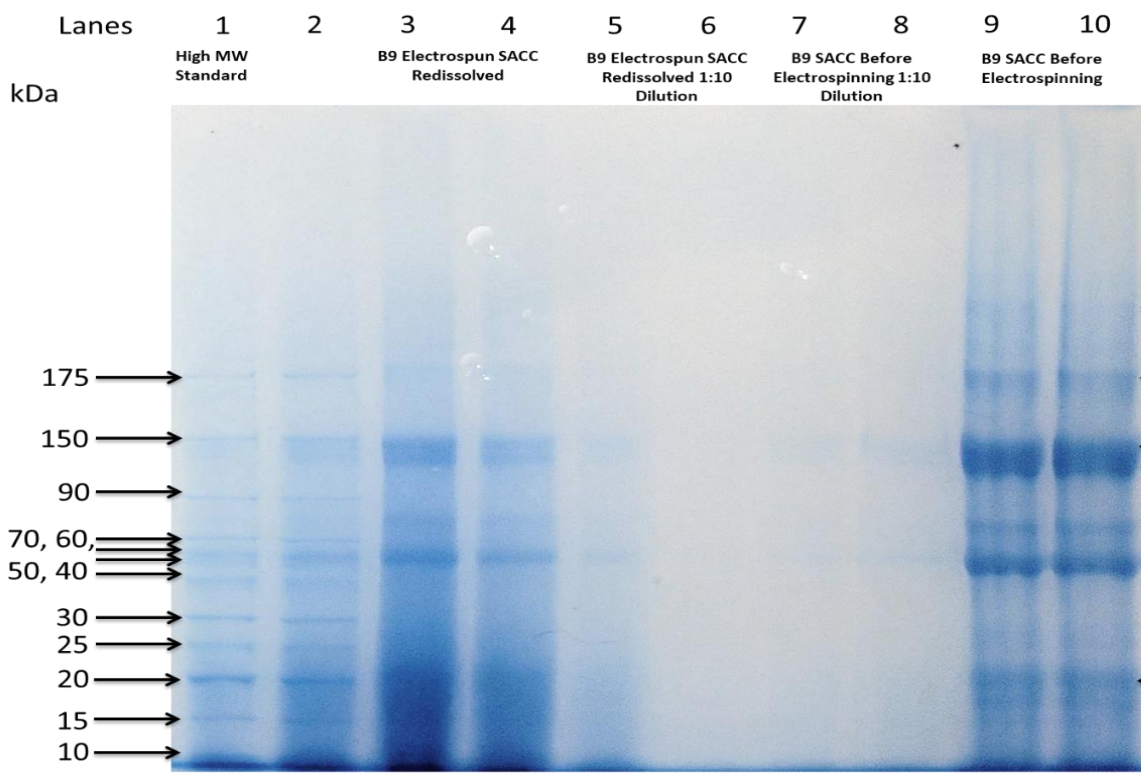

Figure 6.28 SDS PAGE of B9 SACC pre and post electrospinning to observe protein changes c
electrospinning (n=2).

For coaxial electrospun samples, the purpose of the PEO sheath, as well as to permit the electrospinning of ASC collagen solutions, was to ensure the ASC did not undergo degradation during the electrospinning process, due to the potential interactions between the PEO and ASC which stabilise the solution as has been shown to be the case with (Li & Xia, 2004) despite the increased shear on the core solution shown by (Pakravan, Heuzey, and Ajji 2012). To test whether the ASC was adequately protected, samples were examined as to whether the ASC had survived electrospinning or fragmented. The results can be seen in Figure 6.29 with lanes 7 and 8 showing the residual ASC within the dissolved PEO/ASC co-axial sample, without significant change to lane content of α1 & α2 of the B8 solution used in Figure 4.12 (lanes 7-9).

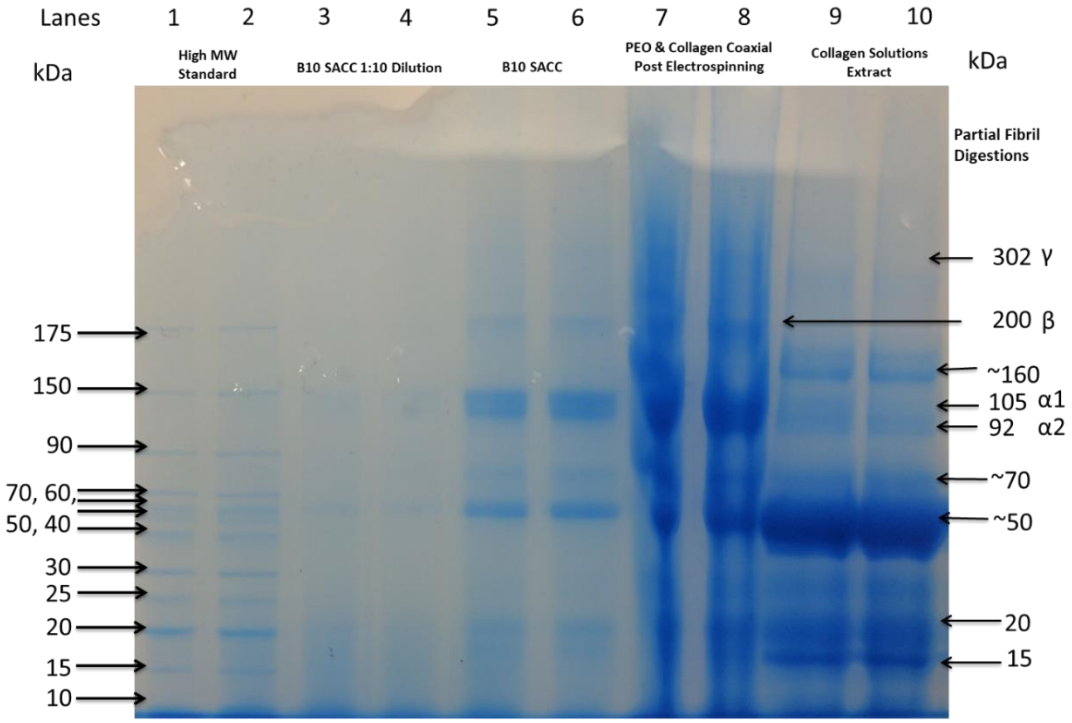

Figure 6.29 SDS PAGE analysis of co-axial electrospun ASC / PEO solutions which were dissolved post electrospinning to observe degradation of the collagen strands.

Following this result, it was important to test whether the electrospun material could survive treatment with pepsin as described in (Zeugolis et al., 2008a), where damaged triple helices would become susceptible to degradation. Figure 6.30 shows the dissolved solutions where lane 3 shows the pepsin treated sample, with lane 4 being untreated. It is clear from this that the triple helical structure of the ASC has been damaged sufficiently by the electrospinning process to permit chain cleavage by pepsin, confirming the findings of (Zeugolis et al., 2008a) that electrospinning itself, regardless of solvent, causes a degree of damage to the protein structure.

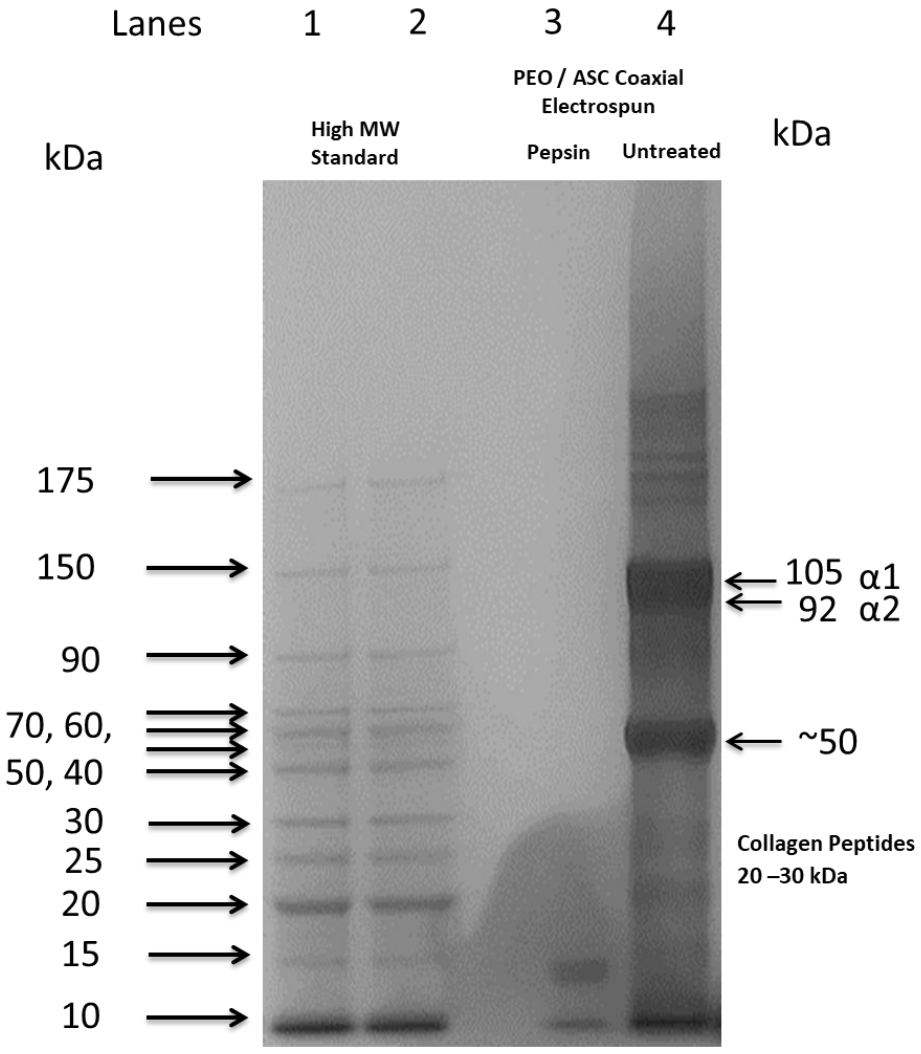

Figure 6.30 SDS PAGE analysis of coaxial electrospun ASC / PEO with treatment of pepsin for 24h to detect whether the triple helix remains resistant to pepsin activity post-electrospinning (n=1).

6.19 FTIR of Electrospun Collagen Samples

To assess the degree of change through the electrospinning of SACC, FTIR was again utilised to compare the samples examined in 5.4 with those which have been electrospun for any changes to the structure of the SACC, or its ability to refibrillise. Figure 6.31 shows the spectra of electrospun SACC from scale up B10 with the pre-spun extract and shows no significant change between the samples, once baseline correction and normalisation had been carried out. Homology between the samples was 95.71% as calculated by the Perkin Elmer Spectrum software. This finding in accompaniment to the SDS PAGE data above shows that there is a degree of strand breakage occurring within the sample, but that the overall secondary structure remains unchanged.

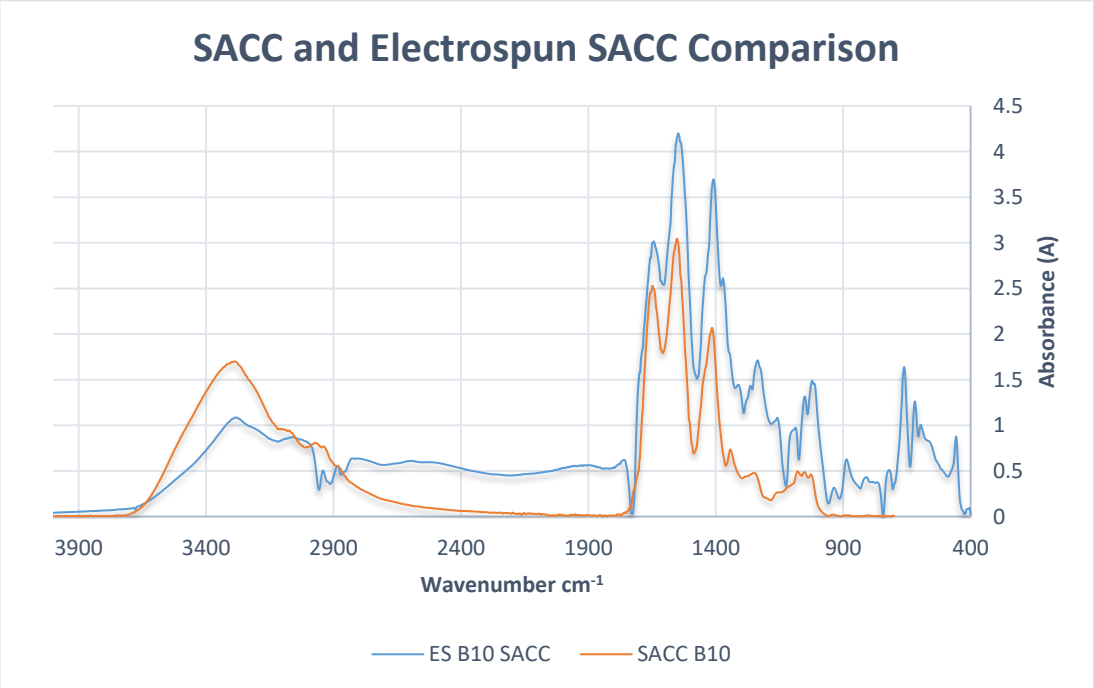

Figure 6.31 FTIR spectra displaying a comparison between electrospun B10 SACC and SACC extracted during scale-up batch 10. SACC has a marked reduction in amide 1 in both samples signifying a reduction in the abundance of triple helix (γ-chains). No significant reduction in amide 1, 2 or 3 are present, with a homology value of 95.71% between the samples when normalised and baseline corrected.

To ensure the degradation effects of electrospinning were not detrimental to the refibrillation properties of SACC, a section of electrospun scaffold was dissolved in a solution of 1X PBS and stored at 4°C for one month. This sample was then lyophilised and tested against the electrospun sample.

Figure 6.32 displays the FTIR spectra of electrospun SACC and refibrillised electrospun SACC displaying a return of the amide 1 peak dominance over amide 2 and confirming that the electrospinning of SACC is not detrimental to its ability to refibrillise into triple helical ASC-like collagen *in vitro*.

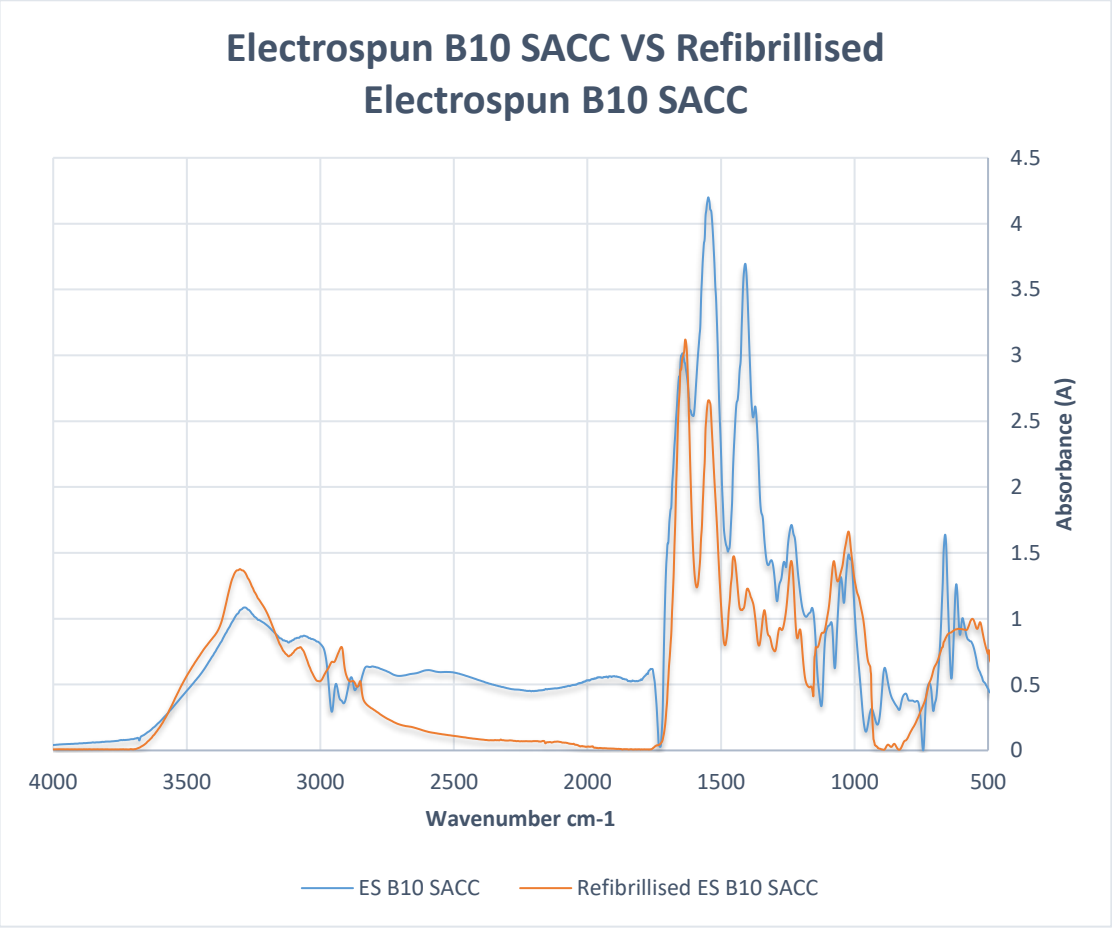

Figure 6.32 FTIR spectra displaying a comparison between electrospun B10 SACC and refibrillised electrospun B10 SACC. The refibrillised electrospun SACC has regained a greater amide 1: amide 2 ratio signifying an increased abundance of triple helix (γ-chains) within the sample.

6.20 FRESH Printing Results

In order to use the Flashforge Creator Pro 3D printer, it was necessary to modify the setup using opensource prints by (Hinton et al. 2015) which were since modified. The version 2.5 was selected for use within these experiments and was printed and assembled as seen in Figure 6.33.

Figure 6.33 Printed Replistruder V2.5 designed by (Hinton et al. 2015) *and modified for opensource release. Assembly of the printer's stock motor allowed for online control of solution deposition and retraction.*

The use of the Replistruder system, designed for the MakerBot replicator was not entirely compatible with the Flashforge Creator Pro (a MakerBot replicator clone), so modifications to the mounting were required, with a custom rail-plate (Figure 6.34(A)) and mounting stand (Figure 6.34 (B)) being produced to give a final setup shown in Figure 6.35. These were designed and implemented after several modifications to successfully give a functioning bioprinter setup.

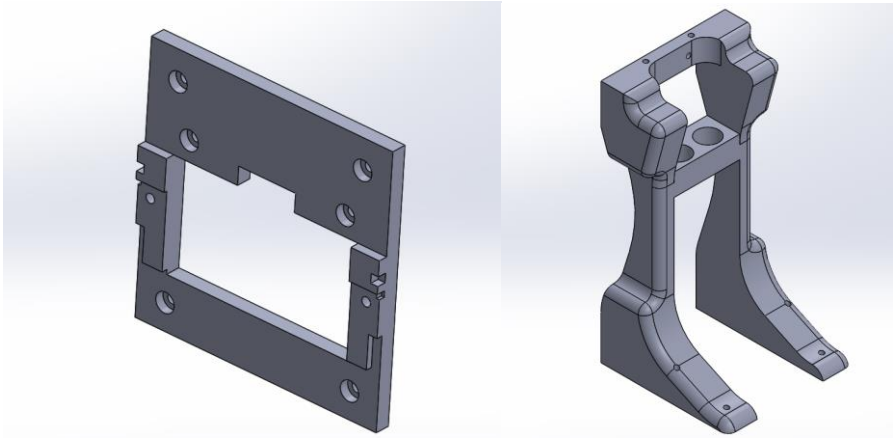

Figure 6.34 (A) Custom rail plate to fit the Flashforge Creator Pro. (B) Custom frame to support and position the Replistruder, with air vents to provide better cooling to the stepper motor.

Figure 6.35 Replistruder mounted to Flashforge Creator Pro and setup to print the solution.

Gelation trials were carried out on several ASC and PSC samples of scale up B9 and B10 to test which conditions would be optimal for printing. Table 6.1 shows the initial results of these trials, in which the sample and conditions from trial 10 were carried forward for FRESH printing.

Table 6.1 Gelation trials of ASC and PSC samples to optimise and select for the most appropriate conditions to carry forward for 3D bioprinting in the FRESH setup.

Trial no.	**Collagen Gel Trials**			
	Collagen Solution	***PBS***	***Genipin %***	***Gelled?***
1	Pepsin solubilised	10x	0.05	No
2	Acid solubilised	10x	0.05	No
3	Pepsin solubilised	10x	0.1	No
4	Acid solubilised	10x	0.1	No
5	Pepsin solubilised	10x	0.1	Partial
6	Acid solubilised	10x	0.1	Partial
7	Pepsin solubilised	10x	1.0	Yes, at 4°C
8	Acid solubilised	10x	1.0	Yes, at 4°C
9	Pepsin solubilised	10x	1.0	Yes, at 20°C
10	Acid solubilised	10x	1.0	Yes, at 20°C

The printing of scaffolds within the gelatin slurry as seen in Figure 6.36 produced samples which were of lower definition than described by (Hinton et al. 2015), as can be seen in the simple face PCL print in Figure 6.37, which printed well but due to a low polymer print concentration led to collapse of the sample and rough edges. The scaffold printed in Figure 6.38 (A) also showed rough edges and an overall poor print quality, due mainly to the use of gelatin as the slurry which is also susceptible to

crosslinking by genipin alongside collagen, leading to scaffolds which were externally fuzzy with a gelatin coating. The move to the coaxial method and the improved ASC gelation time of scale up batch 10 compared with previous batches led to clearer scaffold edges. An example print can be seen in Figure 6.38 (B) where the cross-hatch formation is much clearer.

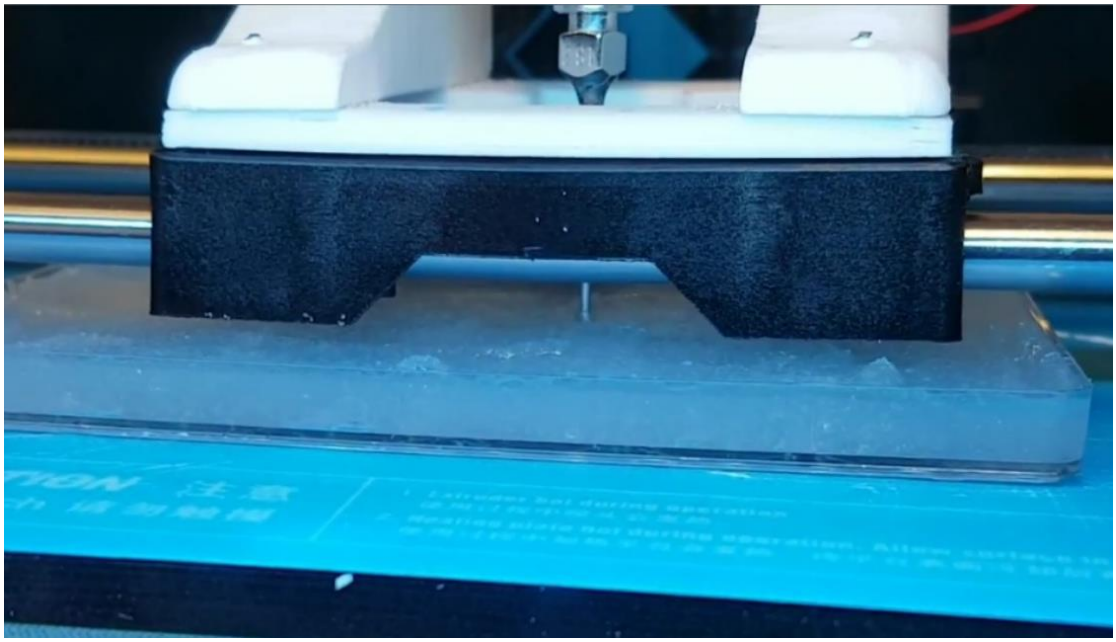

Figure 6.36 Printing of ASC hydrogel into gelatin slurry according to the FRESH setup described by (Hinton et al. 2015).

Figure 6.37 Simple print of a low-poly face to optimise the printing of PCL using the Replistruder setup before progressing onto FRESH printing setup. Left displays the print upon completion while right shows the same sample 1 hour after drying, where the sample has become uneven, with holes and rough edges appearing.

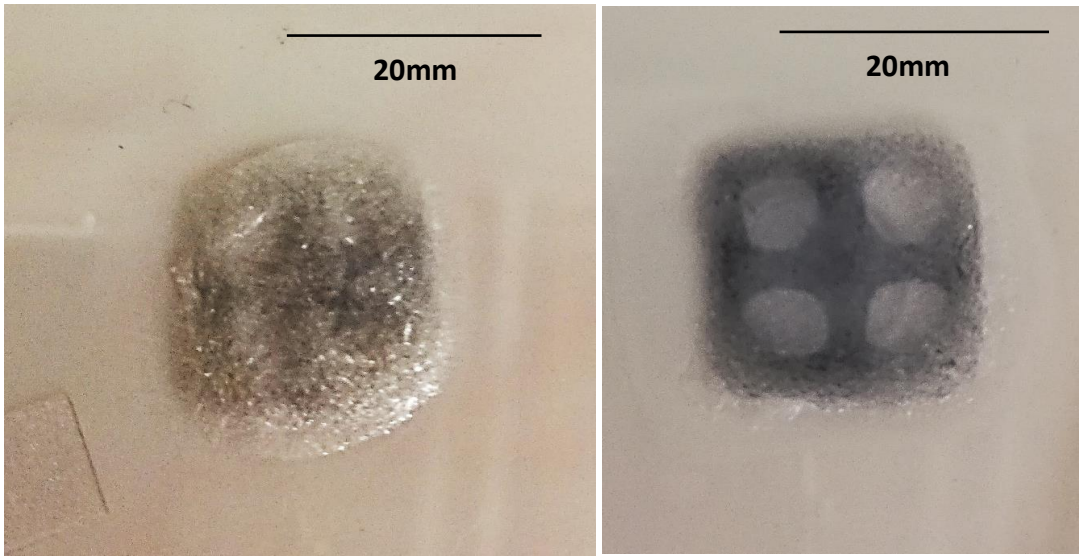

Figure 6.38 (A) Cross-hatch print design in optimisation of ASC bioprinting, where lines are not defined due to the crosslinking of surrounding gelatin slurry with the collagen, leading to an undefined structure. (B) The same cross-hatch print design produced using the improved coaxial printing method, where lines are more defined and gelatin slurry has not been crosslinked, giving clear holes and defined holes within the structure.

Another issue which arose from the FRESH bioprinting setup was the spreading of lower layers which was observed when prints in excess of 10mm height were produced. As seen in Figure 6.39 the scaffold has widened at its base, causing a sloping structure where this should be vertical.

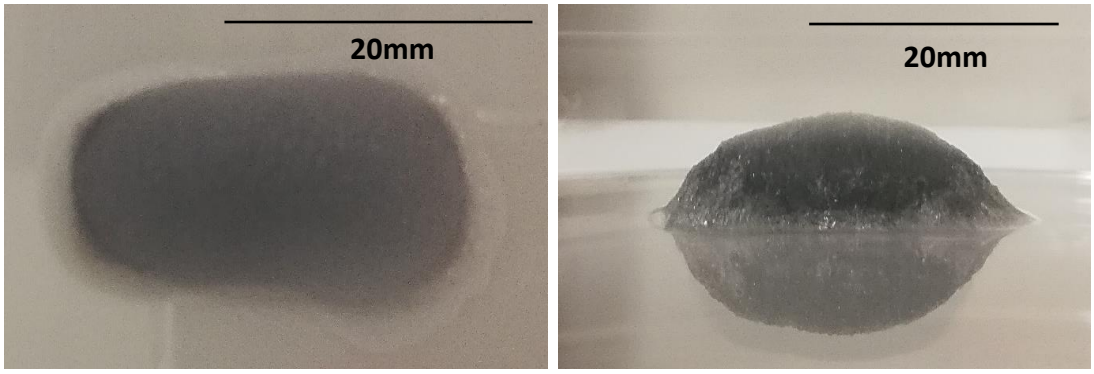

Figure 6.39 The sloping effect observed in FRESH printed ASC samples when height was >10mm. Left shows top down view, right represents side profile.

Overall, the bioprinting of scale up ASC, particularly that of higher quality with faster gelation times, proved successful. The FRESH printing methods produced by (Hinton et al. 2015) were not entirely compatible with the use of collagen as the printing material, due to the crossover in crosslinker effectiveness with methods such as genipin. The use of a more controlled system, such as rose bengal and laser light should permit more accurate control over scaffold crosslinking as used by (Cherfan et al. 2013). Another aspect which would further improve results is to further lower the moisture content of the gelatin slurry, which would provide a firmer support for the printed scaffold. The effectiveness of the improved ASC, from both jellyfish and bovine sources show great potential for use in bioprinting, and the translation from bench prototype to a specialised device such as the 3D-Bioplotter (EnvisionTEC, USA) would be the next logical step.

6.21 Conclusions

Throughout this chapter the progression of electrospinning applications of acid soluble collagen solutions are explored. This has progressed from currently adopted practices that rely on the use of fluorinated alcohols, through the use of coaxial electrospinning to protect the collagenous material from denaturation during electrospinning, to the final application of the single alpha chain collagen material. The use of SACC allowed for the utilisation of benign solvent mixtures which protect the re-fibrillation properties of this novel protein mixture.

This has demonstrated the breadth of applications that have direct relevance to medical device manufacture and tissue engineering for the protein, using needle-less electrospinning to demonstrate the scalability of this process for research commercialisation, making the work of this chapter industrially relevant. The use of FTIR and SDS PAGE confirmed that the protein underwent minor protein degradation observed by SDS PAGE, with chemically identical FTIR spectra shown. Furthermore, the minor degradation seen within Figure 6.28 was not sufficient to prevent the

refibrillation of SACC into an ASC-like protein with triple helical structure. This has significant advantages over the use of HFP, where irreversible degradation in many cases results in ‘an expensive way to make gelatin’. The use of SACC opens new avenues in the manufacture of medical devices through electrospinning, without the harmful denaturation seen when using fluorinated alcohols. The resorb-ability of electrospun SACC in a wound dressing setting, providing a fresh collagen source to the wound which can be remodelled to suit the body’s needs while refibrillising into acid soluble collagen to aid with wound closure will be an interesting application to be explored further in future.

The application of ASC to bioprinting offers an opportunity to a growing field, being simple in composition and use, and acting as the ideal protein for cell adhesion in vitro for the creation of biomimetic scaffolds. Though much further work is required to realise the potential of this novel field, the pace is moving quickly, and ASC has been shown to be particularly suitable to application in bioprinting with reliable and repeatable gel formation. The improved process provided a better-quality solution than in previous iterations, which had a reliable and repeatable gelation profile, with scale up B10 samples gelling in under 30 seconds which was well suited to the coaxial printing method.

7 Summary Conclusions & Further Work.

7.1 Summary Conclusions

The aims of this work were to examine the extraction and characterisation of collagen derived from jellyfish, as well as to assess the applications in tissue engineering and regenerative medicine for this material and scaffolds produced from it. Throughout this thesis, the work carried out has presented several novel discoveries. The scalable manufacturing process developed within chapter 4 permits the production of high-quality acid soluble collagen from both mammalian and non-mammalian animals, with particular focus on increasing both the yield and qualitative quality of extracts. This process acts as an industrially relevant research finding, which has permitted kilogram levels of collagen to be produced using a process that facilitates compliance with key manufacturing objectives such as ISO 13485.

The isolation of single alpha chain collagen described in chapter 5, presents a novel collagen formulation which separates the alpha chains present within acid soluble collagen to give rise to a formulation which benefits from an enhanced solubility profile. This permits a new avenue of medical device development for collagen to be explored. The unique qualities of this protein formulation permit electrospinning in benign solvents such as acetic acid, and more importantly, the use of water-based salt solutions such as PBS as discussed in chapter 6. This produces scaffolds which do not contain harmful residuals as is often the case when fluorinated alcohols such as HFP and TFE are used (Zeugolis et al., 2008a). The application of SACC in this manner results in a major progression for the field of collagen electrospinning, where ongoing debate into the denaturing effects of HFP has prevented progress in electrospun collagen development for medical device and tissue engineering applications.

Finally, the ability of SACC to refibrillise *in vitro* to recreate the triple helical gamma chains presents a key differentiating factor to the use of gelatin, giving the best of both worlds, a high solubility with reformation to acid soluble collagen, the current gold standard, in physiological conditions. This benefit allows SACC to be used in a multitude of applications, such as high-density sprays or films, which may then be used within the body to remodel the damaged area, reducing wound closure times. If

the further work described supports such applications, SACC may be cemented as a vital protein for use in tissue engineering and regenerative medicine.

The use of collagen in the manufacture of medical devices for tissue repair facilitate the move towards personalised medicine. The use of the process developed in chapter 4 allows for the scalable manufacture of ASC, increasing the economic viability of the material for use in medicine. The scalable manufacture of SACC described in chapter 5 also permits the use of this material in medical device contexts. Both processes enhance online quality control over benchtop methods, which may be further enhanced with the use of automation. The removal of the need for centrifugation in this process allows the system to be managed in a closed manner, reducing contamination risks while removing the need for cleanrooms.

Due to the issues which have been seen with electrospinning of collagen, many of the traditionally accepted methods for the fabrication and stabilisation of these membranes has been called into question by the work of (Zeugolis et al. 2008a). The use of fluorocarbon solvents, as well as the use of glutaraldehyde as the 'gold standard' crosslinking agent has caused damage to the collagen nativity, and calcification of surrounding tissues, lowering the efficacy of the scaffold in medically relevant settings.

Aggressive methods such as these are now regarded as incompatible, and the need for a solution to the use of collagen in medical scaffolds is a key target for researchers globally. There remains a great deal of interest, with several research groups attempting to preserve the collagen during electrospinning and to use crosslinkers which show increased biocompatibility.

As the techniques for electrospinning continue to improve, the technology will allow for increased control and a variety of collagen based electrospun scaffolds to be produced, both at bench and commercial scale. Despite the ongoing debate as to the future of electrospun collagen, the biomaterial has shown itself to be extremely useful when interacting with cellular systems. As new techniques enable a more native collagen to be electrospun, the potential improved clinical results may cement collagen's place as the top polymer of choice for clinical applications, including wound, vascular, nervous, bone and dental.

The extraction and purification of SACC creates a novel solution to the electrospinning of collagen nanofibrous membranes that has not been previously

achieved. This material allows the collagen to be electrospun from water-based solutions, and the use of PBS demonstrates clinical integration potential for these nanofibrous membranes. The flexibility of this material in regard to its applications present novel solutions to healthcare, through methods such as the clear dressing casting and electrospinning.

This work, as highlighted in the critical assessment and future work sections, lacks the in-depth cellular analysis for SACC which will confirm whether the exposed α-helices are of benefit or detriment to the immune system either *in vitro* or *in vivo*. Future work to explore the effects of SACC within a cellular environment, in electrospun, film, sponge and spray formats will only then reveal the direct benefits SACC-based devices can provide over existing technologies. The limitations surrounding the use of the membrane extraction system, in relation to the lack of effective removal of contaminants which share the size exclusion range of collagen such as LPS make the removal of these contaminants, should they be present in higher quantities in future harder to remove without the need for additional stages.

In summary, the creation of a scalable manufacturing process for the extraction of acid soluble collagen, and the discovery of a novel collagen formulation in SACC offer promising new avenues for the use of animal derived, and more specifically non-mammalian collagens within tissue engineering and regenerative medicine, as well as to the wider application of collagen.

7.2 Critical Assessment

The aims of this work were the exploration of the use of jellyfish derived collagen, from extraction and characterisation through to its uses in tissue engineering and regenerative medicine. The literature has demonstrated that marine collagens are often shown to be vastly inferior, due not only to their lower denaturation temperature, but to the mismatch of results which have been seen from developing nations, promising vastly different properties than those known to acid soluble collagen extracts. Throughout chapters 5-7, this work found that when handled properly, the use of jellyfish provides an acid soluble collagen solution which matches the characteristics of those from mammalian sources, particularly surrounding the electrospinning characteristics requiring the use of fluorinated alcohols. The implementation of this process required several step-changes in the way jellyfish are commonly handled and does not address the use of salting as a preservation method, commonly employed in Asia, to examine whether this would affect the efficacy of extraction.

The bioprinting of ASC within this body of work remains in its infancy stage, while much greater work is required in order to utilise this material in a quickly developing field.

The creation of SACC as a new material is described within this work as a collagen protein which has the ability to refibrillise into acid soluble – like collagen that contains triple helical gamma chains. The use of this terminology seeks to distinguish the protein from denatured gelatin alternatives, which in certain cases have been shown to exhibit partial renaturation. In order for SACC to be fundamentally distinguished from these materials, it would be necessary to conduct extensive examination of differences, using techniques such as transmission electron microscopy, differential scanning calorimetry, atomic force microscopy (AFM), as well as those already used within this work. Due to time constraints and a lack of access to equipment capable of conducting this work, these further assessments were not carried out, although they should be examined as part of the body of further work described below.

The use of SACC in electrospinning permitted the use of benign solvents, and in particular PBS to be used, however experimentation with other solvent systems, such as buffered media, and even cell electrospinning were not explored. Again, these

should be examined in future, while further testing on the extent of denaturation caused by the electrospinning process to the SACC should be carried out. As is common with new materials, it is not possible to conduct complete characterisation of the material, in particular when the discovery was not made until part-way through the studentship.

The lack of cellular interaction with the SACC materials, in different forms was not conducted during the course of this work, however given the literature on cellular interactions with damaged collagen within a wound (Brett 2008) it is important that this is conducted to better understand how the use of SACC within a wound-based setting would result.

Finally, due to time constraints, the testing and further development of SACC based prototype medical devices, such as the cast film were not fully characterised and again should be included within the body of further work.

7.3 Future Work

The work covered within this thesis lays the groundwork on two novel processes. The first process, described in chapter 4 creates a scalable system for the production of acid soluble collagen, with a particular optimisation for use with jellyfish. This work has since been adapted and scaled for use in the company sponsor's manufacturing facility (Newable 2017). Further work to this should involve adaptations to better suit extraction from mammalian animals, whose sources such as bovine hide, are traditionally more robust than jellyfish, requiring a series of pre-processing stages to improve the extractability of collagen. Furthermore, the process should be further adapted with the addition of several NMWCO membranes between 100 and 300kDa in order to better refine the quantities of alpha, beta and gamma chains within the extract and give a more consistent end product. The implementation of this would also increase solution clarity, due to the complete removal of insoluble fibrils which may remain in the extract.

The second process, covered in chapter 5 describes the extraction of single alpha chain collagens, which are a new addition to the collagen family of industrial proteins, and there are many different areas which require further work in order to fully realise the potential benefits of this material. Primarily, it is important that work relating to the cellular interaction and immunology characteristics are addressed, in order to better understand how the exposed epitopes, present within the collagen alpha chains could cause an immunological response. In this regard, particular focus *in vivo* of the secretion of matrix metalloproteinases (MMPs) should be conducted, as these denature the collagen to gelatine in order to expose the active RGD site (Arg-Gly-Asp) sequences, which are responsible for the creation of granulation tissue within a wound (Brett 2008).

There are other major areas of refinement for SACC which will be further explored in future, surrounding the control of refibrillisation into ASC-like collagen and whether this can be controlled to occur at a specific range, particularly in short timeframes. The knowledge of this control would allow SACC to be used in a variety of medical device applications that cover wound closure. The major experimental technique which has not been covered within this work is the use of transmission electron microscopy, due to the difficulty in accessing this service. Future work into

SACC must include experimentation covering the refibrillisation and whether this also produced fibrils with the defined axial repeat of 67nm.

The development of medical devices as described in chapter 6, is based on the unique properties of SACC and future work would surround its properties for solubility and refibrillisation, and of particular interest is the development of a spray which can contain high quantities of SACC but upon activation at the wound site creates a sealed barrier. The applications of this work would be of particular interest to military and medical response applications, with regenerative medicine at the front line surrounding wound care being a key funding allocation in 2018 (Defence Science and Technology Laboratory 2018). Further developmental optimisations on the film casting of SACC should also be carried forward, while the use of SACC in bioprinting applications is also of future interest, offering solutions to many of the problems experienced within this work.

The electrospinning of SACC has offered a solution to the problems described with the electrospinning of collagens, and their requirement for the use of fluorinated alcohols. SACC now offers a solution to these problems, and its use as a replacement for ASC in electrospinning will be explored in various collaborative avenues in future. The future applications that are of immediate interest within the group surround the addition of other components, co-spun with SACC to produce better biomimetic scaffolds. These include the addition of hydroxyapatite for bone tissue engineering and scaffold coatings with cell migration for use in blood vessel replication, to tackle effective *in vitro* simulation of blood flow.

Bibliography

Addad, Sourour, Jean Yves Exposito, Clément Faye, Sylvie Ricard-Blum, and Claire Lethias. 2011. “Isolation, Characterization and Biological Evaluation of Jellyfish Collagen for Use in Biomedical Applications.” *Marine Drugs* 9 (6): 967–83. https://doi.org/10.3390/md9060967.

Agile Molecule. 2015. “Abalone.” http://www.biomolecular-modeling.com/Abalone/index.html.

Alnasir, Jamie.J. 2017. “Zeus Molecular Viewer and Visualisation Software.” 2017. http://www.al-nasir.com/portfolio/zeus/.

Ashcroft, G S, M A Horan, and M W Ferguson. 1998. “Aging Alters the Inflammatory and Endothelial Cell Adhesion Molecule Profiles during Human Cutaneous Wound Healing.” *Laboratory Investigation; a Journal of Technical Methods and Pathology* 78 (1): 47–58. http://www.ncbi.nlm.nih.gov/pubmed/9461121.

Asher, D M. 1999. “The Transmissible Spongiform Encephalopathy Agents: Concerns and Responses of United States Regulatory Agencies in Maintaining the Safety of Biologics.” *Developments in Biological Standardization* 100: 103–18. http://www.ncbi.nlm.nih.gov/pubmed/10616181.

Aspelund, Matthew T., and Charles E. Glatz. 2010. “Purification of Recombinant Plant-Made Proteins from Corn Extracts by Ultrafiltration.” *Journal of Membrane Science* 353 (1–2): 103–10. https://doi.org/10.1016/J.MEMSCI.2010.02.036.

Bae, Inwoo, Kiyoshi Osatomi, Asami Yoshida, Kazufumi Osako, Atsuko Yamaguchi, and Kenji Hara. 2008. “Biochemical Properties of Acid-Soluble Collagens Extracted from the Skins of Underutilised Fishes.” *Food Chemistry* 108 (1): 49–54. https://doi.org/10.1016/j.foodchem.2007.10.039.

Banerjee, Pradipta, Lonchin Suguna, and C. Shanthi. 2015. “Wound Healing Activity of a Collagen-Derived Cryptic Peptide.” *Amino Acids* 47 (2): 317–28. https://doi.org/10.1007/s00726-014-1860-6.

Barbosa, Oveimar, Claudia Ortiz, Ángel Berenguer-Murcia, Rodrigo Torres, Rafael C. Rodrigues, and Roberto Fernandez-Lafuente. 2014. “Glutaraldehyde in Bio-Catalysts Design: A Useful Crosslinker and a Versatile Tool in Enzyme Immobilization.” *RSC Adv.* 4 (4): 1583–1600. https://doi.org/10.1039/C3RA45991H.

Barnes, Catherine P, Charles W Pemble, David D Brand, David G Simpson, and Gary L Bowlin. 2007. “Cross-Linking Electrospun Type II Collagen Tissue Engineering Scaffolds with Carbodiimide in Ethanol.” *Tissue Engineering* 13 (7): 1593–1605. https://doi.org/10.1089/ten.2006.0292.

Barzideh, Zoha, Aishah Abd Latiff, Chee Yuen Gan, Soottawat Benjakul, and Alias Abd Karim. 2014a. “Isolation and Characterisation of Collagen from the Ribbon Jellyfish (Chrysaora Sp.).” *International Journal of Food Science and Technology* 49 (6): 1490–99. https://doi.org/10.1111/ijfs.12464.

Bayat, A, D A McGrouther, and M W J Ferguson. 2003. “Skin Scarring.” *BMJ (Clinical Research Ed.)* 326 (7380): 88–92. http://www.ncbi.nlm.nih.gov/pubmed/12521975.

Bell, E, H P Ehrlich, D J Buttle, and T Nakatsuji. 1981. “Living Tissue Formed in Vitro and Accepted as Skin-Equivalent Tissue of Full Thickness.” *Science (New York, N.Y.)* 211 (4486): 1052–54. https://doi.org/10.1126/science.7008197.

Bhardwaj, Nandana, and Subhas C. Kundu. 2010. “Electrospinning: A Fascinating Fiber Fabrication Technique.” *Biotechnology Advances* 28 (3): 325–47. https://doi.org/10.1016/J.BIOTECHADV.2010.01.004.

Blatt, William F., Arun Dravid, Alan S. Michaels, and Lita Nelsen. 1970. “Solute Polarization and Cake Formation in Membrane Ultrafiltration: Causes, Consequences, and Control Techniques.” In *Membrane Science and Technology*, 47–97. Boston, MA: Springer US. https://doi.org/10.1007/978-1-4684-1851-4_4.

Boys, Charles Vernon. 1887. “On the Production, Properties, and Some Suggested Uses of the Finest Threads.” *Proceedings of the Physical Society of London* 9 (1): 8.

Brett, David. 2008. “A Review of Collagen and Collagen-Based Wound Dressings.” *Wounds* 20 (12): 1–11.

Burke, Luke, Chris J. Mortimer, Daniel J. Curtis, Aled R. Lewis, Rhodri Williams, Karl Hawkins, Thierry G.G. Maffeis, and Chris J. Wright. 2017. “In-Situ Synthesis of Magnetic Iron-Oxide Nanoparticle-Nanofibre Composites Using Electrospinning.” *Materials Science and Engineering C* 70: 512–19. https://doi.org/10.1016/j.msec.2016.09.014.

Buttafoco, L., N. G. Kolkman, P. Engbers-Buijtenhuijs, a. a. Poot, P. J. Dijkstra, I. Vermes, and J. Feijen. 2006. “Electrospinning of Collagen and Elastin for Tissue Engineering Applications.” *Biomaterials* 27 (5): 724–34.

https://doi.org/10.1016/j.biomaterials.2005.06.024.

Castillo-Briceño Patricia, P., Dominique Bihan, Michael Nilges, Samir Hamaia, José Meseguer, Alfonsa García-Ayala, Richard W. Farndale, and Victoriano Mulero. 2011. "A Role for Specific Collagen Motifs during Wound Healing and Inflammatory Response of Fibroblasts in the Teleost Fish Gilthead Seabream." *Molecular Immunology* 48 (6–7): 826–34. https://doi.org/10.1016/j.molimm.2010.12.004.

Catalina, Mercedes, Jaume Cot, P Celma, Albert M Manich, and Agustín Marsal. 2009. "Molecular Weight Separation of Collagen-Base Biomaterials by Ultrafiltration." In .

Cengiz, F., and O. Jirsak. 2009. "The Effect of Salt on the Roller Electrospinning of Polyurethane Nanofibers." *Fibers and Polymers* 10 (2): 177–84. https://doi.org/10.1007/s12221-009-0177-7.

Chainani, Abby, Kirk J. Hippensteel, Alysha Kishan, N. William Garrigues, David S. Ruch, Farshid Guilak, and Dianne Little. 2013. "Multilayered Electrospun Scaffolds for Tendon Tissue Engineering." *Tissue Engineering Part A* 19 (23–24): 2594–2604. https://doi.org/10.1089/ten.tea.2013.0165.

Chandrakasan, Gowri, Dennis A Torchia, and Karl A Piez. 1976. "Preparation of Intact Monomeric Collagen from Rat Tail Tendon and Skin and the Structure of the Nonhelical Ends in Solution." *Journal of Biological Chemistry* 251 (19): 6062–67. https://doi.org/10.1111/j.1532-5415.2010.03209.x.

Chang, Cheong Ho, Hyeong Woo Jeong, Ji Chul Yoo, Se Ken Yeo, and Dong Sam Suh. 2017. Method for producing high-concentration collagen for using as medical material, issued November 23, 2017. https://patents.google.com/patent/US20170334969A1/en.

Chang, Hsin-I, and Yiwei Wang. 2011. "Cell Responses to Surface and Architecture of Tissue Engineering Scaffolds." *Regenerative Medicine and Tissue Engineering - Cells and Biomaterials*, 569–88. https://doi.org/10.5772/21983.

Chen, S., N. Hirota, M. Okuda, M. Takeguchi, H. Kobayashi, N. Hanagata, and T. Ikoma. 2011. "Microstructures and Rheological Properties of Tilapia Fish-Scale Collagen Hydrogels with Aligned Fibrils Fabricated under Magnetic Fields." *Acta Biomaterialia* 7 (2): 644–52. https://doi.org/10.1016/J.ACTBIO.2010.09.014.

Chen, Z. G., P. W. Wang, B. Wei, X. M. Mo, and F. Z. Cui. 2010. "Electrospun Collagen-Chitosan Nanofiber: A Biomimetic Extracellular Matrix for Endothelial Cell and Smooth Muscle Cell." *Acta Biomaterialia* 6 (2): 372–82.

https://doi.org/10.1016/j.actbio.2009.07.024.

Chen, Zonggang, Xiumei Mo, and Fengling Qing. 2007. “Electrospinning of Collagen-Chitosan Complex.” *Materials Letters* 61 (16): 3490–94. https://doi.org/10.1016/j.matlet.2006.11.104.

Cherfan, Daniel, E. Eri Verter, Samir Melki, Thomas E. Gisel, Francis J. Doyle, Giuliano Scarcelli, Seok Hyun Yun, Robert W. Redmond, and Irene E. Kochevar. 2013. “Collagen Cross-Linking Using Rose Bengal and Green Light to Increase Corneal Stiffness.” *Investigative Ophthalmology and Visual Science* 54 (5): 3426–33. https://doi.org/10.1167/iovs.12-11509.

Chua, Chee Kai, and Wai Yee Yeong. 2015. *Bioprinting*. World Scientific. https://doi.org/10.1142/9193.

Clark, G. L., E. A. Parker, J. A. Schaad, and W. J. Warren. 1935. “NEW Measurements Of Previously Unknown Large Interplanar Spacings In Natural Materials.” *Journal of the American Chemical Society* 57 (8): 1509–1509. https://doi.org/10.1021/ja01311a504.

Clark, R. A. F. (Richard A. F.). 1996. *The Molecular and Cellular Biology of Wound Repair*. Plenum Press.

Clark, Richard. 2012. *The Molecular and Cellular Biology of Wound Repair*.

Clark, Richard A. F. 1998. “Overview and General Considerations of Wound Repair.” In *The Molecular and Cellular Biology of Wound Repair*, 3–33. Boston, MA: Springer US. https://doi.org/10.1007/978-1-4615-1795-5_1.

Clarke, Anthony R, Graham S Jackson, and John Collinge. 2001. “The Molecular Biology of Prion Propagation.” *Philosophical Transactions of the Royal Society of London. Series B, Biological Sciences* 356 (1406): 185–95. https://doi.org/10.1098/rstb.2000.0764.

Corre-Bordes, Deborah Le, Kathleen Hofman, and Bronwyn Hall. 2018. “Guide to Electrospinning Denatured Whole Chain Collagen from Hoki Fish Using Benign Solvents.” *International Journal of Biological Macromolecules* 112 (June): 1289–99. https://doi.org/10.1016/j.ijbiomac.2018.02.088.

“Creative Commons — Attribution 3.0 International — CC BY 3.0.” n.d. Accessed July 25, 2018. https://creativecommons.org/licenses/by-nc-sa/3.0/legalcode.

“Creative Commons — Attribution 4.0 International — CC BY 4.0.” n.d. Accessed July 24, 2018. https://creativecommons.org/licenses/by/4.0/legalcode.

Dallon, John C. 1998. “A Mathematical Model for Fibroblast and Collagen Orientation.” *Bulletin of Mathematical Biology* 60: 101–29. http://www.macs.hw.ac.uk/~jas/paperpdfs/dallon1.pdf.

Dallon, John C, and Jonathan a. Sherratt. 2000. “A Mathematical Model for Spatially Varying Extracellular Matrix Alignment.” *SIAM Journal on Applied Mathematics* 61 (2): 506–27. https://doi.org/10.1137/S0036139999359343.

Dallon, John C, Jonathan A Sherratt, and Philip K Maini-. 1999. “Mathematical Modelling of Extracellular Matrix Dynamics Using Discrete Cells: Fiber Orientation and Tissue Regeneration.” *J. Theor. Biol* 199. http://www.idealibrary.com.

Dealey, Carol. 1999. *The Care of Wounds : A Guide for Nurses*. Blackwell Science. https://capitadiscovery.co.uk/edgehill/items/115403.

Defence Science and Technology Laboratory. 2018. “Competition Document: Regenerative Medicine at the Front Line - GOV.UK.” 2018. https://www.gov.uk/government/publications/accelerator-competition-regenerative-medicine-at-the-front-line/competition-document-regenerative-medicine-at-the-front-line#what-we-want.

Doillon, Charles J., and Frederick H. Silver. 1986. “Collagen-Based Wound Dressing: Effects of Hyaluronic Acid and Firponectin on Wound Healing.” *Biomaterials* 7 (1): 3–8. https://doi.org/10.1016/0142-9612(86)90080-3.

Dong, Bin, Olivier Arnoult, Meghan E. Smith, and Gary E. Wnek. 2009. “Electrospinning of Collagen Nanofiber Scaffolds from Benign Solvents.” *Macromolecular Rapid Communications* 30 (7): 539–42. https://doi.org/10.1002/marc.200800634.

Drexler, Jason W., and Heather M. Powell. 2011. “Dehydrothermal Crosslinking of Electrospun Collagen.” *Tissue Engineering Part C: Methods* 17 (1): 9–17. https://doi.org/10.1089/ten.tec.2009.0754.

Duek, Aviv, Elizabeth Arkhangelsky, Ronit Krush, Asher Brenner, and Vitaly Gitis. 2012. “New and Conventional Pore Size Tests in Virus-Removing Membranes.” *Water Research* 46 (8): 2505–14. https://doi.org/10.1016/j.watres.2011.12.058.

Enea, Davide, Frances Henson, Simon Kew, John Wardale, Alan Getgood, Roger Brooks, and Neil Rushton. 2011. “Extruded Collagen Fibres for Tissue Engineering Applications: Effect of Crosslinking Method on Mechanical and Biological Properties.” *Journal of Materials Science: Materials in Medicine* 22 (6): 1569–78.

https://doi.org/10.1007/s10856-011-4336-1.

Engel, Jürgen, and Hans Peter Bächinger. 2005. “Structure, Stability and Folding of the Collagen Triple Helix.” *Topics in Current Chemistry* 247: 7–33. https://doi.org/10.1007/b103818.

Erencia, Marisa, Francisco Cano, Jose A. Tornero, Jorge Macanás, and Fernando Carrillo. 2014. “Resolving the Electrospinnability Zones and Diameter Prediction for the Electrospinning of the Gelatin/Water/Acetic Acid System.” *Langmuir* 30 (24): 7198–7205. https://doi.org/10.1021/la501183f.

Fiorani, Andrea, Chiara Gualandi, Silvia Panseri, Monica Montesi, Maurilio Marcacci, Maria Letizia Focarete, and Adriana Bigi. 2014. “Comparative Performance of Collagen Nanofibers Electrospun from Different Solvents and Stabilized by Different Crosslinkers.” *Journal of Materials Science: Materials in Medicine* 25 (10): 2313–21. https://doi.org/10.1007/s10856-014-5196-2.

Formhals, a. 1934. “Process and Apparatus for Preparing Artifical Threads Patent,” 1–8.

Formhals, Anton. 1934. “Process and Apparatus for Preparing Artificial Threads: US, 1975504.”

Gallignani, Máximo, Rebeca A Rondón, José F Ovalles, and María R Brunetto. 2015. “Transmission FTIR Derivative Spectroscopy for Estimation of Furosemide in Raw Material and Tablet Dosage Form.” *Acta Pharmaceutica Sinica B* 4: 376–83. https://doi.org/10.1016/j.apsb.2014.06.013.

Gaspar, A, L Moldovan, D Constantin, A M Stanciuc, P M Sarbu Boeti, and I C Efrimescu. 2011. “Collagen-Based Scaffolds for Skin Tissue Engineering.” *Journal of Medicine and Life* 4 (2): 172–77. http://www.ncbi.nlm.nih.gov/pubmed/21776301%0Ahttp://www.pubmedcentral.nih.gov/articlerender.fcgi?artid=PMC3124265.

“Gelatin.” 2018. Encyclopedia of Food and Culture. 2018. https://www.encyclopedia.com/science-and-technology/biochemistry/biochemistry/gelatin.

Gelse, K., E. Pöschl, and T. Aigner. 2003. “Collagens - Structure, Function, and Biosynthesis.” *Advanced Drug Delivery Reviews* 55 (12): 1531–46. https://doi.org/10.1016/j.addr.2003.08.002.

Gilbert, William. 1628. *De Magnete*. London: Peter Short.

Golomb, Gershon, Frederick J Schoen, Mary Sue Smith, Judy Linden, Mark Dixon, and Robert J Levy. 1987. “The Role of Glutaraldehyde-Induced Cross-Links in Calcification of Bovine Pericardium Used in Cardiac Valve Bioprostheses.” *The American Journal of Pathology* 127 (1): 122–30. https://www.ncbi.nlm.nih.gov/pmc/articles/PMC1899585/pdf/amjpathol00145-0127.pdf.

Gourdie, Robert G, and John M Walker. 2013. *Wound Regeneration and Repair IN Series Editor*.

Greenhalgh, David G. 1998. “The Role of Apoptosis in Wound Healing.” *The International Journal of Biochemistry & Cell Biology* 30 (9): 1019–30. https://doi.org/10.1016/S1357-2725(98)00058-2.

Hackett, Joanne M, Thuc Nhi T. Dang, Eve C Tsai, and Xudong Cao. 2010. “Electrospun Biocomposite Polycaprolactone/Collagen Tubes as Scaffolds for Neural Stem Cell Differentiation.” *Materials* 3 (6): 3714–28. https://doi.org/10.3390/ma3063714.

Häggström, Mikael. 2014. “Medical Gallery of Mikael Häggström 2014.” *WikiJournal of Medicine* 1 (2). https://doi.org/10.15347/wjm/2014.008.

Hall Barrientos, Ivan J., Eleonora Paladino, Peter Szabó, Sarah Brozio, Peter J. Hall, Charles I. Oseghale, Melissa K. Passarelli, et al. 2017. “Electrospun Collagen-Based Nanofibres: A Sustainable Material for Improved Antibiotic Utilisation in Tissue Engineering Applications.” *International Journal of Pharmaceutics* 531 (1): 67–79. https://doi.org/10.1016/j.ijpharm.2017.08.071.

Halloran, Damien O., Sibylle Grad, Martin Stoddart, Peter Dockery, Mauro Alini, and Abhay S. Pandit. 2008. “An Injectable Cross-Linked Scaffold for Nucleus Pulposus Regeneration.” *Biomaterials* 29 (4): 438–47. https://doi.org/10.1016/J.BIOMATERIALS.2007.10.009.

Hapach, Lauren A., Jacob A. Vanderburgh, Joseph P. Miller, and Cynthia A. Reinhart-King. 2015. “Manipulation of in Vitro Collagen Matrix Architecture for Scaffolds of Improved Physiological Relevance.” *Physical Biology*. https://doi.org/10.1088/1478-3975/12/6/061002.

Hartman, Olga, Chu Zhang, Elizabeth L Adams, Mary C Farach-Carson, Nicholas J Petrelli, Bruce D Chase, and John F Rabolt. 2009. “Microfabricated Electrospun Collagen Membranes for 3-D Cancer Models and Drug Screening Applications.” *Biomacromolecules* 10 (8): 2019–32. https://doi.org/10.1021/bm8012764.

He, Wei, Thomas Yong, Wee Eong Teo, Zuwei Ma, and Seeram Ramakrishna. 2005. "Fabrication and Endothelialization of Collagen-Blended Biodegradable Polymer Nanofibers: Potential Vascular Graft for Blood Vessel Tissue Engineering." *Tissue Engineering* 11 (9–10): 1574–88. https://doi.org/10.1089/ten.2005.11.1574.

Heydarkhan-Hagvall, Sepideh, Katja Schenke-Layland, Andrew P. Dhanasopon, Fady Rofail, Hunter Smith, Benjamin M. Wu, Richard Shemin, Ramin E. Beygui, and William R. MacLellan. 2008. "Three-Dimensional Electrospun ECM-Based Hybrid Scaffolds for Cardiovascular Tissue Engineering." *Biomaterials* 29 (19): 2907–14. https://doi.org/10.1016/j.biomaterials.2008.03.034.

Hinton, Thomas J, Quentin Jallerat, Rachelle N Palchesko, Joon Hyung Park, Martin S Grodzicki, H.-J. Shue, Mohamed H Ramadan, Andrew R Hudson, and Adam W Feinberg. 2015. "Three-Dimensional Printing of Complex Biological Structures by Freeform Reversible Embedding of Suspended Hydrogels." *Science Advances* 1 (9): e1500758–e1500758. https://doi.org/10.1126/sciadv.1500758.

Holmes, D F, C J Gilpin, C Baldock, U Ziese, a J Koster, and K E Kadler. 2001. "Corneal Collagen Fibril Structure in Three Dimensions: Structural Insights into Fibril Assembly, Mechanical Properties, and Tissue Organization." *Proceedings of the National Academy of Sciences of the United States of America* 98 (13): 7307–12. https://doi.org/10.1073/pnas.111150598.

Holmes, David F, and Karl E Kadler. 2006. "The 10+4 Microfibril Structure of Thin Cartilage Fibrils." *PNAS* 103 (46): 17249–17254. https://doi.org/doi10.1073pnas.0608417103.

Horton, R, L.A Moran, G Scrimgeour, M Perry, and D Rawn. 2006. *Principles of Biochemistry, 4th Edition*. 4th ed. NJ: Pearson. https://www.pearson.com/us/higher-education/product/Horton-Principles-of-Biochemistry-4th-Edition/9780131453067.html.

Hubbell, J a. 1995. "Biomaterials in Tissue Engineering." *Bio/Technology (Nature Publishing Company)* 13 (6): 565–76. https://doi.org/10.1038/nbt0695-565.

Hyman, Libbie Henrietta. 1940. *The Invertebrates-Protozoa Through Ctenophora*. Birchandra State Central Library, Tripura. https://archive.org/details/in.ernet.dli.2015.461506.

Jha, Balendu Shekhar, Chantal E. Ayres, James R. Bowman, Todd A. Telemeco, Scott A. Sell, Gary L. Bowlin, and David G. Simpson. 2011. "Electrospun Collagen: A Tissue

Engineering Scaffold with Unique Functional Properties in a Wide Variety of Applications." *Journal of Nanomaterials* 2011 (April): 1–15. https://doi.org/10.1155/2011/348268.

Jiang, Qiuran, Narendra Reddy, Simeng Zhang, Nicholas Roscioli, and Yiqi Yang. 2013. "Water-Stable Electrospun Collagen Fibers from a Non-Toxic Solvent and Crosslinking System." *Journal of Biomedical Materials Research - Part A* 101 A (5): 1237–47. https://doi.org/10.1002/jbm.a.34422.

Ki, Chang Seok, Doo Hyun Baek, Kyung Don Gang, Ki Hoon Lee, In Chul Um, and Young Hwan Park. 2005. "Characterization of Gelatin Nanofiber Prepared from Gelatin–Formic Acid Solution." *Polymer* 46 (14): 5094–5102. https://doi.org/10.1016/J.POLYMER.2005.04.040.

Kittiphattanabawon, Phanat, Soottawat Benjakul, Wonnop Visessanguan, Hideki Kishimura, and Fereidoon Shahidi. 2010. "Isolation and Characterisation of Collagen from the Skin of Brownbanded Bamboo Shark (Chiloscyllium Punctatum)." *Food Chemistry* 119 (4): 1519–26. https://doi.org/10.1016/j.foodchem.2009.09.037.

Kozlov, P.V., and G.I. Burdygina. 1983. "The Structure and Properties of Solid Gelatin and the Principles of Their Modification." *Polymer* 24 (6): 651–66. https://doi.org/10.1016/0032-3861(83)90001-0.

Krishnamoorthi, Jayalakshmi, Pasiyappazham Ramasamy, Vairamani Shanmugam, and Annaian Shanmugam. 2017. "Isolation and Partial Characterization of Collagen from Outer Skin of Sepia Pharaonis (Ehrenberg, 1831) from Puducherry Coast." *Biochemistry and Biophysics Reports* 10 (March): 39–45. https://doi.org/10.1016/j.bbrep.2017.02.006.

Laemmli, U. K. 1970. "Cleavage of Structural Proteins during the Assembly of the Head of Bacteriophage T4." *Nature* 227 (5259): 680–85. https://doi.org/10.1038/227680a0.

Lau, Ying-Ka Ingar, Andre M. Gobin, and Jennifer L. West. 2006. "Overexpression of Lysyl Oxidase to Increase Matrix Crosslinking and Improve Tissue Strength in Dermal Wound Healing." *Annals of Biomedical Engineering* 34 (8): 1239–46. https://doi.org/10.1007/s10439-006-9130-8.

Law, Jia Xian, Ling Ling Liau, Aminuddin Saim, Ying Yang, and Ruszymah Idrus. 2017. "Electrospun Collagen Nanofibers and Their Applications in Skin Tissue Engineering." *Tissue Engineering and Regenerative Medicine*. Springer Science + Business Media. https://doi.org/10.1007/s13770-017-0075-9.

Lee, Chi H., Anuj Singla, and Yugyung Lee. 2001. “Biomedical Applications of Collagen.” *International Journal of Pharmaceutics* 221 (1–2): 1–22. https://doi.org/10.1016/S0378-5173(01)00691-3.

Lee, Wonhye, Chae Yun Bae, Seyong Kwon, Jaejung Son, Jinho Kim, Yong Jeong, Seung-Schik Yoo, and Je-Kyun Park. 2012. “Cellular Hydrogel Biopaper for Patterned 3D Cell Culture and Modular Tissue Reconstruction.” *Advanced Healthcare Materials* 1 (5): 635–39. https://doi.org/10.1002/adhm.201200158.

Lee, Yun Hui, Jong Hoon Lee, In Gu An, Chan Kim, Doo Sung Lee, Young Kwan Lee, and Jae Do Nam. 2005. “Electrospun Dual-Porosity Structure and Biodegradation Morphology of Montmorillonite Reinforced PLLA Nanocomposite Scaffolds.” *Biomaterials* 26 (16): 3165–72. https://doi.org/10.1016/j.biomaterials.2004.08.018.

Li, Dan, and Younan Xia. 2004. “Direct Fabrication of Composite and Ceramic Hollow Nanofibers by Electrospinning.” *Nano Letters* 4 (5): 933–38. https://doi.org/10.1021/nl049590f.

Li, Jing, and Howard A Chase. 2010. “Applications of Membrane Techniques for Purification of Natural Products.” *Biotechnology Letters*. Springer Verlag. https://doi.org/10.1007/s10529-009-0199-7.

Li, Mengyan, Mark J. Mondrinos, Milind R. Gandhi, Frank K. Ko, Anthony S. Weiss, and Peter I. Lelkes. 2005. “Electrospun Protein Fibers as Matrices for Tissue Engineering.” *Biomaterials* 26 (30): 5999–6008. https://doi.org/10.1016/j.biomaterials.2005.03.030.

Li, Wan-ju, Rabie M Shanti, and Rocky S Tuan. 2006. *Electrospinning Technology for Nanofibrous Scaffolds in Tissue Engineering*. *Nanotechnologies for the Life Sciences*. Vol. 9. https://doi.org/10.1002/9783527610419.ntls0097.

Li, Wan J., Cato T Laurencin, Edward J Caterson, Rocky S Tuan, and Frank K Ko. 2002. “Electrospun Nanofibrous Structure: A Novel Scaffold for Tissue Engineering.” *Journal of Biomedical Materials Research* 60 (4): 613–21. https://doi.org/10.1002/jbm.10167.

Li, Xiaoran, Hui Liang, Jie Sun, Yan Zhuang, Bai Xu, and Jianwu Dai. 2015. “Electrospun Collagen Fibers with Spatial Patterning of SDF1α for the Guidance of Neural Stem Cells.” *Advanced Healthcare Materials* 4 (12): 1869–76. https://doi.org/10.1002/adhm.201500271.

Li, Zhong Rui, Bin Wang, Chang feng Chi, Qi Hong Zhang, Yan dan Gong, Jia Jia Tang,

Hong yu Luo, and Guo fang Ding. 2013. “Isolation and Characterization of Acid Soluble Collagens and Pepsin Soluble Collagens from the Skin and Bone of Spanish Mackerel (Scomberomorous Niphonius).” *Food Hydrocolloids* 31 (1): 103–13. https://doi.org/10.1016/j.foodhyd.2012.10.001.

Liu, Fan, Chen Liu, Qiuhong Chen, Qiang Ao, Xiaohong Tian, Jun Fan, Hao Tong, and Xiaohong Wang. 2018. *International Journal of Bioprinting*. *International Journal of Bioprinting*. Vol. 4. Whioce. http://ijb.whioce.com/index.php/int-j-bioprinting/article/view/128/pdf.

Liu, Ting, Wai Keng Teng, Barbara P. Chan, and Sing Yian Chew. 2010. “Photochemical Crosslinked Electrospun Collagen Nanofibers: Synthesis, Characterization and Neural Stem Cell Interactions.” *Journal of Biomedical Materials Research - Part A* 95 (1): 276–82. https://doi.org/10.1002/jbm.a.32831.

Liu, Yunhuan, Tiequan Shao, Huaqiao Zhang, Qi Wang, Yanan Zhang, Cheng Chen, Yongchun Liang, and Jiaqi Xue. 2017. “A New Scyphozoan from the Cambrian Fortunian Stage of South China.” *Palaeontology* 60 (4): 511–18. https://doi.org/10.1111/pala.12306.

Lodish, Harvey, Arnold Berk, S Lawrence Zipursky, Paul Matsudaira, David Baltimore, and James Darnell. 2000. *Molecular Cell Biology, 4th Edition*. Edited by W H Freeman. New York.

Loeb, Sidney. 1981. “The Loeb-Sourirajan Membrane: How It Came About.” Vol. 14. UTC. https://pubs.acs.org/sharingguidelines.

López, JoséManuel, Santiago Imperial, Rodrigo Valderrama, and Salvador Navarro. 1993. “An Improved Bradford Protein Assay for Collagen Proteins.” *Clinica Chimica Acta* 220 (1): 91–100. https://doi.org/10.1016/0009-8981(93)90009-S.

Lowe, Christopher J, Ian M Reucroft, Matthew C Grota, and David I Shreiber. 2016. “Production of Highly Aligned Collagen Scaffolds by Freeze-Drying of Self-Assembled, Fibrillar Collagen Gels.” *ACS Biomaterials Science and Engineering* 2 (4): 643–51. https://doi.org/10.1021/acsbiomaterials.6b00036.

Lowry, O H, N J Rosebrough, A L Farr, and R J Randall. 1951. “Protein Measurement with the Folin Phenol Reagent.” *The Journal of Biological Chemistry* 193 (1): 265–75. http://www.ncbi.nlm.nih.gov/pubmed/14907713.

Lu, Peng, and Yanchuan Guo. 2018. “Electrospinning of Collagen and Its Derivatives for

Biomedical Biomedical Applications Applications." In *Novel Aspects of Nanofibers*. https://doi.org/10.5772/intechopen.73581.

Lupi, Omar. 2002. "Prions in Dermatology." *Journal of the American Academy of Dermatology* 46 (5): 790–93. https://doi.org/10.1067/mjd.2002.120624.

Ma, Zuwei, Masaya Kotaki, Ryuji Inai, and Seeram Ramakrishna. 2005. "Potential of Nanofiber Matrix as Tissue-Engineering Scaffolds." *Tissue Engineering* 11 (1–2): 101–9. https://doi.org/10.1089/ten.2005.11.101.

Makris, Eleftherios A, Donald J Responte, Nikolaos K Paschos, Jerry C Hu, and Kyriacos A Athanasiou. 2014. "Developing Functional Musculoskeletal Tissues through Hypoxia and Lysyl Oxidase-Induced Collagen Cross-Linking." *Proceedings of the National Academy of Sciences of the United States of America* 111 (45): E4832-41. https://doi.org/10.1073/pnas.1414271111.

Malkoc, Veysi. 2018. "Challenges and the Future of 3D Bioprinting." *Journal of Biomedical Imaging and Bioengineering* 1 (3): 62–63. http://www.alliedacademies.org/biomedical-imaging-and-bioengineering/.

Manappallil, John J. n.d. *Basic Dental Materials*. Accessed October 22, 2018. https://books.google.co.uk/books?id=7cAqCwAAQBAJ&pg=PA417&lpg=PA417&redir_esc=y#v=onepage&q&f=false.

Mathangi Ramakrishnan, K, M Babu, Mathivanan, V Jayaraman, and J Shankar. 2013. "Advantages of Collagen Based Biological Dressings in the Management of Superficial and Superficial Partial Thickness Burns in Children." *Annals of Burns and Fire Disasters* 26 (2): 98–104. http://www.ncbi.nlm.nih.gov/pubmed/24133405.

Matthews, Jamil a., Gary E. Wnek, David G. Simpson, and Gary L. Bowlin. 2002. "Electrospinning of Collagen Nanofibers." *Biomacromolecules* 3 (2): 232–38. https://doi.org/10.1021/bm015533u.

Matthews, Jamil A., Gary E. Wnek, David G. Simpson, and Gary L. Bowlin. 2002. "Electrospinning of Collagen Nanofibers." *Biomacromolecules* 3 (2): 232–38. https://doi.org/10.1021/bm015533u.

Miller, E J. 1972. "Structural Studies on Cartilage Collagen Employing Limited Cleavage and Solubilization with Pepsin." *Biochemistry* 11 (26): 4903–9. https://doi.org/10.1021/bi00776a005.

Min, Su, Song W Wang, and William Orr. 2006a. "Graphic General Pathology: 2.2

Complete Regeneration." Pathology. 2006. https://web.archive.org/web/20160313151452/http://pathol.med.stu.edu.cn/pathol/listengcontent2.aspx?contentid=492.

Min, Su, Song W Wang, and William Orr. 2006b. "Graphic General Pathology: 2.3 Incomplete Regeneration." Pathology. 2006. https://web.archive.org/web/20160311182730/http://pathol.med.stu.edu.cn/pathol/listEngContent2.aspx?contentID=493.

Mocan, E, O Tagadiuc, and V Nacu. 2011. "Aspects of Collagen Isolation Procedure." *Clin. Res. Studies*, 8–10.

Montesano, R., L. Orci, and P. Vassalli. 1983. "In Vitro Rapid Organization of Endothelial Cells into Capillary-like Networks Is Promoted by Collagen Matrices." *Journal of Cell Biology* 97 (5 I): 1648–52. https://doi.org/10.1083/jcb.97.5.1648.

Mortimer, Chris J., Jonathan P. Widdowson, and Chris J. Wright. 2018. "Electrospinning of Functional Nanofibers for Regenerative Medicine: From Bench to Commercial Scale." In *Novel Aspects of Nanofibers,* edited by Tong Lin. Rijeka: InTech. https://doi.org/10.5772/intechopen.73677.

Mruk, Dolores D, and C Yan Cheng. 2011. "Enhanced Chemiluminescence (ECL) for Routine Immunoblotting: An Inexpensive Alternative to Commercially Available Kits." *Spermatogenesis* 1 (2): 121–22. https://doi.org/10.4161/spmg.1.2.16606.

Murray, John C., Sheldon V. Pollack, and Sheldon R. Pinnell. 1981. "Keloids: A Review." *Journal of the American Academy of Dermatology* 4 (4): 461–70. https://doi.org/10.1016/S0190-9622(81)70048-3.

Myllyharju, J, and K I Kivirikko. 2001. "Collagens and Collagen-Related Diseases." *Annals of Medicine* 33 (1): 7–21. https://doi.org/10.3109/07853890109002055.

Nagai, Takeshi, Wanchai Worawattanamateekul, Nobutaka Suzuki, Takashi Nakamura, Tatsumi Ito, Kazuhiro Fujiki, Miki Nakao, and Tomoki Yano. 2000. "Isolation and Characterization of Collagen from Rhizostomous Jellyfish (Rhopilema Asamushi)." *Food Chemistry* 70 (2): 205–8. https://doi.org/10.1016/S0308-8146(00)00081-9.

Nageotte, J. 1927. "Coagulation Fibrillaire in Vitro Du Collagène Dissous Dans Un Acide Dilué." *C.R.Acad.Sci.Paris* 184: 115–17.

Nalinanon, Sitthipong, Soottawat Benjakul, Wonnop Visessanguan, and Hideki Kishimura. 2007. "Use of Pepsin for Collagen Extraction from the Skin of Bigeye Snapper

(Priacanthus Tayenus).” *Food Chemistry* 104 (2): 593–601. https://doi.org/10.1016/j.foodchem.2006.12.035.

Neuhoff, Volker, Norbert Arold, Dieter Taube, and Wolfgang Ehrhardt. 1988. “Improved Staining of Proteins in Polyacrylamide Gels Including Isoelectric Focusing Gels with Clear Background at Nanogram Sensitivity Using Coomassie Brilliant Blue G???250 and R???250.” *ELECTROPHORESIS* 9 (6): 255–62. https://doi.org/10.1002/elps.1150090603.

Newable. 2017. “Jellagen Launches Next-Gen Jellyfish Collagen Facility | News | Newable.” 2017. https://www.newable.co.uk/news-and-views/840433367/jellagen-launches-next-gen-jellyfish-collagen-facility.php.

NICE. 2005. “Monitoring Surgical Wounds for Infection.” *Health Protection Agency*. http://www.guysandstthomas.nhs.uk/patients-and-.

Nisbet, D.R., J.S. Forsythe, W. Shen, D.I. Finkelstein, and M.K. Horne. 2009. “Review Paper: A Review of the Cellular Response on Electrospun Nanofibers for Tissue Engineering.” *Journal of Biomaterials Applications* 24 (1): 7–29. https://doi.org/10.1177/0885328208099086.

Niu, Guoguang, Tracy Criswell, Etai Sapoznik, Sang-jin Lee, and Shay Soker. 2013. “The Influence of Cross-Linking Methods on the Mechanical and Biocompatible Properties of Vascular Scaffold.” *Journal of Science and Applications: Biomedicine* 1 (1): 1–7.

Nocera, Aden Díaz, Romina Comín, Nancy Alicia Salvatierra, and Mariana Paula Cid. 2018. “Development of 3D Printed Fibrillar Collagen Scaffold for Tissue Engineering.” *Biomedical Microdevices* 20 (2): 26. https://doi.org/10.1007/s10544-018-0270-z.

O Halloran, Damien M., Russell J. Collighan, Martin Griffin, and Abhay S. Pandit. 2006. “Characterization of a Microbial Transglutaminase Cross-Linked Type II Collagen Scaffold.” *Tissue Engineering* 12 (6): 1467–74. https://doi.org/10.1089/ten.2006.12.1467.

Okuyama, Kenji. 2008. “Revisiting the Molecular Structure of Collagen.” *Connective Tissue Research* 49 (5): 299–310. https://doi.org/10.1080/03008200802325110.

Orban, Janine M., Lorri B. Wilson, Jessica A. Kofroth, Mohammed S. El-Kurdi, Timothy M. Maul, and David A. Vorp. 2004. “Crosslinking of Collagen Gels by Transglutaminase.” *Journal of Biomedical Materials Research - Part A* 68 (4): 756–62. https://doi.org/10.1002/jbm.a.20110.

Pakravan, Mehdi, Marie-Claude Heuzey, and Abdellah Ajji. 2012. “Core–Shell Structured PEO-Chitosan Nanofibers by Coaxial Electrospinning.” *Biomacromolecules* 13 (2): 412–21. https://doi.org/10.1021/bm201444v.

Panzavolta, Silvia, Michela Gioffrè, Maria Letizia Focarete, Chiara Gualandi, Laura Foroni, and Adriana Bigi. 2011. “Electrospun Gelatin Nanofibers: Optimization of Genipin Cross-Linking to Preserve Fiber Morphology after Exposure to Water.” *Acta Biomaterialia* 7: 1702–9. https://doi.org/10.1016/j.actbio.2010.11.021.

Petibois, Cyril, Gilles Gouspillou, Katia Wehbe, Jean Paul Delage, and Gérard Déléris. 2006. “Analysis of Type i and IV Collagens by FT-IR Spectroscopy and Imaging for a Molecular Investigation of Skeletal Muscle Connective Tissue.” *Analytical and Bioanalytical Chemistry* 386 (7–8): 1961–66. https://doi.org/10.1007/s00216-006-0828-0.

Petruska, J. A., and A. J. Hodge. 1964. “A Subunit Model for the Tropocollagen Macromolecule.” *Proceedings of the National Academy of Sciences* 51 (5): 871–76. https://doi.org/10.1073/pnas.51.5.871.

Pham, Quynh P., Upma Sharma, and Antonios G. Mikos. 2006. “Electrospinning of Polymeric Nanofibers for Tissue Engineering Applications: A Review.” *Tissue Engineering* 12 (5): 1197–1211. https://doi.org/10.1089/ten.2006.12.1197.

Pozzi, Ambra, Kishore K. Wary, Filippo G. Giancotti, and Humphrey A. Gardner. 1998. “Integrin A1β1 Mediates a Unique Collagen-Dependent Proliferation Pathway in Vivo.” *Journal of Cell Biology* 142 (2): 587–94. https://doi.org/10.1083/jcb.142.2.587.

Prabhakaran, Molamma P, Elham Vatankhah, and Seeram Ramakrishna. 2013. “Electrospun Aligned PHBV/Collagen Nanofibers as Substrates for Nerve Tissue Engineering.” *Biotechnol. Bioeng* 110: 2775–84. https://doi.org/10.1002/bit.24937/abstract.

Price, R I, S Lees, and D A Kirschner. 1997. “X-Ray Diffraction Analysis of Tendon Collagen at Ambient and Cryogenic Temperatures: Role of Hydration.” *International Journal of Biological Macromolecules* 20 (1): 23–33. http://www.ncbi.nlm.nih.gov/pubmed/9110182.

Prockop, Darwin J., Kari I. Kivirikko, Leena Tuderman, and Norberto A. Guzman. 1979. “The Biosynthesis of Collagen and Its Disorders.” *New England Journal of Medicine* 301 (2): 77–85. https://doi.org/10.1056/NEJM197907123010204.

Prosapio, Valentina, Ian Norton, and Iolanda De Marco. 2017. “Optimization of Freeze-

Drying Using a Life Cycle Assessment Approach: Strawberries' Case Study." *Journal of Cleaner Production* 168 (December): 1171–79. https://doi.org/10.1016/J.JCLEPRO.2017.09.125.

Ramachandran, G. N., B. B. Doyle, and E. R. Bloot. 1968. "Single-Chain Triple Helical Structure." *Biopolymers* 6 (12): 1771–75. https://doi.org/10.1002/bip.1968.360061213.

Raspanti, M, V Ottani, and A Ruggeri. 1990. "Subfibrillar Architecture and Functional Properties of Collagen: A Comparative Study in Rat Tendons." *Journal of Anatomy* 172 (October): 157–64. http://www.ncbi.nlm.nih.gov/pubmed/2272900.

Ratti, C. 2001. "Hot Air and Freeze-Drying of High-Value Foods: A Review." *Journal of Food Engineering* 49 (4): 311–19. https://doi.org/10.1016/S0260-8774(00)00228-4.

Reed, Lauren. 2016. "Hollow Fiber Membranes for Artificial Lung Applications." http://scholarworks.uark.edu/cheguhthttp://scholarworks.uark.edu/cheguht/99.

Reneker, Darrell H., Alexander L. Yarin, Hao Fong, and Sureeporn Koombhongse. 2000. "Bending Instability of Electrically Charged Liquid Jets of Polymer Solutions in Electrospinning." *Journal of Applied Physics* 87 (9): 4531–47. https://doi.org/10.1063/1.373532.

Reneker, Darrell H, and Iksoo Chun. 1996. "Nanometre Diameter Fibres of Polymer, Produced by Electrospinning." *Nanotechnology* 7 (3): 216–23. https://doi.org/10.1088/0957-4484/7/3/009.

Rey, Louis., and Joan C May. 2010. *Freeze-Drying/Lyophilization of Pharmaceutical and Biological Products*. Informa Healthcare.

Rho, Kyong S., Lim Jeong, Gene Lee, Byoung M. Seo, Yoon Jeong Park, Seong D. Hong, Sangho Roh, Jae Jin Cho, Won H. Park, and Byung M. Min. 2006. "Electrospinning of Collagen Nanofibers: Effects on the Behavior of Normal Human Keratinocytes and Early-Stage Wound Healing." *Biomaterials* 27 (8): 1452–61. https://doi.org/10.1016/j.biomaterials.2005.08.004.

Rigby, B. J. 1968. "Amino-Acid Composition and Thermal Stability of the Skin Collagen of the Antarctic Ice-Fish [19]." *Nature*. Nature Publishing Group. https://doi.org/10.1038/219166a0.

Ryu, Soo Ryeon, Isao Noda, and Young Mee Jung. 2011. "Positional Fluctuation of IR Absorption Peaks: Frequency Shift of a Single Band or Relative Intensity Changes of Overlapped Bands? | American Laboratory." 2011.

https://www.americanlaboratory.com/913-Technical-Articles/1244-Positional-Fluctuation-of-IR-Absorption-Peaks-Frequency-Shift-of-a-Single-Band-or-Relative-Intensity-Changes-of-Overlapped-Bands/.

Sadeghi-Avalshahr, Alireza, Samira Nokhasteh, Amir Mahdi Molavi, Mohammad Khorsand-Ghayeni, and Meysam Mahdavi-Shahri. 2017. "Synthesis and Characterization of Collagen/PLGA Biodegradable Skin Scaffold Fibers." *Regenerative Biomaterials* 4 (5): 309–14. https://doi.org/10.1093/rb/rbx026.

Sadowska, Maria, Ilona Kołodziejska, and Celina Niecikowska. 2003. "Isolation of Collagen from the Skins of Baltic Cod (Gadus Morhua)." *Food Chemistry* 81 (2): 257–62. https://doi.org/10.1016/S0308-8146(02)00420-X.

Saito, M, Y Takenouchi, N Kunisaki, and S Kimura. 2001. "Complete Primary Structure of Rainbow Trout Type I Collagen Consisting of Alpha1(I)Alpha2(I)Alpha3(I) Heterotrimers." *European Journal of Biochemistry / FEBS* 268: 2817–27.

Sajkiewicz, P, and D Kołbuk. 2014. "Electrospinning of Gelatin for Tissue Engineering - Molecular Conformation as One of the Overlooked Problems." *Journal of Biomaterials Science. Polymer Edition* 25 (18): 2009–22. https://doi.org/10.1080/09205063.2014.975392.

Sakai, K. 1994. "Determination of Pore Size and Pore Size Distribution. 2. Dialysis Membranes." *Journal of Membrane Science*. https://doi.org/10.1016/0376-7388(94)00127-8.

Schmidt, M. M., R. C.P. Dornelles, R. O. Mello, E. H. Kubota, M. A. Mazutti, A. P. Kempka, and I. M. Demiate. 2016. "Collagen Extraction Process." *International Food Research Journal* 23 (3): 913–22.

Schultz, Gregory S, and Bruce A Mast. 1999. "Molecular Analysis of the Environments of Healing and Chronic Wounds: Cytokines, Proteases and Growth Factors." *Wounds* 2 (January 1999): 7–14. http://www.awma.com.au/journal/0701_01.pdf.

Sell, Scott a., Michael J. McClure, Koyal Garg, Patricia S. Wolfe, and Gary L. Bowlin. 2009. "Electrospinning of Collagen/Biopolymers for Regenerative Medicine and Cardiovascular Tissue Engineering." *Advanced Drug Delivery Reviews* 61 (12): 1007–19. https://doi.org/10.1016/j.addr.2009.07.012.

Senaratne, L. S., Pyo Jam Park, and Se Kwon Kim. 2006. "Isolation and Characterization of Collagen from Brown Backed Toadfish (Lagocephalus Gloveri) Skin." *Bioresource*

Technology 97 (2): 191–97. https://doi.org/10.1016/j.biortech.2005.02.024.

Shen, Jiang nan, Dan dan Li, Fei yan Jiang, Jun hong Qiu, and Cong jie Gao. 2009. "Purification and Concentration of Collagen by Charged Ultrafiltration Membrane of Hydrophilic Polyacrylonitrile Blend." *Separation and Purification Technology* 66 (2): 257–62. https://doi.org/10.1016/j.seppur.2009.01.002.

Shih, Yu-Ru V., Chung-Nan Chen, Shiao-Wen Tsai, Yng Jiin Wang, and Oscar K. Lee. 2006. "Growth of Mesenchymal Stem Cells on Electrospun Type I Collagen Nanofibers." *Stem Cells* 24 (11): 2391–97. https://doi.org/10.1634/stemcells.2006-0253.

Shoulders, Matthew D., and Ronald T. Raines. 2010. "Collagen Structure and Stability." *Annu Rev Biochem*, 929–58. https://doi.org/10.1146/annurev.biochem.77.032207.120833.COLLAGEN.

Sill, Travis J., and Horst A. von Recum. 2008. "Electrospinning: Applications in Drug Delivery and Tissue Engineering." *Biomaterials* 29 (13): 1989–2006. https://doi.org/10.1016/J.BIOMATERIALS.2008.01.011.

Silvipriya, K. S., K. Krishna Kumar, A. R. Bhat, B. Dinesh Kumar, Anish John, and Panayappan Lakshmanan. 2015. "Collagen: Animal Sources and Biomedical Application." *Journal of Applied Pharmaceutical Science* 5 (3): 123–27. https://doi.org/10.7324/JAPS.2015.50322.

Sim, K. S., Y Y Tan, M A Lai, C P Tso, and W. K. Lim. 2010. "Reducing Scanning Electron Microscope Charging by Using Exponential Contrast Stretching Technique on Post-Processing Images." *Journal of Microscopy* 238 (1): 44–56. https://doi.org/10.1111/j.1365-2818.2009.03328.x.

Simpson, David G, Gary L Bowlin, Gary E Wnek, Peter J Stevens, Marcus E Carr, Jamil A Matthews, and Saravanamoorthy. Rajendran. 2003. Electroprocessed collagen and tissue engineering. *PCT Int. Appl.*, issued May 28, 2003. https://patents.google.com/patent/US20040037813A1/en.

Singh, Deepti, and Daniel Thomas. 2018. "Advances in Medical Polymer Technology towards the Panacea of Complex 3D Tissue and Organ Manufacture." *The American Journal of Surgery*, May. https://doi.org/10.1016/j.amjsurg.2018.05.012.

Sizeland, Katie H., Kathleen A. Hofman, Ian C. Hallett, Danielle E. Martin, Johan Potgieter, Nigel M. Kirby, Adrian Hawley, et al. 2018. "Nanostructure of Electrospun Collagen:

Do Electrospun Collagen Fibers Form Native Structures?" *Materialia* 3 (November): 90–96. https://doi.org/10.1016/j.mtla.2018.10.001.

Smith, Brian C. 2015. "IR Spectral Interpretation Workshop." *Spectroscopy* 30 (1). http://www.spectroscopyonline.com/ir-spectral-interpretation-workshop?pageID=1.

Song, Eun, So Yeon Kim, Taehoon Chun, Hyun Jung Byun, and Young Moo Lee. 2006. "Collagen Scaffolds Derived from a Marine Source and Their Biocompatibility." *Biomaterials* 27 (15): 2951–61. https://doi.org/10.1016/j.biomaterials.2006.01.015.

Taylor, Geoffrey. 1964. "Disintegration of Water Drops in an Electric Field." *Proceedings of the Royal Society of London. Series A. Mathematical and Physical Sciences* 280 (1382): 383–97.

Thoppey, N M, J R Bochinski, L I Clarke, and R E Gorga. 2011. "Edge Electrospinning for High Throughput Production of Quality Nanofibers." *Nanotechnology* 22 (34): 345301. https://doi.org/10.1088/0957-4484/22/34/345301.

Torres-Giner, Sergio, Jose V Gimeno-Alcañ Iz, Maria J Ocio, and Jose M Lagaron. 2009. "Comparative Performance of Electrospun Collagen Nanofibers Cross-Linked by Means of Different Methods." https://doi.org/10.1021/am800063x.

Torres-Giner, Sergio, Jose V. Gimeno-Alcañiz, Maria J. Ocio, and Jose M. Lagaron. 2009a. "Comparative Performance of Electrospun Collagen Nanofibers Cross-Linked by Means of Different Methods." *ACS Applied Materials and Interfaces* 1 (1): 218–23. https://doi.org/10.1021/am800063x.

———. 2009b. "Comparative Performance of Electrospun Collagen Nanofibers Cross-Linked by Means of Different Methods." *ACS Applied Materials and Interfaces* 1 (1): 218–23. https://doi.org/10.1021/am800063x.

Tronci, Giuseppe, Stephen J. Russell, and David J. Wood. 2013. "Photo-Active Collagen Systems with Controlled Triple Helix Architecture." *Journal of Materials Chemistry B* 1 (30): 3705–15. https://doi.org/10.1039/c3tb20720j.

Vasita, Rajesh, and Dhirendra S Katti. 2006. "Nanofibers and Their Applications in Tissue Engineering." *International Journal of Nanomedicine*. Dove Press. https://doi.org/10.2147/nano.2006.1.1.15.

Vijaysree Venkatraman. 2017. "Madras Triple Helix: The World Has Nearly Forgotten the Indian Scientist Who Cracked the Structure of Collagen — Quartz." 2017. https://qz.com/983439/madras-triple-helix-the-world-has-nearly-forgotten-the-indian-

scientist-who-cracked-the-structure-of-collagen/.

Wakuda, Yuka, Shohei Nishimoto, Shin-ichiro Suye, and Satoshi Fujita. 2018. "Native Collagen Hydrogel Nanofibres with Anisotropic Structure Using Core-Shell Electrospinning." *Scientific Reports* 8 (1): 6248. https://doi.org/10.1038/s41598-018-24700-9.

Wang, Yiwei, Paul E. Tomlins, Allan G a Coombes, and Martin Rides. 2010. "On the Determination of Darcy Permeability Coefficients for a Microporous Tissue Scaffold." *Tissue Engineering. Part C, Methods* 16 (2): 281–89. https://doi.org/10.1089/ten.tec.2009.0116.

Wess, T.J., A.P. Hammersley, L. Wess, and A. Miller. 1998. "Molecular Packing of Type I Collagen in Tendon." *Journal of Molecular Biology* 275 (2): 255–67. https://doi.org/10.1006/JMBI.1997.1449.

Wetzel, David L., Ginell R. Post, and Robert A. Lodder. 2005. "Synchrotron Infrared Microspectroscopic Analysis of Collagens I, III, and Elastin on the Shoulders of Human Thin-Cap Fibroatheromas." In *Vibrational Spectroscopy*, 38:53–59. Elsevier. https://doi.org/10.1016/j.vibspec.2005.02.029.

Widdowson, Jonathan P., Alex J. Picton, Valerie Vince, Chris J. Wright, and Andrew Mearns-Spragg. 2017. "*In Vivo* Comparison of Jellyfish and Bovine Collagen Sponges as Prototype Medical Devices." *Journal of Biomedical Materials Research Part B: Applied Biomaterials*, 1–10. https://doi.org/10.1002/jbm.b.33959.

Williams, Jennah. 2015. "Are Jellyfish Taking Over The World?" *Journal of Aquaculture & Marine Biology* 2 (3): 1–13. https://doi.org/10.15406/jamb.2015.02.00026.

Williams, Jessica M., Adebisi Adewunmi, Rachel M. Schek, Colleen L. Flanagan, Paul H. Krebsbach, Stephen E. Feinberg, Scott J. Hollister, and Suman Das. 2005. "Bone Tissue Engineering Using Polycaprolactone Scaffolds Fabricated via Selective Laser Sintering." *Biomaterials* 26 (23): 4817–27. https://doi.org/10.1016/j.biomaterials.2004.11.057.

Wyckoff, R. W. G., R. B. Corey, and J. Biscoe. 1935. "X-RAY REFLECTIONS OF LONG SPACING FROM TENDON." *Science* 82 (2121): 175–76. https://doi.org/10.1126/science.82.2121.175.

Xiong, Xin, Robin Ghosh, Ekkehard Hiller, Friedel Drepper, Bettina Knapp, Herwig Brunner, and Steffen Rupp. 2009. "A New Procedure for Rapid, High Yield

Purification of Type I Collagen for Tissue Engineering." *Process Biochemistry* 44 (11): 1200–1212. https://doi.org/10.1016/j.procbio.2009.06.010.

Xu, Yujia, Manjiri Bhate, and Barbara Brodsky. 2002. "Characterization of the Nucleation Step and Folding of a Collagen Triple-Helix Peptide." *Biochemistry* 41 (25): 8143–51. https://doi.org/10.1021/bi015952b.

Yener, F., and O. Jirsak. 2012. "Comparison between the Needle and Roller Electrospinning of Polyvinylbutyral." *Journal of Nanomaterials* 2012: 1–6. https://doi.org/10.1155/2012/839317.

Zahedi, Payam, Iraj Rezaeian, Seyed Omid Ranaei-Siadat, Seyed Hassan Jafari, and Pitt Supaphol. 2010. "A Review on Wound Dressings with an Emphasis on Electrospun Nanofibrous Polymeric Bandages." *Polymers for Advanced Technologies*. Wiley-Blackwell. https://doi.org/10.1002/pat.1625.

Zeugolis, D I, B Li, R R Lareu, C K Chan, and M Raghunath. 2008. "Collagen Solubility Testing, a Quality Assurance Step for Reproducible Electro-Spun Nano-Fibre Fabrication. A Technical Note." *Journal of Biomaterials Science. Polymer Edition* 19 (10): 1307–17. https://doi.org/10.1163/156856208786052344.

Zeugolis, Dimitrios I., Shih T. Khew, Elijah S Y Yew, Andrew K. Ekaputra, Yen W. Tong, Lin Yue L Yung, Dietmar W. Hutmacher, Colin Sheppard, and Michael Raghunath. 2008a. "Electro-Spinning of Pure Collagen Nano-Fibres - Just an Expensive Way to Make Gelatin?" *Biomaterials* 29 (15): 2293–2305. https://doi.org/10.1016/j.biomaterials.2008.02.009.

Zhang, Junjie, Rui Duan, Lei Huang, Yujie Song, and Joe M. Regenstein. 2014. "Characterisation of Acid-Soluble and Pepsin-Solubilised Collagen from Jellyfish (Cyanea Nozakii Kishinouye)." *Food Chemistry* 150: 22–26. https://doi.org/10.1016/j.foodchem.2013.10.116.

Zhang, Y. Z., J. Venugopal, Z. M. Huang, C. T. Lim, and S. Ramakrishna. 2005. "Characterization of the Surface Biocompatibility of the Electrospun PCL-Collagen Nanofibers Using Fibroblasts." *Biomacromolecules* 6 (5): 2583–89. https://doi.org/10.1021/bm050314k.

Zhang, Zhongkai, Guoying Li, and Bi Shi. 2005. "PHYSICOCHEMICAL PROPERTIES OF COLLAGEN, GELATIN AND COLLAGEN HYDROLYSATE DERIVED FROM BOVINE LIMED SPLIT WASTES." *Journal of the Society of Leather Technologists and Chemists* 90: 23–28.

https://pdfs.semanticscholar.org/3ef8/e7d1c16657823b65e665a7d0663d1317e55a.pdf.

Zhong, S. P., Y. Z. Zhang, and C. T. Lim. 2010. "Tissue Scaffolds for Skin Wound Healing and Dermal Reconstruction." *Wiley Interdisciplinary Reviews: Nanomedicine and Nanobiotechnology* 2 (5): 510–25. https://doi.org/10.1002/wnan.100.

Zhong, Shaoping, Wee Eong Teo, Xiao Zhu, Roger W Beuerman, Seeram Ramakrishna, Lin Yue, and Lanry Yung. 2006. "An Aligned Nanofibrous Collagen Scaffold by Electrospinning and Its Effects on in Vitro Fibroblast Culture." https://doi.org/10.1002/jbm.a.

Zhou, Tian, Nanping Wang, Yang Xue, Tingting Ding, Xin Liu, Xiumei Mo, and Jiao Sun. 2016. "Electrospun Tilapia Collagen Nanofibers Accelerating Wound Healing via Inducing Keratinocytes Proliferation and Differentiation." *Colloids and Surfaces B: Biointerfaces* 143 (July): 415–22. https://doi.org/10.1016/J.COLSURFB.2016.03.052.

Zhu, Chenhui, Daidi Fan, Zhiguang Duan, Wenjiao Xue, Longan Shang, Fulin Chen, and Yane Luo. 2009. "Initial Investigation of Novel Human-like Collagen/Chitosan Scaffold for Vascular Tissue Engineering." *Journal of Biomedical Materials Research - Part A* 89 (3): 829–40. https://doi.org/10.1002/jbm.a.32256.

Zydney, Andrew L. 1998. "Protein Separations Using Membrane Filtration: New Opportunities for Whey Fractionation." *International Dairy Journal* 8 (3): 243–50. https://doi.org/10.1016/S0958-6946(98)00045-4.